The role of chromosome arms and kinetochore architecture in the formation of amphitelic attachments - Implications for mitotic fidelity

Danica Drpic

2017

Tese de Candidatura ao grau de Doutor em Ciências Biomédicas, submetida ao Instituto de Ciências Biomédicas Abel Salazar da Universidade do Porto do Programa Doutoral GABBA

Orientador – Doutor Helder Maiato

Categoria – Investigador Principal,

Professor auxiliar convidado

Afiliação – IBMC/ I3S, FMUP

NOTA EXPLICATIVA

A presente dissertação foi escrita em Inglês na sua quase totalidade devido ao facto dos trabalhos terem sido realizados com colaboração internacional.

Este trabalho foi financiado pela

Fundação para a Ciência e Tecnologia

SFRH/BD/51698/2011

“Nothing in life is to be feared, it is only to be understood”

Marie Curie

Mojim roditeljima, sestri, baki i deki, za svu ljubav i podrsku,

To Waldir

Acknowledgments

One of the dearest advices I got from my mom was: “Don’t go through the school, let the school go through you.” And to be honest that was my main goal during the PhD. But such a task was impossible to achieve without the help of many people I met during the way. And in order to keep my “acknowledgment” section shorter then the rest of the thesis, I will mention just some of these people.

The person from whom I learned a lot and I owe big gratitude is my supervisor Helder Maiato. Foremost, I am thankful for giving me the opportunity to work in the CID lab and introducing me to the beautiful world of cell division and microscopy. I will never forget our first meeting, when Helder showed me the chromosome spread of Indian muntjac cells. Helder’s first advice was that I should be more excited about mitosis. Hmm, I think I took that advice too seriously. That’s how I became privileged to work with the amazing Indian muntjac cells, with which I fell in love after the first Immunofluorescence. (Check figures in Section 4.3 and you will understand). Finally I would like to thank Helder for all the support in and outside the lab. For all inspiring scientific talks and discussions that raised so many ideas and made me “mitotically unfocused”.

Especially, I would like to thank to my “supervisor Brko” Marin, for all the help and knowledge he shared with me since the first minute in the lab. Marin taught me …pretty much everything necessary to study mitosis. But besides big support and help, Marin became my great friend.

Big thank you to my dear Martina, the sunshine of the lab and the source of so much needed smile and positive energy. Thank you for being such a great friend and person.

During all this process so many times I would bother Jorge and Toze with my questions. And they were always so patient and kind with me; answering all possible questions and sharing precious knowledge and advice that helped so many times. Thank you.

And my “trouble makers” Olga, Nina, Luisa, Margarida, Ana Almeida (Bambi). Thank you for making the life inside and outside the lab interesting and for making me smile a lot.

Particularly I would like to thank to Ana Almeida for being such a positive smart and hard working Bambi. It was such a pleasure to work with you; we grew up together as persons and as scientists.

I also need to thank Carolina, my Cross Puncherinha for extremely needed support and positive energy during this last year when I really really needed.

I would like to thank all CID lab members with whom I had the privilege to work since I joined the lab: Zaira, Tatiana, Elsa, Joana, Ana Pereira, Ariana, Paulo Aguiar, Cristina Ferras, Cristina Bebe, Hugo, Filipe, Ana Figueredo, Bernardo, Naoyuki, Danilo, Liam. With you I learned a lot.

A big thank you to all the members of the GMM and the ANA's lab for everyday support and nice environment.

Thank you to my GABBA 15th Edition for the great time we had together. It will always be a pleasure to meet you. Special gratitude to Catarina Corona for help and advice. Professora Maria de Sousa, all my GABBA professors and GABBA PhD program. It has been a great honor to be part of it.

And most of all I would like to thank to my family.

Posebnu zahvalnost dugujem mojim dragim roditeljima, mojoj dragoj sestri i Petruskici. Vasa ljubav I podrska su nesto najvrednije sto postoji. Najvece bogstvo I izvor snage. Otici daleko od vas bila je najteza odluka u zivotu I za vas I za mene. Ali vi ste to nesebicno prihvatili kao I sve ostale moje hirove. Bez vas nista od ovoga ne bi bilo moguce, niti bi imalo smisla. Ova titula je vasa.

Veliku zahvalnost dugujem i mojim voljenim baki I deki, za nesebicnu ljubav, za podrsku i za najbolje savete koje sam ikad dobila. Ponosna sam sto ste moji baka I deka.

Mojim dragim Zivanovicima, mojoj keki, teci, Jovani I Djoletu, Jeleni i Lazi hvala na svim veselim razgovorima, na velikoj podrsci I ljubavi.

To the rest of my family and friends. Big thank you.

And the last, but not least… big thank you to Waldir. For being my dear friend, love, support. You were there when everybody else would leave and give up. Thank you for all the support, for sharing good and bad. For the weekends you spent with me in the lab, for all the days you waited for me, for calming me down when experiments didn't work, for all laughs, patience, for the great time we have together.

Abstract

Proper chromosome segregation and mitotic fidelity depends on previous chromosome bi-orientation. For bi-orientation to occur chromosome have to attach to the microtubules coming from opposite poles, which will create the tension required for attachment stabilization. However, how end-on kinetochore-microtubule attachments are first stabilized in the absence of tension remains a key unanswered question. Moreover, what is the role of kinetochore architecture in proper chromosome congression and segregation stays unknown. Here, taking advantage of two model systems, *Drosophila* S2 cells undergoing mitosis with unreplicated genomes (SMUGs) and Indian muntjac fibroblast we addressed the question of chromosome bi-orientation and mitotic fidelity, focusing on processes that play an important role in initial attachment stabilization, chromosome congression and segregation. To address this we generated *Drosophila* S2 cells undergoing SMUGs. SMUGs retained single condensed chromatids that attached laterally to spindle microtubules. The advantage of this system when compared with MUGs generated in mammalian cells is the preservation of chromatid morphology. Over time, laterally attached kinetochores converted into end-on attachments, experienced intra-kinetochore stretch or structural deformation, and SMUGs eventually exited a delayed mitosis after satisfying the spindle-assembly checkpoint (SAC). Here we show that conversion from lateral to end-on kinetochore-microtubule attachments was promoted by polar ejection forces (PEFs) generated by Chromokinesins ultimately leading to SAC satisfaction in SMUGs. Thus, PEFs convert lateral to stable end-on kinetochore-microtubule attachments, independently of bi-orientation. Besides initial chromosome positioning around the newly formed spindle, changes in kinetochore structure during mitosis increase the probability of formation of amphitelic attachments.

During prometaphase, kinetochores increase in size forming wider crescent structures, which facilitate their capture by microtubules. Upon initial attachments, kinetochore structure decreases, becoming less prone to error formation. However, the physiological relevance of kinetochore size in error formation remains unknown. To investigate whether kinetochore size influences chromosome segregation fidelity we took advantage of immortalized fibroblasts from the Indian muntjac, the mammalian with the lowest known chromosome number (n=3). Indian muntjac chromosomes are morphologically distinct and can be easily tracked by live-cell fluorescence microscopy. One remarkable feature of the Indian muntjac cells is the unusually large kinetochore of chromosome 3+X that can bind up to 100 microtubules. Here we show that large kinetochores are more prompt to establish erroneous attachments

leading to chromosome missegregation. Moreover, our results indicate that kinetochore size affects the pathway of chromosome congression and bi-orientation during mitosis.

Overall, these findings provide direct evidence that kinetochore size is an important determinant of chromosome segregation fidelity in mammals.

Resumo

A segregação correta de cromossomas e a fidelidade do processo de mitose dependem da prévia bi-orientação dos cromossomas. Para que ocorra corretamente, os cromossomas devem ligar-se a microtúbulos provenientes de pólos opostos, o que vai originar a tensão necessária para a estabilização destas ligações. No entanto, de que forma é que a interação cinetocoro-microtúbulo é inicialmente estabilizada na ausência de tensão continua uma questão em aberto. Para além disso, continua por descrever qual a função da arquitetura do cinetocoro no correto deslocamento e posicionamento dos cromossomas na placa equatorial e posterior separação. Aqui, beneficiando das características de dois sistemas modelo, células de Drosophila que entram em mitose com genomas não replicados (SMUGs) e fibroblastos de Indian Muntjac, abordamos a questão da bi-orientação e fidelidade mitótica, focando-nos nos processos que desempenham um papel importante na estabilização inicial das interações, no posicionamento correto dos cromossomas em metáfase e na respetiva separação. Inicialmente geraram-se células Drosophila S2 submetidas a SMUGs. As SMUGs retêm as cromatídeas individuais condensadas e estas ligam-se lateralmente aos microtúbulos do fuso. A vantagem deste sistema comparativamente às MUGs, geradas em células de mamífero, é a preservação da morfologia das cromatídeas. Ao longo do tempo, os cinetocoros conectados lateralmente que passam a interagir com a extremidade do microtúbulo (ligação end-on), experienciam um estiramento intra-cinetocoro e/ou uma deformação estrutural, e as SMUGs saem eventualmente de mitose com um atraso, após a satisfação do ponto de monitorização da mitose (SAC). Assim, mostramos que a conversão de cinetocores-microtúbulos lateralmente ligados para cinetocores-microtúbulos conectados pela extremidade do microtúbulo é promovida por forças de ejeção polar (PEFs) geradas por cromocinesinas que levam em última instância à satisfação do SAC. Deste modo, as PEFs convertem interações laterais em ligações estáveis end-on, independentemente da bi-orientação. Para além do posicionamento inicial dos cromossomas em torno do fuso recém-formado, mudanças na estrutura do cinetocoro durante a mitose aumentam a probabilidade de formação de ligações anfitélicas.

Durante a prometafase, os cinetocoros aumentam de tamanho formando estruturas mais largas, o que facilita a sua captura por microtúbulos. Após as primeiras ligações, a estrutura do cinetocoro diminui, tornando-se menos propenso à formação de erros. Contudo, a relevância fisiológica do tamanho do cinetocoro na formação de erros permanece desconhecida. De modo a investigar se o tamanho do cinetocoro influencia a fidelidade da segregação dos cromossomas, aproveitamos os fibroblastos imortalizados do Indian Muntjac,

o mamífero conhecido com o menor número de cromossomos (n = 3). Os cromossomas deste mamífero possuem uma morfologia distinta e podem ser facilmente identificados por microscopia de fluorescência de células vivas. De destacar que estas células têm características notáveis, nomeadamente possuem um cinetocoro invulgarmente grande que pode ligar até 100 microtúbulos. Neste trabalho, demonstramos que os cinetocoros maiores são mais propensos a estabelecer ligações erradas, o que origina erros na segregação dos cromossomas.

Para além disso, provamos que o tamanho do cinetocoro afeta a via pela qual os cromossomas se deslocam à placa metafásica e a bi-orientação durante a mitose. Em suma, os nossos resultados fornecem evidência direta de que o tamanho do cinetocoro é determinante para a correta separação dos cromossomas em mamíferos. E ainda, estabelecem fundamento para a compreensão dos processos envolvidos na fidelidade mitótica e respetivas aplicações futuras em sistemas mais complexos, como as células humanas.

Contents

Original articles

De acordo com o artigo 8º do Decreto-Lei nº 388/70, fazem parte integrante desta dissertação os seguentes trabalhos publicados:

1. **Danica Drpic***, Marin Barisic*, Diana Pinheiro, Helder Maiato, Selective tracking of template DNA strands after induction of mitosis with unreplicated genomes (MUGs) in *Drosophila* S2 cells. Chromosome Res. 2013 May; 21(3): 329-37. (Cover of the journal).

2. **Danica Drpic**, António J. Pereira, Marin Barisic, Thomas J. Maresca, Helder Maiato, Polar ejection forces and Cdk1 regulate kinetochore-microtubule attachment stability on mono-oriented chromosomes. Cell Reports, 2015, October: 20; 13(3): 460-8.

*os autores tiveram igual contributo para a realização do trabalho. Em cumprimento do disposto no referido Decreto-Lei, declara que participou activamente na recolha e análise de dados e escreveu o artigo 1 e 2 com a colaboração dos co-autores.

Abbreviations

AP	away from the pole
APC/C	Anaphase Promoting Complex/Cyclosome
ATM	Ataxia telangiectasia mutant
ATP	Adenosine Triphosphate
CCAN	Constitutive Centromere Associated Network
H2B	histone H2B like variant
Cdk	Cyclin Dependent Kinase
CENP-A	Centromeric protein A
CFK	centromere-kinetochore fragments
CH	Calponin Homology
CHO	Chinese Hamster ovary
CID	centromere identifier
CIN	Chromosomal Instability
CLEM	Correlative light and electron microscopy
CM	Chinese muntjac
CPC	Chromosomal Passenger Complex
DAPI	4',6-diamino-2'-phenylindole dihydrochloride
DNA	Deoxyribonucleic acid
Dup	Double parked
EM	Electron microscopy
FBS	Fetal Bovine Serum
GDP	Guanosine diphosphate
GFP	Green Fluorescence Protein
GTP	Guanosine-5'-triphosphate
h	Hour
HeLa	Human adenocarcinoma cell line from Henrietta Lacks
HU	hydroxyurea

IF	Immunofluorescence
IM	Indian muntjac
KT	Kinetochore
MAP	Microtubule Associated Proteins
MCAK	Mitotic Centromere Associated Kinase
MCC	Mitotic checkpoint complex
min	Minute
MT	Microtubules
MTOC	Microtubule organizing center
MUG	Mitosis with unreplicated genome
NEB	Nuclear envelope breakdown
NER	Nuclear envelope reformation
P	Poleward
PBS	Phosphate buffered saline
PCM	Pericentriolar material
PEG	Polyethylene glycol
PFA	Paraformaldehyde
PtK1	Potorous tridactylus kidney epithelial cells (female)
PtK2	Potorous tridactylus kidney epithelial cells (male)
PTM	Post-translational Modification
RNAi	Ribonucleic acid interference
RT	Room temperature
SAC	Spindle Assembly Checkpoint
SD	Standard deviation
SHREC	Single-molecule light resolution colocalization
SIM	Structured Illumination Microscopy
SMUG	*Drosophila* S2 cells undergoing mitosis with unreplicated genome
STED	Stimulated Emission Depletion Microscopy
U2OS	Human osteosarcoma epithelial cells
γ-TuRC	γ-tubulin ring complex

List of Figures

List of Tables

Chapter 1

General introduction

1.1 The cell cycle

The cell cycle is a coordinated sequence of periodic events that lead to formation of two cells from a single pre-existing cell. The cell cycle is fundamental for the growth and regeneration of multicellular organisms and requires high regulation and control of each stage in order to prevent errors that could lead to cancer or developmental disorders.

The life cycle of a eukaryotic cell can be divided into two phases: interphase and mitosis. Interphase is the longest phase, compromised of different stages that ensure cell growth, G1 phase, DNA synthesis, S phase and protein synthesis, G2 phase, required for correct cell division during mitosis (reviewed in (Arellano and Moreno, 1997; Vermeulen et al., 2003)) (Figure 1.1). Each stage of the cycle has specialized purposes and requirements for proper cell function. Progression through these phases is controlled by the oscillations in activity of cyclin-dependent kinases (Cdks) (Minshull et al., 1990). As indicated by their name, Cdks are activated through binding to cyclins (Evans et al., 1983), and inactivated once cyclins are degraded. Transition from phase to phase is highly controlled by surveillance mechanisms, called cell cycle checkpoints, whose main purpose is to prevent further progression of the cycle if the requirements from the previous stage are not fulfilled. As a part of the cell cycle, proper cell division requires the successful conclusion of all previous phases in the life of a cell.

1.1.1 Cell cycle stages

After division of the mother cell, the two new daughter cells enter the longest phase, called G1 (GAP1) phase, which is characterized by cell growth and high protein synthesis (Figure 1.1). During this phase, cells can exit the cycle and enter the resting non-proliferative

G0 state. During the G0 phase, cells differentiate and reprogram gene expression in order to fulfill new functions. Cells that continue with the cell cycle will enter the next phase called S phase (Figure 1.1). The essential requirement for cell division is the complete and correct duplication of the genome. This process occurs during the S (synthesis) phase of the cell cycle, when origins of replications are activated and the complete DNA content is duplicated into two identical copies. In the next phase, G2 (GAP-phase), cells undergo high protein synthesis (Figure 1.1). At the end of this phase, the previously replicated genome starts condensing into the individual chromosomes, which will be divided in the following phase called mitosis (M-phase) (reviewed in (Vermeulen et al., 2003) (Figure 1.1).

Mitosis is the shortest phase in the life of the cell, and is characterized by dramatic changes in the cytoskeleton and cell content. Moreover, the duration of M-phase is remarkably constant under normal conditions and independent of cell-cycle length (Araujo et al., 2016).

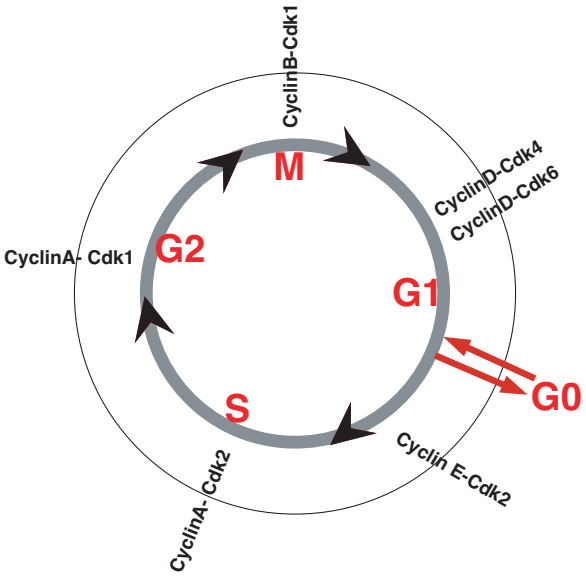

Figure 1.1: **Stages of the cell cycle**. The life cycle of the cell includes several carefully controlled phases, M-mitosis, G1- Gap1, S-synthesis, G2- Gap2 phase. Each phase is characterized by the high concentration of specific cyclins and activity of their associated Cdks. Transition of each phase is controlled by cell cycle checkpoints. The cell cycle starts with G1 phase, in which two new daughter cells, generated during mitosis, initiate cell growth and protein synthesis. In this phase the cell can commit to exit the cell cycle and enter in the non-proliferative G0 phase, or continue with the cell cycle and enter the next S phase. S phase is essential for replicating the genome material into two identical copies that will be divided afterwards. After complete DNA replication, the cell will enter in G2 phase, characterized by protein synthesis and final control of the replicated DNA, which will allow the cell to enter M phase and equally divide two copies of the genome into two new daughter cells.

1.1.2 Mitosis - an overview

Cell division is a fundamental property of every cell and organism. In a single cell organism it is the basis for reproduction, while in multicellular organisms it is essential for growth and regeneration. The main goal of cell division is the proper separation of the previously replicated genetic material into two new daughter cells. The term “mitosis”, nuclear division, was first used by German anatomist Walter Flemming in 1879 (Flemming, 1965). Studying dividing salamander cells, Flemming observed the formation of paired threads (Greek: mythos = treads) and described the series of events that followed (Flemming, 1965).

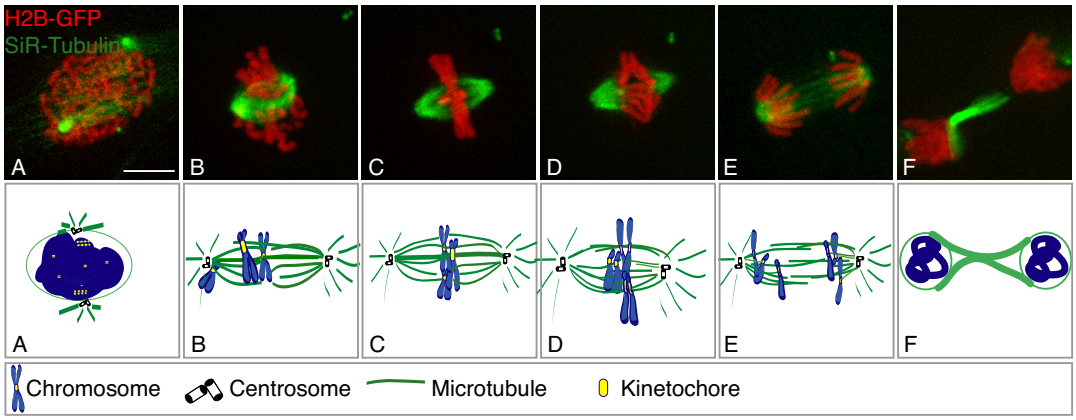

Figure 1.2: **Mitotic phases**. Upper panel represents live cell imaging of Indian muntjac fibroblast undergoing different stages of mitosis. Lower panel is the schematic, simplified representation of the mitotic phases: During (A) prophase, The previously replicated genetic material condenses, and the surrounding nuclear envelope is pushed by the two centrosomes that form a spindle pole. After nuclear envelope breakdown (NEB), the cell enters in (B) prometaphase, the phase in which spindle fibers (microtubules, MTs) invade the nuclear region, capturing chromosomes through protein structures called kinetochores (KTs). In (C) metaphase all chromosomes are correctly attached to opposite poles and align at the spindle equator. Initial separation of sister chromatids in (D) anaphase A, initiates with shortening of microtubules attached to the KTs (K-fibers) and without significant changes in spindle length. Further shortening of K-fibers, pole separation and spindle elongation characterize (E) anaphase B. In (F) telophase both sets of sister chromatids are correctly separated into two nuclei, and the nuclear envelope is reformed (NER). Cell division into two daughter cells ends after cytokinesis, when the cytoplasm of the cell is cleaved. DNA in red, MTs in green; Scale bar 5μm. In the lower panel chromosomes are represented in blue, MTs in green, KTs in yellow, spindle pole in black.

The observed paired threads were condensed chromosomes, the first visible sign of upcoming mitosis. The first phase, known as prophase, (Figure 1.2 A) starts with the condensation of the previously replicated genetic material and ends at the onset of nuclear envelope breakdown (NEB). Removal of the nuclear envelope allows the initial interaction between chromosomes and the spindle leading to mitotic spindle formation. This stage is known as prometaphase (Figure 1.2 B).

Once all chromosomes become correctly attached to opposite spindle poles and aligned at the spindle equator, the cell is considered to be in metaphase (Figure 1.2 C). Pulling forces from MTs coming from the opposite poles result in the separation of aligned sister chromatids during anaphase. Poleward movement of the chromosomes due to shortening of spindle fibers connected to chromosomes is termed as anaphase A (Figure 1.2 D). Further separation of the poles and spindle elongation is defined as anaphase B (Figure 1.2 E). The last stage of mitosis, telophase (Figure 1.2 F), begins when the two identical sets of chromosomes reach opposite poles and integrate into new nuclei following nuclear envelope reformation (NER). Formation of the cleavage furrow takes place in the same plane where chromosomes were previously aligned and its constriction results in the final separation of two daughter cells during cytokinesis (McIntosh and Hays, 2016; Sharp, 1921).

1.1.3 Cell cycle cyclins

As cells progress through the cell cycle, specific proteins are expressed or degraded at distinct time points (Nurse, 1975; Nurse et al., 1976). Some of these specific proteins are called cyclins and play a crucial role in regulating the kinase activity of serine/threonine/protein kinases called cyclin-dependent kinases (Cdks) (Evans et al., 1983; Hartwell et al., 1970; Murray and Kirschner, 1989). While cyclin levels oscillate during the cell cycle, Cdk protein levels are constant, yet their activity depends on the presence of cyclins. In addition to regulation by cyclins, Cdk activity is also controlled by phosphorylation on conserved threonine and tyrosine residues (Leise and Mueller, 2002; Vermeulen et al., 2003). For instance, Cdk1 activity is inhibited by Wee1 and Myt1 kinase-mediated phosphorylation (Leise and Mueller, 2002; Stumpff et al., 2004). This inhibition can be reversed by Cdc25-induced dephosphorylation of the same sites (Furnari et al., 1997; Nurse, 1975; Russell and Nurse, 1986; Sadhu et al., 1990). Moreover cell cycle inhibitory proteins, called Cdk inhibitors (CdkI), counteract and additionally control Cdk activity (reviewed in (Lim and Kaldis, 2013; Morgan, 1995).

Different phases of the cell cycle require different cyclins (Figure 1.1). During G1 phase, cyclin D synthesis, stimulated by growth factors, promotes the activation of Cdk4 and Cdk6 (Sherr, 1994) (Figure 1.1). An increase in Cyclin E levels and its association with Cdk2 allows the transition from G1 to S phase (Ohtsubo et al., 1995). The cyclin A-Cdk2 complex is required for S phase and its high levels together with cyclin B-Cdk1 complex expressed in G2 phase promote mitotic entry (Arellano and Moreno, 1997; Hein and Nilsson, 2016; Minshull et al., 1989; Murray and Kirschner, 1989; Santos et al., 2012) (Figure 1.1). At the

beginning of M-phase, cyclin A levels decrease, which is essential for the initial stabilization of attachments between chromosomes and mitotic spindle (Kabeche and Compton, 2013) (Figure 1.1). As mitosis progress and initial attachments are formed, the E3 ubiquitin ligase APC/C tags cyclin B for degradation, leading to gradual decline in cyclin B levels, consequent decrease in Cdk1 activity and mitotic exit (Alfieri et al., 2016; Clute and Pines, 1999; Collin et al., 2013; Dick and Gerlich, 2013; Pines, 2011).

1.1.4 Cell cycle checkpoints

The orderly sequence of events during the cell cycle is ensured by the existence of multiple cell cycle checkpoints (Hartwell and Weinert, 1989). Cell cycle checkpoints represent constitutive surveillance mechanisms that ensure the tight dependency of cell cycle events (Hartwell and Weinert, 1989; Maiato et al., 2015). In the presence of errors or stress stimuli checkpoints promote a cell cycle delay in order to provide time for error correction. In order to efficiently monitor cell cycle events, checkpoints are constantly active and external to the events that are being monitored (Hartwell and Kastan, 1994; Hartwell and Weinert, 1989; Khodjakov and Rieder, 2009; Maiato et al., 2015). To fulfill such function, checkpoints are composed of three main components: a sensor that detects problems, a signal and response elements (Maiato et al., 2015; Rieder, 2011). To control cell cycle progression checkpoints have an impact on the activity of Cdks and their respective cyclins. However, some experimental procedures (inhibitors, drugs, mutants) can override the checkpoint and allow the cell to proceed with the cell cycle in the presence of errors (Hartwell and Kastan, 1994; Hartwell and Weinert, 1989; Khodjakov and Rieder, 2009; Maiato et al., 2015).

The main task of the cell cycle is to assure the correct division of a completely replicated, undamaged genome. Therefore to ensure genomic integrity DNA damage is controlled several times during the cell cycle (Nelson and Kastan, 1994). During G1 phase DNA damage activates the p53 pathway preventing the progression through the phase. p53 mediated regulation of the cell cycle includes transcriptional, post-transcriptional and post-translational mechanisms (Murray-Zmijewski et al., 2008). Activation of the p53 pathway leads to transcription of CdkI like p16, p21, and p27, which in turn inhibit Cdk2, Cdk4, cyclin D and cyclin E expression (Nelson and Kastan, 1994; Tudzarova et al., 2016).

In S phase, DNA damage and replication stress activate a kinase cascade in response to damage. One of the first examples of the DNA damage checkpoint was reported in primary cells isolated from Ataxia Telangiectasia (AT) patients (Painter and Young, 1980). Even in the presence of radiation induced DNA damage, DNA synthesis in these cells was not perturbed.

The reason for that lays in the mutation in the ataxia telangiectasia mutated (ATM) gene (Painter and Young, 1980; Willis and Rhind, 2009; Zou, 2017). DNA structural alterations (e.g. double strand breaks, gaps) recognized during replication result in stall of replication fork and recruitment of ATM and ATM and Rad3 (ATR) serine/threonine kinases (Harper and Elledge, 2007). DNA bound ATM and ATR bind additional substrates or function as a scaffold to ensemble other complexes required for DNA repair (Harper and Elledge, 2007; van Vugt et al., 2010). The presence of arrested replication forks in S phase is detected by the replication checkpoint which activates the cascade response that abrogates the progression into mitosis. However, the delay in cell cycle induced by ATM activation can be overcome by caffeine treatments (Bode and Dong, 2007).

Once all previous checkpoints are satisfied cells will proceed with mitosis. However, in the presence of stress mitotic entry can be reverted by the antephase checkpoint (Matsusaka and Pines, 2004; Rieder and Cole, 1998). Diverse stress signals during G2 phase activate the p38 protein kinase (Mikhailov et al., 2005). Activated p38 kinase phosphorylates Cdc25B at 14-3-3 binding site which induce its exclusion into the cytoplasm. Since Cdc25B is required for removal of the inhibitory signal from cyclin A/Cdk2 or Cdk1, its sequestration to the cytoplasm results in cyclin A/Cdk2 and cyclinB/ Cdk1 inhibition and arrest in G2 phase (Mikhailov et al., 2005). Moreover cyclin B degradation and APC/C activation during antephase, even after low-doses of radiation results in irreversible cell cycle exit. Observed hypersensitivity to DNA damage in antephase compared with earlier stages of G2 phase comes from the loss of the early mitotic inhibitor 1 (Emi1) shortly before mitosis. Lack of Emi1 and abrupt Cdk inhibition due to DNA damage causes premature APC/C^{Cdh1} activation and cell cycle exit. Thus, induced early cell cycle exit has a role in protecting genome stability by preventing cell division with broken chromosomes (Feringa et al., 2016).

After NEB, the attachment status between chromosomes and the spindle is monitored by the spindle assembly checkpoint (SAC) (Bode and Dong, 2007; Maiato et al., 2015).

As cells proceed into anaphase, another surveillance mechanism plays an important role in controlling chromosome separation during anaphase. An Aurora B mediated phosphorylation gradient along the elongating spindle monitors chromosome separation, by inhibiting premature decondensation and NER. This checkpoint is important for incorporation of lagging chromosomes into daughter nuclei before NER (Afonso et al., 2014b).

Final separation of two newly formed daughter cells is controlled by the abscission (NoCut) checkpoint in cytokinesis, activated by the presence of chromatin in the intracellular bridge (Amaral et al., 2016; Nahse et al., 2017).

1.2 The spindle assembly checkpoint

The SAC is the surveillance mechanism that monitors the attachment status between proteinaceous structures present at the chromosomes, named KTs, and polymers that compose the mitotic spindle, named MTs, during mitosis. Since proper chromosome segregation depends on correct attachments between KTs and MTs, the SAC signal is generated at unattached KTs. The generated signal prevents premature exit from mitosis by inactivating an E3 ubiquitin ligase, the anaphase-promoting complex (APC/C).

1.2.1 The template model

As aforementioned, at the beginning of mitosis, in order to prevent APC/C activity, inhibitory SAC signals are produced at unattached KTs. Initial recruitment of the template composed of Mad1 (mitotic arrest deficient 1) and Mad2 mitotic checkpoint components relies on Mps1 (monopolar spindle 1) kinase activity. Mad1 binding to unattached KTs recruits an inactive form of Mad2 (open o-Mad2), inducing a conformational change into the active closed form (c-Mad2). Thus bound Mad1: cMad2 complex, represent the template for the signal that inhibits cell progression into anaphase. Furthermore, c-Mad2, functions as a receptor for o-Mad2 and catalyzes its conformational change into the active closed form (De Antoni et al., 2005; Fava et al., 2011; Mapelli et al., 2007) (Figure 1.3).

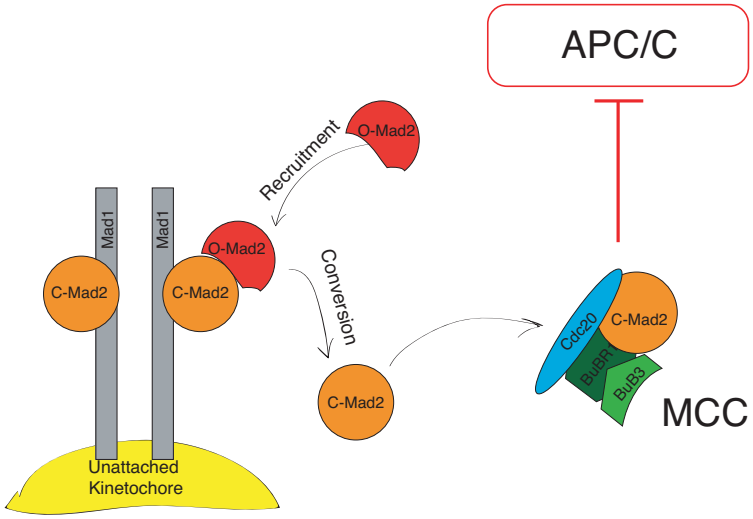

Figure 1.3: **The template model**. Unattached KTs generate an inhibitory SAC signal to prevent premature mitotic exit. On the left side of the image, unattached KT recruits Mad1, which can bind open Mad2 (o-Mad2), inducing its conformational change into the closed (c-Mad2) form. This Mad1: c-Mad2 complex represents a template for further recruitment of the open form of Mad2 and its conversion into closed, through the binding to KT bound c-Mad2. In the closed conformation Mad2 can further bind Cdc20, BuBR1 and Bub3 and form mitotic checkpoint complex (MCC). MCC prevents further mitotic progression by inhibiting Anaphase promoting complex (APC/C).

The conversion of Mad2 from open to closed conformation is required for binding to Cdc20, BuBR1 and Bub3 and assembly of the mitotic checkpoint complex (MCC), the major inhibitor of APC/C (Di Fiore et al., 2016; Faesen et al., 2017; Kulukian et al., 2009; Sudakin et al., 2001) (Figure 1.3). Although a single unattached KT can inhibit further mitotic progression, the strength of the SAC signal and mitotic delay depends on the amount of KT recruited Mad2 and the amount of MCC formed (Collin et al., 2013; Dick and Gerlich, 2013).

1.2.2 SAC silencing

As mitosis progresses, and proper KT- MT attachments are established, SAC components are removed from KTs. One of the proposed mechanisms for removal of SAC proteins upon attachment is MT stripping by the dynein motor protein (Barisic et al., 2010; Gassmann et al., 2010; Hoffman et al., 2001; Wojcik et al., 2001) (Figure 1.4). Dynein is recruited to the KT through the RZZ (Rod/ZW10/Zwilch) complex and Spindly (Chan et al., 2009; Cheerambathur et al., 2013). Spindly is a cell cycle regulated mitotic phosphoprotein that serves as an adaptor between the RZZ complex and dynein. Its KT levels depend on the MT attachment status and tension (Barisic et al., 2010; Gassmann et al., 2010).

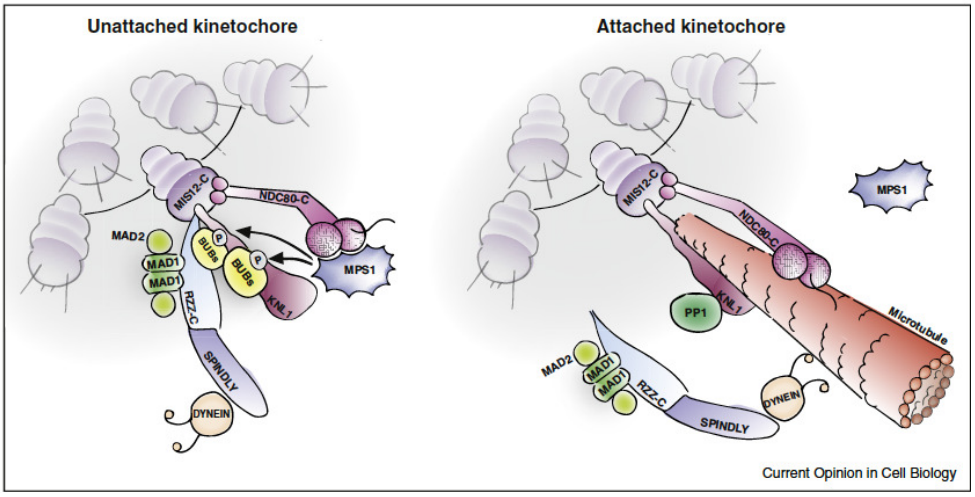

Figure 1.4: **SAC**. At unattached KTs (left image), proteins of the SAC are accumulated at the outer KT, providing an inhibitory signal for the APC/C. After KT-MT attachments are established (right panel) dynein poleward movement on the MTs allows removal of the SAC proteins from the KTs and SAC silencing. For more detailed explanation, consult the subsection 1.2.2 of this thesis. Image adapted from (Etemad and Kops, 2016).

KT localization of many proteins is contingent on the presence of MTs. Recent studies have shown that both Mps1 and MTs compete for binding sites at the calponin domain of the outer KT protein Ndc80/Hec1 (Aravamudhan et al., 2015; Hiruma et al., 2015; Ji et al., 2015). At KTs that displayed clear end-on attachments rebinding of the dynamically cycling

Mps1 was prevented by the presence of MTs bound to Ndc80-complex (Hiruma et al., 2015; Ji et al., 2015).

Besides the physical removal of SAC proteins from the KT, post-translational modifications (mainly phosphorylation) plays a critical role in SAC regulation (Conde et al., 2013; Espert et al., 2014; Gascoigne and Cheeseman, 2013; von Schubert et al., 2015). Removal of Mps1 kinase in the presence of MTs and tension decreases Knl1 phosphorylation, a phospho-docking site for BuBR1/Bub3 SAC proteins (Hiruma et al., 2015).

Aurora B kinase, present at the inner centromere, plays a central role in controlling the attachment status during mitosis (Liu et al., 2009; Vader et al., 2008). By phosphorylating components of the outer KT, in the absence of tension, due to erroneous MT attachments, Aurora B destabilizes the interaction between outer KT proteins and MTs (Liu et al., 2009). Moreover, Mps1 KT localization depends on Aurora B mediated phosphorylation of its N-terminal TPR (tetratricopeptid repeat) domain. Phosphorylation of TPR domain, removes its inhibitory effect on Mps1 localization (Nijenhuis et al., 2013). Additionally, the existence of phosphatases at the outer KT plays an essential role in counteracting the kinase activity of Aurora B and in SAC silencing (Grallert et al., 2015). In eukaryotic cells, this function is promoted by PP1 and PP2A-B56 phosphatases present at the outer KT. While PP2A KT localization depends on BubR1 and PP1 activity, PP1 can directly bind to Knl1, via SILK and RRVSF motifs (Espert et al., 2014; Nijenhuis et al., 2014). By removing Mps1 induced phosphorylation in Knl1 repeated motifs, both PP1 and PP2A have an important role in SAC silencing (Espert et al., 2014).

As aforementioned, when all KTs are attached and chromosomes are prepared for segregation, APC/C is activated to target cyclin B1 and securin for destruction. APC/C activation is controlled through binding of the co-activators Cdc20 (cell division cycle 20) and Cdh1 (Cdc20 homologue1) to the APC 10 subunit, by forming the receptor for at least one of the destruction signals (degrons) (Buschhorn et al., 2011; da Fonseca et al., 2011; Izawa and Pines, 2011). APC/C can recognize diverse primary sequences (destruction motifs) on target proteins, which can be divided in destruction (D)-box and KEN (Lys-Glu-Asn)-box (da Fonseca et al., 2011). The most well described D box is in the N-terminal region of cyclin B1 (Yamano et al., 1998). After cyclin B1 and securin degradation, the APC/C recognizes other substrates through different degrons, mostly Aurora kinases (A box recognition in case of Aurora A) (Littlepage and Ruderman, 2002), Plk1 (Lindon and Pines, 2004), Cdc20 and geminin (McGarry and Kirschner, 1998). It is proposed that the change in specificity for the degron sequence is due to the switch from binding Cdc20 to Cdh1 at the end of mitosis. Although

Cdc20 mediated activation of APC/C is important at the beginning of mitosis, Cdh1 interaction with ubiquitin ligase is crucial during anaphase and after cells exit mitosis (reviewed in (Alfieri et al., 2016; Izawa and Pines, 2011; Kraft et al., 2003; Pines, 2011).

1.3 The mitotic spindle

The mitotic spindle is a distinct hallmark of mitosis. The most abundant component of mitotic spindles are MTs, cytoskeleton straw - shaped structures organized in different populations inside the cell. Each population shows distinct dynamic properties and functions during mitosis (Figure 1.5). For instance, proper spindle positioning depends on interaction between astral MTs and the cell cortex (Wu et al., 2016). Sliding of antiparallel inter-polar MTs defines spindle length and bipolarity (Kapitein et al., 2005), but also regulates chromosome congression and spindle assembly. The most stable population are KT fibers (K-fibers) involved in interactions with KT, proteinaceous structures present at the centromere regions of chromosomes (Maiato et al., 2006; Maiato et al., 2004b; Ye et al., 2016) (Figure 1.5).

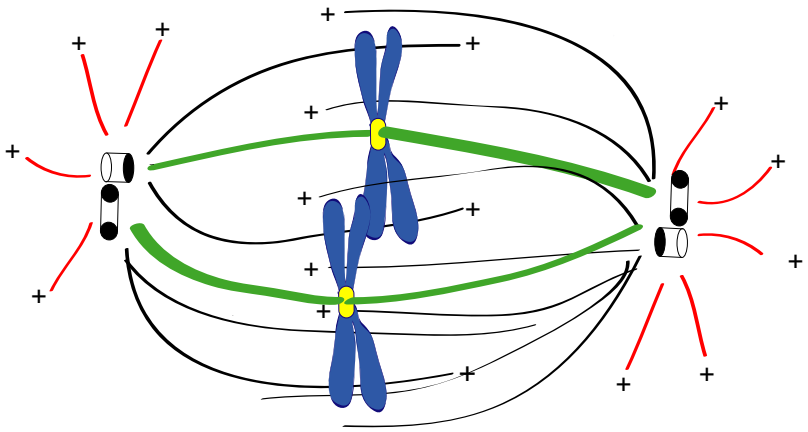

Figure 1.5: **Different populations of MTs build the mitotic spindle.** In red are represented the astral MTs. Emerging form the spindle poles towards the cortex, astral MTs are involved in spindle positioning, and spindle length control. In green are presented the K-fibers, the most stable populations of MTs required for binding to chromosomes (in blue) through their KTs (yellow). In black are interpolar-MTs, important for spindle bi-polarity and stability. Centrosomes at both spindle poles are represented as black cylinders.

The distinct feature of mitotic spindle in animal cells is the presence of two spindle poles located in the opposite side of the mitotic apparatus (Figure 1.5). Spindle poles are formed by centrosomes, the non - membrane bound organelles. In higher eukaryotes, centrosomes act as a main MTOCs (Belmont et al., 1990; Brinkley, 1985; Luders and Stearns, 2007; Rodrigues-Martins et al., 2008). In mitosis, centrosomes play an important role in spindle assembly and positioning, and chromosome segregation fidelity. During interphase, cen-

trosomes regulate diverse processes like cell migration, vesicle trafficking, and cell polarity (Chavali et al., 2014). The majority of cells have two centrosomes each containing two centrioles, the older mother centriole and newly synthesized daughter centriole surrounded by pericentriolar material (PCM) (Mennella et al., 2014).

Beside MTs, microtubule associated proteins (MAPs) and motor proteins have an important role in spindle assembly (Nogales and Zhang, 2016; Pavin and Tolic, 2016). MAPs are involved in control of MT dynamics and stability (e.g. CLASPs, EBs) (Komarova et al., 2009; Maiato et al., 2003a; Mimori-Kiyosue et al., 2005), MT bundling and organization (e.g. HURP) (Wong and Fang, 2006), spindle positioning (e.g. NuMA) (Kiyomitsu and Cheeseman, 2012; Woodard et al., 2010). Motor proteins control MT dynamics (e.g. kinesin 13s) (Manning et al., 2007; Moore et al., 2005), MT sliding (e.g. Eg5, Kif15), spindle length (Goshima et al., 2005b)(dynein, HSET, Eg5), chromosome congression (CENP-E, chromokinesins) (Bancroft et al., 2015; Barisic et al., 2014) and segregation (e.g. dynein, kinesin 13s) (Bakhoum et al., 2009b; Kline-Smith et al., 2004; Kollu et al., 2009; Maney et al., 1998; Manning et al., 2007; Raaijmakers and Medema, 2014). The mitotic spindle is a highly dynamic apparatus with a principal role in establishing correct attachments with chromosomes and allowing equal separation (segregation) of the chromosomes into two daughter cells.

1.3.1 Microtubules

MTs are intrinsically unstable polymers composed of α and β tubulin heterodimers (Carlier et al., 1984; Ponstingl et al., 1981). Although MTs are involved in many processes in the cell, including vesicle/organelle trafficking, motility, and differentiation, here I will only discuss their role during cell division.

The tubulin monomer is a highly conserved protein with a molecular weight of about 55kDa (Downing and Nogales, 1998). It is composed of three functional regions: a GTP-binding N-terminal domain, an intermediate domain and a C-terminal tail (Downing and Nogales, 1998). A longitudinal head-to tail interaction between α and β tubulin subunits builds the long protofilament, which after lateral interactions with 12 additional protofilaments, closes into a cylindrical tube termed MT (Evans et al., 1985; Tilney et al., 1973).

The cloning of the first tubulin genes in 1970's revealed several tubulin isotypes: α, β, γ, δ, ε, ζ, η, ι, $\varkappa$ with a difference in the amino acid sequence in the C-terminal tail (Cleveland et al., 1978; McKean et al., 2001). Different isotypes show distinct cellular localization and functions (Janke, 2014).

In addition to the variability in isotypes, post-translational modifications (PTMs) also contribute to MT diversity (Janke, 2014). Up to date reported PMTs of tubulin include: phosphorylation, acetylation, detyrosination/tyrosination, polyglutamylation and polyglicylation. The combination of different tubulin isotypes and PMTs generates the so called “tubulin code”, that can influence the affinity and activity of motor proteins (Barisic and Maiato, 2016; Barisic et al., 2015; Janke, 2014; Sirajuddin et al., 2014).

1.3.1.1 MT dynamics

One of the intrinsic MT features is their dynamic, unstable nature that changes during the cell cycle. For instance, MT half-life during interphase is around 3 min; while in mitosis it is just a few seconds (measured in Ptk1 cells) (Belmont et al., 1990; Saxton et al., 1984).

The aforementioned head to tail interaction of tubulin subunits defines polymer polarity, with fast growing plus ends (where β tubulin is exposed) and more stable minus ends (α tubulin exposed). Within the mitotic spindle, MT minus ends are facing the MTOC, while MT plus ends are directed towards the periphery (e.g. cortex or KTs) (Figure 1.5).

Two mechanisms can describe the dynamic behavior of MTs. The first, reported by Kirschner and Mitchison in 1984, (Mitchison and Kirschner, 1984) describes the addition and removal of tubulin subunits at the same end of the polymer - a process known as dynamic instability. Moreover, if the addition of subunits occurs at the plus-ends (polymerization) and the removal (depolymerization) at the minus ends, the mechanism is defined as treadmilling (Margolis and Wilson, 1981).

Adding the subunits at the plus ends results in MT growth (Figure 1.6 A), while removal leads to shrinkage (Figure 1.6 B), also termed MT catastrophe. Dynamic MT growth and shrinkage is crucial for initial interaction between KTs and MTs, allowing MTs to search and capture chromosomes during prometaphase (“search and capture model) (Heald and Khodjakov, 2015; Holy and Leibler, 1994; Kirschner and Mitchison, 1986) (Figure 1.6 A-C).

Tubulin incorporation into MTs requires GTP hydrolysis. GTP-bound tubulin associates with plus-ends, forming a cap that protects the rest of the polymer from depolymerization. However, fast GTP hydrolysis leaves GDP tubulin bound to the MT lattice, causing unstable curving of single protofilaments and depolymerization (Carlier et al., 1984; Desai and Mitchison, 1997; Kueh and Mitchison, 2009; Mitchison and Kirschner, 1984) (Figure 1.6 A-C).

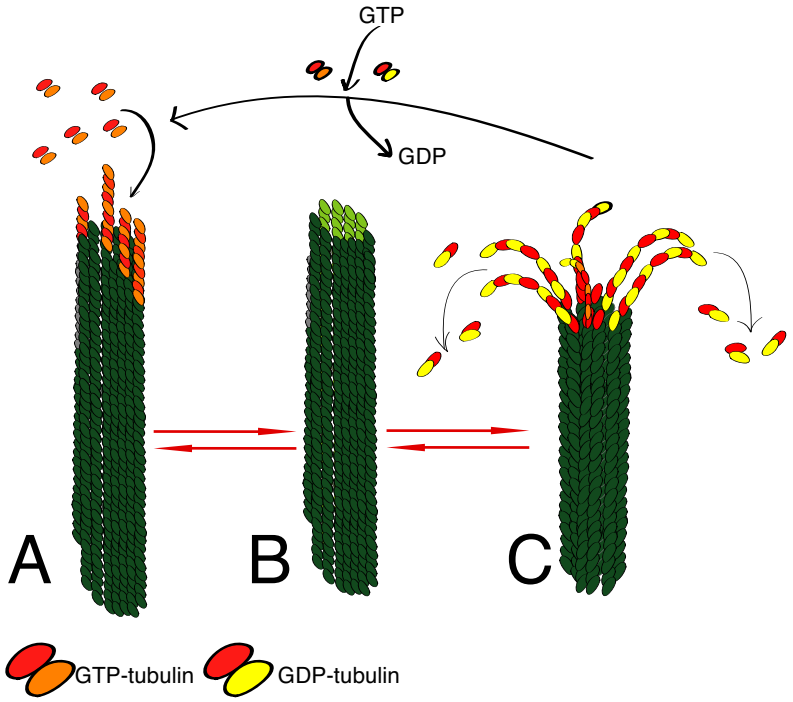

Figure 1.6: **MT dynamics**. MTs are dynamic polymers that undergo constant polymerization and depolymerization. The dynamic nature of MTs is characterized by the (A) addition or removal (C) of tubulin subunits. Incorporation of tubulin dimers at the plus end of the polymer requires binding of the GTP molecule to the tubulin dimer. The added GTP-tubulin cap will rescue the rest of the filament from depolymerization, creating an intermediate meta-stable state (B). However, GTP hydrolysis causes bending of the single protofilaments, removal of GDP-tubulin and shrinking of the polymer, a process known as catastrophe.

During metaphase, when MTs are stably attached to KTs, constant removal of tubulin subunits from the minus ends of the K fiber is compensated by their addition at the plus ends (‘poleward flux’). Thus although tubulin fluxes towards the poles, K-fiber length is constant (Mitchison et al., 1986; Sawin and Mitchison, 1991) (Figure 1.7 A). Since treatment with ATP inhibitors affect MT fluxing in vitro, it indicates involvement of motor proteins (Khodjakov and Kapoor, 2005; Mitchison, 1989; Sawin and Mitchison, 1991). During anaphase, poleward movement of chromosomes is mediated by K-fiber shrinkage (‘Traction fibre model‘) (Downing and Nogales, 1998), when tubulin subunits are removed from the minus ends. Additionally, active depolymerization at the plus ends also results in chromosome movement towards the pole (‘Pac-man‘model) (Gorbsky et al., 1987; Maiato and Lince-Faria, 2010; Mitchison and Salmon, 2001) (Figure 1.7 B).

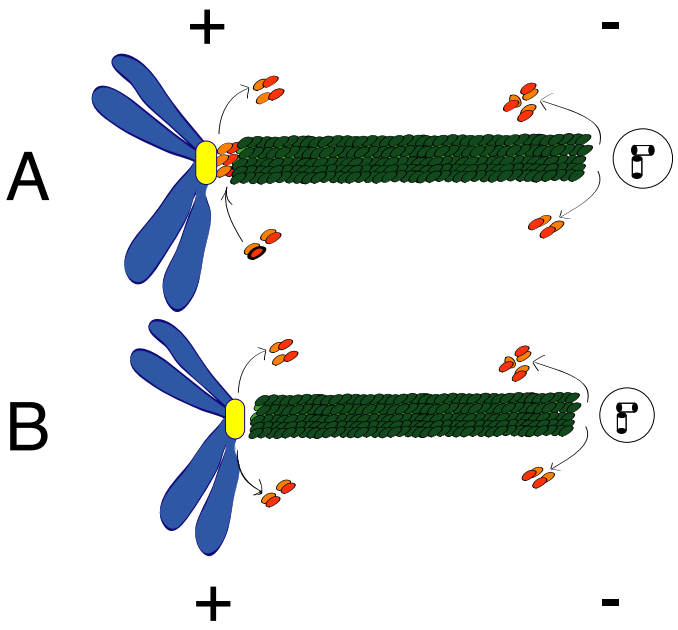

Figure 1.7: **MT poleward flux during metaphase.** (A) MTs attached to the KTs keep a constant length during mitosis due to the removal and addition of the tubulin subunits at opposite sides of the polymer. This process is known as MT flux ('poleward flux'), allows stable positioning of chromosomes at the metaphase plate, while tubulin subunits are moving polewards. (B) At anaphase onset shortening of the K-fiber and chromosome movement towards the poles is orchestrated by tubulin removal from both plus and minus end of the polymer ('Pac man'model) (Khodjakov and Kapoor, 2005).

1.3.2 Role of motor proteins

Besides MTs, proper spindle functioning and mitotic progression depends on MT bound motor proteins. Bipolar spindle formation is the result of balanced inward and outward forces, generated by motor proteins. Increased inward forces lead to spindle collapse and formation of monopolar spindles (Mayer et al., 1999), whereas increased outward forces create unfocused poles and elongated spindles (Goshima et al., 2005a; Goshima et al., 2007; van Heesbeen et al., 2016).

1.3.2.1 Kinesin 5

Inward forces are the result of motor activity of plus-end directed kinesin motor proteins, members of the kinesin-5 and kinesin-12 family.

The kinesin-5, Eg5 (Klp61F in *Drosophila*) is a plus-end directed motor protein that binds anti-parallel interpolar MTs (Figure 1.8 A). In the form of a homotetramer, Eg5 binds to MTs through four globular domains connected with a longer central region (Sawin et al., 1992).

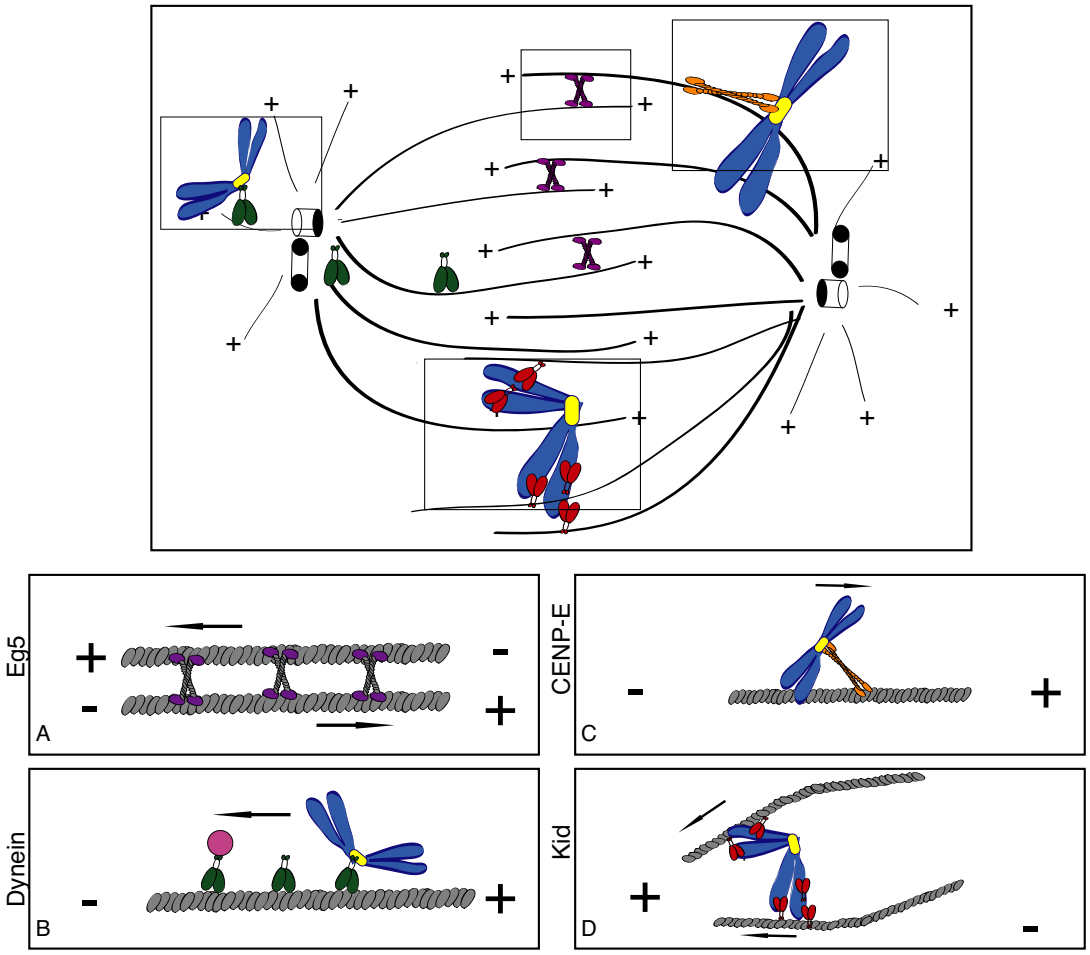

Figure 1.8: **Role of motor proteins**. Mitotic spindle bipolarity is controlled by the coordinated action of minus- and plus-end directed motor proteins. (A) Motor proteins of the kinesin-5 family slide anti - parallel inter - polar MTs, a process important for spindle pole separation and formation of bipolar spindle. (B) Dynein is a highly processive minus-end directed motor protein involved in various processes during cell division. It is involved in SAC silencing, spindle pole focusing and chromosomal movement towards the spindle pole. (C) CENP-E is a plus-end directed motor protein important for chromosome congression. It has a higher affinity for stable detyrosinated K-fibers, which bias chromosome movement towards MT plus ends at the metaphase plate and not towards the cell cortex. (D) Chromokinesins are plus-directed motor proteins present at chromosome arms. Interacting with chromatin through a chromatin binding domain and near passing MTs through a MT binding domain, chromokinesins are involved in the formation of polar ejection forces (PEFs). Plus (+) and minus (-) ends of MTs.

As a result of plus-end directed “walk”, Eg5 slides anti - parallel MTs apart, generating a bipolar spindle (Figure 1.8 A). Inhibition of Eg5 motor activity by drug treatments (monastrol or STLC) results in spindle collapse into monopoles (spindle with unseparated poles) (Cochran et al., 2005; Kapoor et al., 2000; Lampson et al., 2004; Maliga et al., 2002).

1.3.2.2 Dynein

The minus-end directed motor proteins; dynein and kinesin-14 (HSET, Ncd in *Drosophila*) generate inward forces. Dynein is a minus-end directed motor protein with broad mitotic functions due to its localization on spindle MTs, at the cell cortex and at KTs (Figure 1.8 B).

It is a fast, processive motor that uses energy from ATP hydrolysis for its movement. (Mallik et al., 2004; Mallik and Gross, 2004). KT localized dynein has an important role in controlling the SAC through removal of SAC proteins from KTs (Chan et al., 2009; Savoian et al., 2000). Cortical dynein interacts with dynactin and has a role in anchoring astral MTs to the cortex (Sharp et al., 2000). Together with another minus-end directed motor protein, kinesin-14 (Ncd in *Drosophila*), dynein has an important role in pole focusing and poleward movement of chromosomes (Goshima et al., 2005a). RNAi mediated depletion of the dynein heavy chain in *Drosophila* S2 cells results in centrosome separation from the K-fibers (Maiato et al., 2004b). In PtK2 (male rat-kangaroo) cells, newly formed (by laser ablation) spindle minus ends are reincorporated into poles by dynein poleward transport (Elting et al., 2014; Sikirzhytski et al., 2014).

As mentioned above, Eg5 and hKif15 depletion or inhibition results in spindle collapse. However, this can be overcome by co-depletion with dynein, a situation in which opposite forces in the spindle are neutralized (van Heesbeen et al., 2014). Importantly, the motor activity of dynein and Eg5 are not required for maintenance of an already formed bipolar spindle. Depletion of Eg5, dynein and hKif15 does not change the spindle configuration (monopolar or bipolar) that existed in the moment of inhibition. Although these motor proteins are not needed for maintenance of a bipolar spindle they are required for the formation of stable KT-MT attachments (van Heesbeen et al., 2016).

1.3.2.3 CENP-E

Centromere protein-E (CENP-E) belongs to the kinesin-7 family of plus-end directed MT dependent motor proteins (Wood et al., 1997). In the form of a homodimer, it is crucial in moving polar chromosomes towards the equator plate during prometaphase, a process called chromosome congression (Barisic et al., 2014) (Figure 1.8 C). Biased transport of polar chromosomes towards the equator is controlled by different PTMs of spindle and astral MTs (Barisic et al., 2015). Higher CENP-E affinity towards detyrosinated spindle MTs guides chromosomes towards the metaphase plate (Barisic et al., 2015). In vitro studies have reported CENP-E association with MT tips (Sardar et al., 2010), proposing the contribution of motor protein in attachment stability between KTs and dynamic MTs (Gudimchuk et al.,

2013). The small-molecule inhibitor GSK923295 prevents ATP hydrolysis blocking CENP-E in a rigor MT binding state (Bennett et al., 2015). As a result of CENP-E inhibition, most of the chromosomes are able to align at the metaphase plate, however, 15% of the chromosomes in human cells remain clustered near the poles (Barisic et al., 2014).

Similar to other kinesin proteins, it contains two globular regions involved in motor activity and dimerization connected by a long coiled coil domain (Kim et al., 2008) (Figure 1.8 C). However, the elongated stalk of CENP-E motor proteins is longer than in other kinesins (Kim et al., 2008; Vitre et al., 2014). Although complete removal of the stalk region did not compromise the MT walk of Quantum Dots containing motor and tail domain in vitro (Gudimchuk et al., 2013), experiments using a truncated version reported its important role in regulating protein motor activity (Vitre et al., 2014). Eliminating 85% of the stalk region in the 'Bonsai' mutant, affected chromosome congression and KT-MT attachment stability in vivo. Additionally, treatments with proteasome inhibitor in control and 'Bonsai' mutant cells resulted in quicker loss of chromosome alignment in mutant cells when compared to control cells, suggesting the role of stalk region in sustaining stable contacts between KTs and depolymerizing MT ends (Vitre et al., 2014).

1.3.2.4 Chromokinesins

Chromokinesins are plus-end directed motor proteins present at chromosome arms important for generation of the outward force during mitosis (Wandke et al., 2012; Wang and Adler, 1995) (Figure 1.8 D). Chromokinesins contain an N-terminal motor domain involved in interaction with MTs, and a C-terminal domain that binds chromatin (Mazumdar and Misteli, 2005). Through interaction with interpolar MTs, chromokinesins contribute to the polar ejection forces (PEFs) and chromosomal away from the pole movement (Brouhard and Hunt, 2005; Levesque and Compton, 2001; Mazumdar and Misteli, 2005; Rieder et al., 1986) (Figure 1.8 D). KT - free chromosome arms generated after laser ablation are actively transported away from the pole (Rieder et al., 1986). Additionally, KTs at monooriented chromosomes lacking chromosome arms after laser-cutting procedures are pulled polewards due to the absence of ejecting forces (Barisic et al., 2014; Rieder et al., 1986; Rieder and Salmon, 1994).

Kid, one of the two chromokinesins described in human cells, belongs to the kinesin 10 family and is essential in providing PEFs and chromosomal away from the pole movement (Tokai et al., 1996; Tokai-Nishizumi et al., 2005) (Figure 1.7 D). In *Drosophila* cells, the kinesin 10 homolog Nod (non distributive disjunction) plays an important role in KT-MT attachment

stability (Cane et al., 2013; Cochran et al., 2009). Overexpression of Nod in *Drosophila* S2 cells stabilizes erroneous synthelic attachments (both sister KTs attached to the same pole) in a dose - and motor - dependent manner (Cane et al., 2013).

By generating PEFs, hKid expels chromosome arms away from the central region of the newly forming spindle allowing for the formation of the chromosomal ring and initial chromosomal capture during prometaphase. RNAi mediated depletion of kinesin-10 in human cells delays metaphase plate formation and decreases the efficiency of spindle assembly (Magidson et al., 2011).

The second human chromokinesin, Kif4A belongs to the kinesin - 4 family and in contrast to hKid it has limiting effects on generating PEFs (Brouhard and Hunt, 2005; Wandke et al., 2012). However, it contributes to additional functions in mitosis. It has been reported that hKif4A has a role in chromosome congression, MT dynamics (Wandke et al., 2012) and cytokinesis (Kurasawa et al., 2004; Zhu and Jiang, 2005; Zhu et al., 2005b) in human cells. Moreover, Kif4A depleted human cells, had longer mitotic spindles with decreased MT flux (Wandke et al., 2012). A critical role in central spindle assembly and cytokinesis has been reported for the *Drosophila* kinesin 4 homolog, Klp3A (Williams et al., 1995). Interestingly, the major function of the Kif4A *Caenorhabditis elegans* homolog is in the prevention of merotelic attachments. By generating PEFs and thus being functionally more similar to hKid, Klp19 has an important role in metaphase alignment of holocentric chromosomes (Powers et al., 2004).

Although individual contributions of chromokinesins are not fundamental for mitotic progression, codepletion of both chromokinesins led to severe problems in chromosome congression and chromosome segregation both in human and *Drosophila* cells (Goshima and Vale, 2003; Wandke et al., 2012). Increased length of MTs upon loss of both chromokinesins influenced the irregular chromosome oscillations and KT stretching (Wandke et al., 2012).

Elegant studies in human cells have shown that both chromokinesins and motor protein CENP-E (Vitre et al., 2014) are involved in ejecting chromosomes away from the pole. However, KT forces mediated by CENP-E are dominant over chromokinesins in biasing chromosomes towards the metaphase plate. Acentric fragments (without KTs) created by laser ablation were able to move towards the equatorial plate or towards the cortex in the presence of a CENP-E inhibitor. In contrast, KT-containing fragments were ‘locked‘ at the pole, due to dynein motor activity. Even though PEFs are acting on polar chromosomes, KT forces are dominant in bringing chromosomes to the pole via dynein and afterwards towards the equato-

rial plate via CENP-E. This functional hierarchy between motor proteins prevents premature PEF-mediated attachment stabilization of polar chromosomes (Barisic et al., 2014).

1.4 The Kinetochore

During mitosis, the interactions established between spindle MTs and chromosomes are mediated through proteinaceous structures called kinetochores (KT) (Figure 1.4 and Figure 1.5).

The KT is a macromolecular complex present at the centromeric region of chromosomes (Brinkley and Stubblefield, 1966; Rieder, 1982). The name “kinetochore” (movement place) was proposed by J. A. Moore (Sharp, 1934). Besides their key function in providing the attachment site for spindle MTs, KTs also control MT dynamics, SAC signaling and mitotic cell progression by representing the docking sites for proteins involved in these processes (reviewed in (Desai and Mitchison, 1997; Kline-Smith et al., 2005; Rieder and Salmon, 1998)). The importance of KTs during cell division is nicely emphasized by Daniel Mazia in 1961, referring to the KT as “the only essential part of the chromosome so far as mitosis is concerned” (Mazia, 1961). Although the number of characterized KT proteins is increasing, more than 100 proteins have been reported, organized in around 26 core subcomplexes (Petrovic et al., 2016). Early electron microscopy studies have described the KT as a trilayered disk structure, composed of inner and outer electron dense parts separated by a 20-30 nm low contrast gap. At the periphery of the outer KT lies the fibrous corona that extends 100-200 nm away, visible only in the absence of MTs (Brinkley and Stubblefield, 1966; Dong et al., 2007; Maiato et al., 2004a; Maiato et al., 2006) (Figure 1.9).

However, the observed trilaminar structure is the artifact produced by conventional fixations (buffered gluteraldehyde / osmium protocols). In improved forms of fixation, in which specimens are prepared with rapid freezing followed by freeze substitution, trilayered KT is not detected and KTs appear as fibrilar mat-like structures. KT region is recognized by clear zone that excludes ribosomes and other cytoplasmic products (McEwen et al., 1998b) (Figure 1.9).

1.4.1 The centromere

The centromere is a specialized chromatin locus required for KT assembly. Initially, it was described as a primary constriction on condensed chromosomes, which connects chromosomes to spindle MTs (McKinley and Cheeseman, 2016; Rieder, 1982). Centromeres of the nematode *Caenorhabditis elegans*, some insects and lower plants, extend along the length

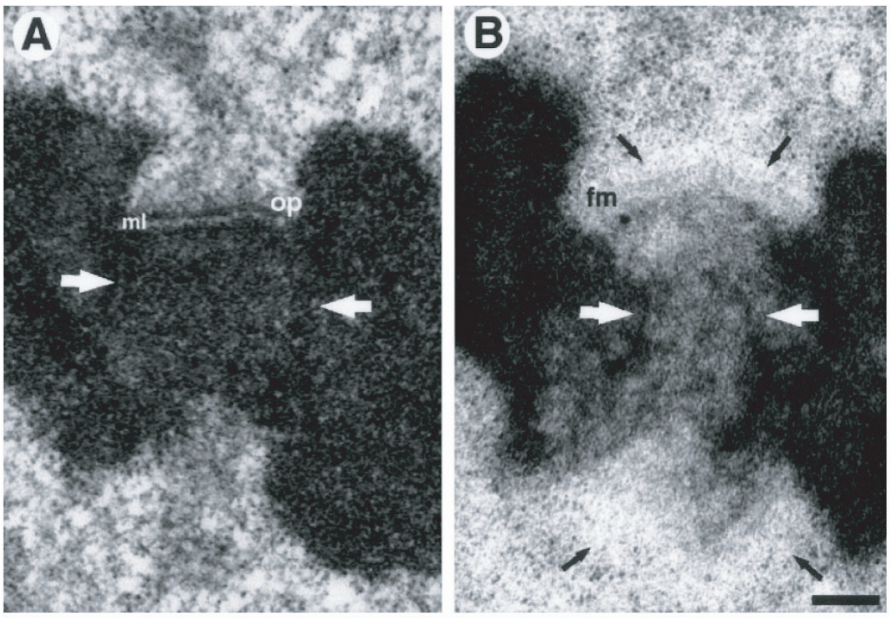

Figure 1.9: **KT ultrastructure of PtK1 cells obtained by electron microscopy**. (A) Trilaminar structure of KT obtained after conventional gluteraldehyde fixation. (B) KT prepared via rapid freezing followed by freeze substitution have fibrous mat like structure. The corona region is clear and does not contain ribosomes and other cytoplasmic products. Image adapted from (McEwen et al., 1998b).

of entire chromosome defined as holocentric centromere (Maddox et al., 2004; Marques and Pedrosa-Harand, 2016). In contrast, other species contain spatially restricted centromeres named as monocentric centromeres. The position of the point centromeres characterizes the chromosomal morphology. Thus, telocentric centromeres are present in the telomere region of the chromosome. Metacentric centromeres equally divide chromosome arms, and centromeres, that divide chromosomes into smaller and larger arms, are named as acrocentric centromeres (Rieder, 1982).

1.4.2 CENP-A

Centromere position is epigenetically defined by the histone H3 variant histone, centromere protein A (CENP-A in humans) (Palmer et al., 1991; Palmer et al., 1987). CENP-A was discovered in 1985 in the experiments using serum from CREST (calcinosis, Raynaud phenomenon, esophageal dysmotility, sclerodactily and telangiectasia) patients (Earnshaw and Rothfield, 1985; Valdivia and Brinkley, 1985). The antibodies from the serum recognize three different bands in the immunobloting experiments and centromere region on the chromosomes after Immunofluorescence. The detected three bands were identified as centromere proteins: CENP-A, CENP-B, and CENP-C (Earnshaw et al., 1986). In contrast to other histones,at the amino acid levels CENP-A is poorly conserved, with homologues found in

all eukaryotic systems: Cid (centromere identifier) in *Drosophila melanogaster* (Blower and Karpen, 2001), Cse4 in *Saccharomyces cerevisiae* (Buchwitz et al., 1999), CenH3 in *Arabidopsis thaliana* (Cooper and Henikoff, 2004). Although CENP-A molecules can be distributed all over the chromatin, the centromeric region shows ~50% enrichment in CENP-A per unit of DNA. It has been reported that typical centromeres of human RPE1 cells contain 400 CENP-A molecules (Bodor et al., 2014). Together with H4, H2A and H2B, CENP-A forms nucleosome core particles that serve as a docking site for downstream complexes involved in the formation of KT (Fachinetti et al., 2013; Hori et al., 2013; Nakano et al., 2008).

Although centromere regions are characterized by specific repetitive DNA sequences, except for *S. cerevisiae* (Spencer and Hieter, 1992), DNA sequence is neither necessary nor sufficient for proper centromere positioning (reviewed in (De Rop et al., 2012; Musacchio and Desai, 2017). The DNA sequence and size of the centromere vary between species. In *Drosophila melanogaster*, centromeres occupy up to 420 kbp repetitive satellite sequences (Murphy and Karpen, 1995). In human cells, this area is characterized by the tandem A/T repeats, 171 bp long, α satellites, ranging from 1 to 5 Mbp (Manuelidis, 1978; Murphy and Karpen, 1998; Willard, 1985). Interestingly, in human cells, centromere size varies between different chromosomes. One of the evidence that centromere identity does not depend on DNA sequence is found in neocentromeres (du Sart et al., 1997). Neocentromeres, discovered in human cells do not contain α satellites, but contain CENP-A and, thus, are able to assemble KTs. Moreover, α satellite DNA present at the non- centromeric loci (inactive centromere) cannot initiate formation of a functional KT (du Sart et al., 1997). Due to the repetitive DNA nature, centromeres play an important role in chromosomal evolution (Murphy and Karpen, 1998). Chromosomal breakpoint regions, involved in chromosomal rearrangements during evolution, are enriched in centromeres (Murphy et al., 2005). Moreover, fusions and fission processes in the centromere regions can lead to differences in karyotype between species that contain a similar DNA sequence (Murphy et al., 2005).

In contrast to other histones, whose recruitment to chromatin occurs during DNA replication, CENP-A recruitment to centromere is cell cycle controlled and concurrent with mitotic exit and G1 phase (Jansen et al., 2007; Silva et al., 2012). During S phase, previously incorporated CENP-A molecules are distributed between two sister chromatids. The formed gaps are completed with H3.3 histone (Bodor et al., 2013; Dunleavy et al., 2011). Snap-tag based experiments have shown that CENP-A loading and assembly is controlled by Cdk1 and Cdk2 kinase activity. At mitotic exit, low Cdk1 and Cdk2 levels trigger CENP-A assembly (Silva et al., 2012). Moreover, inhibition of Cdk1 and Cdk2 in G2 or S phase by small molecule

inhibitors results in stable CENP-A assembly during these phases (Silva et al., 2012). Centromere incorporation of CENP-A requires the activity of the histone chaperones, Mis 18 complex and HJURP (Dunleavy et al., 2009; Foltz et al., 2009; Nardi et al., 2016). The Mis 18 complex bound to Mis 18 binding protein 1 (Mis18BP1 also known as Knl2) recognizes the existing CENP-A molecules and recruits HJURP specifically bound to pre-nucleosomal CENP-A (Bernad et al., 2011; Dunleavy et al., 2009; Foltz et al., 2009; Maddox et al., 2007).

1.4.3 CENP-B

In contrast to CENP-A, whose localization to centromere does not depend on DNA sequence, another member of the centromere protein family, CENP-B, binds to the centromere through recognition of a specific 17 bp sequence inside α satellite region known as CENP-B box (Masumoto et al., 1989). Apart from the Y chromosome, all chromosomes contain a CENP-B box at their centromeric region (Earnshaw et al., 1989; Fachinetti et al., 2015; Miga et al., 2014). CENP-B is also absent from neo-centromeres. Interestingly, deletion of CENP-B in mice does not affect viability (Hudson et al., 1998; Kapoor et al., 1998). Co-depletion of CENP-A and CENP-B leads to chromosome missegregation and cell lethality due to rapid disassembly of downstream KT components (Hoffmann et al., 2016).

1.4.4 Inner KT

The CENP-A nucleosome functions as a docking site for the Constitutive Centromere Associated Network (CCAN), divided into several subcomplexes: (CENP-NL), CENP-HIKM, CENP-TW, CENP-SX and CENP-OPQRU (McKinley et al., 2015; Suzuki et al., 2014) (Figure 1.10). Proteins of the CENP-NL complex and CENP-C interact directly with CENP-A (Falk et al., 2015; Orr and Sunkel, 2011; Petrovic et al., 2016). Moreover, CENP-C is involved in direct binding to the Mis-12 complex, in the outer KT (Klare et al., 2015; Petrovic et al., 2016; Suzuki et al., 2014) (Figure 8). In *Drosophila* cells, except from CENP-C, other members of CCAN complex have not been identified (Erhardt et al., 2008).

1.4.5 Outer KT

The outer KT is involved in the establishment of the direct contacts with spindle MTs, but also functions as a docking site for SAC proteins, some motor proteins (CENP-E, dynein) (Thrower et al., 1996; Yang et al., 2007), plus-end MT binding proteins (CLASPs, CLIP-170, EB1, APC) (Maiato et al., 2005; Maiato et al., 2004b), and MT depolymerizing kinesins (MCAK) (Kline-Smith et al., 2004) (Figure 1.10).

Unlike constitutive centromere proteins that are present at the KT throughout the cell cycle, outer KT proteins are assembled at prophase and removed during the course of mitosis (e.g. SAC proteins). A key component of the outer KT is the KMN network, the core MT binding site, composed of 10-subunits that are part of Knl1, Mis12 and Ndc80 sub complexes. Importantly, the KMN network is conserved in eukaryotes and plays a crucial role in KT-MT interactions (Cheeseman et al., 2006; Kline-Smith et al., 2005) (Figure 1.10).

The Knl1 complex (Knl1 and Zwint) is the largest component of the outer KT involved in mitotic checkpoint control through binding of the SAC proteins through multiple protein docking sites, like Met-Glu-Leu-Thr (MELT) repeats. Together with other members of the KMN complex, Knl1 is involved in MT binding. Its MT binding affinity is regulated by Aurora B phosphorylation (Liu et al., 2009; Welburn et al., 2010). In the absence of attachments, when inter-KT tension is low, phosphorylation levels of Knl1 are increased, which decreases its MT binding affinity. Thus, detection of phosphorylation status of pKnl1 with specific antibodies serves as readout for the tension inside KT (Welburn et al., 2010).

In humans, the Mis12 complex contains four subunits Mis12, Pmf1, Nsl1, and Dsn1. It connects the inner and the outer KT by interacting with CENP-C at one side and Spc24 and Spc25, components of the Ndc80 complex, on the other side (Petrovic et al., 2016; Przewloka et al., 2011; Screpanti et al., 2011) (Figure 1.10). Previous studies have shown that RNAi mediated depletion of the Mis12 complex compromises KT assembly (Feijao et al., 2013).

The Ndc80 complex is composed of four subunits: Ndc80 (Hec1 in humans), Nuf2, Spc24 and Spc 25, and it is conserved from fungi to humans. The dumbbell shaped elongated calponin-homology (CH) domains of Nuf2 and Ndc80 subunits are involved in direct binding of spindle MTs (DeLuca et al., 2006). Depletion of members of the Ndc80 complex abolishes the formation of end-on KT - MT attachments during mitosis (DeLuca et al., 2005; DeLuca et al., 2002; McCleland et al., 2003; McCleland et al., 2004; Miller et al., 2008) (Figure 1.10).

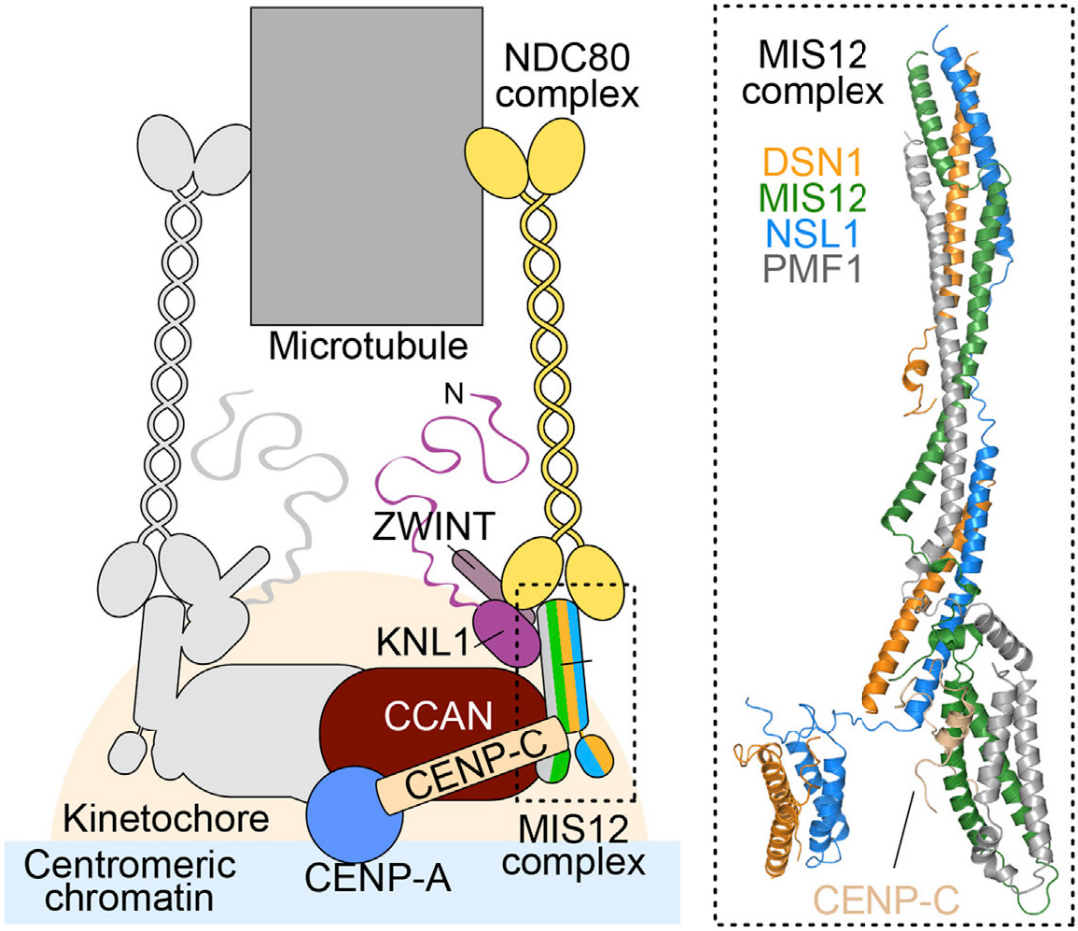

Figure 1.10: **KT structure**. The KT is a proteinaceous structure assembled on the primary chromosomal constrictions –centromeres. CENP-A molecules represent an epigenetic mark for KT assembly. Members of the CCAN complex constitute the inner KT. Connections between the inner and the outer KT are established through a long CENP-C molecule that interacts with both CENP-A (centromere) and Mis12 (outer KT). On the other side Mis12 establishes interactions with the dumbbell shaped Ndc80 complex, crucial for end-on MT binding. Besides Ndc80 and Mis12, the KMN network includes Knl1, important for the recruitment of SAC proteins and binding of the RZZ complex that through interaction with Spindly binds dynein motor protein. Image adapted from (Petrovic et al 216, Cell).

The MT binding affinity of the Ndc80/ Hec1 N-terminal tale is regulated by multiple phosphorylations by the inner centromere Aurora B kinase. Microinjection of PtK1 cells with the antibody (9G3) against the N-terminal region of Hec1 results in an increase in merotelic attachments, chromosome missegregation and a decrease in MT dynamics (DeLuca et al., 2006). Moreover, a non-phosphorylatable mutant Hec1-9A has high affinity for MTs, causing the formation of hyper-stable KT-MT attachments (DeLuca et al., 2006; Guimaraes et al., 2008). By phosphorylating Hec1 at the Ser 4, Ser 5, Ser 8, Ser 15, Ser 44, T 49, Ser 55, Ser 62 and Ser 69 at N-terminal regions, Aurora B decreases the affinity of the Ndc80

complex to incorrectly attached MTs allowing reformation of correct amphitelic attachments (Cheeseman et al., 2006; DeLuca et al., 2011; Nousiainen et al., 2006; Zaytsev et al., 2015).

1.4.6 KT - MT attachments

KTs are dynamic structures that change when encountering MTs during mitosis (Hoffman et al., 2001; Thrower et al., 1996). The initial attachments between KTs and MTs are established soon after NEB.

According to the “search and capture” (S&C) model, interactions between KTs and MTs are established due to constant MT growth and shrinkage. Dynamic MTs are exploring (“searching”) different directions and once they encounter (“capture”) a KT they establish attachments that are selectively stabilized (Kirschner and Mitchison, 1986). However, probing the entire mitotic cytoplasm would take too much time and thus cannot explain the short mitotic timing (40 min in HeLa cells) (Wollman et al., 2005). Thus, it has been proposed that favored position of the chromosomes during prometaphase facilitates the interaction between KTs and MTs of the nascent spindle. After NEB chromosomes are distributed around the zone of the nascent spindle that makes them more visible for the newly formed MTs and facilitates spindle assembly (Magidson et al., 2011).

Considering the S&C model, larger KTs would increase the probability of interactions with MTs. Yet, higher visibility of KTs could also lead to the formation of erroneous attachments. Changes in KT structure allow fast capture by MTs and decrease the possibility of error formation. Soon after NEB, the KT outer layer expands, facilitating MT capture. However, after initial attachments are established, the KT outer layer suffers compaction and rotation, reducing the possibility of establishment of erroneous attachments (Magidson et al., 2015).

Despite changes in KT structure upon MT attachments, erroneous attachments are formed during the course of mitosis and require other mechanisms to be corrected.

1.5 Error correction

Before establishing correct amphitelic attachments, sister KTs can bind to MT coming from the same pole (syntelic attachment) or one of the sister KTs can be attached to both poles (merotelic attachment) (reviewed in (Heald and Khodjakov, 2015) (Figure 1.11). In correct bi-oriented KTs pulling forces coming from opposite poles result in the formation of inter-KT tension between sister KTs. Incorrect syntelic or mono-oriented (attachment to one pole) attachments are destabilized due to the loss of tension, which provides a new possibility to

bi-orient (reviewed in (Godek et al., 2015). In the case of merotelic attachments, one of the sister KTs is simultaneously attached to both spindle poles. Since other sister KT establishes attachment with opposite pole, such bi-orientation in merotelic attachments creates the tension that can be overlooked by the error correction machinery and mitotic checkpoint (Figure 1.11). Erroneously attached sister will create lagging chromosomes during anaphase that can lead to aneuploidy and chromosomal instability (CIN) during cell division. However, when the ratio between MTs coming from opposite poles is unequal, an anaphase correction mechanism can prevent potential segregation errors (Cimini, 2008; Cimini et al., 2004; Cimini et al., 2001).

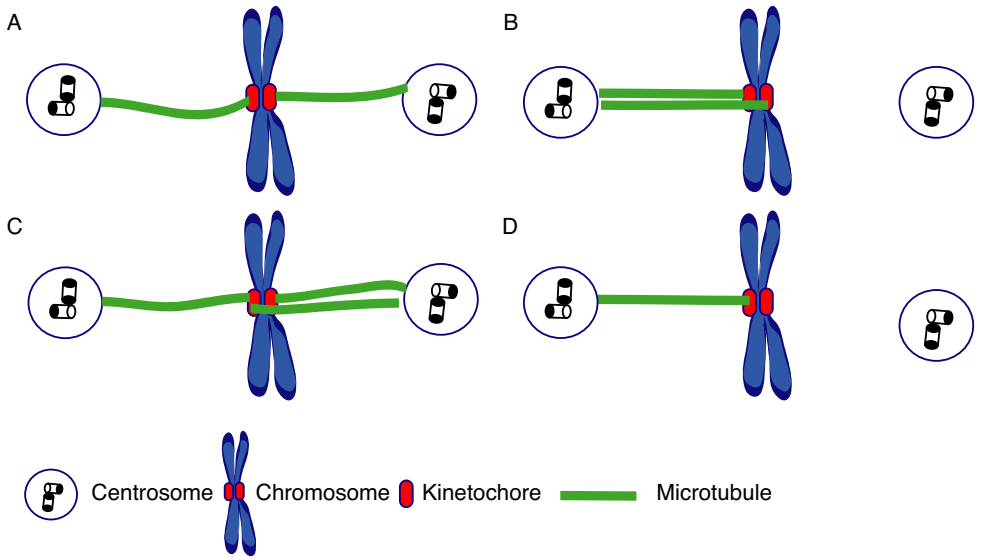

Figure 1.11: **Types of KT-MT attachments.** (A) amphitelic, bi-oriented - both sister KTs are attached to opposite poles; (B) synthelic - both sister KTs attached to the same pole; (C) merotelic - one sister KT attached to both poles; (D) monooriented - only one sister KT attached to one of the poles.

Due to the importance of correct genome division, many proteins are involved in the control of proper KT-MT interactions. The next paragraphs will focus on proteins that regulate inter-KT tension and MT dynamics, two aspects crucial for the establishment and correction of KT-MT attachments.

1.5.1 Chromosomal Passenger Complex (CPC)

Inter-KT tension is sensed by the Aurora B kinase, a catalytic subunit of the Chromosomal Passenger Complex (CPC) (Liu et al., 2009) (Figure 1.12). Besides Aurora B as an enzymatic member of the complex, the CPC contains also Borealin (Dasra), INCENP and Survivin, as regulatory members that direct localization of Aurora B. By changing its location during mitosis, the CPC is involved in the regulation of different aspects of cell division

(reviewed in (Lampson and Cheeseman, 2011; Ruchaud et al., 2007). At the beginning of mitosis, the CPC is present at chromosome arms, where it controls spindle assembly (Maresca et al., 2009; Tseng et al., 2010). As cells progress into metaphase, the CPC localizes to the inner centromere where it plays an important role in error correction (Kelly et al., 2010). At anaphase onset the CPC localizes to the spindle midzone, controlling cytokinesis (Giet and Glover, 2001; Lewellyn et al., 2011; Zhu et al., 2005a). Centromere localization of the CPC depends in the members involved in chromatin binding (Survavin, Borealin and the N-terminal region of INCEP) (Kelly et al., 2010) that recognizes the H3T3ph, phosphorylated by the small Haspin kinase. Depletion of Haspin by RNA interference or microinjection with an H3T3ph specific antibody results in CPC delocalization from the centromere (Kelly et al., 2010; Wang et al., 2010). In fission yeast, centromere localization of CPC is controlled by Cdk1 (cdc2) mediated phosphorylation of Survivin. In human cells Borealin has a comparable role. Cdk1 mediated phosphorylation promotes CPC binding to Shugoshin, which recognizes the H2A histone previously phosphorylated by Bub1 kinase (Tsukahara et al., 2010). Interestingly, the CPC complex is also involved in Shugoshin localization at the centromere (Dai et al., 2006; Resnick et al., 2006). Centromeric localization of the CPC complex allows Aurora B to sense and regulate MT attachment status (Kallio et al., 2002)(Figure 1.12).

1.5.1.1 Aurora kinase family

The Aurora kinase family belongs to serine/threonine protein kinases that phosphorylate substrates at an (RK) x (TS) x (ILV) consensus sequence (Cheeseman et al., 2002). In budding yeast, where it was originally identified in a screen for chromosome-gain or increase-in-ploidy mutants, Aurora kinase family contains only one member Ipl1 (increase in ploidy 1) (Chan and Botstein, 1993). In higher eukaryotes, three genes encode for Aurora A, B and C kinases (reviewed in (Vader and Lens, 2008). Although Aurora kinases share similar sequence identity and substrate phosphorylation sites, they are localized in different cellular compartments. Aurora B is present at the inner- centromere and is important for the phosphorylation of substrates present at the KTs (Liu et al., 2009) (Figure 1.12). Aurora A localizes at centrosomes and besides its role in promoting centrosome maturation, pole separation and spindle assembly (Tsai and Zheng, 2005), it mediates correction of aberrant attachments in the vicinity of poles (Barisic et al., 2014; Barisic and Maiato, 2015; Chmatal et al., 2015; Ye et al., 2015) that could be stabilized due to high PEFs on chromosome arms (Cane et al., 2013). At anaphase onset, Aurora A is degraded, allowing chromosome segregation during anaphase.

The phosphorylation status of Aurora B substrates depends on their distance from the kinase (Liu et al., 2009) (Figure 1.12). Biosensors positioned at the inner centromere are constantly phosphorylated even in the presence of tension. However, delocalizing the same sensor to the outer KT will result in dephosphorylation (Liu et al., 2009). Moreover, targeting Aurora B to the outer KT through Mis12 - INCEP expression in HeLa cells leads to constant phosphorylation of outer KT substrates and KT-MT destabilization (Caldas et al., 2015). Thus at metaphase, when KTs are bi-oriented, pulling forces from the MTs separate outer KT proteins away from the phosphorylation gradient, stabilizing the attachments (Figure 1.12).

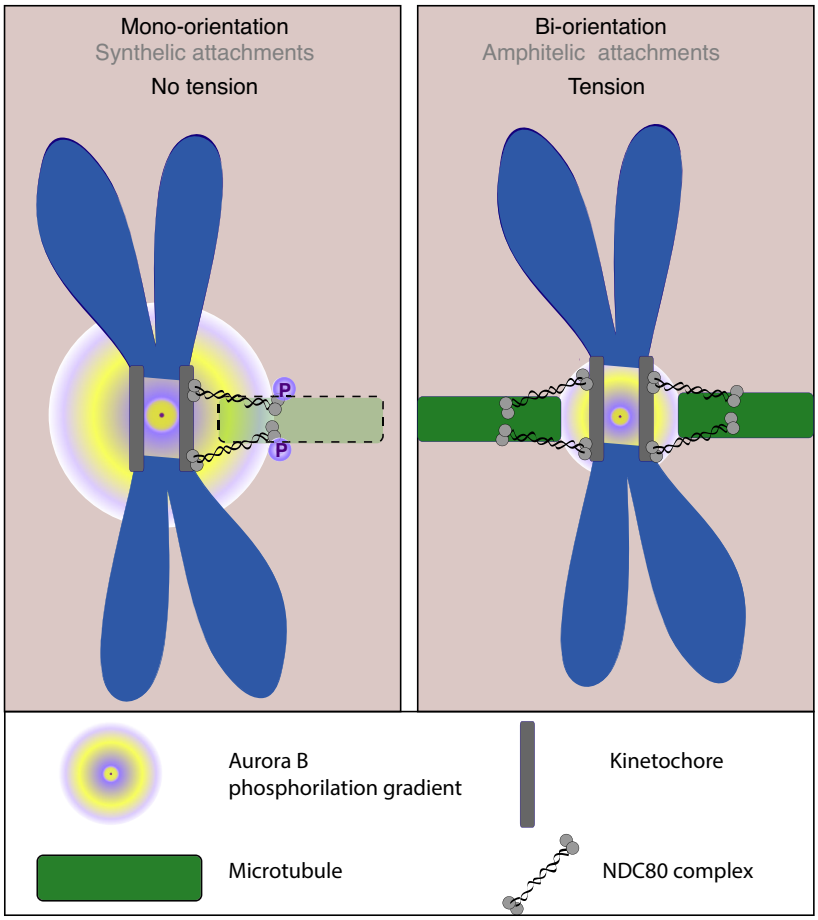

Figure 1.12: **Aurora B kinase regulates KT-MT attachment status**. Aurora B kinase localizes at the inner centromere and regulates KT-MT attachment status through phosphorylation of its substrates at the outer KT. In the left panel, when one (mono-orientation) or both KTs (synthelic attachments) are attached to one pole, the absence of tension between sister KTs brings Aurora B substrates present at the outer KT (KMN network) closer to its phosphorylation gradient. Phosphorylation of the components involved in MT attachment reduces their affinity for MTs and destabilizes the attachment. In the right panel, both sister KTs are attached to opposite spindle poles, which create tension and physically separate the outer KT from phosphorylation activity of Aurora B, and thus attachment stabilization.

Moreover, in stretched KTs, mitotic phosphatases present in the outer KT region (PP1 and PP2A), additionally dephosphorylate the substrates and stabilize the attachments (Egloff et

al., 1997; Liu et al., 2010). At anaphase onset, Aurora B is displaced from centromere into the spindle mid-zone forming the phosphorylation gradient that allows the temporal and spatial control of chromosome separation (Afonso et al., 2014a; Afonso et al., 2014b).

1.5.2 The kinesin-13 family

The dynamic nature of spindle MTs plays an important role in error correction since hyper-stabilization of MTs results in an increased number of lagging chromosomes during anaphase (Bakhoum and Compton, 2012). The essential role in regulating MT end dynamics is performed by a class of depolymerizing kinesin-like proteins, which use their catalytic activities to alter MT dynamics (reviewed in (Manning et al., 2007; Walczak et al., 2013) (Figure 1.13).

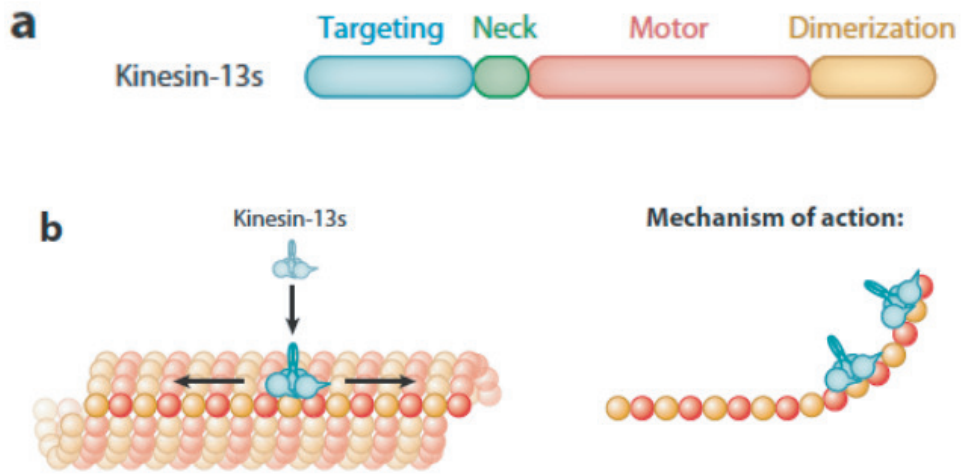

Figure 1.13: **Members of the kinesin-13 family depolymerize spindle MT ends**. (A) The most studied member of the family is MCAK. Its catalytic domain is positioned in the central region of the protein, between the dimerization domain and neck domain. Phosphorylation of the neck domain by Aurora B reduces overall affinity of MCAK for its substrates. (B) Once it binds to microtubules, kinesin-13s can diffuse in both directions. At MT ends, MCAK changes into the closed conformation, allowing tighter binding to the substrate and removal of tubulin dimers. Image adapted from (Walczak et al., 2013)

Members of the kinesin-13 family: Kif2a, Kif2b and Kif2c/MCAK, belong to the group of MT depolymerases (Figure 1.13). Due to their role in controlling MT dynamics, kinesin-13 proteins are involved in diverse functions in cells (Walczak et al., 2013). Importantly, during mitosis, they are implicated in controlling spindle assembly (Manning et al., 2007), error correction (Kline-Smith et al., 2004) and chromosome segregation (Maney et al., 1998). Their subcellular localization at spindle poles, KTs, MTs and in the cytoplasm is temporarily modulated through phosphorylation and protein - protein interactions (Lan et al., 2004; Moore et al., 2005).

The most studied member of the family, kif2C/MCAK (mitotic centromere-associated kinesin) has a catalytic domain, involved in MT and ATP binding, located in the central part of the molecule (Maney et al., 2001; Wordeman and Mitchison, 1995). The N-terminal domain is involved in sub-cellular targeting, whereas a dimerization C-terminal domain contributes to MT tip tracking, KT binding and MT lattice association (Maney et al., 2001). The positively charged neck domain, positioned between the N-terminal and the catalytical domain is crucial for MT depolymerization activity and MT end targeting (Figure 1.13). Moreover, MCAK depolymerization activity is controlled by Aurora B mediated phosphorylation at the S196, located in the neck domain (Andrews et al., 2004; Ems-McClung et al., 2013; Lan et al., 2004). By changing its conformational state through phosphorylation by Aurora B, MCAK reduces its overall affinity for its substrates. In contrast to Aurora B, another mitotic kinase, Plk1 has been reported to stimulate kinesin-13s activity (Hood et al., 2012; Jang et al., 2009; Zhang et al., 2011). Moreover, due to polar localization in mitotic cells, Kif2A activity is suppressed via Aurora A phosphorylation (Jang et al., 2009).

Although the role of Kif2A is more evident in neuronal processes (Silverman et al., 2010), it also functions in mitosis together with Kif2B and MCAK. Since kinesin 13s can depolymerize both MT plus and minus ends, they have a crucial role in chromosome segregation. Moreover, by depolymerizing MT minus ends at the pole, Kif2A plays an important role in the regulation of poleward MT flux (Cameron et al., 2006). Both Kif2A and Kif2B are reported to be required for bipolar spindle assembly since RNAi-induced knockdown of these proteins increases the number of monopolar spindles (Gaetz et al., 2006; Manning et al., 2007).

KT localization of MCAK together with Kif2B is of great importance in destabilizing erroneous attachments during prophase and metaphase. While Kif2B is present at KTs in early prometaphase, and is involved in error correction during this phase, MCAK activity is more relevant during metaphase (Bakhoum et al., 2009b). RNA interference mediated depletion of MCAK or Kif2B kinesins prevents correction of erroneous attachments after monastrol washout, an experimental procedure that increases the number of aberrant attachments (Bakhoum et al., 2009a; Bakhoum et al., 2009b; Kline-Smith et al., 2004; Lampson et al., 2004). In contrast, MCAK or Kif2B overexpression prevents not only erroneous attachments, but also abolishes chromosomal instability (CIN) in already aneuploid cancer cells (Bakhoum et al., 2009b).

1.6 Intra-KT tension

The main stimulus for the error correction machinery is the lack of tension in erroneous attachments (Liu et al., 2009; Vader et al., 2008; van der Horst and Lens, 2014; Nicklas and Koch, 1969). On bi-oriented KTs, the outer components are pulled away through interaction with spindle MTs, resulting in the formation of tension between two sisters KTs (inter-KT tension). Thus, formed tension removes Aurora B substrates present at the outer KT further away form the phosphorylation gradient resulting in the stabilization of the attachment (Lampson and Cheeseman, 2011; Liu et al., 2009; Suzuki et al., 2014) (Figure 1.12).

The importance of tension in mitotic progression was demonstrated by Bruce Nicklas in classic experiments in grasshopper spermatocytes, where pulling the KTs of bivalents with a micro needle resulted in KT-MT stabilization and mitotic progression (Nicklas and Koch, 1969). However, several groups have reported that a stretching occurring inside a single KT (intra-KT stretch) can be sufficient for SAC satisfaction even in the absence of inter- KT tension (Maresca and Salmon, 2009; Uchida et al., 2009). Due to the small size of KTs direct measurements of the stretch inside single KTs are very limiting. Thus, intra-KT distances are measured using single-molecule high-resolution colocalization (SHREC) methods and measured as the difference in distance between the centroids of the fluorescently labeled proteins of the inner and outer KT of both sister pairs, divided by two (**Delta**) (Churchman and Spudich, 2012; Dumont et al., 2012; Maresca and Salmon, 2009) (Figure 1.14).

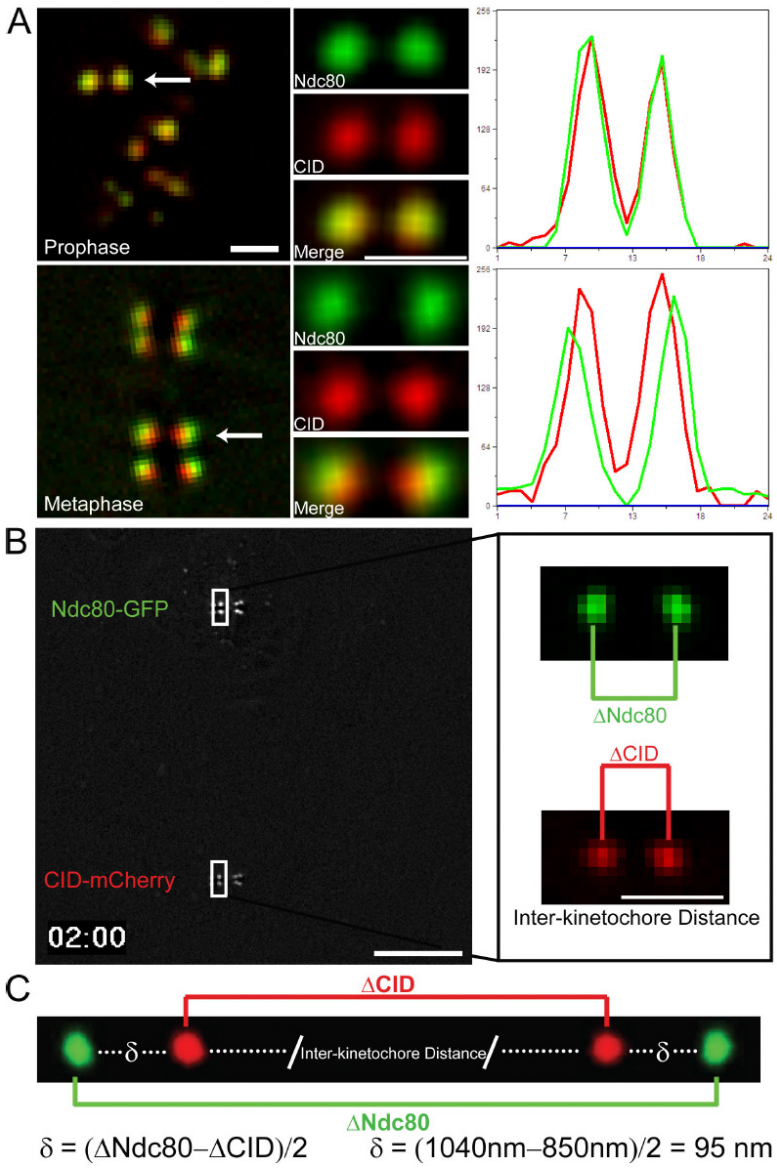

Figure 1.14: **K-tensiometar, of *Drosophila* S2 cells**. Fluorescent labeling of the components of the outer (green) and inner (red) KT used to measure **Delta** values. **Delta** values represent the difference between distance between green and distance between red centroids, divided by two. Image adapted from (Maresca and Salmon, 2009).

Both in human (HeLa) and *Drosophila melanogaster* S2 cells, upon treatments with drugs that interfere with MT dynamics (taxol and low nocodazole doses) and abolish MT induced inter-KT tension, intra-KT stretch was sufficient for SAC satisfaction (Maresca and Salmon, 2009; Uchida et al., 2009).

Nevertheless, the existence and the importance of intra-KT stretch and accuracy of its measurement is controversial (Magidson et al., 2016; Smith et al., 2016). Recent work has shown that human cells expressing a non-phosphorylatable mutant of Hec1 tail (9A-Hec1) can form hyper-stable attachments, which can satisfy the SAC even in the absence of substantial KT stretching (Etemad et al., 2015; Tauchman et al., 2015). However, in the afore-

mentioned reports, it was considered that KTs do not change morphology during mitosis. Magidson et al. have shown that supramolecular structural changes in KT architecture during mitosis can influence the **Delta** values (Magidson et al., 2016). Using correlative light and electron microscopy (CLEM) and super resolution microscopy (SIM) the authors have shown that when attachments are under full tension in metaphase, outer KT proteins are more focused and aligned in the direction of the K-fiber. However, upon nocodazole or taxol treatments, the outer proteins (Hec1 or Mis12) are more dispersed and positioned in different angles relative to K-Fibers (kTilt) or centromeres (cTilt). Furthermore, taxol treatment resulted in mitotic arrest only in cells that had unattached Mad2 positive KTs, emphasizing the importance of attachment over intra-KT tension in mitotic progression (Magidson et al., 2016). Additionally, chemical fixation during experimental procedures can affect **Delta** measurements, since an enlargement of the outer KT can be detected only after gluteraldehyde fixation but not in formaldehyde fixed cells (Magidson et al., 2016).

The interdependence between tension and attachment during mitosis represents the main difficulty in addressing their separate roles in SAC satisfaction. Considering the importance of this question, in Section 4.2 we will discuss how the SAC can be satisfied in the complete absence of inter-KT tension.

1.7 Chromosome congression and bi-orientation

Soon after NEB, chromosomes move toward the spindle equator, where they form amphitelic attachments and align. This migratory event is called chromosome congression (Darlington, 1937; Maiato et al., 2017). Congression away from the poles decreases the probability of erroneous attachments that would occur if chromosomes stay in proximity of one of the poles. Moreover, it allows efficient segregation during anaphase (Maiato et al., 2017).

Pioneering studies on chromosome congression proposed the “traction fiber” model according to which chromosomes are pulled towards the pole with the force that is proportional to the length of the K fiber (Hays and Salmon, 1990; Hays et al., 1982; Oestergren, 1945; Östergren, 1951). As a result of balance between opposing pulling forces on sister KTs chromosomes align at the metaphase plate (Hays and Salmon, 1990; Hays et al., 1982; Oestergren, 1945; Östergren, 1951). However, later studies demonstrated that pulling forces are produced at the KTs and do not depend on the length of the K fiber (Khodjakov and Rieder, 1996; McEwen et al., 1997; Skibbens et al., 1993). Moreover, it has been shown that KT position at the spindle equator is the balance between KT pulling forces and PEFs that act on the chromosome arms. At the beginning of mitosis when chromosome is attached to one

pole (mono-oriented), chromosome is pulled towards the attached pole. Due to higher MT density in the vicinity of the pole that create ejection forces on chromosome arms, mono-oriented chromosomes initiate their oscillatory movements, the process known as dynamic instability (Skibbens et al., 1993). Once chromosome becomes bi-oriented and both KTs are attached to opposite pole, the chromosome congress towards the spindle equator. During congression one sister KT is moved poleward (P) and another trailing sister exerts the away form the pole movement (AP). AP movement is the result of the pulling forces of the other P moving sister KT and ejection forces at the chromosome arms (Khodjakov and Rieder, 1996). Laser ablation of P moving sister KT on bi-oriented chromosomes cause AP moving sister KT to stop and shift the movement towards the pole (Khodjakov and Rieder, 1996).

Moreover, it has been shown that the process of chromosome alignment at the spindle equator is not equal between all chromosomes. Therefore there are two main pathways proposed for chromosome congression. The first named “direct congression” pathway, considers the initial favorable position of the chromosomes between two poles. These chromosomes attach MTs coming from both poles, which results in “direct” bi-orientation and subsequent alignment at the metaphase plate. The second, “peripheral congression” pathway relies on the activity of motor proteins in the alignment of chromosomes that were positioned at the periphery of the poles prior to NEB (Maiato et al., 2017). Although it is clear that chromosome position prior to NEB biases the pathway of chromosome congression, it is still unknown if this bias is chromosome specific. Moreover, if there is a specific chromosome bias towards the congression pathway it remains unclear which chromosome properties drive the preference for one pathway of congression over the other (Figure 1.15).

Important modulators of MT dynamics are also MT depolymerizes of kinesin-13 and kinesin-8 family bound to MT ends (Walczak et al., 2013). While members of kinesin-13 family play important role in error correction (Bakhoum and Compton, 2012; Bakhoum et al., 2009a; Bakhoum et al., 2009b), member of kinesin-8 family, Kif18A is essential for chromosome congression (Mayr et al., 2007; Ye et al., 2011). Kif18A is a motile MT depolymerase with plus-end directed motility. In human cells lacking Kif18A, upon RNAi mediated depletion, chromosomes move in reduced speed and fail to align at the metaphase plate (Mayr et al., 2007) (Figure 1.15).

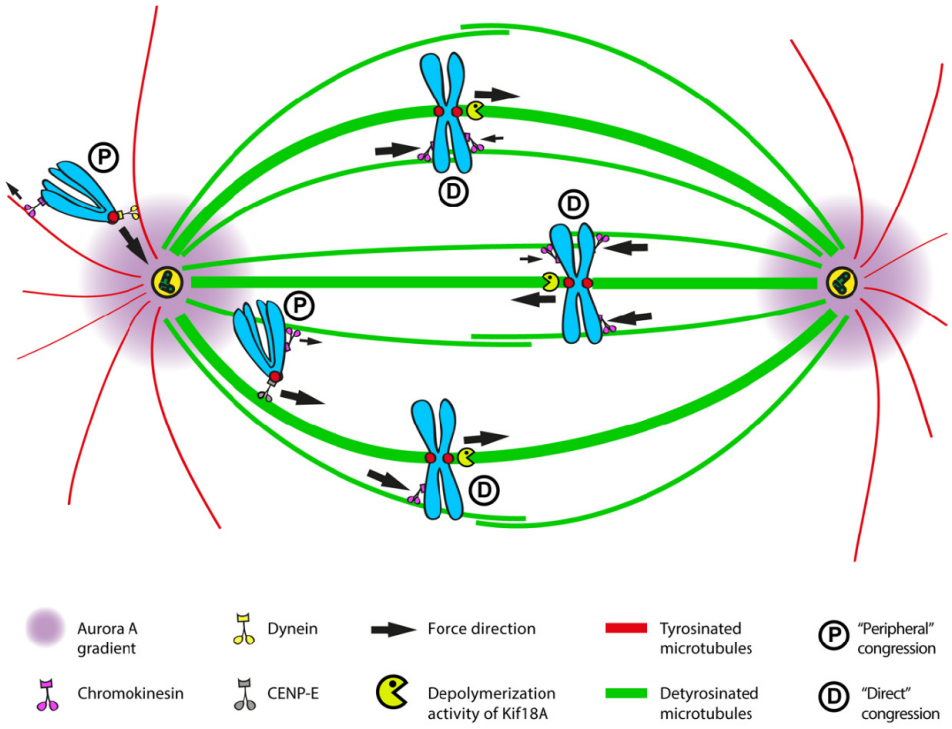

Figure 1.15: **Mechanisms of chromosome congression**. Chromosome alignment at the metaphase plate is result of MT dynamics and coordinated activity of motor proteins. For more details consult the section 1.7 . Image adapted from (Maiato et al., 2017)

Elegant studies have shown that coordinated activity between motor proteins present at the chromosome arms and KTs drives chromosome congression towards the spindle equator (Barisic et al., 2014; Barisic and Maiato, 2015). Perturbation of motor function by small molecule inhibitors and laser microsurgery has shown the dominance of KTs over chromosome arms in chromosome movement. Laser ablated chromosome arms were not able to move in a directed fashion and were randomly ejected towards the cell cortex. However, KT containing fragments were able to align at the metaphase plate (Barisic et al., 2014). During unperturbed mitosis, peripherally positioned chromosomes are moved towards the pole by dynein motor activity (Barisic and Maiato, 2015). By bringing chromosomes closer to polar region allows Aurora A mediated destabilization of premature KT-MT attachments that otherwise would be stabilized due to PEFs (Cane et al., 2013; Ye et al., 2015). At the pole, CENP-E processivity counteracts dynein-mediated poleward motion, resulting in chromosome congression towards the equator plate (Barisic et al., 2014; Kim et al., 2008). As CENP-E moves chromosomes away form the pole the chance for biorientation increases. Additionally chromokinesin mediated PEFs contribute to the formation and stabilization of the attachments (Cane et al., 2013) (Figure 1.15).

The activity of motor proteins involved in chromosome congression is regulated by their PTMs like phosphorylation, sumoylation and fornesylation (Ashar et al., 2000; Kim et al., 2010; Zhang et al., 2008). An Aurora A phosphorylation gradient provides spatial control of motor proteins involved in chromosome congression. Phosphorylation of CENP-E at the conserved T422 site reduces its affinity for MTs (Kim et al., 2010). As CENP-E approaches the spindle equator and Aurora A gradient decreases, dephosphorylation of T422 by PP1 phosphatases allows chromosome bi-orientation (Kim et al., 2010) (Figure 1.15).

Additionally, tubulin PTMs represent spatial cues required for proper directionality of motor proteins during chromosome congression, so called “tubulin code” (Janke, 2014). Distinct populations of MTs inside the mitotic spindle undergo different PTMs. For instance, unstable astral MTs are tyrosinated comparing with more stable K- fibers that lack the last tyrosine at the C-terminal region of α tubulin, and therefore are detyrosinated (Gundersen et al., 1984). Importantly it has been shown that the affinity of motor proteins towards certain MT populations is defined by PTMs (Barisic et al., 2015; Sirajuddin et al., 2014). Combination of such PTMs inside the mitotic spindle functions as a navigation system for motor proteins (Barisic et al., 2015). Recent studies demonstrated that CENP-E shows high preference towards the stable detyrosinated MTs, which biases chromosome congression towards the spindle equator (Figure 1.15).

Chapter 2

Objectives

Correct chromosome attachment to opposite spindle poles is the prerequisite for mitotic fidelity. The main goal of this thesis was to understand the mechanisms involved in chromosome bi-orientation and chromosome segregation fidelity.

In particular we aimed at addressing two main questions:

1. How are the initial attachments stabilized prior to bi-orientation and the establishment of tension?

2. What is the role of KT size in chromosome congression and error formation?

To address these questions we used two model systems- *Drosophila* S2 cells undergoing mitosis with unreplicated genomes (SMUGs) and immortalized Indian muntjac (IM) fibroblasts.

Chapter 3

Model systems

3.1 Mitosis with unreplicated genomes (MUGs)

Mitosis with unreplicated genome (MUG) is an unusual phenomenon during which cells enter the division process without previous replication of the genetic material (O'Connell et al., 2008; Wise and Brinkley, 1997; Zinkowski et al., 1989). Normal cell cycle progression into mitosis requires complete and correct replication of the genome in S phase. Any mistake or damage that can result in stalk in replication fork will be detected by the DNA damage checkpoint which initiates a cascade that prohibits cells to proceed into mitosis (Arellano and Moreno, 1997; Vermeulen et al., 2003). However, experimental treatments with hydroxyurea (HU) and caffeine in mammalian cells lead cells into MUG (O'Connell et al., 2008; Wise and Brinkley, 1997). HU is a potent inhibitor of ribonucleotide reductase (RNR) and by decreasing available dNTPs at the replication fork, it inhibits DNA replication in diverse cells (Koc et al., 2004). Therefore, HU treatment induce replication arrest. Caffeine treatments are known to override DNA - damage induced cell cycle arrest through stabilization of Cdc25 phosphatases and, thus, activation of Cdk1 and Cdk2 required for mitotic entry (Alao et al., 2014; Furnari et al., 1997; Hoffmann and Karsenti, 1994).

Mammalian Hela or Chinese hamster ovary cells (CHO) undergoing MUG enter mitosis with uncondensed chromatin scattered at the spindle periphery during all course of cell division (Brinkley et al., 1988; O'Connell et al., 2008; Wise and Brinkley, 1997). Interestingly, KTs of CHO, Chinese muntjac (CM) and IM cells undergo intensive fragmentation into small centromere-KT fragments (CFKs) that detach from the chromatin and can bind MTs and align at the metaphase plate during MUGs (Wise and Brinkley, 1997; Zinkowski et al., 1989; Zinkowski et al., 1991). Moreover, SAC and motor proteins localize properly on CFKs and KTs during MUGs (Johnson et al., 2008; O'Connell et al., 2008). Although assembling

a normal spindle, these cells do not go through anaphase B (Brinkley et al., 1988; Wise and Brinkley, 1997). Mitotic progression is delayed in MUGs, with the presence of improper attachments (monotelic, merotelic or lateral). However, chromosomes eventually align at the spindle equator and cells proceeded into anaphase, after satisfying the SAC (Brinkley et al., 1988; O'Connell et al., 2008). Even though MUGs were extensively explored for addressing the role of tension and attachment in SAC satisfaction, chromatid decondensation and KT defragmentation represent a limitation of this model system to study the role of chromosome arms in the process.

MUGs in *Drosophila* S2 cells (SMUGs) can be obtained by depletion of the 'Double parked' (Dup) protein. Dup is an origin of replication protein, important for two processes during the cell cycle: initiation of DNA replication and post-replication checkpoint, which controls the transition from G2 phase to mitosis (Whittaker et al., 2000). In contrast to mammalian cells, SMUGs enter mitosis with chromatin condensed into single chromatids scattered over the mitotic spindle. Moreover, KT fragmentation was not detected in SMUGs. Thus, SMUGs represent a good model system for studying the role of tension in single KTs within their native chromatid context.

3.2 Indian muntjac

IM (*Muntiacus muntjac vaginalis*) commonly named as a barking deer, is the mammal with the lowest known chromosome number (2n=6 for female, 2n=7 for male) (Cheng et al., 2009; Wurster and Benirschke, 1970).

Members of the *Genus Muntiacus* (Family Cervidae) are characterized by high variability of chromosome number and represent a good model for studies of karyotype evolution and speciation (Yang et al., 1997). In addition to IM as a member with the lowest diploid number, other two members, the Black muntjac (*M. crinifrous*) and the Gongshan muntjac (*M. gongshanesis*) contain 2n=8 (female) and 2n=9 (male) chromosomes. Moreover the Fea's muntjac (*M. feae*) has a diploid number of 13 and 14 chromosomes (female and male respectively) (Yang et al., 1997). Finally the Chinese muntjac (CM) (*Muntjacus reevesi*) is the member with the highest diploid chromosome number 2n=46 inside the *Muntiacus Genus* (Lin et al., 1991; Murmann et al., 2008). The reason for such a variability in chromosome number lies in repeated tandem fusions from an ancestral genome, 2n=70. It has been suggested that the karyotype of CM has evolved from 17 tandem and 3 centromeric fusion events (Yang et al., 1997). Furthermore, head-to tail (centromere-telomere) fusions were suggested to lead to exceptionally small number of chromosomes reported in IM cells. Hybridization probes

specific for centromeric region, isolated from DNA of female CM cells, after hybridization in IM cells apart from centromere also hybridized with IM chromosome arms. This indicated the existence of remnants of centromeric heterochromatin from ancestral CM chromosomes in IM chromosomes (Lin et al., 1991). Despite the difference in KT size during mitosis, interphase nuclear staining with CREST sera, gave similar bead like patterns in both IM and CM cells. Additionally, total fluorescence intensity of pre-KTs in interphase nuclei does not differ between two species. Hence it has been proposed that the observed non - random clustering of pre-KTs, led to linear tandem fusions during evolution resulting in a decreased number of chromosomes (Brinkley et al., 1984).

Tandem DNA fusions from an ancestral genome, resulted in changes in chromosome number and size, but preserved genome content between the different species (Brinkley et al., 1984; Chi et al., 2005; Johnston et al., 1982; Lin et al., 1991; Murmann et al., 2008; Wurster and Benirschke, 1967; Yang et al., 1997). As a result IM and CM species are phenotypically very similar and can be bred, giving live but sterile offspring (Liming and Pathak, 1981). Since a similar genome content in these two species is packed into a different number of chromosomes it makes them an excellent model for studies of spindle assembly and other processes that might be influenced by the chromosome number.

As a result of tandem fusions during evolution, KTs of IM cells are large; compound structures, composed of subunits that form a bead like structure that can bind up to 100 MTs (Brinkley et al., 1984; Zinkowski et al., 1991). The low number of chromosomes and their big size represent a unique advantage for micromanipulation and high-resolution live-cell studies. Despite that the IM KT has been well characterized at the structural and ultra-structural level (Comings and Okada, 1971; Zinkowski et al., 1991), little is known about the dynamic properties of KT - MT attachments to these compound structures and how this relates with error correction and SAC satisfaction. In Section 4.3, we will discuss the role of KT size in chromosome bi-orientation and investigate the impact on error correction and chromosome segregation fidelity using IM cells as a model system.

Chapter 4

Experimental work

4.1 Experimental work I

Selective tracking of template DNA strands after induction of mitosis with unreplicated genomes in *Drosophila* S2 cells (SMUGs)

(Published in Chromosome Reasearch, 2013 May; 21(3): 329-37)

4.1.1 Introduction

Correct segregation of the genetic material into daughter cells during mitosis depends on previously completed replication of DNA during S phase. In 1975, John Cairns (Cairns, 1975), based on previous reports of non-random segregation of sister chromatids in mammalian cells (Lark et al., 1966), proposed the “immortal strand” hypothesis according to which stem cells would retain template DNA strands, whereas newly synthesized DNA replicas would segregate into differentiated daughter cells. By keeping template strands, stem cells would avoid the accumulation of mutations that can occur during DNA replication. This hypothesis implies a biased/asymmetric distribution of sister chromatids, but the underlying mechanism remains unknown (Tajbakhsh and Gonzalez, 2009). Some possibilities include differences in gene expression, chromatin structure, chromatin modifications between the strands or asymmetry of mitotic spindle components such as centrosomes (Charville and Rando, 2011; Lew et al., 2008; Tajbakhsh and Gonzalez, 2009).

Support for and against asymmetric segregation of all or just a few DNA strands associated with specific chromosomes can be found in the literature in the most diversified systems, from yeast to man (Rocheteau et al., 2012; Tajbakhsh, 2008, Escobar et al., 2011; Schepers et al., 2011, Armakolas and Klar, 2006; Armakolas et al., 2010; Conboy et al., 2007), making this a highly controversial topic, mostly due to current limitations in the molecular identification of truly stem cell populations and to selectively label and track template DNA strands throughout and upon cell division. The latter traditionally involves the administration of labeled nucleotides (e.g. 5-Bromo-deoxyuridine or H3-thymidine) that will mark older or newer DNA strands, depending on the protocol used, but which cannot reliably distinguish stem cells from differentiated cells with a slow cell cycle. Therefore, finding a good model system that would allow not only the monitorization of chromatids containing template DNA strands at high spatial and temporal resolution, but also the dissection of the molecular mechanism that could account for biased/asymmetric strand segregation during cell division will be instrumental to complement existing methodology.

Although correct and complete DNA replication is required to allow cells to proceed with the cell cycle, mammalian cells treated with HU and caffeine can enter mitosis without previously replicating their genomes (Brinkley et al., 1988). HU blocks DNA replication, whereas caffeine allows the override of a post-replication checkpoint. This phenomenon known as MUGs has been used in a number of different studies to demonstrate that KTs, which detach from chromatin in mammalian MUGs, are sufficient to interact with and be segregated autonomously by the mitotic spindle (Brinkley et al., 1988; Johnson and Wise, 2010; O’Connell

et al., 2008; O'Connell et al., 2009; Wise and Brinkley, 1997). An important corollarium from these experiments is that MUGs can satisfy the SAC and proceed with anaphase (O'Connell et al., 2008, Brinkley et al., 1988), thereby allowing the subsequent tracking and fate determination of the segregated DNA.

Drosophila Double parked (Dup) is a conserved origin of replication protein that is essential for the initiation of DNA replication in S phase and is involved in a post-replication checkpoint, thereby preventing cells to enter mitosis without completing DNA replication (Whittaker et al., 2000). We reasoned that Dup knockdown by RNAi would drive cells into mitosis without previous DNA replication, which would represent an efficient way to generate and selectively track single chromatids containing template DNA strands. As proof-of-principle, we tested this idea in *Drosophila* S2 cells in culture, in which it is possible to monitor chromosome and mitotic spindle behavior throughout cell division by stably expressing GFP (or any other fluorescent protein) fusion proteins with core chromosomal and spindle apparatus components. Due to their simple cytology that favors high-resolution imaging studies, the ease of loss-of-function studies by RNAi (Moutinho-Pereira et al., 2010), together with the capacity to induce polarity and asymmetric division in *Drosophila* S2 cells (Johnston et al., 2009), this system may be potentially suited to complement existing methods for the dissection of the molecular mechanism behind asymmetric DNA strand segregation.

4.1.2 Results

With the aim of establishing a tractable cell culture system undergoing MUGs in *Drosophila* S2 cells (SMUGs) we performed Dup knockdown by RNAi in S2 cells stably expressing GFP-H2B /mCherry-α-tubulin or GFP-α-tubulin/CID-mCherry. To confirm that Dup-depleted cells entered mitosis without DNA replication we performed live cell imaging using a spinning disk confocal microscope. As opposed to mammalian cell MUGs in which unreplicated DNA remains decondensed, Dup-depleted S2 cells preserved chromatid morphology (Figure 4.1 B-E), which we used as read-out to validate our experimental strategy.

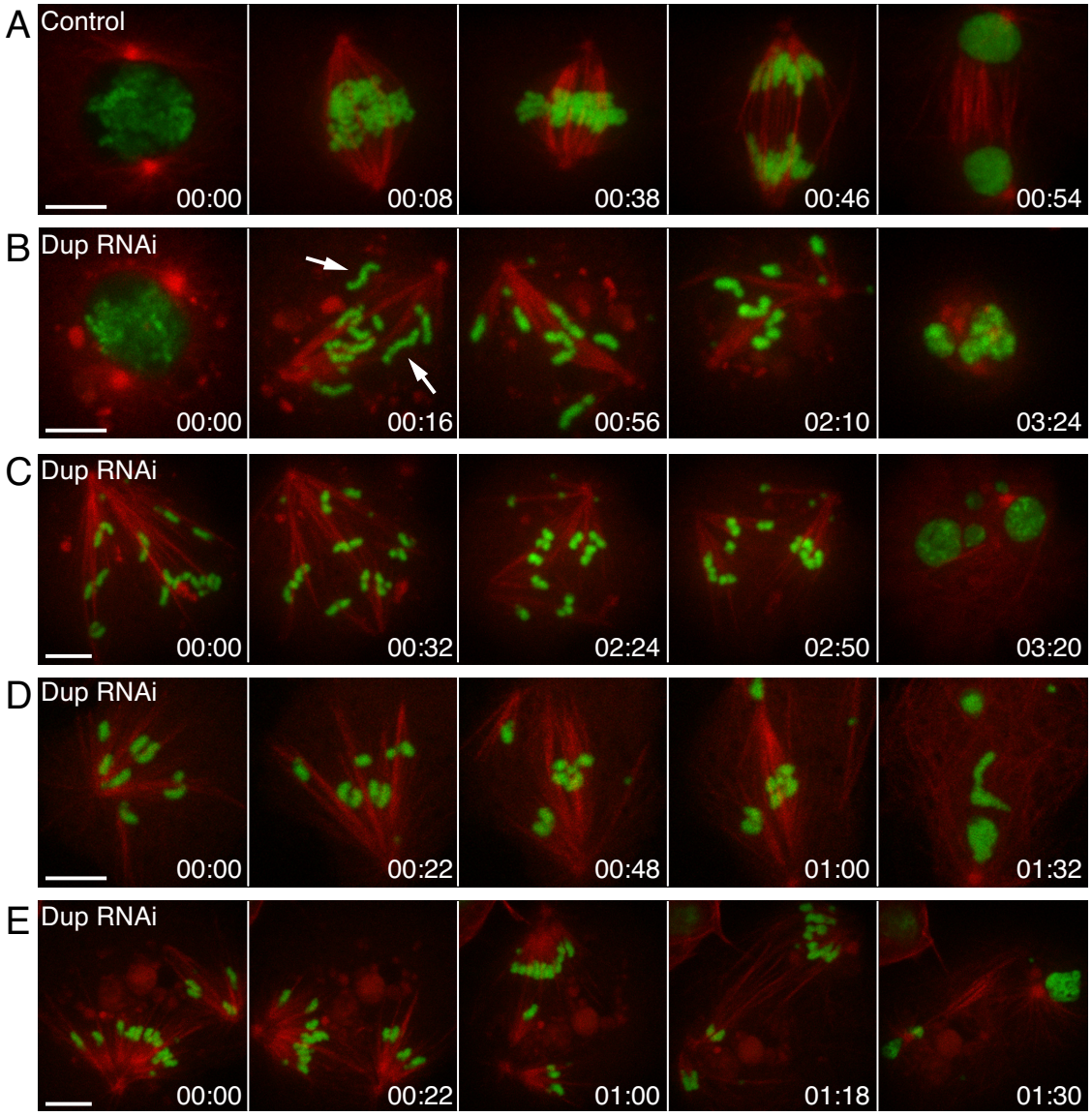

Figure 4.1: **Dup depleted cells enter mitosis with unreplicated genomes (SMUGs) with single, condensed chromatids**. Live cell imaging of control and Dup depleted *Drosophila* S2 cells stably expressing GFP-H2B (shown in green) and mCherry-α-tubulin (shown in red). (A) Control cells containing replicated chromosomes aligned during metaphase and segregated evenly during anaphase. (B-E) SMUGs with single, condensed chromatids (arrows) which remain scattered within the mitotic spindle. Spindle elongation and DNA decondensation can be observed at the end of SMUGs. Scale bar, 5μm. Time is in h:min.

Typically, control S2 cells stably expressing GFP-H2B /mCherry-α-tubulin or GFP-α-tubulin/CID-mCherry established a bipolar spindle with bi-oriented chromosomes aligned at the metaphase plate and mitosis was completed in 32 ± 9 min (mean ± SD; n=11 cells) (Figure 4.1 A and Figure 4.2 A).

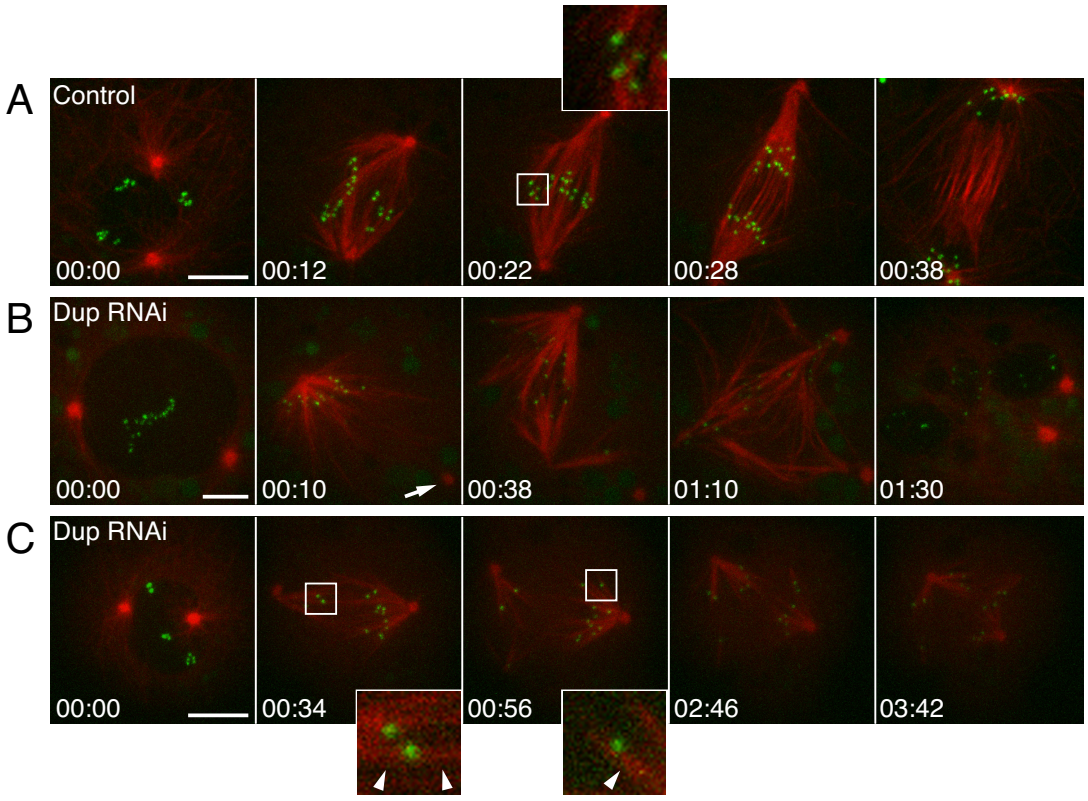

Figure 4.2: **SMUGs contain single KTs improperly attached to the mitotic spindle**. Live cell imaging of control and Dup depleted *Drosophila* S2 cells stably expressing GFP-α-tubulin (shown in red) and CID-mCherry (shown in green). (A) Control cells contain paired, bioriented KTs with amphitelic attachments (boxed, enlarged). (B-C) Single, unpaired KTs of SMUGs. (C) KTs during SMUGs are either merotelic (left box) or monotelic (right box) attached (arrowheads on MTs). (B) Arrow is pointing to the single pole excluded from the mitotic spindle showing lower MT organization capacity. Scale bar, 5μm. Time is in h:min.

In agreement with previous studies in *Drosophila* embryos (Parry et al., 2003), Dup-depleted S2 cells entered mitosis with single chromatids (Figure 4.1 B-E), as predicted for cells undergoing SMUGs. This allowed the unequivocal tracking of chromatids containing template DNA strands. Accordingly, single chromatids upon Dup depletion remained scattered up to several hours (Table 4.1), likely due to the establishment of unstable KT attachments with spindle MT plus ends as result of reduced/absent centromeric tension (King and Nicklas, 2000; Pinsky and Biggins, 2005). Due to these unstable attachments a highly variable number of chromosomes/KTs remained close to the poles throughout mitosis (Figure 4.1 B-E, Figure 4.2 B, C). Interestingly, 3 out of 4 Dup-depleted cells (Table I) showed a

clear asymmetric distribution of chromosomes/KTs between the two poles immediately upon NEB and establishment of initial KT-MT attachments (Figure 4.2 B-C). This correlated with a much higher MT organizing activity from one of the centrosomes, and spindle bipolarity was achieved by means of centrosome-independent mechanisms (Maiato et al., 2004b). Importantly, all recorded SMUGs eventually exited mitosis (Table 4.1), as determined by spindle and cell elongation together with chromatin decondensation (Figure 4.1 B-E). This is consistent with previous studies in mammalian cells undergoing MUGs, which were shown to satisfy the SAC after a mitotic delay (Brinkley et al., 1988; O'Connell et al., 2008). Curiously, mammalian cells undergoing MUGs do not seem to elongate the spindle during anaphase B (Johnson and Wise, 2010), which was not the case in SMUGs (Figure 4.1 E, and Table 4.1).

Table 4.1: Summary of measured parameters from SMUGs.

MUGs	Mitotic entry	Interpolar distribution of single chromatids before NEB	Interpolar distribution of single chromatids after NEB	Mitotic exit	Minimal mitosis duration[a]	Spindle elongation in anaphase	Chromatid segregation in anaphase
Cell 1	yes	even	asymmetric	yes	1 h	yes	asymmetric
Cell 2	yes	even	asymmetric	N.A.	>6 h	N.A.	N.A.
Cell 3	yes	even	asymmetric	N.A.	>1 h	N.A.	N.A.
Cell 4	N.A.	N.A.	N.A.	yes	>2 h	yes	asymmetric
Cell 5	N.A.	N.A.	N.A.	yes	>2 h	yes	asymmetric
Cell 6	N.A.	N.A.	N.A.	yes	>45 min	yes	even
Cell 7	N.A.	N.A.	N.A.	yes	>2 h 20 min	yes	asymmetric
Cell 8	yes	even	even	yes	2 h	yes	even
Cell 9	N.A.	N.A.	N.A.	yes	>2 h	yes	asymmetric
Cell10	N.A.	N.A.	N.A.	yes	>20 min	yes	asymmetric

[a] Defined as the time between nuclear envelope breakdown until chromatin decondensation. In the cases where the entry /exit of mitosis is missing from our recordings, the indicated times are an underestimation of the real mitotic duration.

N.A. = data not available

Contrary to control *Drosophila* S2 cells in which chromosomes segregated evenly during anaphase (Figure 4.1 A and Figure 4.2 A), SMUGs showed a 3:1 bias (n=8 cells) in segregating single chromatids containing template DNA strands in a asymmetric vs. apparently symmetric fashion (Figure 4.1 D, E, and Table 4.1).

4.1.3 Discussion

Here we have established the experimental conditions to generate MUGs in *Drosophila* S2 cells in culture (Figure 4.3). MUGs represent an established model system that helped eluci-

dating a number of important processes in mitosis, such as KT-MT interactions, SAC satisfaction and the role of chromosomes/KTs in spindle assembly (Johnson and Wise, 2010; O'Connell et al., 2008; O'Connell et al., 2009; Wise and Brinkley, 1997). The ability of *Drosophila* S2 cells to preserve condensed DNA morphology during MUGs allowed the unequivocal tracking of single chromatids (Figure 4.1 B-E) containing template DNA strands, which is an advantage relative to mammalian systems where DNA condensation during MUGs is lost.

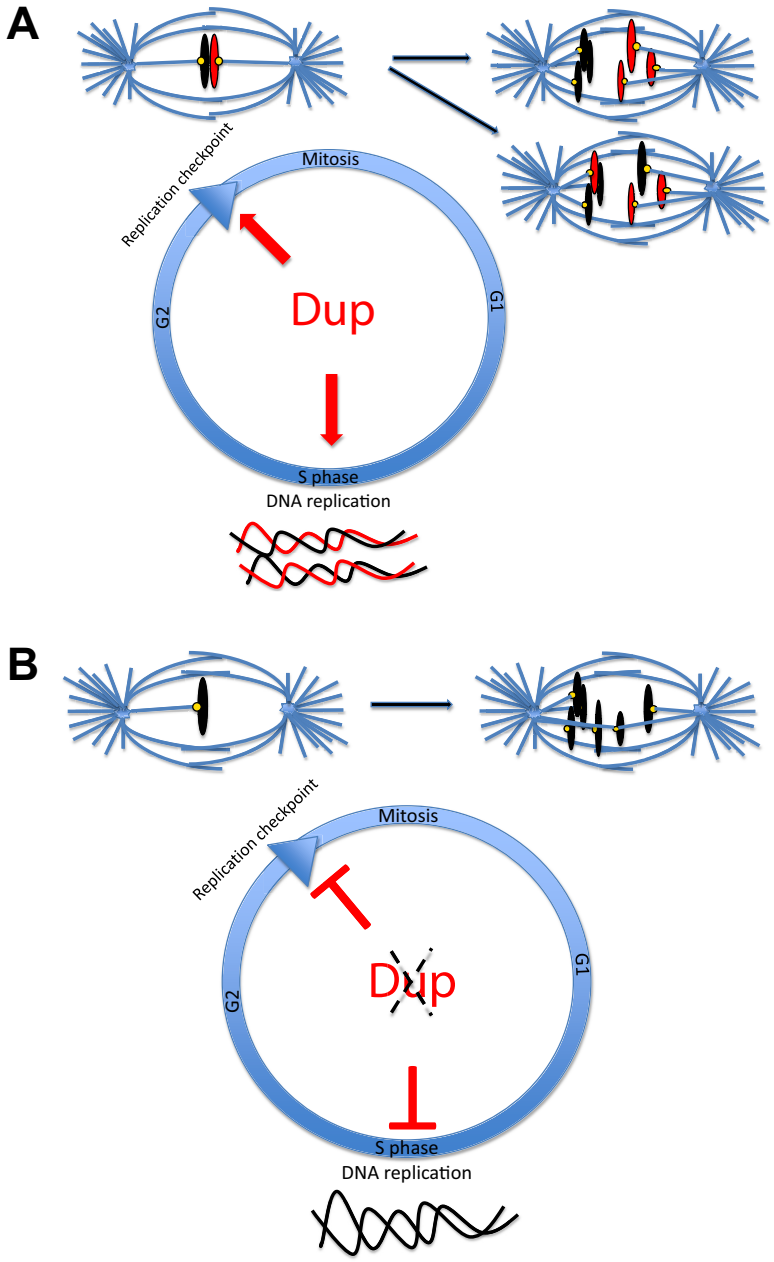

Figure 4.3: **Model of SMUGs**. Model illustrates possible biased/asymmetric segregation of chromosomes in Dup depleted cells in comparison to control. (A) In control cells chromatids equally segregate towards the mitotic poles. (B) Since Dup depleted S2 cells only contain template DNA this system/strategy might be useful to investigate biased/asymmetric segregation of DNA strands.

Although S2 cells are thought to divide in a symmetrical fashion, there are inherent asymmetries that are normally neglected. This is the case for the mother and daughter centrosomes, which will be inherited by the two daughter cells. The template and replicated DNA strands are also inherently asymmetric, in the sense that one is older than the other, but whether they segregate asymmetrically in this system remains unknown. Moreover, even if they do segregate asymmetrically, there is no obvious reasoning for such behavior aside from the potential conservation of mechanisms that maybe present in the stem cells from which S2 cells derived. Importantly, it is possible to induce polarized division in S2 cells in culture, for example through the ectopic expression of aPKC or Pins to cell-cell contact sites (Johnston et al., 2009). The powerful and flexible experimental tools together with the simple cytology of S2 cells makes this system potentially suited for the dissection of the molecular mechanism behind asymmetric DNA strand segregation, namely through the combination of high-resolution live-cell imaging with loss-of-function studies.

Although beyond the scope of this work, we did notice that those SMUGs that were able to exit mitosis showed a 3:1 bias in asymmetric vs. apparently symmetric segregation of single chromatids containing template DNA strands. This was surprising in light of previous studies in CHO cells where it was shown that during MUGs small CKFs segregate evenly to the daughter cells without showing any strong bias or asymmetry (Johnson and Wise, 2010). However, previous studies did detect two populations of CHO cells undergoing MUGs where some showed apparently equal segregation and others where segregation was uneven, depending on whether they had near “diploid” KT numbers (Brinkley et al., 1988). In these cases, the reason for discrepancy might lie in the detection method of small KT fragments, which in SMUGs does not represent a problem since entire chromatids can be tracked. Are these results in SMUGs relevant to the “immortal strand” hypothesis? Maybe not, and our results should be taken with caution given that just a small population of cells was analysed in the present study. Moreover, the observed bias might be due to many other mechanisms unrelated to template strand bias, such as asymmetry in the initial distribution of chromatids towards one of the two centrosomes or unequal MT nucleation capacity of centrosomes, which would bias the capture of a single chromatid by a particular spindle pole. Nevertheless, we do not think this to be the case as during SMUGs initial KT-MT attachments are unstable and therefore cannot account for the segregation bias observed several hours after alternating chromatid excursions to both spindle poles. This is further supported by the observation that those SMUGs that showed a very early bias of chromatids relative to one of the spindle poles immediately upon NEB did not reveal any obvious asymmetry in their

spatial distribution relative to both poles prior to NEB (Table 4.1). These situations are particularly relevant because they further provide an opportunity to dissect and visualize how the initial interactions between KTs from sister chromatids containing template DNA strands and MTs from the mitotic apparatus are established. Finally, our results do show that there is no absolute bias/asymmetry in the segregation of all template DNA strands and, in the best case scenario, there might only be a segregation bias of template DNA strands from some, but not all, chromosomes. It will be interesting in the future to reproduce these experiments upon induction of polarization and selective labeling of mother vs. daughter centrosomes in S2 cells using photo–conversion of centriolar proteins (Januschke et al., 2011; Wang et al., 2009).

One important aspect that deserves further consideration in systems undergoing SMUGs is that KTs are not paired and therefore the entire tension/attachment status of chromosomes is likely to be very different from normal cells, which may influence the segregation pattern of chromatids containing template DNA strands. Accordingly, we observed that the attachments between single chromatids and spindle MTs in Dup depleted S2 cells are unstable, with chromatids often switching orientation between the two poles. This highly dynamic KT-MT interactions and unstable attachments likely result from the lack of tension in the absence of sister chromatid cohesion and is probably the result of Aurora B-mediated corrections of improper KT-MT attachments (e.g. merotelic or monotelic) (Oliveira et al., 2010). Indeed, the majority of Dup-depleted chromatids are scattered around the mitotic spindle and only some are able to align to the spindle equator apparently through the establishment of merotelic attachments, similar to what has been reported in human cells undergoing MUGs (O'Connell et al., 2008). In these cases, segregation bias was shown to depend on the number of MTs associated between pole and the merotelic KT, favoring segregation towards the pole with the higher number of attached MTs (Cimini et al., 2004; Cimini et al., 2003).

Interestingly, all recorded SMUGs exited mitosis but took about 3-4x longer than control S2 cells (Table 4.1). This contrasts with results in *Drosophila* embryos mutant for Dup, which arrested in mitosis as a result of activated SAC, with stabilized mitotic cyclins and Bub1 kinase present on KTs (Garner et al., 2001). On the other hand, mammalian cells undergoing MUGs were able to satisfy the SAC and exited from mitosis (O'Connell et al., 2008), although BubR1 levels on KTs were still high. These differences between systems undergoing MUGs indicate that the detailed mechanism of SAC satisfaction/mitotic exit remains to be elucidated and likely involves structural modifications within the KT itself in addition to centromere stretching (Maresca and Salmon, 2009; Uchida et al., 2009).

Our results in S2 cells in culture mirror previous experiments with *Drosophila* embryos mutant for Dup (Parry et al., 2003; Whittaker et al., 2000). This provides an important advantage over in vitro-limited HU/caffeine induced MUGs in mammalian cells in culture to investigate biased/asymmetric DNA strand segregation in vivo using the powerful genetic tools of *Drosophila*, including the analysis of hypomorphic mutations, in vivo RNAi and clonal cell analysis in specific tissues.

4.1.4 Materials and Methods

4.1.4.1 Cell lines

Drosophila S2 cells stably expressing either GFP-H2B and mCherry -α-tubulin (Maiato and Lince-Faria, 2010) or GFP-α-tubulin and CID-mCherry (Moutinho-Pereira et al., 2010), were grown at 25°C in Schneider's medium (Invitrogen).

4.1.4.2 RNA interference

Synthesis of Dup dsRNA was obtained following the protocol previously described in (Maiato et al., 2003b). For synthetizing Dup dsRNA from *Drosophila* S2 cells genomic DNA, we used the primers: forward TAATACGACTCACTATAGGGGTCATAACGTGTGGATTCATGG and reverse TAATACGACTCACTATAGGGCAAGACTCCCACAAAAATACCG. For RNAi 10^6 of Dup S2 cells were seeded in six well plates and incubated with 1 ml of Schneider's medium without FBS and containing 10μg/ml of Dup dsRNA for 1h (Moutinho-Pereira et al., 2010). After incubation, 2 ml of Schneider's medium with FBS were added and cells were kept for 96h at 25°C.

4.1.4.3 Imaging

Dup depleted S2 cells stably expressing GFP-H2B /mCherry-α-tubulin or GFP-α-tubulin/CID-mCherry were plated on 0.25mg/ml concanavalin A-coated glass-bottom dishes (MatTek) and multipoint time-lapse images of living cells were obtained using a Nikon TE2000U inverted microscope equipped with a Yokogawa CSU-X1 spinning-disc confocal head, two laser lines (488 and 561 nm) and a motorized stage (Marzhauser). Images were collected as a multi (9) 0.5 μm separated z-planes with a time interval of 2 min and detected by an iXonEM+ Electron Multiplying CCD camera (Andor). An effective pixel size of 0.076 μm was achieved using 100x 1.4 NA plan-Apochromatic DIC objective and an 1.5x optivar before the

CCD. The system was controlled by NIS-elements software (Nikon, Japan) and videos were processed and analysed with ImageJ.

4.2 Experimental work II

Polar ejection forces promote the conversion from lateral to end-on KT-MT attachments on mono-oriented chromosomes

(Published in Cell Reports, 2015, Oct 20, 13(3); 460-9)

4.2.1 Introduction

During spindle assembly, the initial lateral interactions between chromosomes and MTs are converted into stable end-on KT-MT attachments that lead to chromosome bi-orientation (Magidson et al., 2011). After chromosome bi-orientation, the opposing spindle forces generate tension on centromeres that is important for the stabilization of correct KT-MT attachments required for error-free chromosome segregation (Nicklas and Koch, 1969; Nicklas and Ward, 1994). Tension has also been shown to be sufficient to satisfy the SAC (Li and Nicklas, 1995), a surveillance mechanism that ensures that all chromosomes are attached to spindle MTs before anaphase onset (Foley and Kapoor, 2013). Tension from spindle forces affects KT chemistry through changes in phosphorylation of “tension-sensitive” proteins at KTs (Gorbsky and Ricketts, 1993; Nicklas et al., 1995). Aurora B, a mitotic kinase present on centromeres, plays a critical role in tension sensing and error correction (Biggins and Murray, 2001; Cheeseman et al., 2002; Lampson et al., 2004) by phosphorylating key substrates at the KT-MT interface, such as the KMN network, in response to tension on bi-oriented chromosomes (DeLuca et al., 2006; Liu et al., 2009; Wang et al., 2011; Welburn et al., 2010). Importantly, recent works in human and *Drosophila* cells have shown that even in the absence of centromeric tension, an intra-KT stretch or structural deformation is sufficient to satisfy the SAC (Maresca and Salmon, 2009; Uchida et al., 2009). However, the underlying mechanism remained unclear.

Chromokinesins are MT plus-end-directed motor proteins present on the chromosome arms harboring both chromatin- and MT-binding domains. As a consequence of their motor activities, chromokinesins move chromosomes away from the poles by generating random PEFs (Barisic et al., 2014; Brouhard and Hunt, 2005; Levesque and Compton, 2001; Rieder et al., 1986; Wandke et al., 2012; Yajima et al., 2003). Recently, elevated PEFs were shown to stabilize erroneous KT-MT attachments (Cane et al., 2013), suggesting a role in the stabilization of KT-MT attachments. Here we found that Chromokinesin-mediated PEFs promote the conversion from lateral to stable end-on KT-MT attachments on mono-oriented chromosomes. These findings contribute to explain how initial end-on KT-MT attachments are stabillized before bi-orientation.

4.2.2 Results

4.2.2.1 The SAC is satisfied in cells with single chromatids after a mitotic delay

To investigate which factors are responsible for KT-MT attachment stability before bi-orientation, we established SMUGs (Drpic et al., 2013). This was achieved by RNAi-mediated depletion of Dup, a conserved protein required for the initiation of DNA replication and post-replication checkpoint response (Whittaker et al., 2000). The main advantage of this system when compared to mammalian cells undergoing MUGs (Brinkley et al., 1988; O'Connell et al., 2009) is that SMUGs preserve their unreplicated genetic material condensed into single chromatids, which never experience bi-orientation due to the absence of sister KTs (Drpic et al., 2013). Thus, the function of individual KTs in SMUGs can be investigated in their native chromatid context.

Spinning-disk confocal live-cell imaging revealed that single chromatids in SMUGs were scattered along the spindle. Because of their low chromosome number, the status of KT-MT attachments could be inferred by careful inspection of the respective z-sections (see Material and Methods). This indicated that SMUGs established mainly lateral and only few merotelic KT-MT attachments. For instance, 20 min after NEB we found that, on average, 8.0 ± 1.6 KTs per cell were laterally attached and 3.0 ± 0.82 KTs established merotelic attachments (mean ± SD, n=5 cells; Figure 4.4 A, 4.5 A). Consequently, SMUGs significantly delayed mitotic exit (t=111 ± 43 min, mean ± SD, n=11 cells, p=<0.001, t-test) when compared to control cells (t=31 ± 8 min, mean ± SD, n=11 cells; Figure 4.4 A, C). Indeed, while Cyclin B1 levels abruptly decreased at the metaphase-anaphase transition in control cells, Cyclin B1 levels decreased more slowly over time in SMUGs (Figure 4.5 E, F), suggesting a delay in SAC satisfaction. To investigate whether the delayed mitotic exit in SMUGs is SAC dependent, we co-depleted Mad2 and Dup by RNAi (Figure 4.4 C and 4.5 B, C). We found that, similar to control cells, Mad2 co-depletion overcomes the mitotic delay in SMUGs (Mad2/Dup-depleted cells: t=22.1 ± 6.0 min, mean ± SD, n=31 cells; Mad2-depleted cells: t=18.0 ± 5.6 min, Mean ± SD, n=19 cells), indicating that the mitotic delay in SMUGs is SAC dependent.

Next, we tested SAC response in SMUGs by adding colchicine immediately after NEB to generate unattached KTs, and monitored mitotic progression by live-cell imaging. Both control cells and SMUGs were arrested in mitosis for more than 10 h before undergoing slippage (Rieder and Maiato, 2004) (control t=18.4 ± 1.23h, Mean ± SD, n=7 cells; SMUGs t=10.4 ± 2.6h, Mean ± SD, n=24 cells; Figure 4.4 B, C). These results indicate that SMUGs have an active SAC, which is however less robust than in control cells.

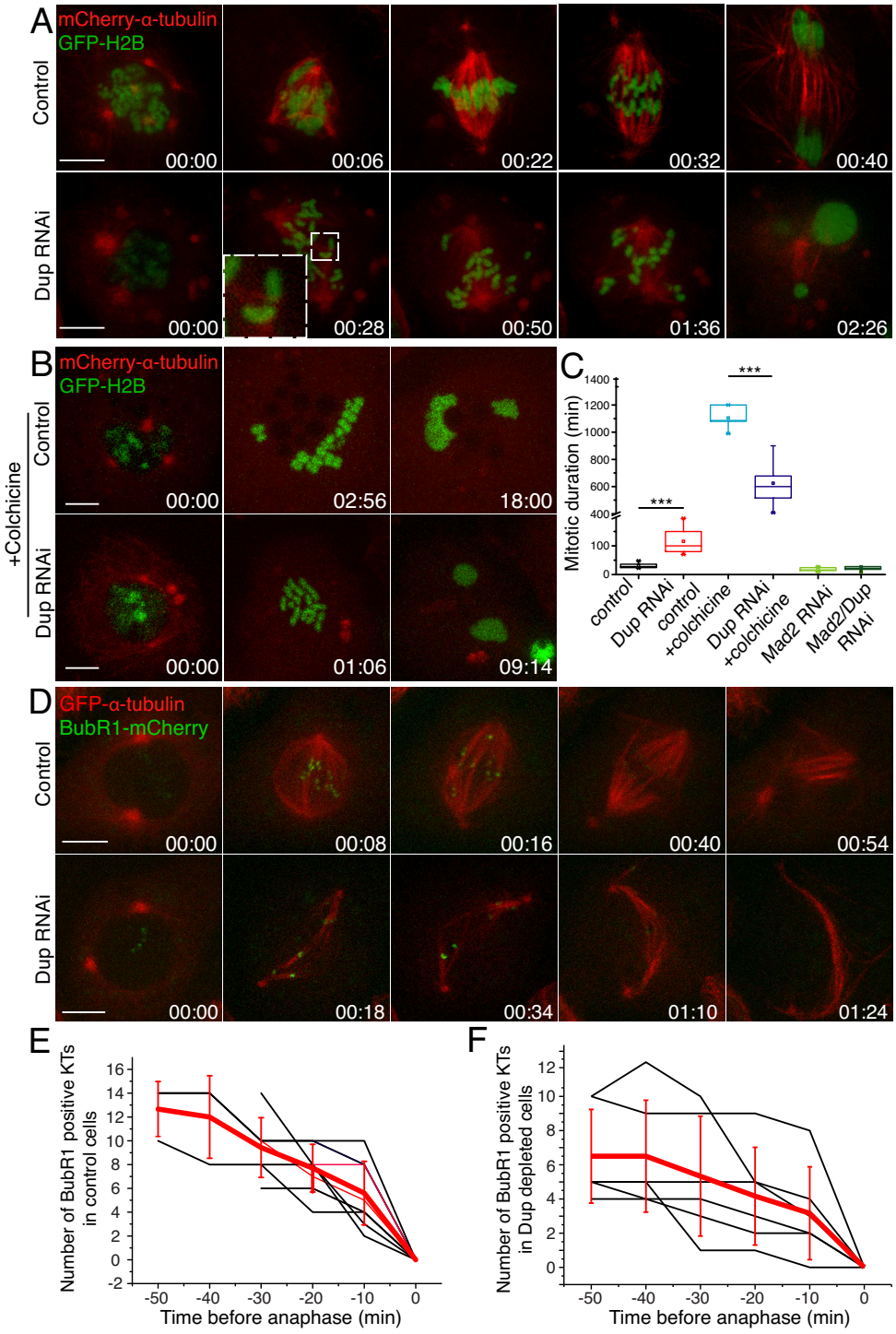

Figure 4.4: **Cells with single chromatids satisfy the SAC after a mitotic delay**. (A) Live cell imaging of *Drosophila* S2 cells (control and Dup-depleted) stably expressing H2B-GFP and mCherry-α-tubulin. Dashed box indicates a single, condensed chromatid. (B) Similar conditions, but in which cells were treated with 200 μM colchicine immediately after NEB. (C) Quantification of mitotic duration (control n=11 cells; Dup-depleted n=11 cells; control cells treated with colchicine n=7 cells; Dup-depleted cells treated with colchicine n=24 cells; Mad2-depleted cells treated with colchicine n=19 cells; Mad2/dup-depleted cells treated with colchicine, n=31 cells). (D) Live cell imaging of S2 cells stably expressing BubR1-mCherry and GFP-α-tubulin. (E, F) Quantification of the number of BubR1 positive KTs during normal mitosis (n=10 cells) and SMUGs (n=10 cells). Zero time point refers to anaphase onset. *** $p < 0.001$. Black lines indicate individual cells and red lines represent the average. Error bars represent standard deviation. Time = h:min. Scale bar= 5 μm.

Interestingly, the total levels of Mad2 and the recruitment of Mad2 and active Aurora B to unattached KTs in SMUGs were unaltered relative to controls; Figure 4.5 D and 4.6 A-D).

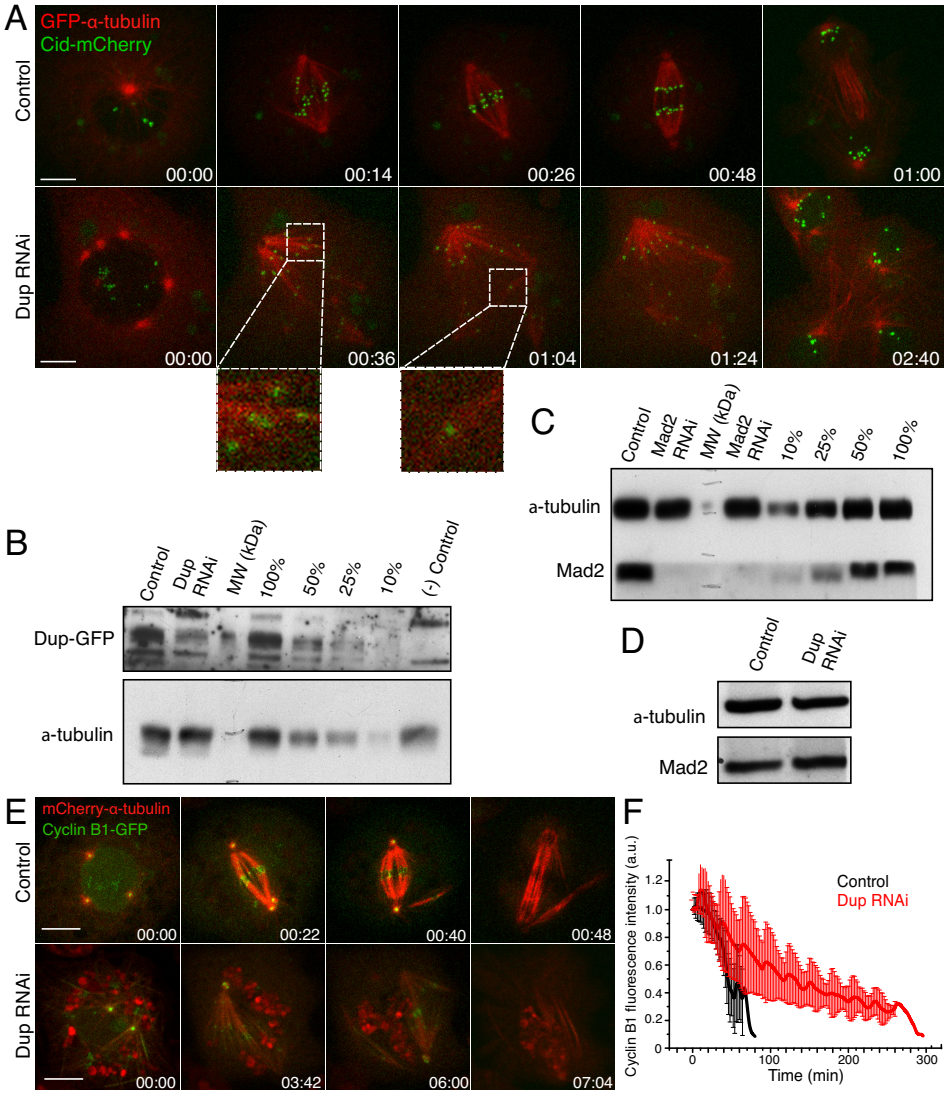

Figure 4.5: **Single chromatids in SMUGs are laterally attached to spindle MTs causing slow cyclin B1 degradation and a mitotic delay**. (A) Live cell imaging of *Drosophila* S2 cells (control and Dup-depleted) stably expressing GFP-α-tubulin (red) and Cid-mCherry (green). Dashed boxes illustrate examples of single KTs (lateral and merotelic attachments). (B) Immunoblot showing Dup depletion efficiency. Total cell protein extracts from *Drosophila* S2 cells stably expressing Dup-GFP were loaded into the wells. Dup depletion was monitored by using a rabbit anti-GFP antibody. A cell line stably expressing another GFP-tagged protein (Cyclin B1-GFP) was used as negative control. (C) Rabbit anti-Mad2 antibody was used to monitor Mad2 depletion. Mouse anti-tubulin was used to detect α-tubulin (loading control). Handwritten lines are from our annotations in the original film and represent the molecular weight (kDa). (D) Immunoblot showing the total amount of Mad2 in control and Dup-depleted cells. (E) Live cell imaging of control and Dup depleted cells stably expressing Cyclin B1-GFP (green) and mCherry-α-tubulin (red). (F) Cyclin B1 degradation profile in normal mitosis (black) (n=12 cells) and SMUGs (red) (n=4 cells) as indicated by fluorescence intensity quantification of Cyclin B1-GFP. The oscillatory decay pattern resulted from an artifact during image acquisition (periodic alterations in the focal plane). Zero time point=NEB. Time is in min. Scale bar = 5 μm. Error bars represent standard deviation.

Thus, despite normal SAC signaling at individual KTs, the number of cumulative unattached KTs that are able to inhibit the APC/C in SMUGs is reduced by half relative to controls cells. This explains the weakened SAC response in SMUGs and is in line with previous reports in human cells (Collin et al., 2013; Dick and Gerlich, 2013). Importantly, these data strongly suggest that SMUGs normally exit mitosis after SAC satisfaction, as they took more than five times longer to slip out of mitosis in the presence of colchicine.

To directly test whether SMUGs satisfy the SAC after a mitotic delay, we investigated the behavior of another SAC protein, BubR1, using live-cell imaging of SMUGs stably expressing BubR1-mCherry/α-tubulin-GFP. BubR1 is normally recruited to unattached KTs and its levels decrease significantly as chromosomes bi-orient, becoming undetectable on anaphase KTs (Howell et al., 2004; Maiato et al., 2002). In contrast, BubR1 remains associated with KTs in cells that slip out of mitosis without satisfying the SAC (Brito and Rieder, 2006). We found that, despite of a mitotic delay, SMUGs lost BubR1 from KTs just before exiting from mitosis (Figure 4.4 D-F). This demonstrates that the SAC in SMUGs with single chromatids can be satisfied without bi-orientation.

4.2.2.2 Single chromatids in SMUGs experience intra-KT stretch/structural deformation after a mitotic delay

Intra-KT stretch or structural deformation is sufficient to satisfy the SAC even with reduced centromeric tension (Maresca and Salmon, 2009; Uchida et al., 2009). To investigate whether SMUGs experience intra-KT stretch/structural deformation, we measured the absolute distance between the inner KT protein Cid-mCherry and the outer KT protein Ndc80-GFP (Maresca and Salmon, 2009) at individual KTs (see Materials and Methods) from control cells treated with colchicine (reference for relaxed KTs) or MG132 (reference for bi-oriented chromosomes under tension), as well as from Dup-depleted cells treated with MG132 for 2h (to normalize the mitotic delay). We found that under these conditions single chromatids in SMUGs experienced a significant intra-KT stretch/structural deformation relative to relaxed KTs (Mann-Whitney Rank Sum Test, $p<0.001$) that was almost comparable to bi-oriented chromosomes under tension (Figure 4.7 A, C).

In line with these measurements, we further observed intermediate levels of Aurora B-mediated phosphorylation of the outer KT protein Knl1 (Welburn et al., 2010) relative to unattached controls and bi-oriented chromosomes (Figure 4.7 B, C), suggesting that intra-KT stretch/structural deformation positively correlates with KT-MT attachment stability. Taken to-

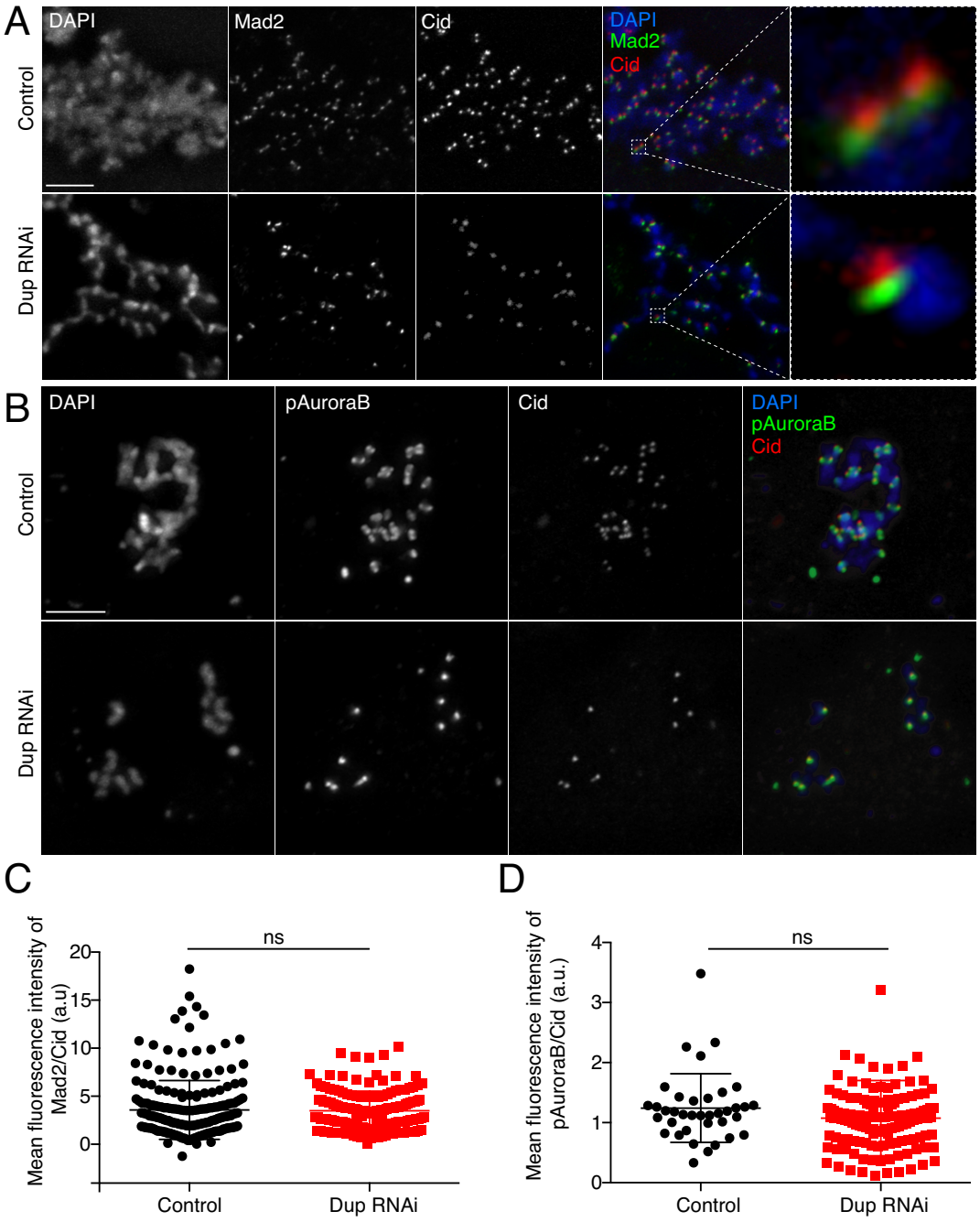

Figure 4.6: **Unattached KTs in SMUGs have normal Mad2 and active Aurora B levels**. (A, B) Immunofluorescence of *Drosophila* S2 control and Dup RNAi cells using an antibody against Mad2 (green) or pAuroraB T232 (green). Cid is shown in red and DNA (DAPI) in blue. (C) Mean Fluorescence Intensity of Mad2 levels normalized to Cid levels in control (n=207 KTs) and DupRNAi (n=160 KTs) depleted *Drosophila* S2 cells. (D) Mean Fluorescence Intensity of p-T232 AuroraB levels normalized to Cid levels in control (n=37 KTs) and Dup RNAi (n=119 KTs) *Drosophila* S2 cells. There was no difference in the protein levels per KT (normalized to Cid levels) between Dup RNAi and control cells. Scale bar = 5 μm. Error bars represent standard deviation. (ns = non-significant; a.u = arbitrary units).

gether, these data indicate that single chromatids in SMUGs experience sufficient intra-KT stretch/structural deformation to satisfy the SAC.

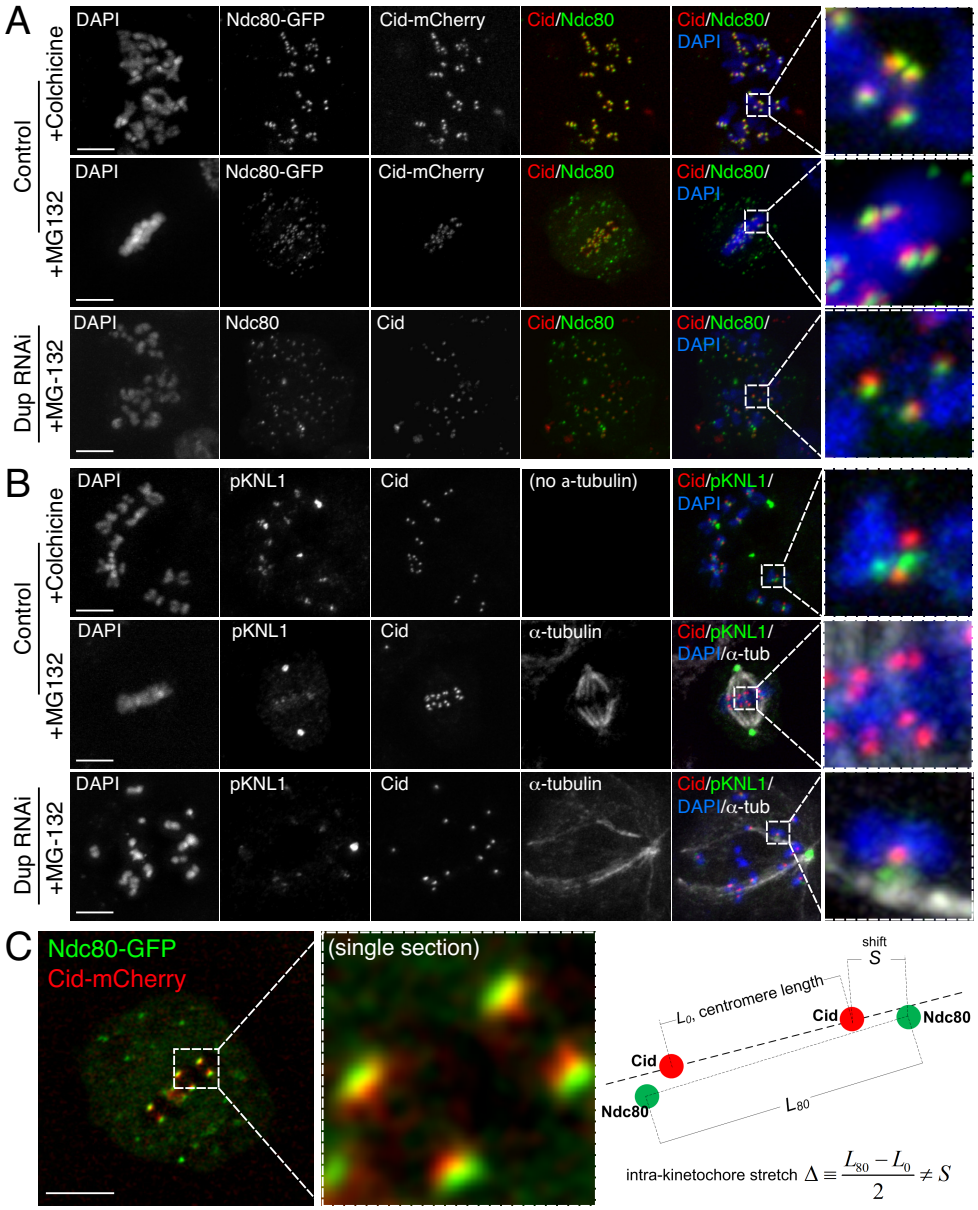

Treatment	Intra-KT stretch ± SD (nm)	Nr. of KTs	Mean Fluorescence Intensity of pKNL1/Cid ± SD (a.u.)	Nr. of KTs
Control + colchicine	103 ± 52	255	0.511 ± 0.385	351
Control + MG132	130 ± 62	890	0.353 ± 0.204	300
Dup + MG132	126 ± 68	475	0.438 ± 0.228	472

Figure 4.7: **Single chromatids in SMUGs experience intra-KT stretch after a mitotic delay**. (A) Fixed control cells stably expressing Cid-mCherry/Ndc80-GFP were treated with colchicine or MG132 (2h) and compared with Dup depleted cells treated with MG132 (2h). (B) Immunofluorescence analysis of Aurora-B phosphorylation of the outer KT protein Knl1 in SMUGs and control cells in the same conditions as in A. (C) Quantification of pKnl1 and intra-KT stretch (shift) by measuring absolute distance between red (Cid) and green (Ndc80) centroids in control cells vs. SMUGs.

4.2.2.3 PEFs stabilize KT-MT attachments and promote SAC satisfaction independently of chromosome bi-orientation

Elevated PEFs on chromosome arms after overexpression of the Chromokinesin Nod lead to the stabilization of syntelic KT-MT attachments in *Drosophila* S2 cells (Cane et al., 2013). To test whether the KT-MT stabilizing role of PEFs is involved in SAC satisfaction in SMUGs, we co-depleted Dup and Nod. This resulted in a SAC-dependent increase in mitotic duration when compared to Dup-depleted cells (t=208 ± 109 min, mean ± SD, n=25 cells, p=0.007, t-test; Figure 4.8 B, D). Co-depletion of both Chromokinesins, Nod and Klp3A, with Dup caused an even longer mitotic delay (t=304 ± 66 min, Mean ± SD, n=8 cells, p=<0.001, t-test; Figure 4.8 D and 4.9 E).

Interestingly, Nod depletion in control cells caused chromosome alignment defects and also significantly increased the duration of mitosis (t=44 ± 12 min, Mean ± SD, n=26, p=0.005, Mann- Whitney Rank Sum test; Figure 4.8 A, D), in line with previous findings in human cells (Levesque and Compton, 2001; Magidson et al., 2011). This phenotype was exacerbated when Nod and Klp3A were co-depleted (t=62 ± 29 min, mean ± SD, n=20, p=0.003, t-test; Figure 4.8 D and 4.9 E), suggesting that PEFs play an important role in the stabilization of KT-MT attachments during a normal mitosis. Thus, in the absence of Chromokinesin-mediated PEFs, SAC satisfaction is delayed and the delay is more pronounced in the absence of chromosome bi-orientation.

One prediction from these data is that elevated PEFs should promote the stabilization of KT-MT attachments and consequently accelerate SAC satisfaction in SMUGs. To test this we overexpressed Nod-mCherry in Dup-depleted cells stably expressing GFP-α-tubulin (Cane et al., 2013). In agreement with our prediction, Nod overexpression significantly shortened the mitotic duration in Dup-depleted cells (t=46.5 ± 22 min, mean ± SD, n=12 cells, p=<0.001, t-test; Figure 4.8 C, D). In contrast, elevated PEFs caused by Nod overexpression in control cells increased mitotic duration (t=67 ± 27 min, Mean±SD, n=22 cells p=0.003, Mann-Whitney Rank Sum test; Figure 4.8 C, D), which might be due to random ejection of chromosomes after stabilization of monotelic attachments, thereby preventing bi-orientation and timely SAC satisfaction (Barisic et al., 2014).

Overall, these data suggest that Chromokinesin-mediated PEFs promote SAC satisfaction in SMUGs by stabilizing KT-MT attachments independently of chromosome bi-orientation.

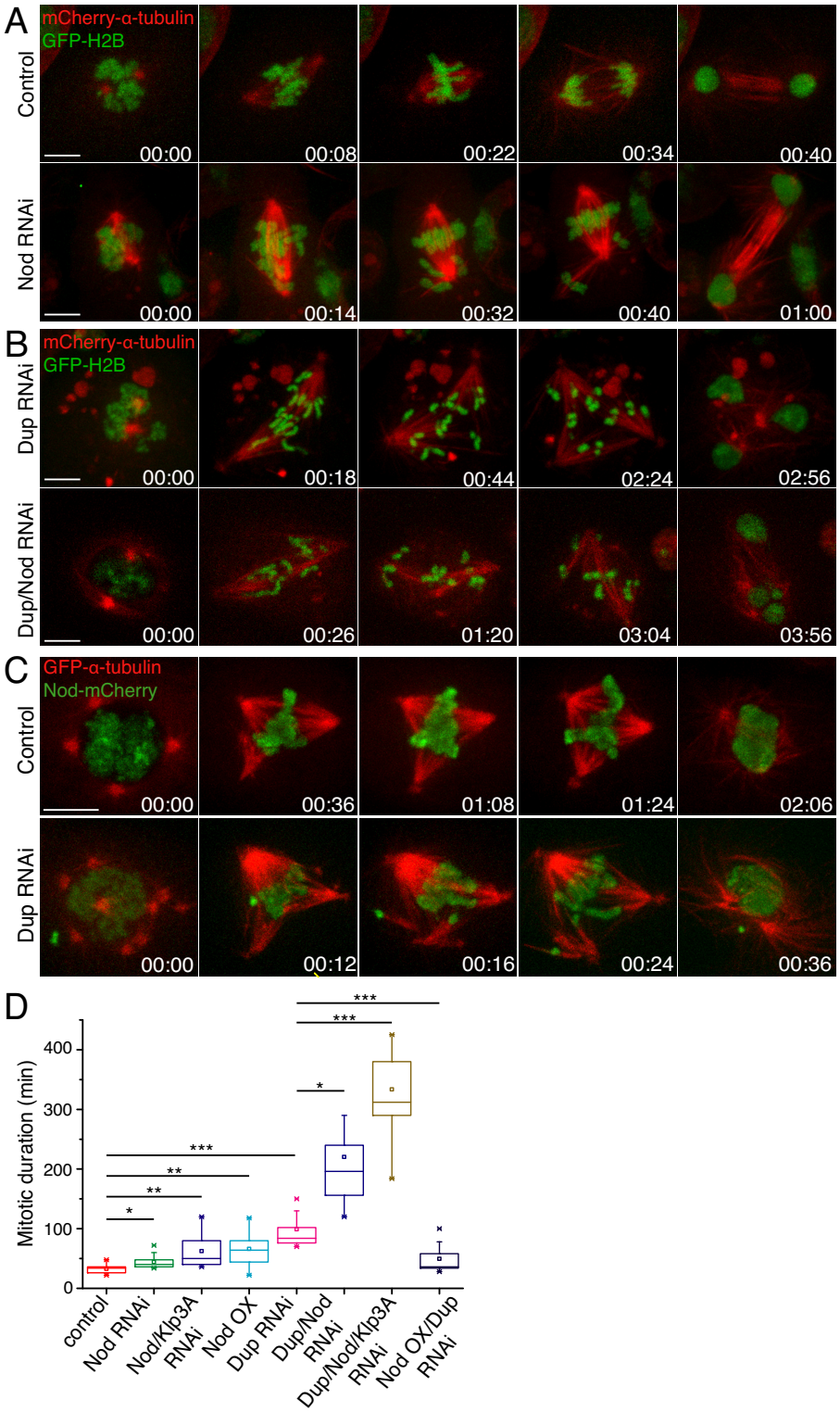

Figure 4.8: **PEFs are involved in SAC satisfaction independently of chromosome bi-orientation.** (A, B) Live cell imagining of *Drosophila* S2 cells stably expressing H2B-GFP and mCherry-α-tubulin. The panels illustrate control, Nod depleted, Dup depleted, as well as Nod and Dup co-depleted situations, as indicated. (C) Live cell imaging of Nod-mCherry over-expressing cells with and without Dup depletion. (D) Mitotic duration of control (n=11 cells), Nod depleted (n=26 cells), Nod/Klp3A depleted (n=20 cells), Nod overexpressing (OX) (n=22 cells), Dup-depleted (n=10), Nod/Dup-depleted (n=25), Nod/Klp3A/Dup depleted (n=8) and Nod OX SMUGs (n=12). * $p < 0.05$, ** $p < 0.01$, *** $p < 0.001$. Time = h:min. Scale bar = 5 μm. Error bars represent standard deviation.

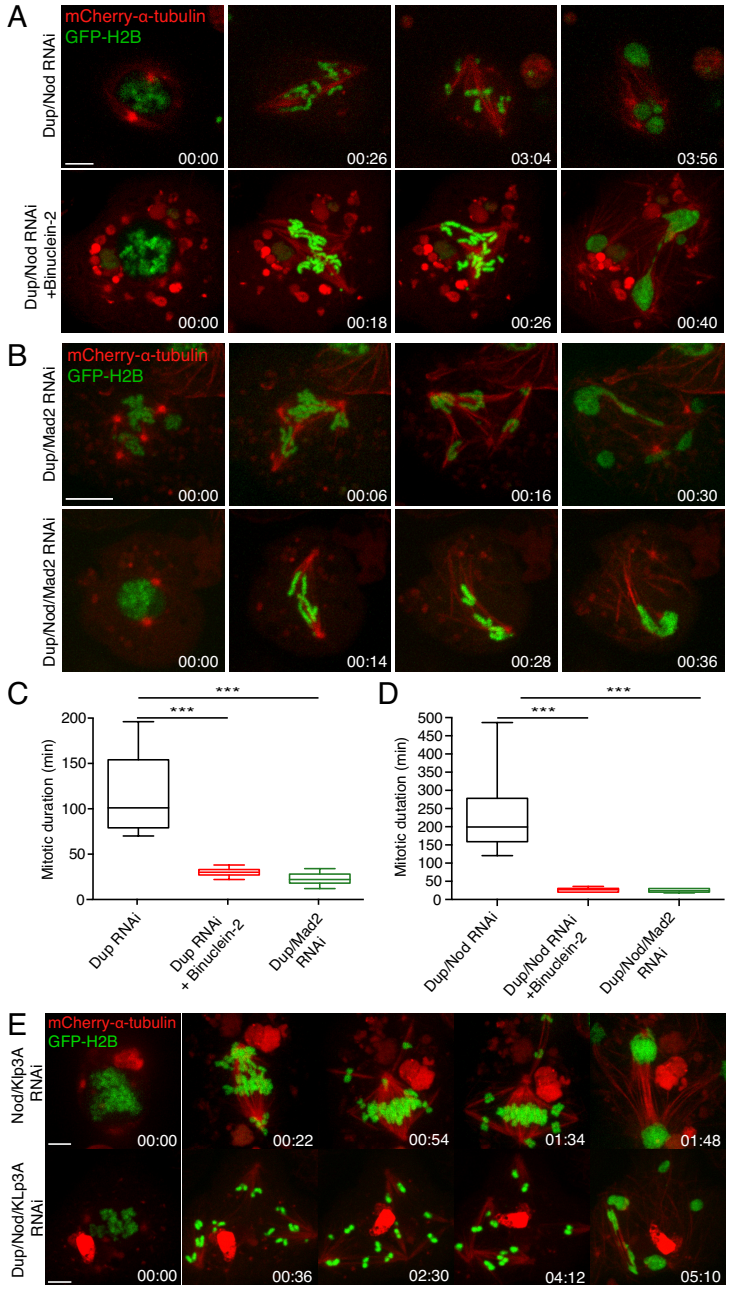

Figure 4.9: **Chromokinesin-mediated PEFs are required for timely SAC satisfaction in SMUGs.** (A) Live cell imaging of H2B-GFP (green) and mCherry-α-tubulin (red) Dup and Dup/Nod depleted *Drosophila* S2 cells treated with 40 μM Binucleine-2 immediately after NEB. (B) Live cell imaging of H2B-GFP (green) and mCherry-α-tubulin (red) Dup/Mad2 RNAi and Dup/Nod/Mad2 RNAi *Drosophila* S2 cells. (C) Mitotic duration of Dup RNAi (t=111 ± 43 min, Mean ± SD, n=11 cells), Dup RNAi after Binucleine-2 addition (t=29.65 ± 4.31 min Mean ± SD, n=18), Dup/ Mad2 RNAi (t=22.1 ± 6.0 min, Mean ± SD, n=31 cells, $p<0.001$, Mann-Whitney Rank Sum test). (D) Mitotic duration of Dup/Nod RNAi, (t=208 ± 109 min, Mean ± SD, n=25 cells), Dup/Nod RNAi + Binuclein-2 (t= 26.71 ± 5.52 min, Mean ± SD, n=15), Dup/Nod/ Mad2 RNAi (t=24 ± 4.9, n=7, $p<0.001$, Mann-Whitney Rank Sum test) showing that the mitotic delay observed in chromokinesin-depleted SMUGs is due to inefficient satisfaction of the SAC. (E) Live cell imaging of Nod/Klp3A and Dup/Nod/Klp3A depleted *Drosophila* S2 cells stably expressing H2B-GFP (green) and mCherry-α-tubulin (red). Depletion of both Chromokinesins led to increased mitotic duration and chromosome alignment defects in control cells and SMUGs. Time=h:min. Scale bar = 5 μm. Error bars represent standard deviation.

4.2.2.4 PEFs promote the conversion from lateral to end-on KT-MT attachments on mono-oriented chromosomes

HeLa cells undergoing MUGs satisfy the SAC independently of bi-orientation mainly by establishing merotelic attachments (O'Connell et al., 2008). Due to opposite spindle forces, merotelic attachments might cause KT deformation that generates sufficient intra-KT stretch that would satisfy the SAC (Maresca and Salmon, 2009; Uchida et al., 2009). Importantly, the contribution of PEFs for SAC satisfaction could not be investigated in this system because KTs detach from chromatin, which remains decondensed during MUGs (Brinkley et al., 1988; O'Connell et al., 2009). Although we cannot exclude that, in addition to PEFs, some merotelic attachments contribute to SAC silencing in SMUGs, these attachments were rare, as indicated by our live-cell recordings and careful inspection of the respective z-stacks (Figure 4.4 A, 4.5 A).

To test whether PEFs are required to satisfy the SAC in SMUGs, independently of chromosome bi-orientation and the establishment of merotelic attachments, we investigated the duration of mitosis in Nod- depleted cells with a monopolar spindle configuration (in which only monotelic attachments can be established), after co-depletion of the kinesin-5 protein Klp61F by RNAi (Cane et al., 2013) (Figure 4.10 A). We found that SMUGs with monopolar spindles were also able to exit mitosis after a delay (t=178 ± 59 min, mean ± SD, n=9; Figure 4.10 A), which was exacerbated after Nod co-depletion (t=379 min ± 132 min, Mean ± SD, n=4, p=0.011, Mann-Whitney Rank Sum test; Figure 4.10 A). Closer inspection of z-stacks from live-cell images of monopolar spindles in SMUGs revealed a clear transition from lateral to end-on KT-MT attachments prior to mitotic exit, and the presence of Nod-mediated PEFs promoted this transition (Figure 4.10 B, C). Immunofluorescence analysis with a Mad1 antibody confirmed that the percentage of unattached KTs in SMUGs with monopolar spindles (35%) increased after Nod depletion (62%, p=0.028, t-test; Figure 4.10 D). Overall, these data demonstrate that Chromokinesin-mediated PEFs promote the conversion from lateral to stable end-on KT-MT attachments, independently of bi-orientation and merotely.

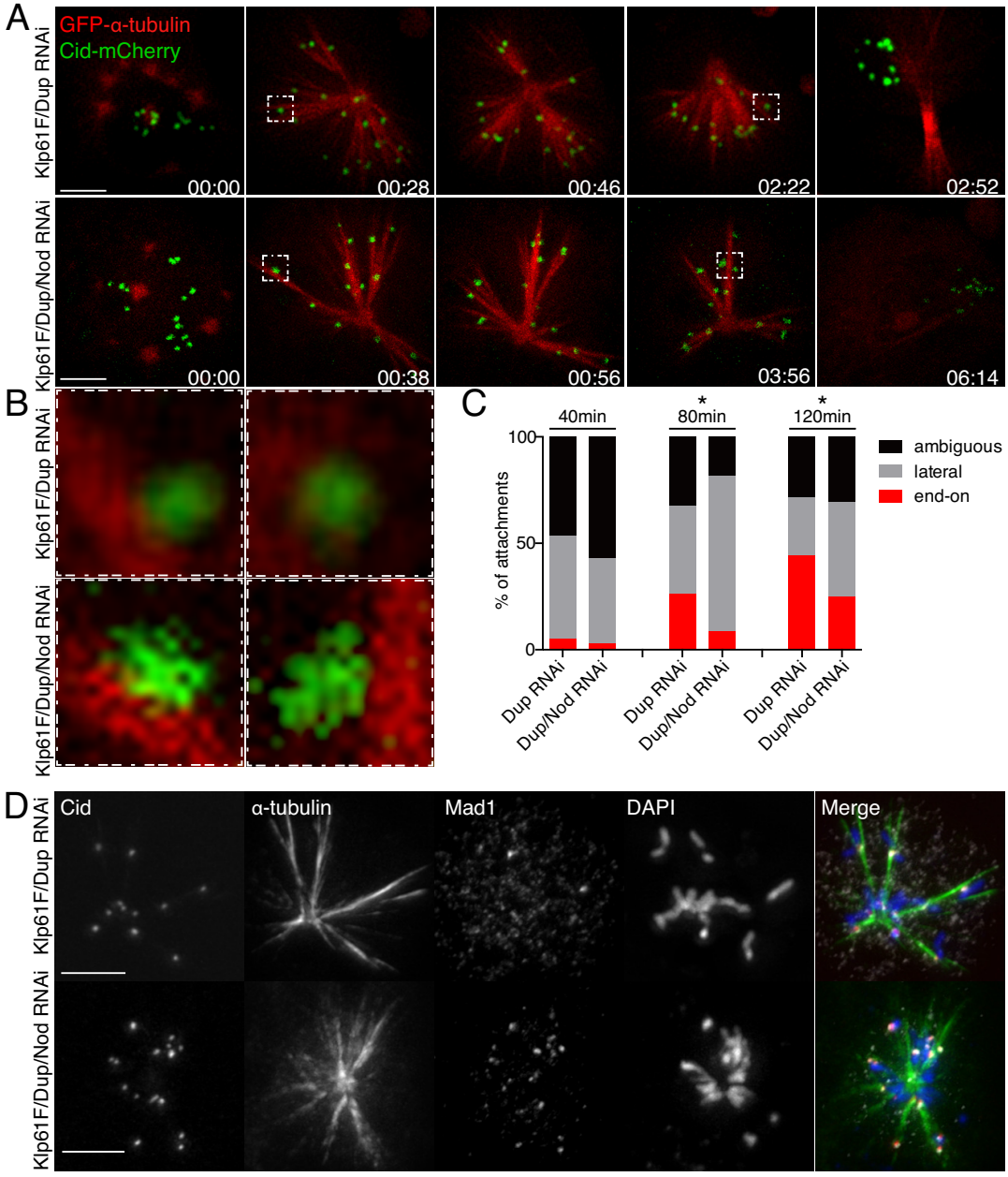

Figure 4.10: **PEFs promote the conversion from lateral to end-on KT-MT attachments on mono-oriented chromosomes.** A) Live cell imaging of Klp61F/Dup and Klp61F/Dup/Nod depleted S2 cells stably expressing GFP-α-tubulin and Cid-mCherry. (B) Respective higher magnifications of lateral and end-on attachments from A. (C) Quantification of the different KT-MT attachments (through z-stacks) in Klp61F/Dup/Nod RNAi and Klp61F/Dup RNAi cells. The difference in the percentage of end-on attachments between Klp61F/Dup RNAi (n=7 cells) and Klp61F/Dup/Nod RNAi cells (n=5 cells) at 80 min and 120 min after NEB are statistically significant (Z-test compare proportions, $p<0.05$). (D) Immunofluorescence of Klp61F/Dup and Klp61F/Dup/Nod depleted S2 cells. Nod depletion in monopolar SMUGs lead to increased number of Mad1 positive KTs. Time = h:min. Scale bar = 5 μm. Scale bar in higher magnification panels = 2 μm. *** $p < 0.001$ relative to the previous time point, t-test. Error bars represent standard deviation.

4.2.3 Discussion

Chromosome bi-orientation is a critical requirement for accurate chromosome segregation during mitosis and requires that both KTs are stably attached to spindle MTs. Tension from spindle forces has long been known to stabilize correct KT-MT attachments (King and Nicklas, 2000), but how the first end-on attachments are stabilized before the development of tension has remained unknown. Here we found that PEFs promote the conversion from lateral to stable end-on KT-MT attachments on mono-oriented chromosomes. Lateral attachments to spindle MTs are insensitive to Aurora B activity (Kalantzaki et al., 2015) and are initially mediated by KT dynein, which is dominant over PEFs at the spindle poles (Barisic et al., 2014) and inhibits the action of the Ndc80 complex required for stable end-on attachments (Cheerambathur et al., 2013). Despite not being dominant at this stage, PEFs promote the exclusion of chromosomes from the central area of the mitotic spindle (Magidson et al., 2011), but chromosomes remain tethered to the MT walls by CENP-E/Kinesin-7 (Shrestha and Draviam, 2013), which slides chromosomes preferentially along detyrosinated MTs towards the spindle equator (Barisic et al., 2015). At the equator PEFs become critical to stabilize end-on KT-MT attachments required for chromosome bi-orientation (Barisic et al., 2014; Magidson et al., 2011; Wandke et al., 2012).

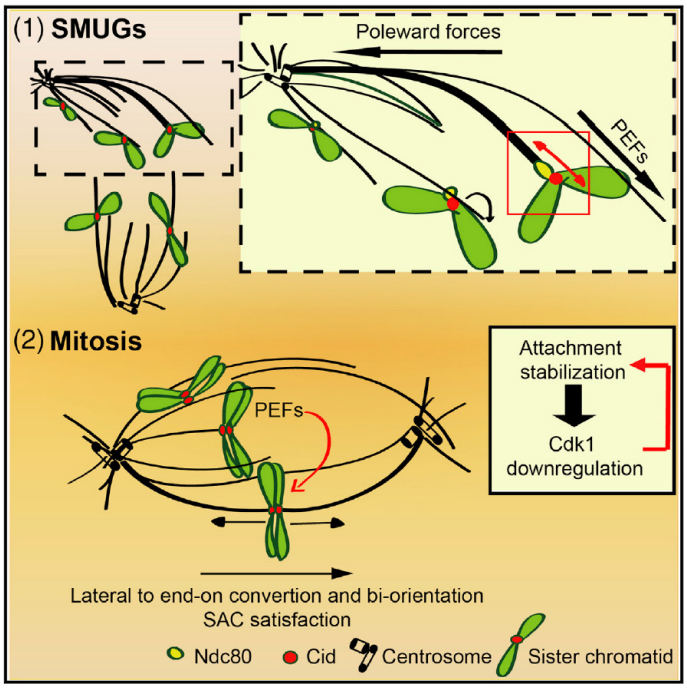

Figure 4.11: **PEFs contribute to the lateral to end-on conversion of KT-MT attachments.** Model illustration of the SMUGs, shows the role of PEFs in lateral to end-on attachment conversion of mono-oriented chromosomes. Due to the opposite directionality of poleward forces and PEFs, intra-KT stretch/structural deformation lead to stabilization of end-on attachments, cyclin B1degradation induced Cdk 1downregulation and mitotic exit.

In this context, our data can be best explained by a model in which the lateral to end-on conversion of KT-MT attachments near the equator requires the contribution of Chromokinesin-mediated PEFs acting on the arms of mono-oriented chromosomes to counteract MT depolymerization-driven poleward motion. This might generate sufficient intra-KT stretch or structural deformation (Maresca and Salmon, 2009; Uchida et al., 2009) that leads to the stabilization of end-on KT-MT attachments (Figure 4.11).

Cdk1 down-regulation due to Cyclin A and B1 degradation might generate positive feedback loops that, in coordination with PEFs, further stabilize KT-MT attachments (Collin et al., 2013; Kabeche and Compton, 2013). While this eventually leads to SAC satisfaction after a significant mitotic delay in SMUGs, we propose that during normal mitosis this mechanism contributes to the stabilization of initial end-on KT-MT attachments, before tension from opposing spindle forces is established during bi-orientation.

4.2.4 Materials and methods

4.2.4.1 Cell culture and drug treatments

Drosophila S2 cells were kept in Schneider's medium (Gibco-BRL) containing 10% heat inactivated fetal bovine serum (FBS) (Invitrogen) at 25°C incubator.

For live cell imaging, we used cell lines stably expressing fluorescent proteins: GFP-H2B/mCherry-α-tubulin (Afonso et al., 2014a), GFP- α tubulin/Cid-mCherry (Matos et al., 2009), Cyclin B1-GFP/mCherry- α -tubulin (Afonso et al., 2014a), BubR1-mCherry/GFP- α tubulin (Matos et al., 2009), GFP- α tubulin/Nod-mCherry (Cane et al., 2013), and Cid-mCherry/Ndc80-GFP (Maresca and Salmon, 2009). For colchicine treatment, 200 μM Colchicine (Sigma-Aldrich) was added immediately after NEB both in control cells and SMUGs. Dup and Dup/Nod RNAi cells were treated with 40 μM Binucleine -2 (Sigma-Aldrich) after NEB to inhibit SAC response (Moutinho-Pereira et al., 2013).

4.2.4.2 RNA interference

S2 cells were plated in six-well plates (1x10^6 cells/well), and incubated for 2 h with Schneider's medium without FBS containing 10 μg/ml of Dup, Nod or Mad2 dsRNA. For dsRNA synthesis, we used following primers:
(Dup) forward: 5'-TAATACGACTCACTATAGGGGTCATAACGTGTGGATTCATGG-3' and reverse: 5'-TAATACGACTCACTATAGGGCAAGACTCCCACAAAAATACCG-3';
(Nod) forward TAATACGACTCACTATAGGGACCTGGGTATTCTGCCTCG-3' and

reverse 5'-TAATACGACTCACTATAGGGGTATGGTATCACTGTGTGGCCC-3';
(Klp3a) forward 5'-TAATACGACTCACTATAGGGCTTACTAACCGTCCTGGACTCG-3',
reverse 5' - TAATACGACTCACTATAGGGAATCCAAGGTGAAGCTCATACG-3';
(Mad2) forward 5'-TAATACGACTCACTATAGGGAATAGCGGCAATTTAGC- 3',
reverse 5'-TAATACGACTCACTATAGGGAGAAGCGCAGCTGGA-3' (Orr et al., 2007),
(Klp61F) forward 5'-TAATACGACTCACTATAGGGCAAAAATAGCATCAGCATGTCC-3',
reverse 5'-TAATACGACTCACTATAGGGGGATAAACGAAATCCCTTTTGG-3'. After 2 h, normal Schneider's medium (Gibco-BRL) with 10% FBS was added and cells were kept for 96 h at 25°C for efficient knockdown (Maiato et al., 2003b).

4.2.4.3 Immunofluorescence

Control cells and SMUGs were seeded on Concanavalin A (Merk Milipore) treated coverslips. Fixation was performed with 4% paraformaldehyde, followed by extraction with 0.3%Triton in PBS for 10 min. Cells were washed three times with PBS + 0.05% Tween, and blocked in 10% FBS for 1h, followed by primary antibody incubation for 1h at room temperature (RT). After primary antibody incubation, coverslips were washed three times with PBS + 0.05% Tween and incubated for 45 min at RT with the secondary antibodies (Alexa 488, Alexa 568, Alexa 647, Invitrogen 1:1000 dilutions) in blocking solution. After washing, cells were incubated 5 min with DAPI (Sigma, 1 μg/ml), washed with PBS and sealed on slides using mounting media (20 mM Tris pH8, 0.5 N-propyl gallate, 90% glycerol). Primary antibodies used were: mouse anti–tubulin (1:2000; B-512 clone, Sigma); rat anti-Cid (1:2000), rabbit-anti-Mad2 and rabbit-anti-Mad1 (1:1000) (kind gifts from Claudio Sunkel, IBMC, University of Porto, Portugal) (Conde et al., 2013), rabbit anti-pKnl1 (1:1000) (Welburn et al., 2010) (kind gift from Iain Cheeseman, Whitehead Institute, MIT, Boston), rabbit anti-pT232 AuroraB (Rockland Immunochemicals). For image analysis and acquisition we used a Zeiss AxioObserver Z1 wide-field microscope equipped with a plan-apochromat (1.46 NA 100x) DIC objective and a cooled CCD (Hamamatsu Orca R2). Images were deconvolved using Autoquant X (Media Cybernetics) and processed for publication with Fiji (ImageJ) and Adobe Photoshop CS4 (Adobe Systems).

4.2.4.4 Live cell imaging

Drosophila S2 cells were plated on Concanavalin A coated (0.25 mg/ml) MatTek dishes (MatTekCorporation) 2-3 h prior to live cell imaging. Live imaging of GFP-α-tubulin/Cid-mCherry, H2B-GFP/mCherry-α-tubulin, CyclinB1-GFP/mCherry-α-tubulin,

BubR1-mCherry/GFP-α-tubulin, GFP-α-tubulin /Nod-mCherry was performed on a temperature-controlled Nikon TE2000 microscope equipped at the camera port with a modified Yokogawa CSU-X1 spinning-disc head (Solamere Technology), an ASI FW-1000 filterwheel and an Andor iXon+ DU-897 EM-CCD. The excitation optics is composed of two sapphire lasers at 488 nm and 561 nm (Coherent), which are shuttered by an acousto-optic tunable filter (Gooche&Housego, model R64040-150) and injected into the Yokogawa head via a polarization-maintaining single-mode optical fiber (OZ optics). Sample position is controlled by a SCAN-IM stage (Marzhauser) and a 541.ZSL piezo (Physik Instrumente). The objective is an oil-immersion 100x 1.4 NA Plan-Apo DIC CFI (Nikon, VC series), yielding an overall (including the pinhole-imaging lens) 112 nm/pixel sampling. A 1.5x tube lens (optivar) was also used (75 nm/pixel sampling). A 2 min time-lapse interval and 0.5 μm step image stack was used in all acquisitions, except for intra-KT stretch measurements where it was used a 15 min time interval and 0.22 μm step image stack. The system was controlled by NIS-Elements via a DAC board (National Instruments, PCI-6733).

4.2.4.5 Immunoblotting

Immunoblotting was used to confirm protein depletion. After boiling protein extracts for 5 min in SDS sample buffer, samples were run on SDS-PAGE and transferred to nitrocellulose membranes. Blots containing proteins were incubated with primary antibodies: mouse anti–tubulin (1:2000; B-512 clone, Sigma), rabbit anti-GFP (kindly provided by Frederico Silva, IBMC, University of Porto, Portugal), rabbit-anti-Mad2 (1:1000) (kind gift from Claudio Sunkel, IBMC, University of Porto, Portugal) (Conde et al., 2013).

4.2.4.6 Quantification of KT-MT attachments

In order to distinguish the different types of KT-MT attachments in SMUGs, we performed live-cell imaging in *Drosophila* S2 cells stably expressing GFP-α-tubulin/Cid-mCherry. Images were analyzed using FIJI (ImageJ) software through z-stacks (0.5 μm). KT-MT attachments were quantified after tracing MT positioning in relation to the Cid signal (KTs). When MTs passed by the Cid signal the attachment was considered as lateral. When MTs ended at the KT they were considered as end-on attachments. Since in SMUGs chromosomes do not align in the spindle equator, merotelic attachments were rarely observed and were distinguished as having long K-fibers coming from opposite poles that ended on the same KT.

4.2.4.7 Measurement of Intra-KT stretch/deformation

Drosophila S2 cells stably expressing Cid-mCherry/Ndc80-GFP (Maresca and Salmon, 2009) were used for intra-KT stretch measurements in fixed (4% paraformaldehyde) material and for live cell imaging (intra-KT stretch measurements over time). Sub-pixel determination of fluorescent spot localization was performed using a home-written Matlab script (Mathworks). A sequential refinement of the spot position starts with manual (mouse) selection of the KT ensemble to be measured. A neighborhood (ROI) (11 x 11 pixels) is defined around each selected point, the boundary of which is used to estimate average background signal per pixel. This background value is subtracted and the centroid is then calculated to allow recentering of the ROI. This first part of the script is meant as a coarse correction of the mouse-defined points. Before fitting a circular two-dimensional Gaussian function to each ROI intensity map, an empirical parameter of 1/2 was chosen as the fraction of (highest gray-value) ROI pixels to be fed into the fitting procedure thus avoiding the bias induced by residual fluorescence of adjacent structures (e.g., defocused adjacent KTs). Fitting is performed using the least-squares fitting routine lsqcurvefit.

4.3 Experimental work III

KT size generates a bias in the chromosome congression and bi-orientation pathway

4.3.1 Introduction

After NEB, MT coming from the spindle poles explore cytoplasm “searching” for chromosomes, and “capturing” them via protein structures called KTs (Kirschner and Mitchison, 1986). Mitotic fidelity depends on the establishment of correct attachments between KTs and spindle MTs. Theoretical models have shown that after NEB, chromosomes are spatially positioned in a ring around the newly formed mitotic spindle, which facilitates their capture by MTs (Magidson et al., 2011). Disruption of such prepositioning by MT depolymerizing drugs (eg. nocodazole) at the prometaphase, increases the rate of error formation (Magidson et al., 2011).

In the instances when chromosomes are positioned favorably between two poles at NEB, sister KTs become directly attached to the MTs coming from opposite poles (amphitelic attachments). In other cases, when chromosomes are closer to one of the poles, their alignment towards the equatorial plate depends on the coordinated activity of motor proteins like Cenp-E (kinesin-7), dynein and chromokinesins (Barisic et al., 2014; Li et al., 2007; Maiato et al., 2017; Walczak et al., 2010). During mammalian mitosis, only few chromosomes depend on motor proteins to align at the metaphase plate. Which depends on their position relative to spindle poles at NEB (Barisic et al., 2014). Yet, it remains unclear whether there is a bias for specific chromosomes to preferably locate at the periphery near the poles prior to alignment (Maiato et al., 2017).

It is widely accepted that KT size and composition changes as a response to MT attachment status. In the beginning of the mitosis, as well as in the absence of MTs (nocodazole treatment), outer KTs increase forming wide crescent structures (Hoffman et al., 2001; Magidson et al., 2015; Maiato et al., 2006; Rieder, 1982). These changes in KT structure are due to the recruitment of KT proteins that form the outer corona, and include SAC proteins and some motor proteins (CENP-E, dynein) (Thrower et al., 1996; Wynne and Funabiki, 2015). Based on theoretical predictions, upon initial attachments, these crescent structures reduce their size lowering the probability for error formation (Magidson et al., 2015; Thrower et al., 1996; Zaytsev and Grishchuk, 2015). However, how KT size influences MT capture and attachment formation remains unknown.

Importantly, centromere size of human chromosomes is highly variable (e.g. centromeres of chromosome 18 are several fold bigger than the ones of the y chromosome) (Cherry et al., 1989; Cherry and Johnston, 1987). Addressing the aforementioned questions in human cells is bound with technical limitations and distinction of KT size amongst most chromosomes

(except the y chromosome) is limited by diffraction and thus cannot be resolved by light microscopy.

In order to address the role of KT size during mitosis we took advantage of an IM fibroblast cells, the mammalian cells with the lowest chromosome number (2n=6,7, female and male respectively) (Brinkley et al., 1984; Carrano et al., 1976; Wurster and Benirschke, 1970; Zinkowski et al., 1991; Zou et al., 2002). Besides the low chromosomal number, DNA fusions during evolution from an ancestor genome, also give rise to large chromosomes with unusually big compound KTs (Brinkley et al., 1984; Chi et al., 2005; He and Brinkley, 1996; Johnston et al., 1982; Lin et al., 1991; Murmann et al., 2008; Tsipouri et al., 2008; Yang et al., 1997; Zhou et al., 2006; Zinkowski et al., 1991). One of the chromosomes, that represents the fusion between autosome 3 and the X chromosome, contain remarkably large compound KT that can bind up to 100 MTs (Brinkley et al., 1984; Comings and Okada, 1971; Wurster and Benirschke, 1970; Zinkowski et al., 1991). Since the three pairs of IM chromosomes are morphologically distant (metacentric vs acrocentric) they can also be easily tracked by live cell imaging. Using this model system and state-of the art microscopy, we studied the effect of KT size during mitosis. Our experimental data show that chromosomes with bigger KTs tend to align more efficiently at the metaphase plate in a CENP-E independent manner comparing with the chromosomes that contain smaller KTs. However, formation of erroneous attachments is more frequent in chromosomes with large KTs. Thus, our experimental results show that although bigger KTs facilitate the initial capture by MTs and bias for direct bi-orientation soon after NEB, they are also more prone for errors, supporting a model in which control of KT size is critical for mitotic fidelity.

4.3.2 Results

4.3.2.1 Mitosis in IM fibroblast cells

To investigate the role of KT size during mitosis we took advantage of IM fibroblast cells stably expressing H2B-GFP (Kanda et al., 1998) or CENP-A-GFP (Figure 4.12, A, B). Since these cells were previously immortalized with human telomerase- hTERT (Zou et al., 2002), adding a third plasmid (besides H2B-GFP or CENP-A-GP) for dual-color labeling was technically very difficult. To overcome this limitation we used sir Tubulin dyes, to label spindle MTs and follow mitosis in these cells (Figure 4.12 A, B).

Their low diploid chromosome number (2n=6 for female, 2n= 7 male) and their big size, represents a unique advantage for micromanipulation and high-resolution live-cell studies (Cheng et al., 2009). As a result of DNA fusions during evolution, KTs of IM cells are large;

compound structures, composed of a line of subunits that form a bead like structure that can bind up to 100 MTs (Brinkley et al., 1984; Wurster and Benirschke, 1970; Zinkowski et al., 1991). Chromosome spreads of IM fibroblasts showed 3 pairs of morphologically different chromosomes (one metacentric and two acrocentric) (Figure 4.12 C). One of the chromosomes that contain unusually large KT (KT length = 1.99 μm ± 0,50, mean± SD; n= 85 KTs measured in chromosome spreads) is a result of the fusion between autosome 3 and X chromosome (Figure 4.12 C) (Brinkley et al., 1984; Lin et al., 1991; Murmann et al., 2008; Yang et al., 1997; Zhou et al., 2006; Zinkowski et al., 1991).

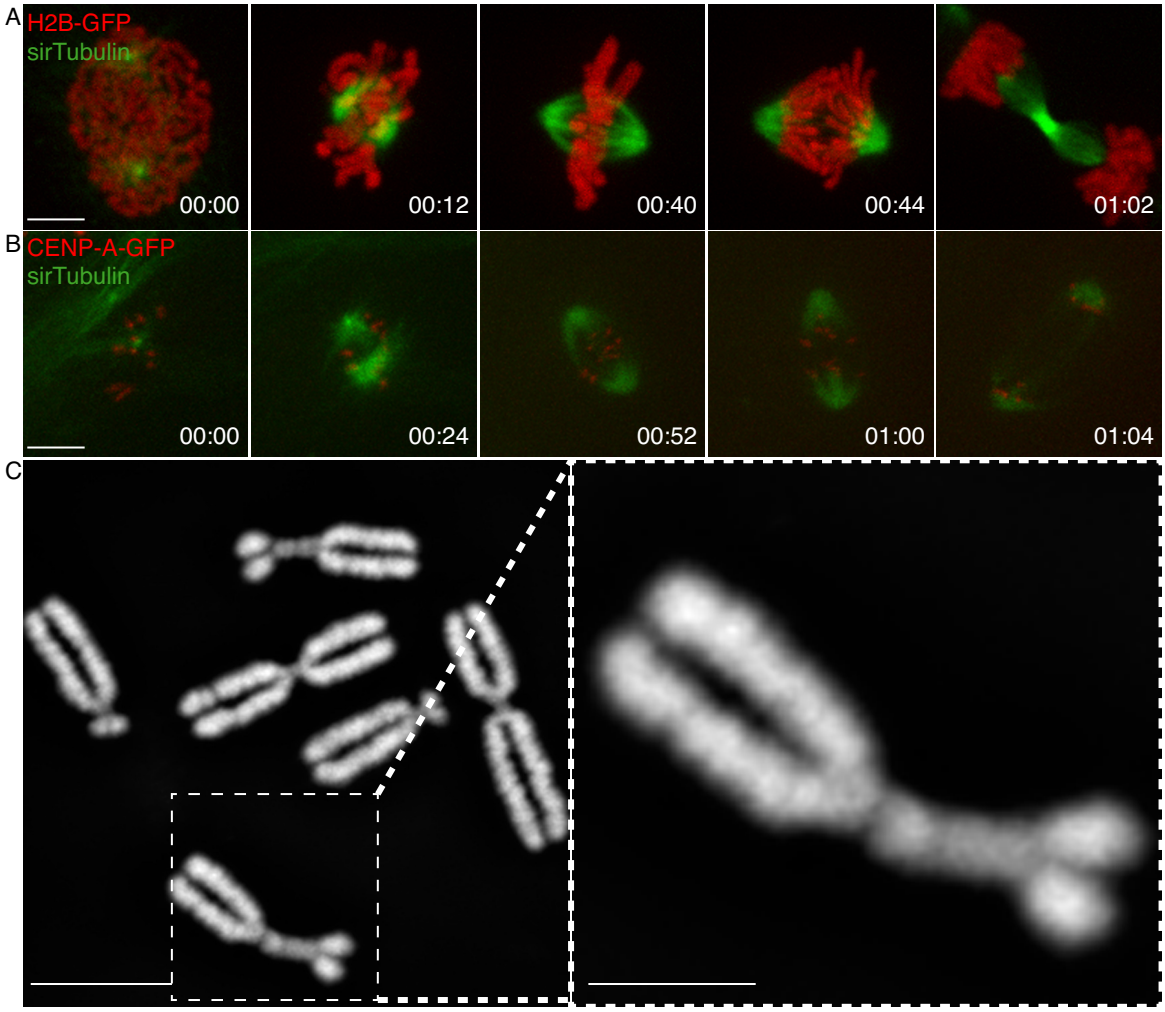

Figure 4.12: Indian muntjac cells as a model system, (A) Live-cell imagining of IM fibroblast cell stably expressing human H2B-GFP and treated with 20nM sirTubulin dye, H2B-GFP in red, sirTubulin in green, (B) Live cell imaging of IM fibroblast cells stably expressing human CENP-A-GFP and treated with 20nM sirTubulin dye, CENP-A-GFP in red, SirTubulin in green (C) Chromosome spread of immortalized female IM fibroblast cells, chromosomes labeled with DAPI, Scale bar 5 μm, Scale bar in cropped single chromosome 2 μm, Time in h : min.

In our experiments we used female immortalized cell line that contains two of 3 + X chromosomes with big KT and 4 chromosomes with smaller KTs. The apparent difference be-

tween KT size in the chromosomes of IM cells, allowed us to perform live cell imaging and track the chromosomes in H2B-GFP and CENP-A-GFP cell lines. (Figure 4.12 C). Using live - cell spinning - disc confocal imaging, we were able to follow mitosis in IM cells (Figure 4.12 A, B). Typically control IM cells spend t= 40.76 ± 12.49 min, (mean ± SD; n= 42 cells) in mitosis, measured from NEB to anaphase.

4.3.2.2 The congression pathway does not depend on the type of the chromosome

To gain deeper insights about the role of KT size in chromosome congression we performed live cell imaging using IM fibroblasts stably expressing CENP-A-GFP. Previous studies have shown that after disassembly of the nuclear envelope, chromosomes can undergo one of two congression pathways (Barisic et al., 2014; Maiato et al., 2017). First, chromosomes can bi-orient soon after NEB and align at the metaphase plate. Or, they depend on lateral sliding along MTs by motor proteins to align at the equator zone of mitotic spindle (Barisic et al., 2014; Maiato et al., 2017). In human cells, after inhibiting CENP-E (kinesin-7) motor protein, around 15 – 20 % of the chromosomes stay attached to one of the poles, while the rest of the chromosomes align at the metaphase plate. Barisic et al, showed that chromosome alignment is determined on chromosome position relative to the poles at the moment of NEB (Barisic et al., 2014). However, which chromosomes depend on CENP-E motor activity to align remains unknown due to the limitation in distinguishing different chromosomes in human cells. To address this question we treated IM cells with 20 nM CENP-E inhibitor, GSK923295, (acts by locking the motor protein on MTs) one hour before NEB (Bennett et al., 2015; Wood et al., 2010) (Figure 4.13 B, C, D).

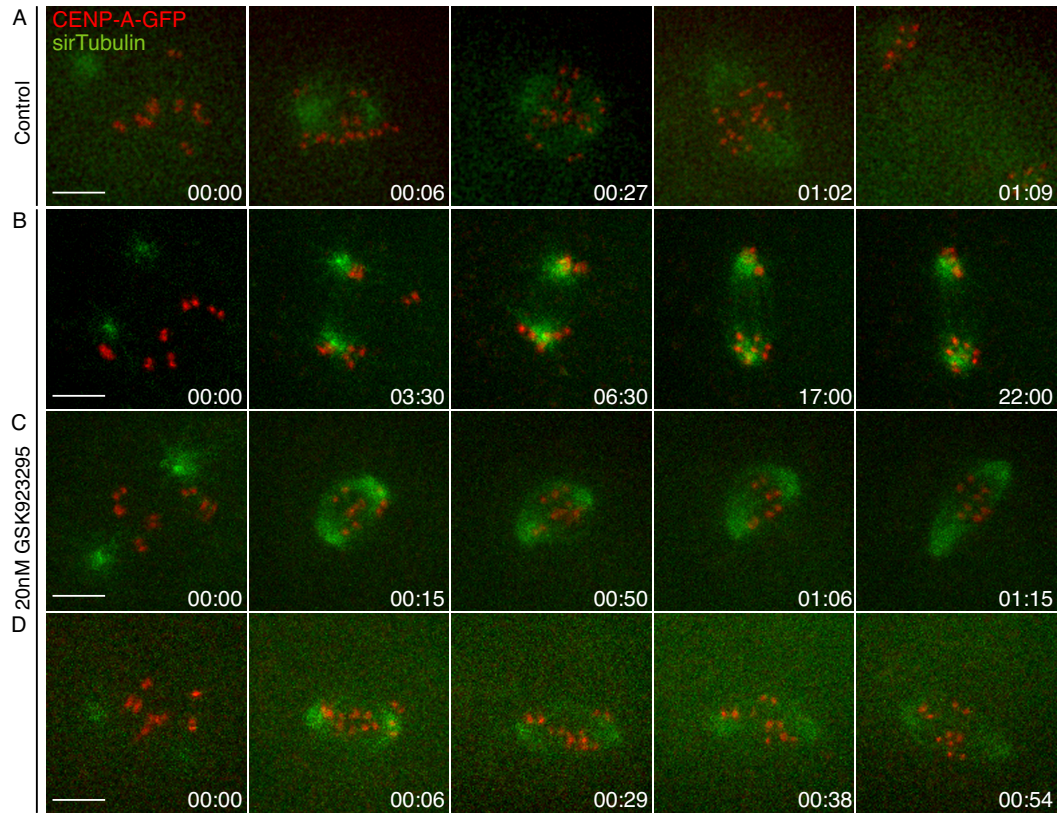

Figure 4.13: **The congression pathway does not depend on the type of the chromosome.** IM fibroblast cells stably expressing CENP-A-GFP (red) and treated with 20nM sir-Tubulin (green) (A) Control cells (B-D) Cells after CENP-E inhibition with 20nM GSK923295, CENP-A-GFP in red, Sir Tubulin in green, Scale bars 5 μm, Time in min : sec, except in second panel time in sec : sec

Live cell imaging revealed that upon CENP-E inhibition in IM cells, three different scenarios can occur: 1) In very few cells when centrosomes didn't separate fully before NEB, all chromosomes went to the poles (n = 2 cells from 28 cells, 6 independent experiments) (Figure 4.13 B). 2) In most of cases chromosomes would align at the metaphase plate and some would attach to the pole (Figure 4.13 C) (n = 20 cells from 28 cells, 6 independent experiments). 3) In the third situation, all chromosomes managed to align at the metaphase plate soon after NEB (Figure 4.13 D) (n = 6 cells form 28 cells, 6 independent experiments). From these data we can conclude that any chromosome can use one or the other pathway depending on the position relative to the poles.

4.3.2.3 KT size can bias the chromosome congression pathway

To investigate whether KT size influences the congression pathway as seen by the probability of finding chromosomes with big or small KT size at the pole. Since IM fibroblast cells exhibit high percentage of aneuploidy and polyploidy, we screened only for the cells that con-

tain 6 chromosomes. Immunofluorescence images were analyzed for the position of each chromosome in mitotic spindle after CENP-E inhibition (Figure 4.14 A). The position of the 4 chromosomes with small KTs and the 2 chromosomes with big KTs was quantified and statistical analyses were performed (n= 300 cells, 5 independent experiments). The data allowed the construction of a joint probability table involving two defined random variables: S, the number of chromosomes with small KTs that stay at the pole; and B, the number of chromosomes with big KTs that stay at the pole. From the analysis of the joint probability table it was possible to draw the following conclusions: 1) The number of small KTs, and big KTs, that stay at the pole is well described by a binomial distribution. This means that the fate of each chromosome is independent of the other chromosomes in the same class (with small or big KTs). 2) The two random variables S and B are roughly independent. This means that the state of the small KTs says nothing about the state of the big KTs, and vice-versa. 3) Under the binomial distributions description, the probability of each individual chromosome with small KTs to stay at the pole is almost double of the probability for chromosomes with big KTs: 22% for small KTs versus 12% for big KTs. (Figure 4.14 B).

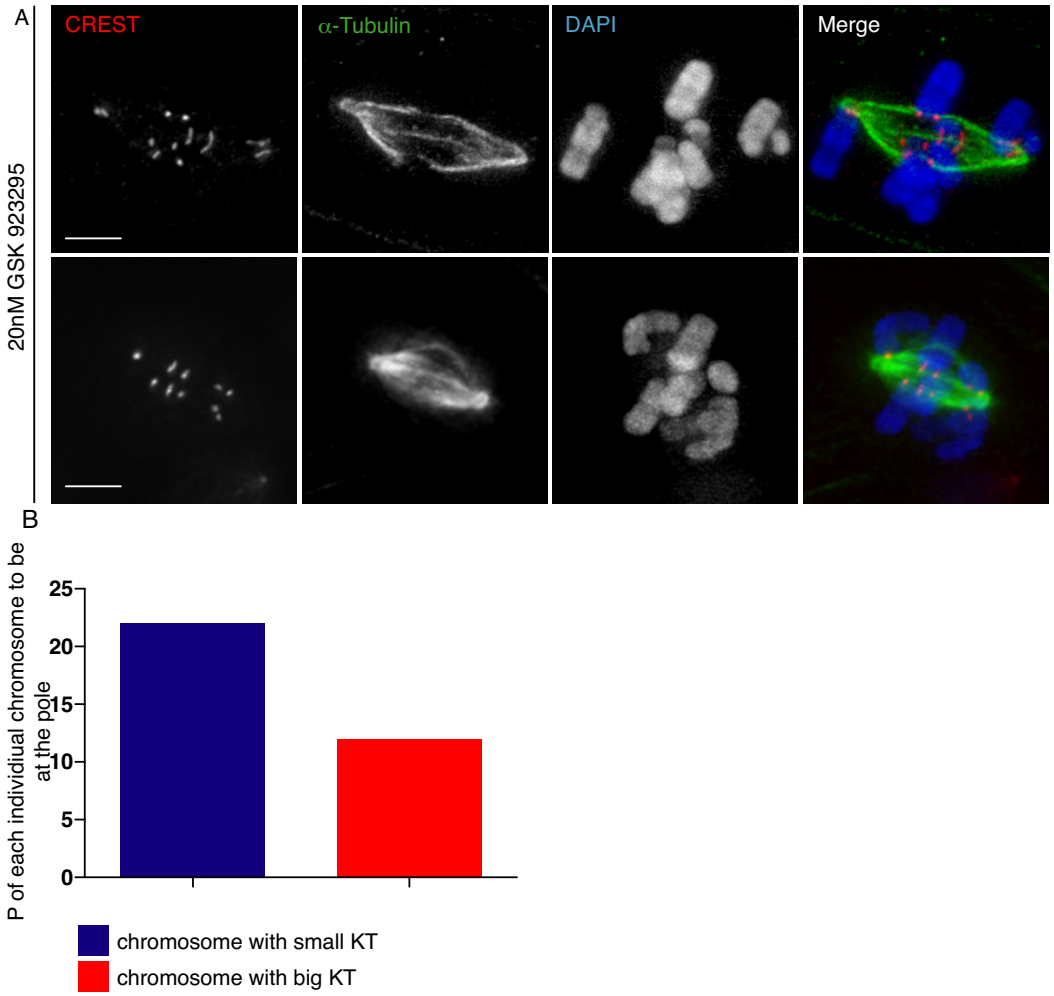

Figure 4.14: **KT size influences the congression pathway.** Chromosomes with bigger KTs have a higher probability to use a direct pathway of congression. (A) Immunofluorescence images of IM fibroblast cells after CENP-E inhibition, (cells were incubated 1h with 20nM GSK923295 before fixation), KTs in red, α-tubulin in green, chromosomes in blue, (B) Immunofluorescence quantifications of IM fibroblast cells. Graph shows probability of each individual chromosome containing big KT or small KT to stay bound at the pole after CENP-E inhibition, (n=300 cells, 3 independent experiments). Blue-Percentage of chromosomes with small KTs at the pole, Red - percentage of chromosomes with big KTs at the pole. Scale bar 5 μm

In contrast, chromosomes with smaller KTs depend more on CENP-E motor activity to align (Figure 4.15 B). Given that we can find both types of chromosomes at the pole, we can conclude that every chromosome, independently of KT size, can use any of the two pathways to congress (Figure 4.14 A). Yet, chromosomes with bigger KTs have higher probability to bi-orient and align more efficiently when, compared with chromosomes with smaller KTs which rely more on the activity of CENP-E.

Previous reports in human cells have shown that the position of the chromosomes prior to NEB defines the chromosome congression pathway (Barisic et al., 2014). To test weather the aforementioned bias was due to initial position of chromosomes with bigger KT at NEB,

we performed four-dimensional (4D, x,y,z,t) tracking of big KTs 30 min after NEB in cells treated with CENP-E inhibitor. After analyzing KT-tracking data, (n= 8 cells, 14 big KTs) we were unable to find a correlation between the position of the chromosomes with big KT and the congression pathway (Figure 4.15).

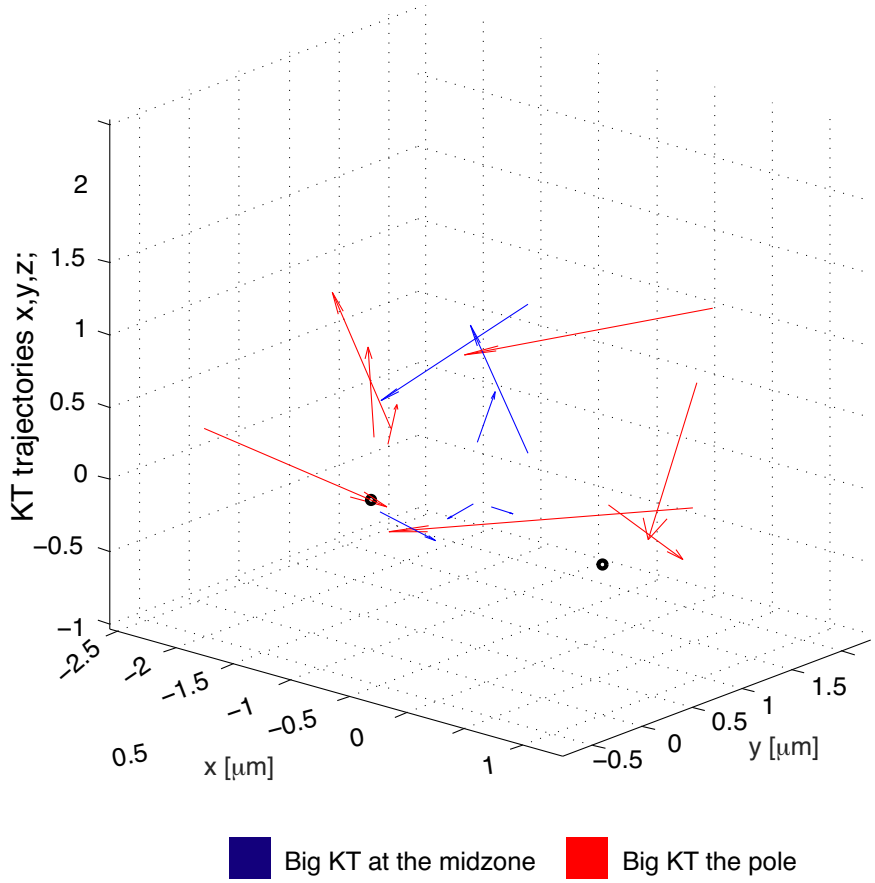

Figure 4.15: **Congression pathway does not depend on preposition of chromosome.** 4D (x, y, z, t)- KT tracking of chromosomes with big KT 30 min after NEB, upon CENP-E inhibition (n= 14 big KTs from 8 cells). Red arrows indicate the position of big KTs that finish at the pole 30 min upon CENP-E inhibition. Blue arrows indicate the position of big KTs that aligned at the midzone at the presence of CENP-E inhibitor. Black dots represent spindle poles.

These results suggest that the congression pathway does not depend on the type and preposition of the chromosomes. However chromosomes with bigger KTs are more probable to bi-orient by MTs coming from opposite poles and align at metaphase plate soon after NEB indicating the importance of KT size in initial MT attachments.

4.3.2.4 KT size affects chromosome segregation

We next tested the importance of KT size in error formation. The consequence of erroneous attachments in the first stages of mitosis is the formation of merotelic chromosomes during anaphase (Bakhoum et al., 2009; Bakhoum et al., 2014; Cimini et al., 2004). Screening for IM anaphase cells by Immunofluorescence we revealed a very low rate of lagging chromosomes. In 267 control anaphase cells (from 3 independent experiments) we detected only 4 cells with lagging chromosomes (1.49 %) indicating that IM cells are very efficient in mitosis, which might be due to their low chromosome number (Figure 4.16 A). In order to increase the number of lagging chromosomes, we treated cells with monastrol, inhibitor of the kinesin-5 (Eg5). By inhibiting Eg5 motor activity, during prophase centrosome separation, leads to bipolar spindle collapse and formation of monopolar spindles (Lampson and Kapoor, 2006). In monopolar spindles, chromosomes are not able to establish amphitelic attachments, and form unstable and erroneous monotelic, syntelic or lateral attachments (Loncarek et al., 2007) (Figure 4.16 C).

After 12h of incubation with 100 μM monastrol, cells were washed out into fresh Minimum Essential Media (MEM) with or without ZM 447439 (Aurora B inhibitor) to inhibit error correction (Lampson and Kapoor, 2006; Lampson et al., 2004) (Figure 4.16 A - C). As a result of monastrol treatment the number of lagging chromosomes in anaphase cells increased to 5.49% (n= 2603 anaphase cells, of which 143 cells with lagging chromosomes, 9 independent experiments). As expected, an increase in the number of cells with lagging chromosomes was even more evident when we performed monastrol washout into MEM medium containing Aurora B inhibition, 7.71%, (n= 1323 anaphase cells of which 102 had lagging chromosome, 6 independent experiments) (Figure 4.16 A - C).

By using a KT marker and DNA staining (DAPI) in fixed cell analysis we were able to differentiate the type of lagging chromosome. Although most of the cells with lagging chromosomes were triploid or tetraploid, we restricted statistical analysis only to the cells with 6 chromosomes (Figure 4.16 C).

In 35 diploid IM cells after monastrol washout into MEM, in 66% of the cells the lagging chromosome had a big KT. In contrast 29% of the cells the laggards contained a small KT (5% of the cells was not clear which chromosomes are lagging, so its defined as non applicable n.a.). In anaphase cells in which the chromosome with a big KT was lagging, the big KT was hyper-stretched, as a result of merotelic attachments and opposing pulling forces (Figure 4.16 C) (Cimini et al., 2001). These results show that KT size affects chromosome segregation, with a tendency for chromosomes with big KTs to lag more.

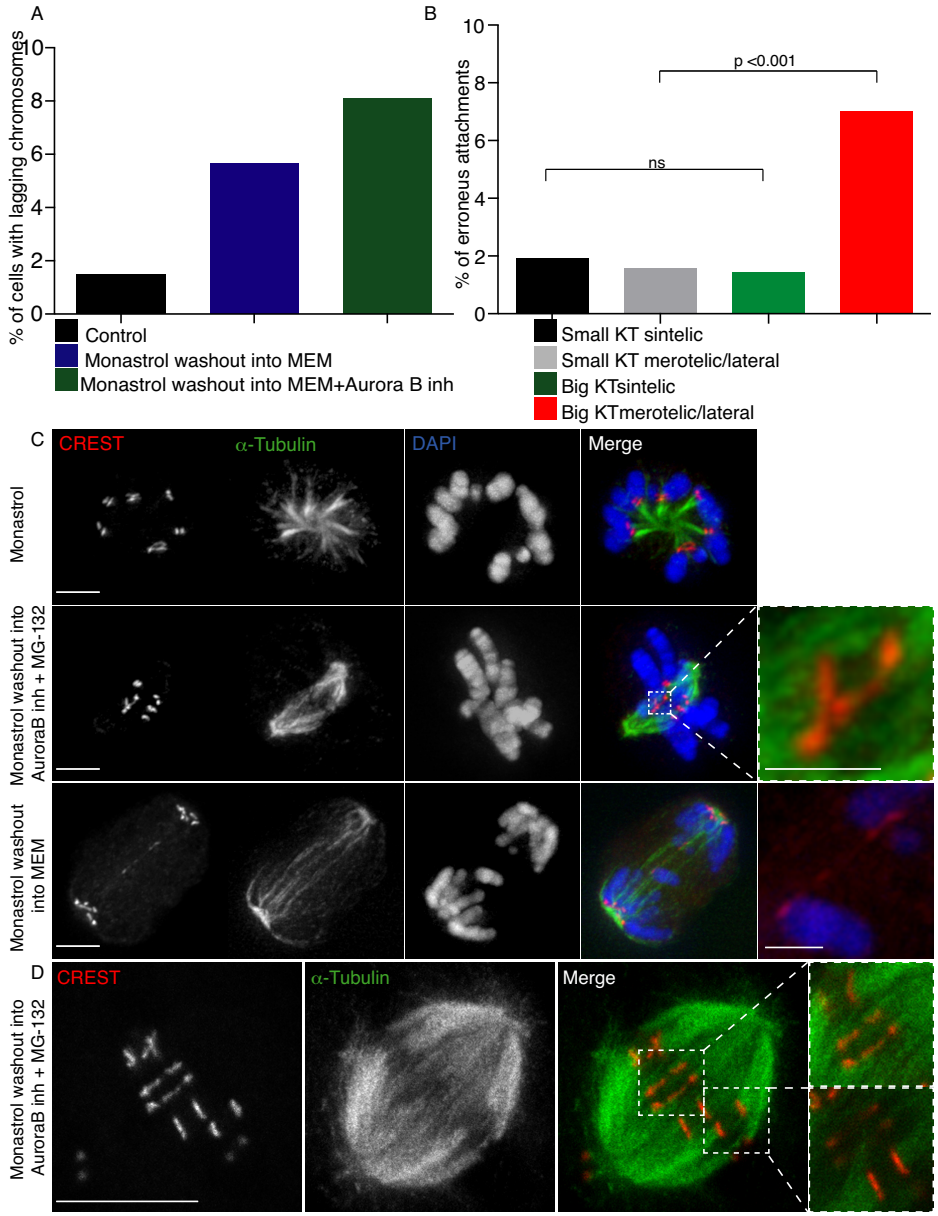

Figure 4.16: **Chromosomes with bigger KTs are more prone to form erroneous attachments during mitosis.** (A) Immunofluorescence quantifications analysis. Graph represents percentage of anaphase cells containing lagging chromosomes in control IM cells (n= 267 anaphase cells, of which 4 lagging chromosomes) IM cells washed out from monastrol into MEM medium (n=2603 anaphase cells, of which 143 with lagging chromosomes) and IM cells washed from monastrol into MEM medium containing Aurora B inhibitor (n=1323 anaphase cells, of which 102 with lagging chromosomes. (B) Quantification of KT-MT attachments of chromosomes with small and big KTs in IM cells after monastrol washout into Aurora B inhibitor and MG-132 (n=220 cells, 3 independent experiments, total number of chromosomes with small KT=828, total number of chromosomes with big KT=414). Graph represents percentage of erroneous attachments. Percentages of the KT-MT attachments were compared by statistical analysis : comparison of proportions (Chi-squared test), (C) Immunofluorescence images of IM fibroblast cells treated with 100 μM monastrol-first panel, washed out from monastrol into MEM medium containing 1 μM Aurora B inhibitor (ZM 447439) and MG-132-second panel, washed out from monastrol into MEM medium- third panel. KTs in red, α-tubulin in green, chromosomes in blue. (D) STED images of IM cells treated with Aurora B inhibitor and MG-132 inhibitor after monastrol treatment. KTs in red, α-tubulin in green. Scale bar 5 μm.

4.3.2.5 Chromosomes with bigger KTs are more prone to form erroneous attachments

To further investigate if the chromosomes with big KTs are more prone to form errors or less efficient in correcting them we inhibited the Aurora B activity after monastrol washout. By this experimental procedure we were able to prevent correction of already formed erroneous attachments. We used 1 μM concentration of Aurora B inhibitor in order to partially inhibit Aurora B, and thus avoid effects of Aurora B inhibition on spindle formation (van der Horst and Lens, 2014) (Figure 4.17 A-C).

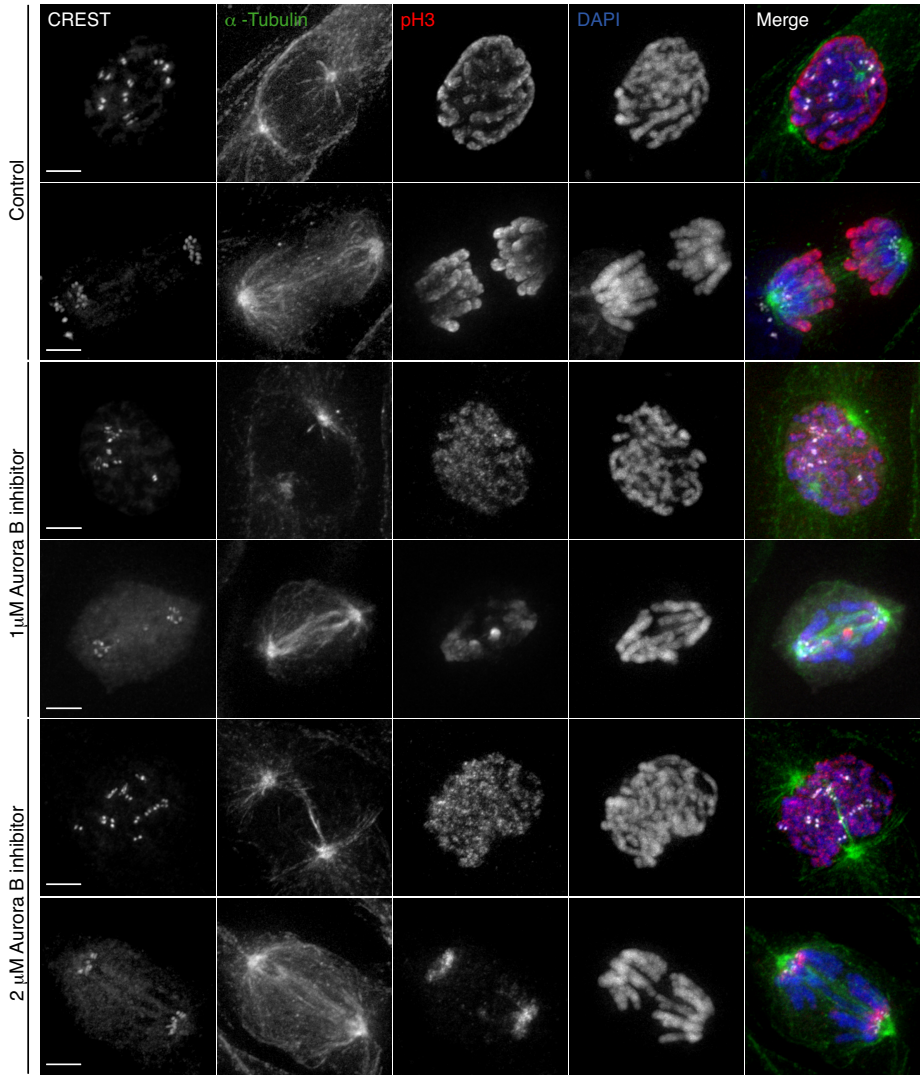

Figure 4.17: **Titration of Aurora B inhibitor in IM fibroblast cells**. Immunofluorescence images of IM fibroblast cells inhibited with Aurora B inhibitor- ZM 447439 (A) Control cells, (B) 2μM Aurora B inhibitor, (C) 1μM Aurora B inhibitor, Cells were incubated for 40 min before fixation, pH3 in red, α-tubulin in green, chromosomes in blue. Scale bar 5μm

We first tested whether there is a difference in Aurora B activity between smaller and bigger KTs, which might lead to differences in the efficiency in error correction between chromo-

somes with KTs of different sizes (Figure 4.18). By performing Immunofluorescence analysis in nocodazole treated cells, we couldn't detect any difference in Aurora B activity as determining by quantification of pKnl1.

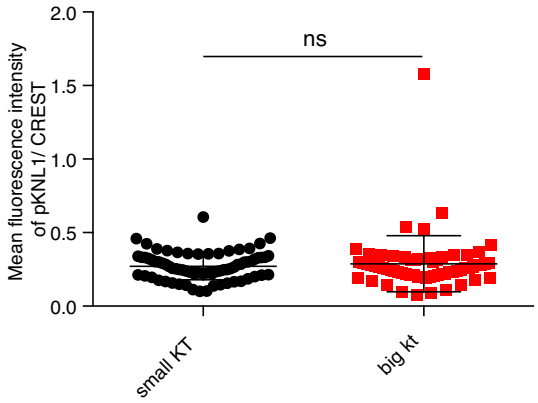

Figure 4.18: **Chromosomes with small and big KTs have equivalent Aurora B activity.** (A) Quantification of pKnl1 levels in IM cells, pKnl levels were subtracted of background, and afterwards normalized to CREST levels, also subtracted of background. (n = 63 big KTs, n= 76 small KTs, n= 50 cells). Mann- Whitney test.

We next performed an error correction assay (Lampson et al., 2004) (Figure 4.16 B). After 12h of monastrol treatment, cells were released into MEM containing 1 μM Aurora B inhibitor and 20 μM proteasome inhibitor MG-132, to prevent anaphase onset and allow the quantification of type of attachments in metaphase cells. For each cell we defined the attachment type for chromosomes with small and big KTs. We analyzed 220 cells (3 independent experiments, total number of chromosomes with small KTs=828, total number of chromosomes with big KTs= 414). The percentage of cells where chromosomes with small KT formed erroneous merotelic attachments was 1,5%, while 7% of chromosomes with big KTs formed merotelic/lateral attachments (Figure 4.16 B-D). These results demonstrated that chromosomes containing big KTs are more prone to form erroneous attachments (Figure 4.16 B-D) which is in correlation with aforementioned quantifications of error correction assay in IM cells. Using super resolution images, we could detect the cells with chromosomes containing big KTs, positioned perpendicularly to the spindle axis, after establishing merotelic attachments on both sister KTs (Figure 4.16 B-D). All together our results indicate the importance of KT size in error formation.

4.3.3 Discussion

Using immortalized IM fibroblast, here we demonstrate that KT size has an important role during mitosis. Our model proposes that soon after NEB, big KTs, due to their large surface,

efficiently capture MTs coming from the opposite poles, which results in direct alignment in the metaphase plate. However, in some cases, large area of one of the sister KTs can bind MTs coming from the opposite poles resulting in merotelic attachments and lagging chromosomes during anaphase (Figure 4.19).

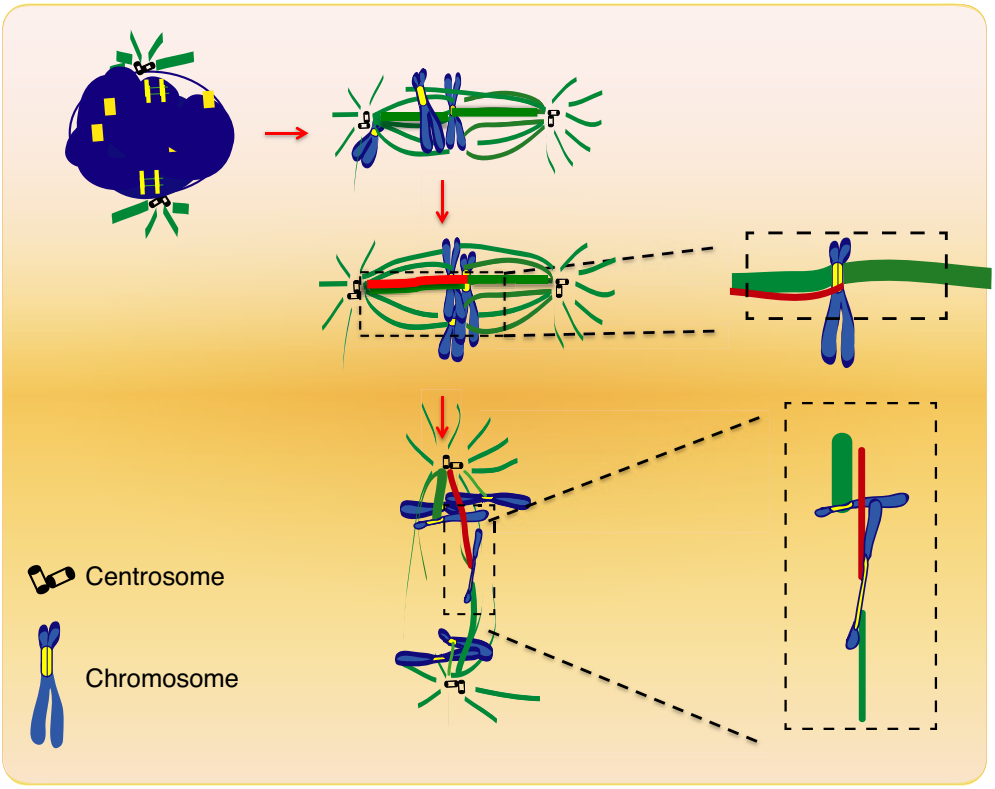

Figure 4.19: **Model for the role of KT size in error formation and chromosome segregation.** During mitosis chromosomes can align at the metaphase plate via motor proteins (“peripheral pathway” of congression) or can be directly attached by MTs coming from the opposite poles (“direct pathway” of congression). KT size biases the pathway of congression, where chromosomes with bigger KTs tend to preferably align by direct pathway. Bigger KT size, increases visibility for the attachment with MTs, however it increases the chance for erroneous attachment formation.

Extensive work has been done addressing the role of KTs in establishment of KT-MT attachment (Magidson et al., 2011; McEwen et al., 1998; O’Connell et al., 2012; Zaytsev and Grishchuk, 2015). In the chromosomes, sister KTs are turned “back-to back” conformation in order to facilitate the capture by MTs coming from the opposite poles (Zaytsev and Grishchuk, 2015). The “back-to back” position can be deformed if both sister KTs become attached to the same pole (syntelic) attachments (Loncarek et al., 2007). Once distorted, the position of sister KTs requires external forces in order to position sister KTs to opposite sides. This emphasizes the importance of the centromere and KT geometry and architecture on high fidelity chromosome segregation (Loncarek et al., 2007).

Previous work has been focused on changes in the outer KT structure during mitosis and depending on MT attachment status. However, in all these studies, after initial attachments KTs decrease in size, hence avoiding erroneous attachments (Magidson et al., 2015; Rieder, 1982; Wynne and Funabiki, 2015; Zaytsev and Grishchuk, 2015). The advantage of IM model system used in this studies is that the KT size, remains extraordinary big during all course of mitosis. We could predict that KTs of IM also form large crescent structures at the beginning of mitosis that eventually decrease upon attachment. Nevertheless, the difference in KT size between chromosomes in IM cells stays evident and considerable during all mitosis. Besides the important role in attachment stabilization, KTs also play dominant role in "chromosome-mediated pathway of spindle assembly" (Heald and Khodjakov, 2015; Maiato et al., 2004; O'Connell et al., 2012). It would be interesting to address the role of tick K fibers (100 MTs) of IM 3+X chromosomes in spindle assembly. Moreover detailed studies of big IM KTs that represent a fusion of single smaller KTs, might tell us more about the behavior of single subunits during attachment formation.

The difference in KT size is not only characteristic of IM cells, although it is the most evident one. In human cells, chromosomes contain different centromeric regions and the difference in centromere size between some chromosomes can be several fold (chromosome 18 and y chromosome) (Cherry et al., 1989; Cherry and Johnston, 1987).

Up to date literature contains extensive data that correlates the aneuploidy of some chromosomes to certain type of cancers (Haugvik et al., 2014; Salido et al., 2005; Zimonjic et al., 2000). Yet, until now a clear connection has not been found. The common conclusion of all the studies is that CIN and aneuploidy are the hallmark of all cancers (Cimini, 2008; Naylor and van Deursen, 2016). Due to the technical limitations it is still difficult to follow the different chromosomes during mitosis. Using IM as a model system, we could study the mechanisms that lie behind important processes during mitosis and were difficult to address in human cells due to complexity of the system or small size of the chromosomes/KTs. Employing that knowledge we could later approach the more complex (human) systems.

4.3.4 Material and methods

4.3.4.1 Cell culturing

IM fibroblast cells, immortalized with human hTERT (pBabe puro hTERT) were kind gift from Jerry W Shay, (University of Texas Southwestern Medical Center, Dallas, Texas) (Zou et al., 2002). Cells were grown in Minimum Essential Media (MEM) (Gibco, Life Technologies), supplemented with 20%FBS (Gibco, Life Technologies), 2mM L-Glutamine (Alfagene) at 37°C in humidified conditions with 5% CO2. To collect IM fibroblasts, we used Trypsin (Gibco, Life Technologies). Due to the natural properties of these cells to become aneuploid and polyploid, for the purpose of our studies we used only diploid cells, which was controlled by counting the number of KTs (2n=6).

4.3.4.2 Cell transfection

IM cells were transfected with human H2B-GFP (from Geoff Wahl lab (Addgene plasmid # 11680) and pSV-IRESneo3-CENP-A-EGFP (kind gift from Patrick Meraldi, University of Geneva) plasmids using Lipofectamine 2000 (Invitrogen) to generate a new stable cell line. At day 1 cells were seeded in 6-well plate at 60-70% confluence in MEM containing 20% FBS. The day after, cells were washed 3x with PBS and incubated with Optimem ((Gibco, Life Technologies) medium containing Lipofectamine 2000 (Invitrogen) and respective DNA for 4h. Optimem with DNA and Lipofectamine 2000 were previously mixed and incubated for 20 min before adding to the cells. After 4 hours Optimem medium was exchanged to MEM supplemented with 20% FBS and cells were selected with G418 (Merck Millipore) after 48h.

4.3.4.3 Error correction assay

IM cells were seeded on poly-L-lysin-coated (Sigma-Aldrich) coverslips 2 days before experiment. Initially, cells were incubated for 12h with 100 μM monastrol (Tocris bioscience) and after that washed out into MEM or MEM medium containing 1μM Aurora B inhibitor (ZM 447439, Selleckchem.com) or MEM containing 1μM Aurora B inhibitor and 20 μM MG-132, proteasome inhibitor, (Calbiochem). Afterwards cells were fixed with ice-cold methanol for 4 min at -20 °C (Invitrogen) or 4% paraformaldehyde (Electron Microscopy Sciences) for further immunofluorescence analysis.

4.3.4.4 Cenp-E inhibition

To inhibit CENP-E cells were treated with 20 nM Cenp-E inhibitor (GSK 923295, Selleckchem.com) 1h before fixation or live cell imaging.

4.3.4.5 Imunofluorescence

IM cells were seeded on poly - L - lysin-coated coverslips 2 days before the experiment. After fixation with ice-cold methanol (Invitrogen) or 4% paraformaldehyde (Electron Microscopy Sciences), IM fibroblast cells were washed with PBS-0.05%Tween 20 (Sigma-Aldrich) or cytoskeleton buffer pH 6.1 (274 mM NaCl, 10mM KCl, 2.2 mM Na2HPO4, 0.8mM KH2PO4, 4mM EGTA, 4mM MgCl2, 10mM Pipes, 10mM Glucose). Extraction after paraformaldehyde fixation was performed using PBS-0,1%Triton (Sigma-Aldrich). Coverslips were incubates with primary antibody in blocking solution for 1h. We used following primary antibodies: anti-human centromere antiserum (CREST) 1:2000 (Fitzgerald), mouse anti-α-tubulin (1:2000; B-512 clone, Sigma) rabbit anti-pKnl1 (1:1000) (Welburn et al., 2010) (kind gift from Iain Cheeseman, Whitehead Institute, MIT, Boston), rabbit anti-pT232 Aurora B (Rockland Immunochemicals). Afterwards cells were washed 3x with PBS- 0.05% Tween or cytoskeleton buffer and incubated 45 min with secondary antibodies (Alexa-488, 568 and 647, (Invitrogen) and (Abberior STAR 580 and Abberior STAR 635p (Abberior Instruments) for Stimulated emission depletion (STED) microscopy. For STED microscopy, both primary and secondary antibodies were used at 1:100 concentrations. After adding DAPI (1:500.000) (4'6'-Diamidino-2-phenylindole, Sigma Aldrich) for 5 min, coverslips were washed in PBS and sealed on glass slides using mounting medium (20 mM Tris pH8, 0.5 N-propyl gallate, 90% glycerol).

4.3.4.6 Live cell imaging

IM cells stably expressing human CENP-A-GFP and H2B-GFP were plated on fibronectin (Sigma-Aldrich) coated in 35mm glass-bottom dishes (14 mm, No 1.5, MatTek Corporation) 2 days before imaging. Before live cell imaging cells were cultured in Leibovitz's - L15 medium (Gibco, Life Technologies). For tubulin staining, we used 20nM sirTubulin dye (Spirochrome) and incubated for 6-12h. Live cell imaging was performed on a temperature-controlled Nikon TE2000 microscope equipped at the camera port with a modified Yokogawa CSU-X1 spinning-disc head (Solamere Technology), an ASI FW-1000 filter-wheel and an Andor iXon+ DU-897 EM-CCD. The excitation optics is composed of two sapphire lasers

at 488 nm and 647 nm (Coherent), which are shuttered by an acousto-optic tunable filter (Gooche&Housego, model R64040-150) and injected into the Yokogawa head via a polarization-maintaining single-mode optical fiber (OZ optics). Sample position is controlled by a SCAN-IM stage (Marzhauser) and a 541.ZSL piezo (Physik Instrumente). The objective was an oil-immersion 60x 1.4 NA Plan-Apo DIC CFI (Nikon, VC series), yielding an overall (including the pinhole-imaging lens) 190 nm/pixel sampling. A 1.5x tube lens (optivar) was also used (126 nm/pixel sampling). Eleven 1 μm separated z-stacks were acquired every 2 min while recording control IM cells stably expressing H2B-GFP cell line. For KT tracking we used 30 seconds and 10 seconds time interval and 0.75 μm separated z-stack. The system was controlled by NIS-Elements via a DAC board (National Instruments, PCI-6733).

4.3.4.7 Image analysis

Image acquisition (0.22 μm thin Z stacks) was performed on a Zeiss AxioObserver Z1 wide-field microscope equipped with a plan-apochromat (1.46 NA 60x) DIC objective and a cooled CCD (Hamamatsu Orca R2). For image analysis we used Autoquant X (Media Cybernetics) for deconvolution and Fiji (ImageJ) for attachment quantifications and KT tracking. Adobe Photoshop CS4 and Adobe Illustrator (Adobe Systems) were used for image preparation for publication.

Merotelic/ lateral attachments were defined by the position of the KTs (bent or parallel to the spindle axis) and by defining the MTs passing by (defined through Z stacks). The pKnl1 levels were analyzed using ROI manager in Fiji (ImageJ) . The pKnl1 levels corrected for the background were normalized to CREST levels (also corrected for the background).

4.3.4.8 Stimulated emission depletion (STED) microscopy

For STED imaging we used a pulsed gated-STED microscope (Abberior Instruments) with excitation wavelengths at 561nm and 640nm doughnut-depleted with a single laser at 775nm. All acquisitions were made using an 1.4NA oil-immersion and a pixel size set to 35nm.

4.3.4.9 Frequency analysis and joint probability tables

Custom-made scripts were developed in MATLAB 8.1 (The MathWorks Inc.) to perform the frequency analysis for the number of chromosomes with small and big KTs staying at the pole (Immunofluorescence analysis of CENP-E inhibited IM cells). Joint probability tables were calculated for three independent sets of mitotic cells (n = 110, 100, 101). The tables

were used to calculate the marginal and the conditional probabilities of the number of chromosomes with small/big KTs which remain at the pole. The random variables considered for the joint probability table were S, the number of chromosomes with small KTs that stay at the pole, and B, the number of chromosomes with big KTs that stay at the pole. Binomial distributions were fitted to both random variables, using information about the number of independent components (2 for big KTs, and 4 for small KTs) and the respective experimental expected values. All data are represented as the mean ± SD.

4.3.4.10 KT tracking

Live cell imaging of IM stably expressing CENP-A-GFP obtained on Nikon TE2000 microscope every 30 seconds or 1 min, were analyzed using TrackMate Tool in Fiji (Image J). KTs and pole positions were manually tracked in four dimensions (x,y,z,t) using Manual Tracking Tool. Further analyses and plotting were performed using MATLAB to assess the influence of the initial position of the chromosome and its KT size, on its later location during metaphase (at equatorial plate or at poles). Data from different cells (n = 8) was pooled together by applying geometric affine transformations (without shear) to generate overlap the poles location. Initial and final positions of the chromosomes (with reference to its KT size) were plotted on this standardized geometrical representation of the mitotic spindle.

Chapter 5

General discussion

Correct KT-MT attachments are the uppermost requirement for faithful cell division. Errors generated during this process can be deleterious for the cell and the organism, since they are linked to developmental disorders, neurodegenerative diseases and cancer (Bakhoum and Compton, 2012; Bakhoum et al., 2014; Bakhoum et al., 2009b; Cimini, 2008; Cimini et al., 2001). The process of error formation and correction during mitosis has been subject to detailed investigation in different model systems and in different stages of mitosis (Kline-Smith et al., 2005; Lampson et al., 2004; Salemi et al., 2013). However, many questions regarding initial attachment stabilization, formation of bi-orientation, role of KT and chromosome size in error correction still remain to be answered.

During the course of this thesis, we explored two important aspects of KT-MT interaction: how initial attachments are stabilized without tension and the importance of KT size. We tackled these questions by using two different model systems SMUGs (Whittaker et al., 2000) and immortalized IM fibroblasts (Zou et al., 2002). Each model system has unique features that are appropriate to address these specific questions. The results from this thesis help us to understand the pathways leading to bi-orientation.

5.1 The role of PEFs in the stabilization of initial KT-MT attachments

Incorrect attachments are recognized by the error correction machinery due to the lack of tension between two sister KTs (Vader et al., 2008). Paradoxically, as same attachments cannot be stabilized without tension, tension also cannot be established without attachments. To form stable bi-orientation, sister KTs would have to attach simultaneously to opposite

poles, unless there is a mechanism that promotes initial attachment stabilization before bi-orientation.

In this thesis, we established SMUGs after depletion of origin of replication protein Dup (Whittaker et al., 2000).

SMUGs represent an important tool to study KT - MT attachments, and single KT behavior in the absence of tension. In contrast to mammalian cells, SMUGs enter mitosis with condensed single chromatids, representing a good model system to explore KT-MT attachment formation in their native chromatid context. Here we show that SMUGs were able to exit mitosis even in the absence of bi-orientation. This delay was increased after RNAi mediated depletion of chromokinesins Nod, involved in generation of PEFs. However, Nod overexpression significantly shortened the mitotic duration in SMUGs. Our results demonstrated that PEFs have important role in the initial attachment stabilization through conversion from lateral to end-on KT - MT attachment on mono-oriented chromosomes. This mechanism allows cells to form the intermediate, quasi-stable attachments, and allows transition towards the final stable bi-orientation. Even though mitotic progression was delayed in SMUGs compared with control cells, lack of inter-KT tension did not prevent SMUGs to exit mitosis. Decrease in Knl1 phosphorylation levels indicates that during SMUGs outer KT proteins in a single KT position further away from Aurora B phosphorylation activity, which allowed stabilization of the attachment and SAC satisfaction. These changes in KT structure are small, and reflect the reorganization of the KT proteins during mitosis. Measurement of this delocalization, named as intra-KT stretch, and its importance in attachment stabilization has been controversial in the field of cell division (Etemad et al., 2015; Magidson et al., 2016; Maresca and Salmon, 2009; Smith et al., 2016; Tauchman et al., 2015; Uchida et al., 2009). Existence of intra-KT stretch as a form of “stretching” inside the single KT, measured by the SHREC method, was criticized as an overestimation of the tension importance in SAC satisfaction. The detected changes inside the single KT were reported to be structural deformations caused by the presence of MTs (Magidson et al., 2016).

More detailed study on the SMUG KTs, using super resolution microscopy or electron microscopy (EM), would give more informative data about the changes inside the single KT. Thus, the question of the importance of tension versus attachment in SAC silencing still stays as an inspiration for future studies.

5.2 The role of KT size in KT-MT attachments and mitotic fidelity

One important contribution of this thesis was the reestablishment of IM cells as a model system for the study of mitosis. Although these cells have been comprehensively used as a model system in the field of cell division three decades ago (Brinkley et al., 1984; Carrano et al., 1976; Comings and Okada, 1971; He and Brinkley, 1996; Liming and Pathak, 1981; Wurster and Benirschke, 1970; Zinkowski et al., 1991), a gap in the literature demonstrates that they were put aside as a model system in mitotic studies. Reasons for this might be technical limitations at the time and no available genome information and difficulties in culturing and transfecting these cells compared with other cell lines (e.g. HeLa or U2OS).

Here we used immortalized IM cells (Zou et al., 2002). By stably expressing fluorescently labeled proteins, we were able to follow mitosis in IM cells using live cell imaging. The simplicity of the model allowed us to follow single KT and address the role of KT size in mitosis.

It has been well established that KT shape and size change during mitosis (Magidson et al., 2015; Maiato et al., 2004a; Rieder, 1982) as a function of MT attachment. In the beginning of mitosis KTs are wider, more exposed structures. After initial interactions with MTs, KTs become more focused decreasing the chance of repeated erroneous attachments (Magidson et al., 2015). In human cells, the variability in KT size between different chromosomes is very small and difficult to detect by light microscopy. The distinct morphology of the IM chromosomes facilitates their identification during mitosis. One of the chromosomes, results from the fusion between autosome 3 and X chromosome and contains a 2 μm long KT that can bind up to 100 MTs (Brinkley et al., 1984; Zinkowski et al., 1991). Therefore, by taking advantage of IM cells, we studied the role of KT size in chromosome congression and segregation. Our data demonstrated that larger KTs become attached more efficiently. However, large KTs show increase in formation of erroneous KT - MT attachments.

The simplicity of this model system opens many questions that were not addressable in other more complex systems. Moreover, IM is a mammal, which makes it evolutionary closer to humans comparing with other simpler systems like *Drosophila melanogaster*, *Caenorhabditis elegans* or other mammalian model like mice. This increases the probability that the studied mechanisms in mitosis of IM cells might be similar or identical in humans. Moreover, RNAi based protein depletion using human sequences for some mitotic proteins efficiently depleted the proteins in IM cells. Overall, using IM cells allows us to study some of the important mechanisms behind mitosis in much simpler, still mammalian concept.

As mentioned before, tandem head-to-tail fusion during evolution gives rise to elongated KTs, composed of several subunits - a repeat subunit model (Brinkley et al., 1984; He and Brinkley, 1996; Tsipouri et al., 2008; Wurster and Benirschke, 1970; Zinkowski et al., 1991; Zou et al., 2002). The subunit, bead-like property of these KTs is more evident in interphase nuclei (Brinkley et al., 1984) or after HU and caffeine treatment that induce KT fragmentation into 80-100 smaller units (Zinkowski et al., 1991). Nevertheless, the behavior of single subunits during mitosis has not yet been addressed. Whether each of these subunits acts as an independent KT, or their attachment to MTs is orchestrated stay unanswered. Such a question can be tackled using laser microsurgery, optogenetics (Ballister et al., 2015) or rapamycin induced dimerization (Ballister and Lampson, 2016), which will allow controlled deactivation of the fragments of one or both sister KTs.

The thick K-fiber bound to compound KT of X+3 chromosome contains 100 MTs (Brinkley et al., 1984). Due to their dynamic nature, MTs undergo constant polymerization and depolymerization. How MT dynamics is regulated in the single K-fiber stays unknown. Following the MT (+) tips, in high temporal and spatial resolution, can give the information about the behavior of single MTs or batches of MTs inside the single K-fiber.

Another member of *Genus Muntiacus,* CM (*Muntjacus reevesi*), although phenotypically similar to IM contains 2n= 46 chromosomes (Johnston et al., 1982; Murmann et al., 2008). According to the data from the literature these two species share identical genome content, however organized in different number of chromosomes (Johnston et al., 1982; Murmann et al., 2008). This characteristic of Muntjac *Genus* can be used to address the effect of different chromosome number on spindle size and mitotic progression, in existing natural conditions. More detailed comparison of these two model systems will require further proteome comparison of the cells, before other future steps. A fascinating characteristic of these animals is that they can mate and give birth to live, but sterile offspring (Liming and Pathak, 1981). The chromosome number of this hybrid species is 26 (23 chromosomes form paternal CM gametes and 3 from maternal IM gametes). In the opposite combination, hybrid would have 27 chromosomes (Liming and Pathak, 1981). Since hybrid cells contain 23 small and 3 significantly larger chromosomes, it would be interesting to address how spindle and mitosis adapts to substantial difference in chromosome size inside a single cell. Moreover, it is unknown if the chromosomes, coming from IM and CM parents, change their condensation status, becoming more similar in size inside the cells of F1 offspring. Besides using hybrid specie, similar questions could be addressed using polyethylene glycol (PEG) mediated cell fusion experiments of IM and CM cells. It has been shown that the single unattached KT

can activate the SAC and arrest cells in mitosis (Rieder et al., 1995). However, the strength of the SAC signal depends of the amount of MCC formed, indicating that SAC functions as a rheostat (Collin et al., 2013; Dick and Gerlich, 2013). It would be interesting to study the contribution of the bigger IM KTs in SAC signal formation comparing with smaller CM-derived KTs in the hybrid cells. Thus, we could further understand the dose dependent nature of SAC signaling and how it can be regulated in sub-KT levels by laser ablating parts of bigger IM KTs.

The benefits of the Muntjac model system go beyond cell division. Evolution of Muntjac *Genus* has been the focus of many karyotype and genetic studies (Lin et al., 1991; Murmann et al., 2008; Tsipouri et al., 2008; Zhou et al., 2006). As previously mentioned, the chromosome that contains large KT was a result of DNA fusion between autosome 3 and X chromosome (Brinkley et al., 1984; Chi et al., 2005; Yang et al., 1997). Extensive studies have shown that in female mammalian cells one of the X chromosomes is inactivated through DNA methylation- imprinting (reviewed in (Elhamamsy, 2016). Thus, it would be interesting to address how are imprinting and gene expression locally regulated in the fused chromosome of female IM cells.

Bibliography

Afonso, O., I. Matos, and H. Maiato. 2014a. Spatial control of the anaphase-telophase transition. Cell Cycle. 13:2985-2986.

Afonso, O., I. Matos, A.J. Pereira, P. Aguiar, M.A. Lampson, and H. Maiato. 2014b. Feedback control of chromosome separation by a midzone Aurora B gradient. Science. 345:332-336.

Alao, J.P., J.J. Sjolander, J. Baar, N. Ozbaki-Yagan, B. Kakoschky, and P. Sunnerhagen. 2014. Caffeine stabilizes Cdc25 independently of Rad3 in Schizosaccharomyces pombe contributing to checkpoint override. Mol Microbiol. 92:777-796.

Alfieri, C., L. Chang, Z. Zhang, J. Yang, S. Maslen, M. Skehel, and D. Barford. 2016. Molecular basis of APC/C regulation by the spindle assembly checkpoint. Nature. 536:431-436.

Alsop, A.E., A.E. Teschendorff, and P.A. Edwards. 2006. Distribution of breakpoints on chromosome 18 in breast, colorectal, and pancreatic carcinoma cell lines. Cancer Genet Cytogenet. 164:97-109.

Amaral, N., A. Vendrell, C. Funaya, F.Z. Idrissi, M. Maier, A. Kumar, G. Neurohr, N. Colomina, J. Torres-Rosell, M.I. Geli, and M. Mendoza. 2016. The Aurora-B-dependent No-Cut checkpoint prevents damage of anaphase bridges after DNA replication stress. Nature cell biology. 18:516-526.

Andrews, P.D., Y. Ovechkina, N. Morrice, M. Wagenbach, K. Duncan, L. Wordeman, and J.R. Swedlow. 2004. Aurora B regulates MCAK at the mitotic centromere. Developmental cell. 6:253-268.

Araujo, A.R., L. Gelens, R.S. Sheriff, and S.D. Santos. 2016. Positive Feedback Keeps Duration of Mitosis Temporally Insulated from Upstream Cell-Cycle Events. Mol Cell. 64:362-375.

Aravamudhan, P., A.A. Goldfarb, and A.P. Joglekar. 2015. The kinetochore encodes a mechanical switch to disrupt spindle assembly checkpoint signalling. Nature cell biology. 17:868-879.

Arellano, M., and S. Moreno. 1997. Regulation of CDK/cyclin complexes during the cell cycle. Int J Biochem Cell Biol. 29:559-573.

Armakolas, A., and A.J. Klar. 2006. Cell type regulates selective segregation of mouse chromosome 7 DNA strands in mitosis. Science. 311:1146-1149.

Armakolas, A., M. Koutsilieris, and A.J. Klar. 2010. Discovery of the mitotic selective chromatid segregation phenomenon and its implications for vertebrate development. Current opinion in cell biology. 22:81-87.

Ashar, H.R., L. James, K. Gray, D. Carr, S. Black, L. Armstrong, W.R. Bishop, and P. Kirschmeier. 2000. Farnesyl transferase inhibitors block the farnesylation of CENP-E and CENP-F and alter the association of CENP-E with the microtubules. The Journal of biological chemistry. 275:30451-30457.

Bakhoum, S.F., and D.A. Compton. 2012. Kinetochores and disease: keeping microtubule dynamics in check! Current opinion in cell biology. 24:64-70.

Bakhoum, S.F., G. Genovese, and D.A. Compton. 2009a. Deviant kinetochore microtubule dynamics underlie chromosomal instability. Current biology : CB. 19:1937-1942.

Bakhoum, S.F., W.T. Silkworth, I.K. Nardi, J.M. Nicholson, D.A. Compton, and D. Cimini. 2014. The mitotic origin of chromosomal instability. Current biology : CB. 24:R148-149.

Bakhoum, S.F., S.L. Thompson, A.L. Manning, and D.A. Compton. 2009b. Genome stability is ensured by temporal control of kinetochore-microtubule dynamics. Nature cell biology. 11:27-35.

Ballister, E.R., S. Ayloo, D.M. Chenoweth, M.A. Lampson, and E.L. Holzbaur. 2015. Optogenetic control of organelle transport using a photocaged chemical inducer of dimerization. Current biology : CB. 25:R407-408.

Ballister, E.R., and M.A. Lampson. 2016. Probing Mitosis by Manipulating the Interactions of Mitotic Regulator Proteins Using Rapamycin-Inducible Dimerization. Methods Mol Biol. 1413:325-331.

Bancroft, J., P. Auckland, C.P. Samora, and A.D. McAinsh. 2015. Chromosome congression is promoted by CENP-Q- and CENP-E-dependent pathways. Journal of cell science. 128:171-184.

Barisic, M., P. Aguiar, S. Geley, and H. Maiato. 2014. Kinetochore motors drive congression of peripheral polar chromosomes by overcoming random arm-ejection forces. Nat Cell Biol. 16:1249-1256.

Barisic, M., and H. Maiato. 2015. Dynein prevents erroneous kinetochore-microtubule attachments in mitosis. Cell Cycle. 14:3356-3361.

Barisic, M., and H. Maiato. 2016. The Tubulin Code: A Navigation System for Chromosomes during Mitosis. Trends in cell biology. 26:766-775.

Barisic, M., R. Silva e Sousa, S.K. Tripathy, M.M. Magiera, A.V. Zaytsev, A.L. Pereira, C. Janke, E.L. Grishchuk, and H. Maiato. 2015. Mitosis. Microtubule detyrosination guides chromosomes during mitosis. Science. 348:799-803.

Barisic, M., B. Sohm, P. Mikolcevic, C. Wandke, V. Rauch, T. Ringer, M. Hess, G. Bonn, and S. Geley. 2010. Spindly/CCDC99 is required for efficient chromosome congression and mitotic checkpoint regulation. Molecular biology of the cell. 21:1968-1981.

Belmont, L.D., A.A. Hyman, K.E. Sawin, and T.J. Mitchison. 1990. Real-time visualization of cell cycle-dependent changes in microtubule dynamics in cytoplasmic extracts. Cell. 62:579-589.

Bennett, A., B. Bechi, A. Tighe, S. Thompson, D.J. Procter, and S.S. Taylor. 2015. Cenp-E inhibitor GSK923295: Novel synthetic route and use as a tool to generate aneuploidy. Oncotarget. 6:20921-20932.

Bernad, R., P. Sanchez, T. Rivera, M. Rodriguez-Corsino, E. Boyarchuk, I. Vassias, D. Ray-Gallet, A. Arnaoutov, M. Dasso, G. Almouzni, and A. Losada. 2011. Xenopus HJURP and condensin II are required for CENP-A assembly. The Journal of cell biology. 192:569-582.

Biggins, S., and A.W. Murray. 2001. The budding yeast protein kinase Ipl1/Aurora allows the absence of tension to activate the spindle checkpoint. Genes & development. 15:3118-3129.

Blower, M.D., and G.H. Karpen. 2001. The role of Drosophila CID in kinetochore formation, cell-cycle progression and heterochromatin interactions. Nature cell biology. 3:730-739.

Bode, A.M., and Z. Dong. 2007. The enigmatic effects of caffeine in cell cycle and cancer. Cancer Lett. 247:26-39.

Bodor, D.L., J.F. Mata, M. Sergeev, A.F. David, K.J. Salimian, T. Panchenko, D.W. Cleveland, B.E. Black, J.V. Shah, and L.E. Jansen. 2014. The quantitative architecture of centromeric chromatin. eLife. 3:e02137.

Bodor, D.L., L.P. Valente, J.F. Mata, B.E. Black, and L.E. Jansen. 2013. Assembly in G1 phase and long-term stability are unique intrinsic features of CENP-A nucleosomes. Molecular biology of the cell. 24:923-932.

Brinkley, B.R. 1985. Microtubule organizing centers. Annu Rev Cell Biol. 1:145-172.

Brinkley, B.R., and E. Stubblefield. 1966. The fine structure of the kinetochore of a mammalian cell in vitro. Chromosoma. 19:28-43.

Brinkley, B.R., M.M. Valdivia, A. Tousson, and S.L. Brenner. 1984. Compound kinetochores of the Indian muntjac. Evolution by linear fusion of unit kinetochores. Chromosoma. 91:1-11.

Brinkley, B.R., R.P. Zinkowski, W.L. Mollon, F.M. Davis, M.A. Pisegna, M. Pershouse, and P.N. Rao. 1988. Movement and segregation of kinetochores experimentally detached from mammalian chromosomes. Nature. 336:251-254.

Brito, D.A., and C.L. Rieder. 2006. Mitotic checkpoint slippage in humans occurs via cyclin B destruction in the presence of an active checkpoint. Curr Biol. 16:1194-1200.

Brouhard, G.J., and A.J. Hunt. 2005. Microtubule movements on the arms of mitotic chromosomes: polar ejection forces quantified in vitro. Proceedings of the National Academy of Sciences of the United States of America. 102:13903-13908.

Buchwitz, B.J., K. Ahmad, L.L. Moore, M.B. Roth, and S. Henikoff. 1999. A histone-H3-like protein in C. elegans. Nature. 401:547-548.

Buschhorn, B.A., G. Petzold, M. Galova, P. Dube, C. Kraft, F. Herzog, H. Stark, and J.M. Peters. 2011. Substrate binding on the APC/C occurs between the coactivator Cdh1 and the processivity factor Doc1. Nat Struct Mol Biol. 18:6-13.

Cairns, J. 1975. Mutation selection and the natural history of cancer. Nature. 255:197-200.

Caldas, G.V., T.R. Lynch, R. Anderson, S. Afreen, D. Varma, and J.G. DeLuca. 2015. The RZZ complex requires the N-terminus of KNL1 to mediate optimal Mad1 kinetochore localization in human cells. Open Biol. 5.

Cameron, L.A., G. Yang, D. Cimini, J.C. Canman, O. Kisurina-Evgenieva, A. Khodjakov, G. Danuser, and E.D. Salmon. 2006. Kinesin 5-independent poleward flux of kinetochore microtubules in PtK1 cells. The Journal of cell biology. 173:173-179.

Cane, S., A.A. Ye, S.J. Luks-Morgan, and T.J. Maresca. 2013. Elevated polar ejection forces stabilize kinetochore-microtubule attachments. J Cell Biol. 200:203-218.

Carlier, M.F., T.L. Hill, and Y. Chen. 1984. Interference of GTP hydrolysis in the mechanism of microtubule assembly: an experimental study. Proceedings of the National Academy of Sciences of the United States of America. 81:771-775.

Carrano, A.V., J.W. Gray, D.H. Moore, 2nd, J.L. Minkler, B.H. Mayall, M.A. van Dilla, and M.L. Mendelsohn. 1976. Purification of the chromosomes of the Indian muntjac by flow sorting. J Histochem Cytochem. 24:348-354.

Chan, C.S., and D. Botstein. 1993. Isolation and characterization of chromosome-gain and increase-in-ploidy mutants in yeast. Genetics. 135:677-691.

Chan, Y.W., L.L. Fava, A. Uldschmid, M.H. Schmitz, D.W. Gerlich, E.A. Nigg, and A. Santamaria. 2009. Mitotic control of kinetochore-associated dynein and spindle orientation by human Spindly. The Journal of cell biology. 185:859-874.

Charville, G.W., and T.A. Rando. 2011. Stem cell ageing and non-random chromosome segregation. Philosophical transactions of the Royal Society of London. Series B, Biological sciences. 366:85-93.

Chavali, P.L., M. Putz, and F. Gergely. 2014. Small organelle, big responsibility: the role of centrosomes in development and disease. Philos Trans R Soc Lond B Biol Sci. 369.

Cheerambathur, D.K., R. Gassmann, B. Cook, K. Oegema, and A. Desai. 2013. Crosstalk between microtubule attachment complexes ensures accurate chromosome segregation. Science. 342:1239-1242.

Cheeseman, I.M., S. Anderson, M. Jwa, E.M. Green, J. Kang, J.R. Yates, 3rd, C.S. Chan, D.G. Drubin, and G. Barnes. 2002. Phospho-regulation of kinetochore-microtubule attachments by the Aurora kinase Ipl1p. Cell. 111:163-172.

Cheeseman, I.M., J.S. Chappie, E.M. Wilson-Kubalek, and A. Desai. 2006. The conserved KMN network constitutes the core microtubule-binding site of the kinetochore. Cell. 127:983-997.

Cheng, Y.M., T.S. Li, L.J. Hsieh, P.C. Hsu, Y.C. Li, and C.C. Lin. 2009. Complex genomic organization of Indian muntjac centromeric DNA. Chromosome research : an international journal on the molecular, supramolecular and evolutionary aspects of chromosome biology. 17:1051-1062.

Cherry, L.M., A.J. Faulkner, L.A. Grossberg, and R. Balczon. 1989. Kinetochore size variation in mammalian chromosomes: an image analysis study with evolutionary implications. Journal of cell science. 92 (Pt 2):281-289.

Cherry, L.M., and D.A. Johnston. 1987. Size variation in kinetochores of human chromosomes. Hum Genet. 75:155-158.

Chi, J.X., L. Huang, W. Nie, J. Wang, B. Su, and F. Yang. 2005. Defining the orientation of the tandem fusions that occurred during the evolution of Indian muntjac chromosomes by BAC mapping. Chromosoma. 114:167-172.

Chmatal, L., K. Yang, R.M. Schultz, and M.A. Lampson. 2015. Spatial Regulation of Kinetochore Microtubule Attachments by Destabilization at Spindle Poles in Meiosis I. Current biology : CB. 25:1835-1841.

Churchman, L.S., and J.A. Spudich. 2012. Single-molecule high-resolution colocalization of single probes. Cold Spring Harb Protoc. 2012:242-245.

Cimini, D. 2008. Merotelic kinetochore orientation, aneuploidy, and cancer. Biochim Biophys Acta. 1786:32-40.

Cimini, D., L.A. Cameron, and E.D. Salmon. 2004. Anaphase spindle mechanics prevent mis-segregation of merotelically oriented chromosomes. Current biology : CB. 14:2149-2155.

Cimini, D., B. Howell, P. Maddox, A. Khodjakov, F. Degrassi, and E.D. Salmon. 2001. Merotelic kinetochore orientation is a major mechanism of aneuploidy in mitotic mammalian tissue cells. The Journal of cell biology. 153:517-527.

Cimini, D., B. Moree, J.C. Canman, and E.D. Salmon. 2003. Merotelic kinetochore orientation occurs frequently during early mitosis in mammalian tissue cells and error correction is achieved by two different mechanisms. J Cell Sci. 116:4213-4225.

Cleveland, D.W., M.W. Kirschner, and N.J. Cowan. 1978. Isolation of separate mRNAs for alpha- and beta-tubulin and characterization of the corresponding in vitro translation products. Cell. 15:1021-1031.

Clute, P., and J. Pines. 1999. Temporal and spatial control of cyclin B1 destruction in metaphase. Nature cell biology. 1:82-87.

Cochran, J.C., J.E. Gatial, 3rd, T.M. Kapoor, and S.P. Gilbert. 2005. Monastrol inhibition of the mitotic kinesin Eg5. The Journal of biological chemistry. 280:12658-12667.

Cochran, J.C., C.V. Sindelar, N.K. Mulko, K.A. Collins, S.E. Kong, R.S. Hawley, and F.J. Kull. 2009. ATPase cycle of the nonmotile kinesin NOD allows microtubule end tracking and drives chromosome movement. Cell. 136:110-122.

Collin, P., O. Nashchekina, R. Walker, and J. Pines. 2013. The spindle assembly checkpoint works like a rheostat rather than a toggle switch. Nat Cell Biol. 15:1378-1385.

Comings, D.E., and T.A. Okada. 1971. Fine structure of kinetochore in Indian muntjac. Experimental cell research. 67:97-110.

Conboy, M.J., A.O. Karasov, and T.A. Rando. 2007. High incidence of non-random template strand segregation and asymmetric fate determination in dividing stem cells and their progeny. PLoS Biol. 5:e102.

Conde, C., M. Osswald, J. Barbosa, T. Moutinho-Santos, D. Pinheiro, S. Guimaraes, I. Matos, H. Maiato, and C.E. Sunkel. 2013. Drosophila Polo regulates the spindle assembly checkpoint through Mps1-dependent BubR1 phosphorylation. The EMBO journal. 32:1761-1777.

Cooper, J.L., and S. Henikoff. 2004. Adaptive evolution of the histone fold domain in centromeric histones. Mol Biol Evol. 21:1712-1718.

da Fonseca, P.C., E.H. Kong, Z. Zhang, A. Schreiber, M.A. Williams, E.P. Morris, and D. Barford. 2011. Structures of APC/C(Cdh1) with substrates identify Cdh1 and Apc10 as the D-box co-receptor. Nature. 470:274-278.

Dai, J., B.A. Sullivan, and J.M. Higgins. 2006. Regulation of mitotic chromosome cohesion by Haspin and Aurora B. Developmental cell. 11:741-750.

Darlington, C.D. 1937. Recent advances in cytology. Philadelphia, P. Blakiston´s son & co.,inc:671.

De Antoni, A., C.G. Pearson, D. Cimini, J.C. Canman, V. Sala, L. Nezi, M. Mapelli, L. Sironi, M. Faretta, E.D. Salmon, and A. Musacchio. 2005. The Mad1/Mad2 complex as a template for Mad2 activation in the spindle assembly checkpoint. Current biology : CB. 15:214-225.

De Rop, V., A. Padeganeh, and P.S. Maddox. 2012. CENP-A: the key player behind centromere identity, propagation, and kinetochore assembly. Chromosoma. 121:527-538.

DeLuca, J.G., Y. Dong, P. Hergert, J. Strauss, J.M. Hickey, E.D. Salmon, and B.F. McEwen. 2005. Hec1 and nuf2 are core components of the kinetochore outer plate essential for organizing microtubule attachment sites. Molecular biology of the cell. 16:519-531.

DeLuca, J.G., W.E. Gall, C. Ciferri, D. Cimini, A. Musacchio, and E.D. Salmon. 2006. Kinetochore microtubule dynamics and attachment stability are regulated by Hec1. Cell. 127:969-982.

DeLuca, J.G., B. Moree, J.M. Hickey, J.V. Kilmartin, and E.D. Salmon. 2002. hNuf2 inhibition blocks stable kinetochore-microtubule attachment and induces mitotic cell death in HeLa cells. The Journal of cell biology. 159:549-555.

DeLuca, K.F., S.M. Lens, and J.G. DeLuca. 2011. Temporal changes in Hec1 phosphorylation control kinetochore-microtubule attachment stability during mitosis. Journal of cell science. 124:622-634.

Desai, A., and T.J. Mitchison. 1997. Microtubule polymerization dynamics. Annual review of cell and developmental biology. 13:83-117.

Di Fiore, B., C. Wurzenberger, N.E. Davey, and J. Pines. 2016. The Mitotic Checkpoint Complex Requires an Evolutionary Conserved Cassette to Bind and Inhibit Active APC/C. Mol Cell. 64:1144-1153.

Dick, A.E., and D.W. Gerlich. 2013. Kinetic framework of spindle assembly checkpoint signalling. Nature cell biology. 15:1370-1377.

Dong, Y., K.J. Vanden Beldt, X. Meng, A. Khodjakov, and B.F. McEwen. 2007. The outer plate in vertebrate kinetochores is a flexible network with multiple microtubule interactions. Nature cell biology. 9:516-522.

Downing, K.H., and E. Nogales. 1998. Tubulin structure: insights into microtubule properties and functions. Curr Opin Struct Biol. 8:785-791.

Drpic, D., M. Barisic, D. Pinheiro, and H. Maiato. 2013. Selective tracking of template DNA strands after induction of mitosis with unreplicated genomes (MUGs) in Drosophila S2 cells. Chromosome research : an international journal on the molecular, supramolecular and evolutionary aspects of chromosome biology. 21:329-337.

du Sart, D., M.R. Cancilla, E. Earle, J.I. Mao, R. Saffery, K.M. Tainton, P. Kalitsis, J. Martyn, A.E. Barry, and K.H. Choo. 1997. A functional neo-centromere formed through activation of a latent human centromere and consisting of non-alpha-satellite DNA. Nat Genet. 16:144-153.

Dumont, S., E.D. Salmon, and T.J. Mitchison. 2012. Deformations within moving kinetochores reveal different sites of active and passive force generation. Science. 337:355-358.

Dunleavy, E.M., G. Almouzni, and G.H. Karpen. 2011. H3.3 is deposited at centromeres in S phase as a placeholder for newly assembled CENP-A in G(1) phase. Nucleus. 2:146-157.

Dunleavy, E.M., D. Roche, H. Tagami, N. Lacoste, D. Ray-Gallet, Y. Nakamura, Y. Daigo, Y. Nakatani, and G. Almouzni-Pettinotti. 2009. HJURP is a cell-cycle-dependent maintenance and deposition factor of CENP-A at centromeres. Cell. 137:485-497.

Earnshaw, W., B. Bordwell, C. Marino, and N. Rothfield. 1986. Three human chromosomal autoantigens are recognized by sera from patients with anti-centromere antibodies. The Journal of clinical investigation. 77:426-430.

Earnshaw, W.C., H. Ratrie, 3rd, and G. Stetten. 1989. Visualization of centromere proteins CENP-B and CENP-C on a stable dicentric chromosome in cytological spreads. Chromosoma. 98:1-12.

Earnshaw, W.C., and N. Rothfield. 1985. Identification of a family of human centromere proteins using autoimmune sera from patients with scleroderma. Chromosoma. 91:313-321.

Egloff, M.P., D.F. Johnson, G. Moorhead, P.T. Cohen, P. Cohen, and D. Barford. 1997. Structural basis for the recognition of regulatory subunits by the catalytic subunit of protein phosphatase 1. The EMBO journal. 16:1876-1887.

Elhamamsy, A.R. 2016. DNA methylation dynamics in plants and mammals: overview of regulation and dysregulation. Cell Biochem Funct. 34:289-298.

Elting, M.W., C.L. Hueschen, D.B. Udy, and S. Dumont. 2014. Force on spindle microtubule minus ends moves chromosomes. The Journal of cell biology. 206:245-256.

Ems-McClung, S.C., S.G. Hainline, J. Devare, H. Zong, S. Cai, S.K. Carnes, S.L. Shaw, and C.E. Walczak. 2013. Aurora B inhibits MCAK activity through a phosphoconformational switch that reduces microtubule association. Current biology : CB. 23:2491-2499.

Erhardt, S., B.G. Mellone, C.M. Betts, W. Zhang, G.H. Karpen, and A.F. Straight. 2008. Genome-wide analysis reveals a cell cycle-dependent mechanism controlling centromere propagation. The Journal of cell biology. 183:805-818.

Escobar, M., P. Nicolas, F. Sangar, S. Laurent-Chabalier, P. Clair, D. Joubert, P. Jay, and C. Legraverend. 2011. Intestinal epithelial stem cells do not protect their genome by asymmetric chromosome segregation. Nature communications. 2:258.

Espert, A., P. Uluocak, R.N. Bastos, D. Mangat, P. Graab, and U. Gruneberg. 2014. PP2A-B56 opposes Mps1 phosphorylation of Knl1 and thereby promotes spindle assembly checkpoint silencing. The Journal of cell biology. 206:833-842.

Etemad, B., and G.J. Kops. 2016. Attachment issues: kinetochore transformations and spindle checkpoint silencing. Current opinion in cell biology. 39:101-108.

Etemad, B., T.E. Kuijt, and G.J. Kops. 2015. Kinetochore-microtubule attachment is sufficient to satisfy the human spindle assembly checkpoint. Nat Commun. 6:8987.

Evans, L., T. Mitchison, and M. Kirschner. 1985. Influence of the centrosome on the structure of nucleated microtubules. The Journal of cell biology. 100:1185-1191.

Evans, T., E.T. Rosenthal, J. Youngblom, D. Distel, and T. Hunt. 1983. Cyclin: a protein specified by maternal mRNA in sea urchin eggs that is destroyed at each cleavage division. Cell. 33:389-396.

Fachinetti, D., H.D. Folco, Y. Nechemia-Arbely, L.P. Valente, K. Nguyen, A.J. Wong, Q. Zhu, A.J. Holland, A. Desai, L.E. Jansen, and D.W. Cleveland. 2013. A two-step mechanism for epigenetic specification of centromere identity and function. Nature cell biology. 15:1056-1066.

Fachinetti, D., J.S. Han, M.A. McMahon, P. Ly, A. Abdullah, A.J. Wong, and D.W. Cleveland. 2015. DNA Sequence-Specific Binding of CENP-B Enhances the Fidelity of Human Centromere Function. Developmental cell. 33:314-327.

Faesen, A.C., M. Thanasoula, S. Maffini, C. Breit, F. Muller, S. van Gerwen, T. Bange, and A. Musacchio. 2017. Basis of catalytic assembly of the mitotic checkpoint complex. Nature.

Falk, S.J., L.Y. Guo, N. Sekulic, E.M. Smoak, T. Mani, G.A. Logsdon, K. Gupta, L.E. Jansen, G.D. Van Duyne, S.A. Vinogradov, M.A. Lampson, and B.E. Black. 2015. Chromosomes. CENP-C reshapes and stabilizes CENP-A nucleosomes at the centromere. Science. 348:699-703.

Fava, L.L., M. Kaulich, E.A. Nigg, and A. Santamaria. 2011. Probing the in vivo function of Mad1:C-Mad2 in the spindle assembly checkpoint. The EMBO journal. 30:3322-3336.

Feijao, T., O. Afonso, A.F. Maia, and C.E. Sunkel. 2013. Stability of kinetochore-microtubule attachment and the role of different KMN network components in Drosophila. Cytoskeleton (Hoboken). 70:661-675.

Feringa, F.M., L. Krenning, A. Koch, J. van den Berg, B. van den Broek, K. Jalink, and R.H. Medema. 2016. Hypersensitivity to DNA damage in antephase as a safeguard for genome stability. Nat Commun. 7:12618.

Flemming, W. 1965. Contributions to the Knowledge of the Cell and Its Vital Processes. The Journal of cell biology. 25:3-69.

Foley, E.A., and T.M. Kapoor. 2013. Microtubule attachment and spindle assembly checkpoint signalling at the kinetochore. Nature reviews. 14:25-37.

Foltz, D.R., L.E. Jansen, A.O. Bailey, J.R. Yates, 3rd, E.A. Bassett, S. Wood, B.E. Black, and D.W. Cleveland. 2009. Centromere-specific assembly of CENP-a nucleosomes is mediated by HJURP. Cell. 137:472-484.

Furnari, B., N. Rhind, and P. Russell. 1997. Cdc25 mitotic inducer targeted by chk1 DNA damage checkpoint kinase. Science. 277:1495-1497.

Gaetz, J., Z. Gueroui, A. Libchaber, and T.M. Kapoor. 2006. Examining how the spatial organization of chromatin signals influences metaphase spindle assembly. Nature cell biology. 8:924-932.

Garner, M., S. van Kreeveld, and T.T. Su. 2001. mei-41 and bub1 block mitosis at two distinct steps in response to incomplete DNA replication in Drosophila embryos. Current biology : CB. 11:1595-1599.

Gascoigne, K.E., and I.M. Cheeseman. 2013. CDK-dependent phosphorylation and nuclear exclusion coordinately control kinetochore assembly state. The Journal of cell biology. 201:23-32.

Gassmann, R., A.J. Holland, D. Varma, X. Wan, F. Civril, D.W. Cleveland, K. Oegema, E.D. Salmon, and A. Desai. 2010. Removal of Spindly from microtubule-attached kinetochores controls spindle checkpoint silencing in human cells. Genes & development. 24:957-971.

Giet, R., and D.M. Glover. 2001. Drosophila aurora B kinase is required for histone H3 phosphorylation and condensin recruitment during chromosome condensation and to organize the central spindle during cytokinesis. The Journal of cell biology. 152:669-682.

Godek, K.M., L. Kabeche, and D.A. Compton. 2015. Regulation of kinetochore-microtubule attachments through homeostatic control during mitosis. Nat Rev Mol Cell Biol. 16:57-64.

Gorbsky, G.J., and W.A. Ricketts. 1993. Differential expression of a phosphoepitope at the kinetochores of moving chromosomes. The Journal of cell biology. 122:1311-1321.

Gorbsky, G.J., P.J. Sammak, and G.G. Borisy. 1987. Chromosomes move poleward in anaphase along stationary microtubules that coordinately disassemble from their kinetochore ends. The Journal of cell biology. 104:9-18.

Goshima, G., F. Nedelec, and R.D. Vale. 2005a. Mechanisms for focusing mitotic spindle poles by minus end-directed motor proteins. The Journal of cell biology. 171:229-240.

Goshima, G., and R.D. Vale. 2003. The roles of microtubule-based motor proteins in mitosis: comprehensive RNAi analysis in the Drosophila S2 cell line. The Journal of cell biology. 162:1003-1016.

Goshima, G., R. Wollman, S.S. Goodwin, N. Zhang, J.M. Scholey, R.D. Vale, and N. Stuurman. 2007. Genes required for mitotic spindle assembly in Drosophila S2 cells. Science. 316:417-421.

Goshima, G., R. Wollman, N. Stuurman, J.M. Scholey, and R.D. Vale. 2005b. Length control of the metaphase spindle. Current biology : CB. 15:1979-1988.

Grallert, A., E. Boke, A. Hagting, B. Hodgson, Y. Connolly, J.R. Griffiths, D.L. Smith, J. Pines, and I.M. Hagan. 2015. A PP1-PP2A phosphatase relay controls mitotic progression. Nature. 517:94-98.

Gregan, J., S. Polakova, L. Zhang, I.M. Tolic-Norrelykke, and D. Cimini. 2011. Merotelic kinetochore attachment: causes and effects. Trends in cell biology. 21:374-381.

Gudimchuk, N., B. Vitre, Y. Kim, A. Kiyatkin, D.W. Cleveland, F.I. Ataullakhanov, and E.L. Grishchuk. 2013. Kinetochore kinesin CENP-E is a processive bi-directional tracker of dynamic microtubule tips. Nature cell biology. 15:1079-1088.

Guimaraes, G.J., Y. Dong, B.F. McEwen, and J.G. Deluca. 2008. Kinetochore-microtubule attachment relies on the disordered N-terminal tail domain of Hec1. Current biology : CB. 18:1778-1784.

Gundersen, G.G., M.H. Kalnoski, and J.C. Bulinski. 1984. Distinct populations of microtubules: tyrosinated and nontyrosinated alpha tubulin are distributed differently in vivo. Cell. 38:779-789.

Harper, J.W., and S.J. Elledge. 2007. The DNA damage response: ten years after. Mol Cell. 28:739-745.

Hartwell, L.H., J. Culotti, and B. Reid. 1970. Genetic control of the cell-division cycle in yeast. I. Detection of mutants. Proceedings of the National Academy of Sciences of the United States of America. 66:352-359.

Hartwell, L.H., and M.B. Kastan. 1994. Cell cycle control and cancer. Science. 266:1821-1828.

Hartwell, L.H., and T.A. Weinert. 1989. Checkpoints: controls that ensure the order of cell cycle events. Science. 246:629-634.

Haugvik, S.P., L. Gorunova, L. Haugom, A.M. Eibak, I.P. Gladhaug, S. Heim, and F. Micci. 2014. Loss of 11p11 is a frequent and early event in sporadic nonfunctioning pancreatic neuroendocrine neoplasms. Oncol Rep. 32:906-912.

Hays, T.S., and E.D. Salmon. 1990. Poleward force at the kinetochore in metaphase depends on the number of kinetochore microtubules. The Journal of cell biology. 110:391-404.

Hays, T.S., D. Wise, and E.D. Salmon. 1982. Traction force on a kinetochore at metaphase acts as a linear function of kinetochore fiber length. The Journal of cell biology. 93:374-389.

He, D., and B.R. Brinkley. 1996. Structure and dynamic organization of centromeres/prekinetochores in the nucleus of mammalian cells. Journal of cell science. 109 (Pt 11):2693-2704.

Heald, R., and A. Khodjakov. 2015. Thirty years of search and capture: The complex simplicity of mitotic spindle assembly. The Journal of cell biology. 211:1103-1111.

Hein, J.B., and J. Nilsson. 2016. Interphase APC/C-Cdc20 inhibition by cyclin A2-Cdk2 ensures efficient mitotic entry. Nat Commun. 7:10975.

Hiruma, Y., C. Sacristan, S.T. Pachis, A. Adamopoulos, T. Kuijt, M. Ubbink, E. von Castelmur, A. Perrakis, and G.J. Kops. 2015. CELL DIVISION CYCLE. Competition between MPS1 and microtubules at kinetochores regulates spindle checkpoint signaling. Science. 348:1264-1267.

Hoffman, D.B., C.G. Pearson, T.J. Yen, B.J. Howell, and E.D. Salmon. 2001. Microtubule-dependent changes in assembly of microtubule motor proteins and mitotic spindle checkpoint proteins at PtK1 kinetochores. Molecular biology of the cell. 12:1995-2009.

Hoffmann, I., and E. Karsenti. 1994. The role of cdc25 in checkpoints and feedback controls in the eukaryotic cell cycle. J Cell Sci Suppl. 18:75-79.

Hoffmann, S., M. Dumont, V. Barra, P. Ly, Y. Nechemia-Arbely, M.A. McMahon, S. Herve, D.W. Cleveland, and D. Fachinetti. 2016. CENP-A Is Dispensable for Mitotic Centromere Function after Initial Centromere/Kinetochore Assembly. Cell reports. 17:2394-2404.

Holy, T.E., and S. Leibler. 1994. Dynamic instability of microtubules as an efficient way to search in space. Proceedings of the National Academy of Sciences of the United States of America. 91:5682-5685.

Hood, E.A., A.N. Kettenbach, S.A. Gerber, and D.A. Compton. 2012. Plk1 regulates the kinesin-13 protein Kif2b to promote faithful chromosome segregation. Molecular biology of the cell. 23:2264-2274.

Hori, T., W.H. Shang, K. Takeuchi, and T. Fukagawa. 2013. The CCAN recruits CENP-A to the centromere and forms the structural core for kinetochore assembly. The Journal of cell biology. 200:45-60.

Howell, B.J., B. Moree, E.M. Farrar, S. Stewart, G. Fang, and E.D. Salmon. 2004. Spindle checkpoint protein dynamics at kinetochores in living cells. Curr Biol. 14:953-964.

Hudson, D.F., K.J. Fowler, E. Earle, R. Saffery, P. Kalitsis, H. Trowell, J. Hill, N.G. Wreford, D.M. de Kretser, M.R. Cancilla, E. Howman, L. Hii, S.M. Cutts, D.V. Irvine, and K.H. Choo. 1998. Centromere protein B null mice are mitotically and meiotically normal but have lower body and testis weights. The Journal of cell biology. 141:309-319.

Izawa, D., and J. Pines. 2011. How APC/C-Cdc20 changes its substrate specificity in mitosis. Nature cell biology. 13:223-233.

Jang, C.Y., J.A. Coppinger, A. Seki, J.R. Yates, 3rd, and G. Fang. 2009. Plk1 and Aurora A regulate the depolymerase activity and the cellular localization of Kif2a. Journal of cell science. 122:1334-1341.

Janke, C. 2014. The tubulin code: molecular components, readout mechanisms, and functions. The Journal of cell biology. 206:461-472.

Jansen, L.E., B.E. Black, D.R. Foltz, and D.W. Cleveland. 2007. Propagation of centromeric chromatin requires exit from mitosis. The Journal of cell biology. 176:795-805.

Januschke, J., S. Llamazares, J. Reina, and C. Gonzalez. 2011. Drosophila neuroblasts retain the daughter centrosome. Nat Commun. 2:243.

Ji, Z., H. Gao, and H. Yu. 2015. CELL DIVISION CYCLE. Kinetochore attachment sensed by competitive Mps1 and microtubule binding to Ndc80C. Science. 348:1260-1264.

Johnson, M.K., A.M. Cooksey, and D.A. Wise. 2008. Localization of spindle checkpoint proteins in cells undergoing mitosis with unreplicated genomes. Cell motility and the cytoskeleton. 65:890-895.

Johnson, M.K., and D.A. Wise. 2010. Distribution of kinetochore fragments during mitosis with unreplicated genomes. Cytoskeleton (Hoboken). 67:172-177.

Johnston, C.A., K. Hirono, K.E. Prehoda, and C.Q. Doe. 2009. Identification of an Aurora-A/PinsLINKER/Dlg spindle orientation pathway using induced cell polarity in S2 cells. Cell. 138:1150-1163.

Johnston, F.P., R.B. Church, and C.C. Lin. 1982. Chromosome rearrangement between the Indian muntjac and Chinese muntjac is accompanied by a delection of middle repetitive DNA. Can J Biochem. 60:497-506.

Kabeche, L., and D.A. Compton. 2013. Cyclin A regulates kinetochore microtubules to promote faithful chromosome segregation. Nature. 502:110-113.

Kalantzaki, M., E. Kitamura, T. Zhang, A. Mino, B. Novak, and T.U. Tanaka. 2015. Kinetochore-microtubule error correction is driven by differentially regulated interaction modes. Nat Cell Biol. 17:421-433.

Kallio, M.J., M.L. McCleland, P.T. Stukenberg, and G.J. Gorbsky. 2002. Inhibition of aurora B kinase blocks chromosome segregation, overrides the spindle checkpoint, and perturbs microtubule dynamics in mitosis. Current biology : CB. 12:900-905.

Kanda, T., K.F. Sullivan, and G.M. Wahl. 1998. Histone-GFP fusion protein enables sensitive analysis of chromosome dynamics in living mammalian cells. Current biology : CB. 8:377-385.

Kapitein, L.C., E.J. Peterman, B.H. Kwok, J.H. Kim, T.M. Kapoor, and C.F. Schmidt. 2005. The bipolar mitotic kinesin Eg5 moves on both microtubules that it crosslinks. Nature. 435:114-118.

Kapoor, M., R. Montes de Oca Luna, G. Liu, G. Lozano, C. Cummings, M. Mancini, I. Ouspenski, B.R. Brinkley, and G.S. May. 1998. The cenpB gene is not essential in mice. Chromosoma. 107:570-576.

Kapoor, T.M., T.U. Mayer, M.L. Coughlin, and T.J. Mitchison. 2000. Probing spindle assembly mechanisms with monastrol, a small molecule inhibitor of the mitotic kinesin, Eg5. The Journal of cell biology. 150:975-988.

Kelly, A.E., C. Ghenoiu, J.Z. Xue, C. Zierhut, H. Kimura, and H. Funabiki. 2010. Survivin reads phosphorylated histone H3 threonine 3 to activate the mitotic kinase Aurora B. Science. 330:235-239.

Khodjakov, A., and T. Kapoor. 2005. Microtubule flux: what is it good for? Current biology : CB. 15:R966-968.

Khodjakov, A., and C.L. Rieder. 1996. Kinetochores moving away from their associated pole do not exert a significant pushing force on the chromosome. The Journal of cell biology. 135:315-327.

Khodjakov, A., and C.L. Rieder. 2009. The nature of cell-cycle checkpoints: facts and fallacies. J Biol. 8:88.

Kim, Y., J.E. Heuser, C.M. Waterman, and D.W. Cleveland. 2008. CENP-E combines a slow, processive motor and a flexible coiled coil to produce an essential motile kinetochore tether. The Journal of cell biology. 181:411-419.

Kim, Y., A.J. Holland, W. Lan, and D.W. Cleveland. 2010. Aurora kinases and protein phosphatase 1 mediate chromosome congression through regulation of CENP-E. Cell. 142:444-455.

King, J.M., and R.B. Nicklas. 2000. Tension on chromosomes increases the number of kinetochore microtubules but only within limits. J Cell Sci. 113 Pt 21:3815-3823.

Kirschner, M., and T. Mitchison. 1986. Beyond self-assembly: from microtubules to morphogenesis. Cell. 45:329-342.

Kiyomitsu, T., and I.M. Cheeseman. 2012. Chromosome- and spindle-pole-derived signals generate an intrinsic code for spindle position and orientation. Nature cell biology. 14:311-317.

Klare, K., J.R. Weir, F. Basilico, T. Zimniak, L. Massimiliano, N. Ludwigs, F. Herzog, and A. Musacchio. 2015. CENP-C is a blueprint for constitutive centromere-associated network assembly within human kinetochores. The Journal of cell biology. 210:11-22.

Kline-Smith, S.L., A. Khodjakov, P. Hergert, and C.E. Walczak. 2004. Depletion of centromeric MCAK leads to chromosome congression and segregation defects due to improper kinetochore attachments. Molecular biology of the cell. 15:1146-1159.

Kline-Smith, S.L., S. Sandall, and A. Desai. 2005. Kinetochore-spindle microtubule interactions during mitosis. Current opinion in cell biology. 17:35-46.

Koc, A., L.J. Wheeler, C.K. Mathews, and G.F. Merrill. 2004. Hydroxyurea arrests DNA replication by a mechanism that preserves basal dNTP pools. The Journal of biological chemistry. 279:223-230.

Kollu, S., S.F. Bakhoum, and D.A. Compton. 2009. Interplay of microtubule dynamics and sliding during bipolar spindle formation in mammalian cells. Current biology : CB. 19:2108-2113.

Komarova, Y., C.O. De Groot, I. Grigoriev, S.M. Gouveia, E.L. Munteanu, J.M. Schober, S. Honnappa, R.M. Buey, C.C. Hoogenraad, M. Dogterom, G.G. Borisy, M.O. Steinmetz, and A. Akhmanova. 2009. Mammalian end binding proteins control persistent microtubule growth. The Journal of cell biology. 184:691-706.

Kraft, C., F. Herzog, C. Gieffers, K. Mechtler, A. Hagting, J. Pines, and J.M. Peters. 2003. Mitotic regulation of the human anaphase-promoting complex by phosphorylation. The EMBO journal. 22:6598-6609.

Kueh, H.Y., and T.J. Mitchison. 2009. Structural plasticity in actin and tubulin polymer dynamics. Science. 325:960-963.

Kulukian, A., J.S. Han, and D.W. Cleveland. 2009. Unattached kinetochores catalyze production of an anaphase inhibitor that requires a Mad2 template to prime Cdc20 for BubR1 binding. Developmental cell. 16:105-117.

Kurasawa, Y., W.C. Earnshaw, Y. Mochizuki, N. Dohmae, and K. Todokoro. 2004. Essential roles of KIF4 and its binding partner PRC1 in organized central spindle midzone formation. The EMBO journal. 23:3237-3248.

Lampson, M.A., and I.M. Cheeseman. 2011. Sensing centromere tension: Aurora B and the regulation of kinetochore function. Trends in cell biology. 21:133-140.

Lampson, M.A., and T.M. Kapoor. 2006. Unraveling cell division mechanisms with small-molecule inhibitors. Nat Chem Biol. 2:19-27.

Lampson, M.A., K. Renduchitala, A. Khodjakov, and T.M. Kapoor. 2004. Correcting improper chromosome-spindle attachments during cell division. Nature cell biology. 6:232-237.

Lan, W., X. Zhang, S.L. Kline-Smith, S.E. Rosasco, G.A. Barrett-Wilt, J. Shabanowitz, D.F. Hunt, C.E. Walczak, and P.T. Stukenberg. 2004. Aurora B phosphorylates centromeric MCAK and regulates its localization and microtubule depolymerization activity. Current biology : CB. 14:273-286.

Lark, K.G., R.A. Consigli, and H.C. Minocha. 1966. Segregation of sister chromatids in mammalian cells. Science. 154:1202-1205.

Leise, W., 3rd, and P.R. Mueller. 2002. Multiple Cdk1 inhibitory kinases regulate the cell cycle during development. Developmental biology. 249:156-173.

Levesque, A.A., and D.A. Compton. 2001. The chromokinesin Kid is necessary for chromosome arm orientation and oscillation, but not congression, on mitotic spindles. J Cell Biol. 154:1135-1146.

Lew, D.J., D.J. Burke, and A. Dutta. 2008. The immortal strand hypothesis: how could it work? Cell. 133:21-23.

Lewellyn, L., A. Carvalho, A. Desai, A.S. Maddox, and K. Oegema. 2011. The chromosomal passenger complex and centralspindlin independently contribute to contractile ring assembly. The Journal of cell biology. 193:155-169.

Li, X., and R.B. Nicklas. 1995. Mitotic forces control a cell-cycle checkpoint. Nature. 373:630-632.

Li, Y., W. Yu, Y. Liang, and X. Zhu. 2007. Kinetochore dynein generates a poleward pulling force to facilitate congression and full chromosome alignment. Cell Res. 17:701-712.

Lim, S., and P. Kaldis. 2013. Cdks, cyclins and CKIs: roles beyond cell cycle regulation. Development. 140:3079-3093.

Liming, S., and S. Pathak. 1981. Gametogenesis in a male Indian muntjac x Chinese muntjac hybrid. Cytogenet Cell Genet. 30:152-156.

Lin, C.C., R. Sasi, Y.S. Fan, and Z.Q. Chen. 1991. New evidence for tandem chromosome fusions in the karyotypic evolution of Asian muntjacs. Chromosoma. 101:19-24.

Lindon, C., and J. Pines. 2004. Ordered proteolysis in anaphase inactivates Plk1 to contribute to proper mitotic exit in human cells. The Journal of cell biology. 164:233-241.

Littlepage, L.E., and J.V. Ruderman. 2002. Identification of a new APC/C recognition domain, the A box, which is required for the Cdh1-dependent destruction of the kinase Aurora-A during mitotic exit. Genes & development. 16:2274-2285.

Liu, D., G. Vader, M.J. Vromans, M.A. Lampson, and S.M. Lens. 2009. Sensing chromosome bi-orientation by spatial separation of aurora B kinase from kinetochore substrates. Science. 323:1350-1353.

Liu, D., M. Vleugel, C.B. Backer, T. Hori, T. Fukagawa, I.M. Cheeseman, and M.A. Lampson. 2010. Regulated targeting of protein phosphatase 1 to the outer kinetochore by KNL1 opposes Aurora B kinase. The Journal of cell biology. 188:809-820.

Loncarek, J., O. Kisurina-Evgenieva, T. Vinogradova, P. Hergert, S. La Terra, T.M. Kapoor, and A. Khodjakov. 2007. The centromere geometry essential for keeping mitosis error free is controlled by spindle forces. Nature. 450:745-749.

Luders, J., and T. Stearns. 2007. Microtubule-organizing centres: a re-evaluation. Nat Rev Mol Cell Biol. 8:161-167.

Maddox, P.S., F. Hyndman, J. Monen, K. Oegema, and A. Desai. 2007. Functional genomics identifies a Myb domain-containing protein family required for assembly of CENP-A chromatin. The Journal of cell biology. 176:757-763.

Maddox, P.S., K. Oegema, A. Desai, and I.M. Cheeseman. 2004. "Holo"er than thou: chromosome segregation and kinetochore function in C. elegans. Chromosome research : an international journal on the molecular, supramolecular and evolutionary aspects of chromosome biology. 12:641-653.

Magidson, V., J. He, J.G. Ault, C.B. O'Connell, N. Yang, I. Tikhonenko, B.F. McEwen, H. Sui, and A. Khodjakov. 2016. Unattached kinetochores rather than intrakinetochore tension arrest mitosis in taxol-treated cells. The Journal of cell biology. 212:307-319.

Magidson, V., C.B. O'Connell, J. Loncarek, R. Paul, A. Mogilner, and A. Khodjakov. 2011. The spatial arrangement of chromosomes during prometaphase facilitates spindle assembly. Cell. 146:555-567.

Magidson, V., R. Paul, N. Yang, J.G. Ault, C.B. O'Connell, I. Tikhonenko, B.F. McEwen, A. Mogilner, and A. Khodjakov. 2015. Adaptive changes in the kinetochore architecture facilitate proper spindle assembly. Nature cell biology. 17:1134-1144.

Maiato, H., O. Afonso, and I. Matos. 2015. A chromosome separation checkpoint: A midzone Aurora B gradient mediates a chromosome separation checkpoint that regulates the anaphase-telophase transition. Bioessays. 37:257-266.

Maiato, H., J. DeLuca, E.D. Salmon, and W.C. Earnshaw. 2004a. The dynamic kinetochore-microtubule interface. Journal of cell science. 117:5461-5477.

Maiato, H., E.A. Fairley, C.L. Rieder, J.R. Swedlow, C.E. Sunkel, and W.C. Earnshaw. 2003a. Human CLASP1 is an outer kinetochore component that regulates spindle microtubule dynamics. Cell. 113:891-904.

Maiato, H., A.M. Gomes, F. Sousa, and M. Barisic. 2017. Mechanisms of Chromosome Congression during Mitosis. Biology (Basel). 6.

Maiato, H., P.J. Hergert, S. Moutinho-Pereira, Y. Dong, K.J. Vandenbeldt, C.L. Rieder, and B.F. McEwen. 2006. The ultrastructure of the kinetochore and kinetochore fiber in Drosophila somatic cells. Chromosoma. 115:469-480.

Maiato, H., A. Khodjakov, and C.L. Rieder. 2005. Drosophila CLASP is required for the incorporation of microtubule subunits into fluxing kinetochore fibres. Nature cell biology. 7:42-47.

Maiato, H., and M. Lince-Faria. 2010. The perpetual movements of anaphase. Cellular and molecular life sciences : CMLS. 67:2251-2269.

Maiato, H., C.L. Rieder, and A. Khodjakov. 2004b. Kinetochore-driven formation of kinetochore fibers contributes to spindle assembly during animal mitosis. The Journal of cell biology. 167:831-840.

Maiato, H., P. Sampaio, C.L. Lemos, J. Findlay, M. Carmena, W.C. Earnshaw, and C.E. Sunkel. 2002. MAST/Orbit has a role in microtubule-kinetochore attachment and is essential for chromosome alignment and maintenance of spindle bipolarity. The Journal of cell biology. 157:749-760.

Maiato, H., C.E. Sunkel, and W.C. Earnshaw. 2003b. Dissecting mitosis by RNAi in Drosophila tissue culture cells. Biological procedures online. 5:153-161.

Maliga, Z., T.M. Kapoor, and T.J. Mitchison. 2002. Evidence that monastrol is an allosteric inhibitor of the mitotic kinesin Eg5. Chemistry & biology. 9:989-996.

Mallik, R., B.C. Carter, S.A. Lex, S.J. King, and S.P. Gross. 2004. Cytoplasmic dynein functions as a gear in response to load. Nature. 427:649-652.

Mallik, R., and S.P. Gross. 2004. Molecular motors: strategies to get along. Current biology : CB. 14:R971-982.

Maney, T., A.W. Hunter, M. Wagenbach, and L. Wordeman. 1998. Mitotic centromere-associated kinesin is important for anaphase chromosome segregation. The Journal of cell biology. 142:787-801.

Maney, T., M. Wagenbach, and L. Wordeman. 2001. Molecular dissection of the microtubule depolymerizing activity of mitotic centromere-associated kinesin. The Journal of biological chemistry. 276:34753-34758.

Manning, A.L., N.J. Ganem, S.F. Bakhoum, M. Wagenbach, L. Wordeman, and D.A. Compton. 2007. The kinesin-13 proteins Kif2a, Kif2b, and Kif2c/MCAK have distinct roles during mitosis in human cells. Molecular biology of the cell. 18:2970-2979.

Manuelidis, L. 1978. Chromosomal localization of complex and simple repeated human DNAs. Chromosoma. 66:23-32.

Mapelli, M., L. Massimiliano, S. Santaguida, and A. Musacchio. 2007. The Mad2 conformational dimer: structure and implications for the spindle assembly checkpoint. Cell. 131:730-743.

Maresca, T.J., A.C. Groen, J.C. Gatlin, R. Ohi, T.J. Mitchison, and E.D. Salmon. 2009. Spindle assembly in the absence of a RanGTP gradient requires localized CPC activity. Current biology : CB. 19:1210-1215.

Maresca, T.J., and E.D. Salmon. 2009. Intrakinetochore stretch is associated with changes in kinetochore phosphorylation and spindle assembly checkpoint activity. The Journal of cell biology. 184:373-381.

Margolis, R.L., and L. Wilson. 1981. Microtubule treadmills–possible molecular machinery. Nature. 293:705-711.

Marques, A., and A. Pedrosa-Harand. 2016. Holocentromere identity: from the typical mitotic linear structure to the great plasticity of meiotic holocentromeres. Chromosoma. 125:669-681.

Masumoto, H., H. Masukata, Y. Muro, N. Nozaki, and T. Okazaki. 1989. A human centromere antigen (CENP-B) interacts with a short specific sequence in alphoid DNA, a human centromeric satellite. The Journal of cell biology. 109:1963-1973.

Matos, I., A.J. Pereira, M. Lince-Faria, L.A. Cameron, E.D. Salmon, and H. Maiato. 2009. Synchronizing chromosome segregation by flux-dependent force equalization at kinetochores. The Journal of cell biology. 186:11-26.

Matsusaka, T., and J. Pines. 2004. Chfr acts with the p38 stress kinases to block entry to mitosis in mammalian cells. The Journal of cell biology. 166:507-516.

Mayer, T.U., T.M. Kapoor, S.J. Haggarty, R.W. King, S.L. Schreiber, and T.J. Mitchison. 1999. Small molecule inhibitor of mitotic spindle bipolarity identified in a phenotype-based screen. Science. 286:971-974.

Mayr, M.I., S. Hummer, J. Bormann, T. Gruner, S. Adio, G. Woehlke, and T.U. Mayer. 2007. The human kinesin Kif18A is a motile microtubule depolymerase essential for chromosome congression. Current biology : CB. 17:488-498.

Mazia, D. 1961. How cells divide. Sci Am. 205:100-120.

Mazumdar, M., and T. Misteli. 2005. Chromokinesins: multitalented players in mitosis. Trends in cell biology. 15:349-355.

McCleland, M.L., R.D. Gardner, M.J. Kallio, J.R. Daum, G.J. Gorbsky, D.J. Burke, and P.T. Stukenberg. 2003. The highly conserved Ndc80 complex is required for kinetochore assembly, chromosome congression, and spindle checkpoint activity. Genes & development. 17:101-114.

McCleland, M.L., M.J. Kallio, G.A. Barrett-Wilt, C.A. Kestner, J. Shabanowitz, D.F. Hunt, G.J. Gorbsky, and P.T. Stukenberg. 2004. The vertebrate Ndc80 complex contains Spc24 and Spc25 homologs, which are required to establish and maintain kinetochore-microtubule attachment. Current biology : CB. 14:131-137.

McEwen, B.F., Y. Ding, and A.B. Heagle. 1998a. Relevance of kinetochore size and microtubule-binding capacity for stable chromosome attachment during mitosis in PtK1 cells. Chromosome research : an international journal on the molecular, supramolecular and evolutionary aspects of chromosome biology. 6:123-132.

McEwen, B.F., A.B. Heagle, G.O. Cassels, K.F. Buttle, and C.L. Rieder. 1997. Kinetochore fiber maturation in PtK1 cells and its implications for the mechanisms of chromosome congression and anaphase onset. The Journal of cell biology. 137:1567-1580.

McEwen, B.F., C.E. Hsieh, A.L. Mattheyses, and C.L. Rieder. 1998b. A new look at kinetochore structure in vertebrate somatic cells using high-pressure freezing and freeze substitution. Chromosoma. 107:366-375.

McGarry, T.J., and M.W. Kirschner. 1998. Geminin, an inhibitor of DNA replication, is degraded during mitosis. Cell. 93:1043-1053.

McIntosh, J.R., and T. Hays. 2016. A Brief History of Research on Mitotic Mechanisms. Biology (Basel). 5.

McKean, P.G., S. Vaughan, and K. Gull. 2001. The extended tubulin superfamily. Journal of cell science. 114:2723-2733.

McKinley, K.L., and I.M. Cheeseman. 2016. The molecular basis for centromere identity and function. Nat Rev Mol Cell Biol. 17:16-29.

McKinley, K.L., N. Sekulic, L.Y. Guo, T. Tsinman, B.E. Black, and I.M. Cheeseman. 2015. The CENP-L-N Complex Forms a Critical Node in an Integrated Meshwork of Interactions at the Centromere-Kinetochore Interface. Mol Cell. 60:886-898.

Mennella, V., D.A. Agard, B. Huang, and L. Pelletier. 2014. Amorphous no more: subdiffraction view of the pericentriolar material architecture. Trends in cell biology. 24:188-197.

Miga, K.H., Y. Newton, M. Jain, N. Altemose, H.F. Willard, and W.J. Kent. 2014. Centromere reference models for human chromosomes X and Y satellite arrays. Genome Res. 24:697-707.

Mikhailov, A., M. Shinohara, and C.L. Rieder. 2005. The p38-mediated stress-activated checkpoint. A rapid response system for delaying progression through antephase and entry into mitosis. Cell Cycle. 4:57-62.

Miller, S.A., M.L. Johnson, and P.T. Stukenberg. 2008. Kinetochore attachments require an interaction between unstructured tails on microtubules and Ndc80(Hec1). Current biology : CB. 18:1785-1791.

Mimori-Kiyosue, Y., I. Grigoriev, G. Lansbergen, H. Sasaki, C. Matsui, F. Severin, N. Galjart, F. Grosveld, I. Vorobjev, S. Tsukita, and A. Akhmanova. 2005. CLASP1 and CLASP2 bind to EB1 and regulate microtubule plus-end dynamics at the cell cortex. The Journal of cell biology. 168:141-153.

Minshull, J., J.J. Blow, and T. Hunt. 1989. Translation of cyclin mRNA is necessary for extracts of activated xenopus eggs to enter mitosis. Cell. 56:947-956.

Minshull, J., R. Golsteyn, C.S. Hill, and T. Hunt. 1990. The A- and B-type cyclin associated cdc2 kinases in Xenopus turn on and off at different times in the cell cycle. The EMBO journal. 9:2865-2875.

Mitchison, T., L. Evans, E. Schulze, and M. Kirschner. 1986. Sites of microtubule assembly and disassembly in the mitotic spindle. Cell. 45:515-527.

Mitchison, T., and M. Kirschner. 1984. Dynamic instability of microtubule growth. Nature. 312:237-242.

Mitchison, T.J. 1989. Polewards microtubule flux in the mitotic spindle: evidence from photoactivation of fluorescence. The Journal of cell biology. 109:637-652.

Mitchison, T.J., and E.D. Salmon. 2001. Mitosis: a history of division. Nature cell biology. 3:E17-21.

Moore, A.T., K.E. Rankin, G. von Dassow, L. Peris, M. Wagenbach, Y. Ovechkina, A. Andrieux, D. Job, and L. Wordeman. 2005. MCAK associates with the tips of polymerizing microtubules. The Journal of cell biology. 169:391-397.

Morgan, D.O. 1995. Principles of CDK regulation. Nature. 374:131-134.

Moutinho-Pereira, S., I. Matos, and H. Maiato. 2010. Drosophila S2 cells as a model system to investigate mitotic spindle dynamics, architecture, and function. Methods in cell biology. 97:243-257.

Moutinho-Pereira, S., N. Stuurman, O. Afonso, M. Hornsveld, P. Aguiar, G. Goshima, R.D. Vale, and H. Maiato. 2013. Genes involved in centrosome-independent mitotic spindle assembly in Drosophila S2 cells. Proceedings of the National Academy of Sciences of the United States of America. 110:19808-19813.

Murmann, A.E., A. Mincheva, M.O. Scheuermann, M. Gautier, F. Yang, J. Buitkamp, P.L. Strissel, R. Strick, J.D. Rowley, and P. Lichter. 2008. Comparative gene mapping in cattle, Indian muntjac, and Chinese muntjac by fluorescence in situ hybridization. Genetica. 134:345-351.

Murphy, T.D., and G.H. Karpen. 1995. Localization of centromere function in a Drosophila minichromosome. Cell. 82:599-609.

Murphy, T.D., and G.H. Karpen. 1998. Centromeres take flight: alpha satellite and the quest for the human centromere. Cell. 93:317-320.

Murphy, W.J., D.M. Larkin, A. Everts-van der Wind, G. Bourque, G. Tesler, L. Auvil, J.E. Beever, B.P. Chowdhary, F. Galibert, L. Gatzke, C. Hitte, S.N. Meyers, D. Milan, E.A. Ostrander, G. Pape, H.G. Parker, T. Raudsepp, M.B. Rogatcheva, L.B. Schook, L.C. Skow, M. Welge, J.E. Womack, J. O'Brien S, P.A. Pevzner, and H.A. Lewin. 2005. Dynamics of mammalian chromosome evolution inferred from multispecies comparative maps. Science. 309:613-617.

Murray, A.W., and M.W. Kirschner. 1989. Cyclin synthesis drives the early embryonic cell cycle. Nature. 339:275-280.

Murray-Zmijewski, F., E.A. Slee, and X. Lu. 2008. A complex barcode underlies the heterogeneous response of p53 to stress. Nat Rev Mol Cell Biol. 9:702-712.

Musacchio, A., and A. Desai. 2017. A Molecular View of Kinetochore Assembly and Function. Biology (Basel). 6.

Nahse, V., L. Christ, H. Stenmark, and C. Campsteijn. 2017. The Abscission Checkpoint: Making It to the Final Cut. Trends in cell biology. 27:1-11.

Nakano, M., S. Cardinale, V.N. Noskov, R. Gassmann, P. Vagnarelli, S. Kandels-Lewis, V. Larionov, W.C. Earnshaw, and H. Masumoto. 2008. Inactivation of a human kinetochore by specific targeting of chromatin modifiers. Developmental cell. 14:507-522.

Nardi, I.K., E. Zasadzinska, M.E. Stellfox, C.M. Knippler, and D.R. Foltz. 2016. Licensing of Centromeric Chromatin Assembly through the Mis18alpha-Mis18beta Heterotetramer. Mol Cell. 61:774-787.

Naylor, R.M., and J.M. van Deursen. 2016. Aneuploidy in Cancer and Aging. Annu Rev Genet. 50:45-66.

Nelson, W.G., and M.B. Kastan. 1994. DNA strand breaks: the DNA template alterations that trigger p53-dependent DNA damage response pathways. Mol Cell Biol. 14:1815-1823.

Nicklas, R.B., and C.A. Koch. 1969. Chromosome micromanipulation. 3. Spindle fiber tension and the reorientation of mal-oriented chromosomes. The Journal of cell biology. 43:40-50.

Nicklas, R.B., and S.C. Ward. 1994. Elements of error correction in mitosis: microtubule capture, release, and tension. J Cell Biol. 126:1241-1253.

Nicklas, R.B., S.C. Ward, and G.J. Gorbsky. 1995. Kinetochore chemistry is sensitive to tension and may link mitotic forces to a cell cycle checkpoint. The Journal of cell biology. 130:929-939.

Nijenhuis, W., G. Vallardi, A. Teixeira, G.J. Kops, and A.T. Saurin. 2014. Negative feedback at kinetochores underlies a responsive spindle checkpoint signal. Nature cell biology. 16:1257-1264.

Nijenhuis, W., E. von Castelmur, D. Littler, V. De Marco, E. Tromer, M. Vleugel, M.H. van Osch, B. Snel, A. Perrakis, and G.J. Kops. 2013. A TPR domain-containing N-terminal

module of MPS1 is required for its kinetochore localization by Aurora B. The Journal of cell biology. 201:217-231.

Nogales, E., and R. Zhang. 2016. Visualizing microtubule structural transitions and interactions with associated proteins. Curr Opin Struct Biol. 37:90-96.

Nousiainen, M., H.H. Sillje, G. Sauer, E.A. Nigg, and R. Korner. 2006. Phosphoproteome analysis of the human mitotic spindle. Proceedings of the National Academy of Sciences of the United States of America. 103:5391-5396.

Nurse, P. 1975. Genetic control of cell size at cell division in yeast. Nature. 256:547-551.

Nurse, P., P. Thuriaux, and K. Nasmyth. 1976. Genetic control of the cell division cycle in the fission yeast Schizosaccharomyces pombe. Mol Gen Genet. 146:167-178.

Nusbaum, C., M.C. Zody, M.L. Borowsky, M. Kamal, C.D. Kodira, T.D. Taylor, C.A. Whittaker, J.L. Chang, C.A. Cuomo, K. Dewar, M.G. FitzGerald, X. Yang, A. Abouelleil, N.R. Allen, S. Anderson, T. Bloom, B. Bugalter, J. Butler, A. Cook, D. DeCaprio, R. Engels, M. Garber, A. Gnirke, N. Hafez, J.L. Hall, C.H. Norman, T. Itoh, D.B. Jaffe, Y. Kuroki, J. Lehoczky, A. Lui, P. Macdonald, E. Mauceli, T.S. Mikkelsen, J.W. Naylor, R. Nicol, C. Nguyen, H. Noguchi, S.B. O'Leary, K. O'Neill, B. Piqani, C.L. Smith, J.A. Talamas, K. Topham, Y. Totoki, A. Toyoda, H.M. Wain, S.K. Young, Q. Zeng, A.R. Zimmer, A. Fujiyama, M. Hattori, B.W. Birren, Y. Sakaki, and E.S. Lander. 2005. DNA sequence and analysis of human chromosome 18. Nature. 437:551-555.

O'Connell, C.B., A. Khodjakov, and B.F. McEwen. 2012. Kinetochore flexibility: creating a dynamic chromosome-spindle interface. Current opinion in cell biology. 24:40-47.

O'Connell, C.B., J. Loncarek, P. Hergert, A. Kourtidis, D.S. Conklin, and A. Khodjakov. 2008. The spindle assembly checkpoint is satisfied in the absence of interkinetochore tension during mitosis with unreplicated genomes. The Journal of cell biology. 183:29-36.

O'Connell, C.B., J. Loncarek, P. Kalab, and A. Khodjakov. 2009. Relative contributions of chromatin and kinetochores to mitotic spindle assembly. The Journal of cell biology. 187:43-51.

Oestergren, G. 1945. Equilibrium of trivalents and the mechanism of chromosome movements. Hereditas. 31:498.

Ohtsubo, M., A.M. Theodoras, J. Schumacher, J.M. Roberts, and M. Pagano. 1995. Human cyclin E, a nuclear protein essential for the G1-to-S phase transition. Mol Cell Biol. 15:2612-2624.

Oliveira, R.A., R.S. Hamilton, A. Pauli, I. Davis, and K. Nasmyth. 2010. Cohesin cleavage and Cdk inhibition trigger formation of daughter nuclei. Nat Cell Biol. 12:185-192.

Orr, B., H. Bousbaa, and C.E. Sunkel. 2007. Mad2-independent spindle assembly checkpoint activation and controlled metaphase-anaphase transition in Drosophila S2 cells. Molecular biology of the cell. 18:850-863.

Orr, B., and C.E. Sunkel. 2011. Drosophila CENP-C is essential for centromere identity. Chromosoma. 120:83-96.

Östergren, G. 1951. THE MECHANISM OF CO-ORIENTATION IN BIVALENTS AND MULTIVALENTS

THE THEORY OF ORIENTATION BY PULLING. Hereditas. 37:85-156.

Painter, R.B., and B.R. Young. 1980. Radiosensitivity in ataxia-telangiectasia: a new explanation. Proceedings of the National Academy of Sciences of the United States of America. 77:7315-7317.

Palmer, D.K., K. O'Day, H.L. Trong, H. Charbonneau, and R.L. Margolis. 1991. Purification of the centromere-specific protein CENP-A and demonstration that it is a distinctive histone. Proceedings of the National Academy of Sciences of the United States of America. 88:3734-3738.

Palmer, D.K., K. O'Day, M.H. Wener, B.S. Andrews, and R.L. Margolis. 1987. A 17-kD centromere protein (CENP-A) copurifies with nucleosome core particles and with histones. The Journal of cell biology. 104:805-815.

Parry, D.H., G.R. Hickson, and P.H. O'Farrell. 2003. Cyclin B destruction triggers changes in kinetochore behavior essential for successful anaphase. Current biology : CB. 13:647-653.

Pavin, N., and I.M. Tolic. 2016. Self-Organization and Forces in the Mitotic Spindle. Annu Rev Biophys. 45:279-298.

Petrovic, A., J. Keller, Y. Liu, K. Overlack, J. John, Y.N. Dimitrova, S. Jenni, S. van Gerwen, P. Stege, S. Wohlgemuth, P. Rombaut, F. Herzog, S.C. Harrison, I.R. Vetter, and A.

Musacchio. 2016. Structure of the MIS12 Complex and Molecular Basis of Its Interaction with CENP-C at Human Kinetochores. Cell. 167:1028-1040 e1015.

Pines, J. 2011. Cubism and the cell cycle: the many faces of the APC/C. Nat Rev Mol Cell Biol. 12:427-438.

Pinsky, B.A., and S. Biggins. 2005. The spindle checkpoint: tension versus attachment. Trends in cell biology. 15:486-493.

Ponstingl, H., E. Krauhs, M. Little, and T. Kempf. 1981. Complete amino acid sequence of alpha-tubulin from porcine brain. Proceedings of the National Academy of Sciences of the United States of America. 78:2757-2761.

Powers, J., D.J. Rose, A. Saunders, S. Dunkelbarger, S. Strome, and W.M. Saxton. 2004. Loss of KLP-19 polar ejection force causes misorientation and missegregation of holocentric chromosomes. The Journal of cell biology. 166:991-1001.

Przewloka, M.R., Z. Venkei, V.M. Bolanos-Garcia, J. Debski, M. Dadlez, and D.M. Glover. 2011. CENP-C is a structural platform for kinetochore assembly. Current biology : CB. 21:399-405.

Raaijmakers, J.A., and R.H. Medema. 2014. Function and regulation of dynein in mitotic chromosome segregation. Chromosoma. 123:407-422.

Resnick, T.D., D.L. Satinover, F. MacIsaac, P.T. Stukenberg, W.C. Earnshaw, T.L. Orr-Weaver, and M. Carmena. 2006. INCENP and Aurora B promote meiotic sister chromatid cohesion through localization of the Shugoshin MEI-S332 in Drosophila. Developmental cell. 11:57-68.

Rieder, C.L. 1982. The formation, structure, and composition of the mammalian kinetochore and kinetochore fiber. International review of cytology. 79:1-58.

Rieder, C.L. 2011. Mitosis in vertebrates: the G2/M and M/A transitions and their associated checkpoints. Chromosome research : an international journal on the molecular, supramolecular and evolutionary aspects of chromosome biology. 19:291-306.

Rieder, C.L., and R.W. Cole. 1998. Entry into mitosis in vertebrate somatic cells is guarded by a chromosome damage checkpoint that reverses the cell cycle when triggered during early but not late prophase. The Journal of cell biology. 142:1013-1022.

Rieder, C.L., R.W. Cole, A. Khodjakov, and G. Sluder. 1995. The checkpoint delaying anaphase in response to chromosome monoorientation is mediated by an inhibitory signal produced by unattached kinetochores. The Journal of cell biology. 130:941-948.

Rieder, C.L., E.A. Davison, L.C. Jensen, L. Cassimeris, and E.D. Salmon. 1986. Oscillatory movements of monooriented chromosomes and their position relative to the spindle pole result from the ejection properties of the aster and half-spindle. The Journal of cell biology. 103:581-591.

Rieder, C.L., and H. Maiato. 2004. Stuck in division or passing through: what happens when cells cannot satisfy the spindle assembly checkpoint. Dev Cell. 7:637-651.

Rieder, C.L., and E.D. Salmon. 1994. Motile kinetochores and polar ejection forces dictate chromosome position on the vertebrate mitotic spindle. The Journal of cell biology. 124:223-233.

Rieder, C.L., and E.D. Salmon. 1998. The vertebrate cell kinetochore and its roles during mitosis. Trends in cell biology. 8:310-318.

Rocheteau, P., B. Gayraud-Morel, I. Siegl-Cachedenier, M.A. Blasco, and S. Tajbakhsh. 2012. A subpopulation of adult skeletal muscle stem cells retains all template DNA strands after cell division. Cell. 148:112-125.

Rodrigues-Martins, A., M. Riparbelli, G. Callaini, D.M. Glover, and M. Bettencourt-Dias. 2008. From centriole biogenesis to cellular function: centrioles are essential for cell division at critical developmental stages. Cell Cycle. 7:11-16.

Ruchaud, S., M. Carmena, and W.C. Earnshaw. 2007. Chromosomal passengers: conducting cell division. Nat Rev Mol Cell Biol. 8:798-812.

Russell, P., and P. Nurse. 1986. cdc25+ functions as an inducer in the mitotic control of fission yeast. Cell. 45:145-153.

Sadhu, K., S.I. Reed, H. Richardson, and P. Russell. 1990. Human homolog of fission yeast cdc25 mitotic inducer is predominantly expressed in G2. Proceedings of the National Academy of Sciences of the United States of America. 87:5139-5143.

Salemi, J.D., P.T. McGilvray, and T.J. Maresca. 2013. Development of a Drosophila cell-based error correction assay. Frontiers in oncology. 3:187.

Salido, M., I. Tusquets, J.M. Corominas, M. Suarez, B. Espinet, C. Corzo, M. Bellet, X. Fabregat, S. Serrano, and F. Sole. 2005. Polysomy of chromosome 17 in breast cancer tumors showing an overexpression of ERBB2: a study of 175 cases using fluorescence in situ hybridization and immunohistochemistry. Breast Cancer Res. 7:R267-273.

Santos, S.D., R. Wollman, T. Meyer, and J.E. Ferrell, Jr. 2012. Spatial positive feedback at the onset of mitosis. Cell. 149:1500-1513.

Sardar, H.S., V.G. Luczak, M.M. Lopez, B.C. Lister, and S.P. Gilbert. 2010. Mitotic kinesin CENP-E promotes microtubule plus-end elongation. Current biology : CB. 20:1648-1653.

Satge, D., M. Nishi, N. Sirvent, and M. Vekemans. 2016. A tumor profile in Edwards syndrome (trisomy 18). Am J Med Genet C Semin Med Genet. 172:296-306.

Savoian, M.S., M.L. Goldberg, and C.L. Rieder. 2000. The rate of poleward chromosome motion is attenuated in Drosophila zw10 and rod mutants. Nature cell biology. 2:948-952.

Sawin, K.E., K. LeGuellec, M. Philippe, and T.J. Mitchison. 1992. Mitotic spindle organization by a plus-end-directed microtubule motor. Nature. 359:540-543.

Sawin, K.E., and T.J. Mitchison. 1991. Poleward microtubule flux mitotic spindles assembled in vitro. The Journal of cell biology. 112:941-954.

Saxton, W.M., D.L. Stemple, R.J. Leslie, E.D. Salmon, M. Zavortink, and J.R. McIntosh. 1984. Tubulin dynamics in cultured mammalian cells. The Journal of cell biology. 99:2175-2186.

Schepers, A.G., R. Vries, M. van den Born, M. van de Wetering, and H. Clevers. 2011. Lgr5 intestinal stem cells have high telomerase activity and randomly segregate their chromosomes. The EMBO journal. 30:1104-1109.

Screpanti, E., A. De Antoni, G.M. Alushin, A. Petrovic, T. Melis, E. Nogales, and A. Musacchio. 2011. Direct binding of Cenp-C to the Mis12 complex joins the inner and outer kinetochore. Current biology : CB. 21:391-398.

Sharp, D.J., H.M. Brown, M. Kwon, G.C. Rogers, G. Holland, and J.M. Scholey. 2000. Functional coordination of three mitotic motors in Drosophila embryos. Molecular biology of the cell. 11:241-253.

Sharp, L.W. 1921. Introduction To Cytology. New York: McGraw Hill Book Company Inc. p. 143. New York: McGraw Hill Book Company Inc. p. 143. 1.

Sharp, L.W. 1934. Introduction to cytology. McGraw-Hill Book Co. Inc. New York & London.

Sherr, C.J. 1994. G1 phase progression: cycling on cue. Cell. 79:551-555.

Shrestha, R.L., and V.M. Draviam. 2013. Lateral to end-on conversion of chromosome-microtubule attachment requires kinesins CENP-E and MCAK. Curr Biol. 23:1514-1526.

Sikirzhytski, V., V. Magidson, J.B. Steinman, J. He, M. Le Berre, I. Tikhonenko, J.G. Ault, B.F. McEwen, J.K. Chen, H. Sui, M. Piel, T.M. Kapoor, and A. Khodjakov. 2014. Direct kinetochore-spindle pole connections are not required for chromosome segregation. The Journal of cell biology. 206:231-243.

Silva, M.C., D.L. Bodor, M.E. Stellfox, N.M. Martins, H. Hochegger, D.R. Foltz, and L.E. Jansen. 2012. Cdk activity couples epigenetic centromere inheritance to cell cycle progression. Developmental cell. 22:52-63.

Silverman, M.A., S. Kaech, E.M. Ramser, X. Lu, M.R. Lasarev, S. Nagalla, and G. Banker. 2010. Expression of kinesin superfamily genes in cultured hippocampal neurons. Cytoskeleton (Hoboken). 67:784-795.

Sirajuddin, M., L.M. Rice, and R.D. Vale. 2014. Regulation of microtubule motors by tubulin isotypes and post-translational modifications. Nature cell biology. 16:335-344.

Skibbens, R.V., V.P. Skeen, and E.D. Salmon. 1993. Directional instability of kinetochore motility during chromosome congression and segregation in mitotic newt lung cells: a push-pull mechanism. The Journal of cell biology. 122:859-875.

Smith, C.A., A.D. McAinsh, and N.J. Burroughs. 2016. Human kinetochores are swivel joints that mediate microtubule attachments. eLife. 5.

Spencer, F., and P. Hieter. 1992. Centromere DNA mutations induce a mitotic delay in Saccharomyces cerevisiae. Proceedings of the National Academy of Sciences of the United States of America. 89:8908-8912.

Stumpff, J., T. Duncan, E. Homola, S.D. Campbell, and T.T. Su. 2004. Drosophila Wee1 kinase regulates Cdk1 and mitotic entry during embryogenesis. Current biology : CB. 14:2143-2148.

Sudakin, V., G.K. Chan, and T.J. Yen. 2001. Checkpoint inhibition of the APC/C in HeLa cells is mediated by a complex of BUBR1, BUB3, CDC20, and MAD2. The Journal of cell biology. 154:925-936.

Suzuki, A., B.L. Badger, X. Wan, J.G. DeLuca, and E.D. Salmon. 2014. The architecture of CCAN proteins creates a structural integrity to resist spindle forces and achieve proper Intrakinetochore stretch. Developmental cell. 30:717-730.

Tajbakhsh, S. 2008. Stem cell identity and template DNA strand segregation. Current opinion in cell biology. 20:716-722.

Tajbakhsh, S., and C. Gonzalez. 2009. Biased segregation of DNA and centrosomes: moving together or drifting apart? Nature reviews. Molecular cell biology. 10:804-810.

Tauchman, E.C., F.J. Boehm, and J.G. DeLuca. 2015. Stable kinetochore-microtubule attachment is sufficient to silence the spindle assembly checkpoint in human cells. Nat Commun. 6:10036.

Thrower, D.A., M.A. Jordan, and L. Wilson. 1996. Modulation of CENP-E organization at kinetochores by spindle microtubule attachment. Cell motility and the cytoskeleton. 35:121-133.

Tilney, L.G., J. Bryan, D.J. Bush, K. Fujiwara, M.S. Mooseker, D.B. Murphy, and D.H. Snyder. 1973. Microtubules: evidence for 13 protofilaments. The Journal of cell biology. 59:267-275.

Tokai, N., A. Fujimoto-Nishiyama, Y. Toyoshima, S. Yonemura, S. Tsukita, J. Inoue, and T. Yamamota. 1996. Kid, a novel kinesin-like DNA binding protein, is localized to chromosomes and the mitotic spindle. The EMBO journal. 15:457-467.

Tokai-Nishizumi, N., M. Ohsugi, E. Suzuki, and T. Yamamoto. 2005. The chromokinesin Kid is required for maintenance of proper metaphase spindle size. Molecular biology of the cell. 16:5455-5463.

Tsai, M.Y., and Y. Zheng. 2005. Aurora A kinase-coated beads function as microtubule-organizing centers and enhance RanGTP-induced spindle assembly. Current biology : CB. 15:2156-2163.

Tseng, B.S., L. Tan, T.M. Kapoor, and H. Funabiki. 2010. Dual detection of chromosomes and microtubules by the chromosomal passenger complex drives spindle assembly. Developmental cell. 18:903-912.

Tsipouri, V., M.G. Schueler, S. Hu, N.C.S. Program, A. Dutra, E. Pak, H. Riethman, and E.D. Green. 2008. Comparative sequence analyses reveal sites of ancestral chromosomal fusions in the Indian muntjac genome. Genome Biol. 9:R155.

Tsukahara, T., Y. Tanno, and Y. Watanabe. 2010. Phosphorylation of the CPC by Cdk1 promotes chromosome bi-orientation. Nature. 467:719-723.

Tudzarova, S., P. Mulholland, A. Dey, K. Stoeber, A.L. Okorokov, and G.H. Williams. 2016. p53 controls CDC7 levels to reinforce G1 cell cycle arrest upon genotoxic stress. Cell Cycle. 15:2958-2972.

Uchida, K.S., K. Takagaki, K. Kumada, Y. Hirayama, T. Noda, and T. Hirota. 2009. Kinetochore stretching inactivates the spindle assembly checkpoint. J Cell Biol. 184:383-390.

Vader, G., and S.M. Lens. 2008. The Aurora kinase family in cell division and cancer. Biochim Biophys Acta. 1786:60-72.

Vader, G., A.F. Maia, and S.M. Lens. 2008. The chromosomal passenger complex and the spindle assembly checkpoint: kinetochore-microtubule error correction and beyond. Cell division. 3:10.

Valdivia, M.M., and B.R. Brinkley. 1985. Fractionation and initial characterization of the kinetochore from mammalian metaphase chromosomes. The Journal of cell biology. 101:1124-1134.

van der Horst, A., and S.M. Lens. 2014. Cell division: control of the chromosomal passenger complex in time and space. Chromosoma. 123:25-42.

van Heesbeen, R.G., J.A. Raaijmakers, M.E. Tanenbaum, V.A. Halim, D. Lelieveld, C. Lieftink, A.J. Heck, D.A. Egan, and R.H. Medema. 2016. Aurora A, MCAK, and Kif18b promote Eg5-independent spindle formation. Chromosoma.

van Heesbeen, R.G., M.E. Tanenbaum, and R.H. Medema. 2014. Balanced activity of three mitotic motors is required for bipolar spindle assembly and chromosome segregation. Cell reports. 8:948-956.

van Vugt, M.A., A.K. Gardino, R. Linding, G.J. Ostheimer, H.C. Reinhardt, S.E. Ong, C.S. Tan, H. Miao, S.M. Keezer, J. Li, T. Pawson, T.A. Lewis, S.A. Carr, S.J. Smerdon, T.R. Brummelkamp, and M.B. Yaffe. 2010. A mitotic phosphorylation feedback network connects Cdk1, Plk1, 53BP1, and Chk2 to inactivate the G(2)/M DNA damage checkpoint. PLoS Biol. 8:e1000287.

Vermeulen, K., D.R. Van Bockstaele, and Z.N. Berneman. 2003. The cell cycle: a review of regulation, deregulation and therapeutic targets in cancer. Cell Prolif. 36:131-149.

Vitre, B., N. Gudimchuk, R. Borda, Y. Kim, J.E. Heuser, D.W. Cleveland, and E.L. Grishchuk. 2014. Kinetochore-microtubule attachment throughout mitosis potentiated by the elongated stalk of the kinetochore kinesin CENP-E. Molecular biology of the cell. 25:2272-2281.

von Schubert, C., F. Cubizolles, J.M. Bracher, T. Sliedrecht, G.J. Kops, and E.A. Nigg. 2015. Plk1 and Mps1 Cooperatively Regulate the Spindle Assembly Checkpoint in Human Cells. Cell reports. 12:66-78.

Walczak, C.E., S. Cai, and A. Khodjakov. 2010. Mechanisms of chromosome behaviour during mitosis. Nat Rev Mol Cell Biol. 11:91-102.

Walczak, C.E., S. Gayek, and R. Ohi. 2013. Microtubule-depolymerizing kinesins. Annual review of cell and developmental biology. 29:417-441.

Wandke, C., M. Barisic, R. Sigl, V. Rauch, F. Wolf, A.C. Amaro, C.H. Tan, A.J. Pereira, U. Kutay, H. Maiato, P. Meraldi, and S. Geley. 2012. Human chromokinesins promote chromosome congression and spindle microtubule dynamics during mitosis. The Journal of cell biology. 198:847-863.

Wang, E., E.R. Ballister, and M.A. Lampson. 2011. Aurora B dynamics at centromeres create a diffusion-based phosphorylation gradient. J Cell Biol. 194:539-549.

Wang, F., J. Dai, J.R. Daum, E. Niedzialkowska, B. Banerjee, P.T. Stukenberg, G.J. Gorbsky, and J.M. Higgins. 2010. Histone H3 Thr-3 phosphorylation by Haspin positions Aurora B at centromeres in mitosis. Science. 330:231-235.

Wang, S.Z., and R. Adler. 1995. Chromokinesin: a DNA-binding, kinesin-like nuclear protein. The Journal of cell biology. 128:761-768.

Wang, X., J.W. Tsai, J.H. Imai, W.N. Lian, R.B. Vallee, and S.H. Shi. 2009. Asymmetric centrosome inheritance maintains neural progenitors in the neocortex. Nature. 461:947-955.

Welburn, J.P., M. Vleugel, D. Liu, J.R. Yates, 3rd, M.A. Lampson, T. Fukagawa, and I.M. Cheeseman. 2010. Aurora B phosphorylates spatially distinct targets to differentially regulate the kinetochore-microtubule interface. Mol Cell. 38:383-392.

Whittaker, A.J., I. Royzman, and T.L. Orr-Weaver. 2000. Drosophila double parked: a conserved, essential replication protein that colocalizes with the origin recognition complex and links DNA replication with mitosis and the down-regulation of S phase transcripts. Genes & development. 14:1765-1776.

Willard, H.F. 1985. Chromosome-specific organization of human alpha satellite DNA. Am J Hum Genet. 37:524-532.

Williams, B.C., M.F. Riedy, E.V. Williams, M. Gatti, and M.L. Goldberg. 1995. The Drosophila kinesin-like protein KLP3A is a midbody component required for central spindle assembly and initiation of cytokinesis. The Journal of cell biology. 129:709-723.

Willis, N., and N. Rhind. 2009. Regulation of DNA replication by the S-phase DNA damage checkpoint. Cell division. 4:13.

Wise, D.A., and B.R. Brinkley. 1997. Mitosis in cells with unreplicated genomes (MUGs): spindle assembly and behavior of centromere fragments. Cell motility and the cytoskeleton. 36:291-302.

Wojcik, E., R. Basto, M. Serr, F. Scaerou, R. Karess, and T. Hays. 2001. Kinetochore dynein: its dynamics and role in the transport of the Rough deal checkpoint protein. Nature cell biology. 3:1001-1007.

Wollman, R., E.N. Cytrynbaum, J.T. Jones, T. Meyer, J.M. Scholey, and A. Mogilner. 2005. Efficient chromosome capture requires a bias in the 'search-and-capture' process during mitotic-spindle assembly. Current biology : CB. 15:828-832.

Wong, J., and G. Fang. 2006. HURP controls spindle dynamics to promote proper interkinetochore tension and efficient kinetochore capture. The Journal of cell biology. 173:879-891.

Wood, K.W., L. Lad, L. Luo, X. Qian, S.D. Knight, N. Nevins, K. Brejc, D. Sutton, A.G. Gilmartin, P.R. Chua, R. Desai, S.P. Schauer, D.E. McNulty, R.S. Annan, L.D. Belmont, C. Garcia, Y. Lee, M.A. Diamond, L.F. Faucette, M. Giardiniere, S. Zhang, C.M. Sun, J.D. Vidal, S. Lichtsteiner, W.D. Cornwell, J.D. Greshock, R.F. Wooster, J.T. Finer, R.A. Copeland, P.S. Huang, D.J. Morgans, Jr., D. Dhanak, G. Bergnes, R. Sakowicz, and J.R. Jackson. 2010. Antitumor activity of an allosteric inhibitor of centromere-associated protein-E. Proceedings of the National Academy of Sciences of the United States of America. 107:5839-5844.

Wood, K.W., R. Sakowicz, L.S. Goldstein, and D.W. Cleveland. 1997. CENP-E is a plus end-directed kinetochore motor required for metaphase chromosome alignment. Cell. 91:357-366.

Woodard, G.E., N.N. Huang, H. Cho, T. Miki, G.G. Tall, and J.H. Kehrl. 2010. Ric-8A and Gi alpha recruit LGN, NuMA, and dynein to the cell cortex to help orient the mitotic spindle. Mol Cell Biol. 30:3519-3530.

Wordeman, L., and T.J. Mitchison. 1995. Identification and partial characterization of mitotic centromere-associated kinesin, a kinesin-related protein that associates with centromeres during mitosis. The Journal of cell biology. 128:95-104.

Wu, H.Y., E. Nazockdast, M.J. Shelley, and D.J. Needleman. 2016. Forces positioning the mitotic spindle: Theories, and now experiments. Bioessays.

Wurster, D.H., and K. Benirschke. 1967. Chromosome studies in some deer, the springbok, and the pronghorn, with notes on placentation in deer. Cytologia (Tokyo). 32:273-285.

Wurster, D.H., and K. Benirschke. 1970. Indian muntjac, Muntiacus muntjak: a deer with a low diploid chromosome number. Science. 168:1364-1366.

Wynne, D.J., and H. Funabiki. 2015. Kinetochore function is controlled by a phospho-dependent coexpansion of inner and outer components. The Journal of cell biology. 210:899-916.

Yajima, J., M. Edamatsu, J. Watai-Nishii, N. Tokai-Nishizumi, T. Yamamoto, and Y.Y. Toyoshima. 2003. The human chromokinesin Kid is a plus end-directed microtubule-based motor. EMBO J. 22:1067-1074.

Yamano, H., C. Tsurumi, J. Gannon, and T. Hunt. 1998. The role of the destruction box and its neighbouring lysine residues in cyclin B for anaphase ubiquitin-dependent proteolysis in fission yeast: defining the D-box receptor. The EMBO journal. 17:5670-5678.

Yang, F., P.C. O'Brien, J. Wienberg, and M.A. Ferguson-Smith. 1997. A reappraisal of the tandem fusion theory of karyotype evolution in Indian muntjac using chromosome painting. Chromosome research : an international journal on the molecular, supramolecular and evolutionary aspects of chromosome biology. 5:109-117.

Yang, Z., U.S. Tulu, P. Wadsworth, and C.L. Rieder. 2007. Kinetochore dynein is required for chromosome motion and congression independent of the spindle checkpoint. Current biology : CB. 17:973-980.

Ye, A.A., S. Cane, and T.J. Maresca. 2016. Chromosome biorientation produces hundreds of piconewtons at a metazoan kinetochore. Nat Commun. 7:13221.

Ye, A.A., J. Deretic, C.M. Hoel, A.W. Hinman, D. Cimini, J.P. Welburn, and T.J. Maresca. 2015. Aurora A Kinase Contributes to a Pole-Based Error Correction Pathway. Current biology : CB. 25:1842-1851.

Ye, F., L. Tan, Q. Yang, Y. Xia, L.W. Deng, M. Murata-Hori, and Y.C. Liou. 2011. HURP regulates chromosome congression by modulating kinesin Kif18A function. Current biology : CB. 21:1584-1591.

Zaytsev, A.V., and E.L. Grishchuk. 2015. Basic mechanism for biorientation of mitotic chromosomes is provided by the kinetochore geometry and indiscriminate turnover of kinetochore microtubules. Molecular biology of the cell. 26:3985-3998.

Zaytsev, A.V., J.E. Mick, E. Maslennikov, B. Nikashin, J.G. DeLuca, and E.L. Grishchuk. 2015. Multisite phosphorylation of the NDC80 complex gradually tunes its microtubule-binding affinity. Molecular biology of the cell. 26:1829-1844.

Zhang, L., H. Shao, Y. Huang, F. Yan, Y. Chu, H. Hou, M. Zhu, C. Fu, F. Aikhionbare, G. Fang, X. Ding, and X. Yao. 2011. PLK1 phosphorylates mitotic centromere-associated kinesin and promotes its depolymerase activity. The Journal of biological chemistry. 286:3033-3046.

Zhang, X.D., J. Goeres, H. Zhang, T.J. Yen, A.C. Porter, and M.J. Matunis. 2008. SUMO-2/3 modification and binding regulate the association of CENP-E with kinetochores and progression through mitosis. Mol Cell. 29:729-741.

Zhou, Q., L. Huang, J. Zhang, X. Zhao, Q. Zhang, F. Song, J. Chi, F. Yang, and W. Wang. 2006. Comparative genomic analysis links karyotypic evolution with genomic evolution in the Indian muntjac (Muntiacus muntjak vaginalis). Chromosoma. 115:427-436.

Zhu, C., E. Bossy-Wetzel, and W. Jiang. 2005a. Recruitment of MKLP1 to the spindle midzone/midbody by INCENP is essential for midbody formation and completion of cytokinesis in human cells. Biochem J. 389:373-381.

Zhu, C., and W. Jiang. 2005. Cell cycle-dependent translocation of PRC1 on the spindle by Kif4 is essential for midzone formation and cytokinesis. Proceedings of the National Academy of Sciences of the United States of America. 102:343-348.

Zhu, C., J. Zhao, M. Bibikova, J.D. Leverson, E. Bossy-Wetzel, J.B. Fan, R.T. Abraham, and W. Jiang. 2005b. Functional analysis of human microtubule-based motor proteins, the kinesins and dyneins, in mitosis/cytokinesis using RNA interference. Molecular biology of the cell. 16:3187-3199.

Zimonjic, D.B., C.L. Keck-Waggoner, B.Z. Yuan, M.H. Kraus, and N.C. Popescu. 2000. Profile of genetic alterations and tumorigenicity of human breast cancer cells. Int J Oncol. 16:221-230.

Zinkowski, R.P., S.L. McCune, R.D. Balczon, P.N. Rao, and B.R. Brinkley. 1989. The centromere and aneuploidy: I. Caffeine-induced detachment and fragmentation of kinetochores of mammalian chromosomes. Prog Clin Biol Res. 318:43-60.

Zinkowski, R.P., J. Meyne, and B.R. Brinkley. 1991. The centromere-kinetochore complex: a repeat subunit model. The Journal of cell biology. 113:1091-1110.

Zou, L. 2017. DNA Replication Checkpoint: New ATR Activator Identified. Current biology : CB. 27:R33-R35.

Zou, Y., X. Yi, W.E. Wright, and J.W. Shay. 2002. Human telomerase can immortalize Indian muntjac cells. Experimental cell research. 281:63-76.

Annex

A.1 - Selective tracking of template DNA strands after induction of mitosis with unreplicated genomes (MUGs) in *Drosophila* S2 cells

Chromosome Res (2013) 21:329–337
DOI 10.1007/s10577-013-9354-z

Selective tracking of template DNA strands after induction of mitosis with unreplicated genomes (MUGs) in *Drosophila* S2 cells

Danica Drpic · Marin Barisic · Diana Pinheiro · Helder Maiato

Abstract According to the "immortal" DNA strand hypothesis (Cairns Nature 255:197–200, 1975), stem cells would keep their template strands in order to prevent the accumulation of mutations, which could occur during DNA replication. Despite the growing number of studies that attempt to test this hypothesis, the conclusions remain highly controversial. In the base of this controversy lie the current limitations of available methodology to selectively and faithfully track the fate of template DNA strands throughout and upon cell division. Here, we developed a method that allows the unequivocal tracking of single chromatids containing template DNA strands in *Drosophila* S2 cells in culture. This method consists in the induction of mitosis with unreplicated genomes (MUGs) in which cells are allowed to enter mitosis without prior DNA replication. This is achieved by RNAi-mediated knockdown of Double parked, a conserved protein required for the initiation of DNA replication and post-replication checkpoint response. The advantages of this system when compared with MUGs generated in mammalian cells is the preservation of chromatid morphology, the ease of loss-of-function studies and the possibility of in vivo applications. Altogether, this approach allows for the readily visualization and tracking of template DNA strands by simply monitoring cells stably expressing GFP-fusions with either Histone H2B or the centromeric Histone variant CID/CENP-A by time-lapse fluorescence microscopy. This might be useful for the dissection of the molecular mechanism behind asymmetric DNA strand segregation.

Responsible Editor: Yves Barral.

Danica Drpic and Marin Barisic contributed equally to this work.

Electronic supplementary material The online version of this article (doi:10.1007/s10577-013-9354-z) contains supplementary material, which is available to authorized users.

D. Drpic · M. Barisic · H. Maiato (✉)
Chromosome Instability & Dynamics Laboratory, Instituto de Biologia Molecular e Celular, University of Porto, Rua do Campo Alegre, 823, 4150-180 Porto, Portugal
e-mail: maiato@ibmc.up.pt

D. Drpic · D. Pinheiro
Graduate Program in Areas of Basic and Applied Biology, University of Porto, Porto, Portugal

H. Maiato
Cell Division Unit, Department of Experimental Biology, Faculty of Medicine, University of Porto, Alameda Prof. Hernâni Monteiro, 4200-319 Porto, Portugal

Present Address:
D. Pinheiro
Polarity Division and Morphogenesis Team, Institut Curie, CNRS UMR 3215, INSERM U934, 26 rue d'Ulm, 75248 Paris Cedex 05, France

Keywords Immortal strand · Template DNA · Random segregation · Biased segregation · Asymmetric division

Abbreviations

MUGs	Mitosis with unreplicated genomes
Dup	Double parked
HU	Hydroxyurea
SAC	Spindle assembly checkpoint
NEB	Nuclear envelope breakdown

Introduction

Correct segregation of genetic material into daughter cells during mitosis depends on previously completed replication of DNA during S phase. In 1975, John Cairns (Cairns 1975), based on previous reports of non-random segregation of sister chromatids in mammalian cells (Lark et al. 1966), proposed the "immortal strand" hypothesis according to which stem cells would retain template DNA strands, whereas newly synthesized DNA replicas would segregate into differentiating daughter cells. By keeping template strands, stem cells would avoid the accumulation of mutations that could occur during DNA replication. This hypothesis implies a biased/asymmetric distribution of sister chromatids, but the underlying mechanism remains unknown (Tajbakhsh and Gonzalez 2009). Some possibilities include differences in gene expression, chromatin structure, chromatin modifications between the strands or asymmetry of mitotic spindle components such as centrosomes (Lew et al. 2008, Tajbakhsh and Gonzalez 2009, Charville and Rando 2011).

Support for and against asymmetric segregation of all or just a few DNA strands associated with specific chromosomes can be found in the literature in the most diversified systems, from yeast to man (Tajbakhsh 2008, Rocheteau et al. 2012, Escobar et al. 2011, Schepers et al. 2011, Armakolas and Klar 2006, Conboy et al. 2007, Armakolas et al. 2010), making this a highly controversial topic, mostly due to current limitations in the molecular identification of truly stem cell populations and to selectively label and track template DNA strands throughout and upon cell division. The latter traditionally involves the administration of labelled nucleotides (e.g., 5-bromo-deoxyuridine or H^3-thymidine) that will mark older or newer DNA strands, depending on the protocol used, but which cannot reliably distinguish stem cells from differentiated cells with a slow cell cycle. Therefore, finding a good model system that would allow not only the monitorization of chromatids containing template DNA strands at high spatial and temporal resolution, but also the dissection of the molecular mechanism that could account for biased/asymmetric strand segregation during cell division will be detrimental to complement existing methodology.

Although correct and complete DNA replication is required to allow cells to proceed with the cell cycle, mammalian cells treated with hydroxyurea (HU) and caffeine can enter mitosis without previously replicating their genomes (Brinkley et al. 1988). Hydroxyurea blocks DNA replication, whereas caffeine allows the override of a post-replication checkpoint. This phenomenon known as mitosis with unreplicated genomes (MUGs) has been used in a number of different studies to demonstrate that kinetochores, which detach from chromatin in mammalian MUGs, are sufficient to interact with and be segregated autonomously by the mitotic spindle (Brinkley et al. 1988, Wise and Brinkley 1997, O'Connell et al. 2008, O'Connell et al. 2009, Johnson and Wise 2010). An important corollarium from these experiments is that MUGs can satisfy the spindle assembly checkpoint (SAC) and proceed with anaphase (Brinkley et al. 1988, O'Connell et al. 2008), thereby allowing the subsequent tracking and fate determination of the segregated DNA.

Drosophila Double parked (Dup) is a conserved origin of replication protein that is essential for the initiation of DNA replication in S phase and is involved in a post-replication checkpoint, thereby preventing cells to enter mitosis without completing DNA replication (Whittaker et al. 2000). We reasoned that Dup knockdown by RNAi would drive cells into mitosis without previous DNA replication, which would represent an efficient way to generate and selectively track single chromatids containing template DNA strands. As proof-of-principle, we tested this idea in *Drosophila* S2 cells in culture, in which it is possible to monitor chromosome and mitotic spindle behaviour throughout cell division by stably expressing GFP (or any other fluorescent protein) fusion proteins with core chromosomal and spindle apparatus components. Due to their simple cytology that favours high-resolution imaging studies, the ease of loss-of-function studies by RNAi (Moutinho-Pereira et al. 2010), together with the capacity to induce polarity and asymmetric division in *Drosophila* S2 cells (Johnston et al. 2009), this system may be potentially

suited to complement existing methods for the dissection of the molecular mechanism behind asymmetric DNA strand segregation.

Materials and methods

Cell lines

Drosophila S2 cells stably expressing either GFP-H2B Histone and mCherry-α-tubulin (Maiato and Lince-Faria 2010) or GFP-α-tubulin and CID-mCherry (Moutinho-Pereira et al. 2010), were grown at 25 °C in Schneider's medium (Invitrogen).

RNA interference

Dup dsRNA was obtained following the protocol previously described in (Maiato et al. 2003). For synthetizing Dup dsRNA from *Drosophila* S2 cells genomic DNA, we used the primers: forward TAATACGACTCACTATAGGGGTCATAACGTGTGGATTCATGG and reverse TAATACGACTCACTATAGGGCAAGACTCCCACAAAAATACCG. For RNAi of Dup 10^6 S2 cells were seeded in six well plates and incubated with 1 ml of Schneider´s medium without FBS and containing 10 μg/ml of Dup dsRNA for 1 h (Moutinho-Pereira et al. 2010). After incubation, 2 ml of Schneider´s medium with FBS were added and cells were kept for 96 h at 25 °C.

Imaging

Dup-depleted S2 cells stably expressing GFP-H2B Histone /mCherry-α-tubulin or GFP-α-tubulin/CID-mCherry were plated on 0.25 mg/ml concanavalin A-coated glass-bottom dishes (MatTek) and multipoint time-lapse images of living cells were obtained using a Nikon TE2000U inverted microscope equipped with a Yokogawa CSU-X1 spinning-disc confocal head, two laser lines (488 and 561 nm) and a motorized stage (Marzhauser). Images were collected as a multi (9) 0.5 μm separated *z*-planes with a time interval of 2 min and detected by an iXon^{EM}+Electron Multiplying CCD camera (Andor). An effective pixel size of 0.076 μm was achieved using ×100 1.4 NA plan-Apochromatic DIC objective and two additional lenses: an ×1.5 optivar and a ×1.41 plan-apochromatic imaging lens before the CCD. The system was controlled by NIS-elements software (Nikon, Japan) and videos were processed and analysed with ImageJ.

Results

With the aim of establishing a tractable cell culture system undergoing MUGs in *Drosophila* we performed Dup Histone knockdown by RNAi in S2 cells stably expressing GFP-H2B Histone /mCherry-α-tubulin or GFP-α-tubulin/CID-mCherry. To confirm that Dup-depleted cells entered mitosis without DNA replication we performed live cell imaging using a spinning-disc confocal microscope. As opposed to mammalian cell MUGs in which unreplicated DNA remains decondensed, Dup-depleted S2 cells preserved chromatid morphology (Fig. 1b–e, Movies S2–5), which we used as read-out to validate our experimental strategy. Typically, control S2 cells stably expressing GFP-H2B Histone /mCherry-α-tubulin or GFP-α-tubulin/CID-mCherry established a bipolar spindle with bioriented chromosomes aligned at the metaphase plate and mitosis was completed in 32±9 min (mean±SD; n=11 cells) (Fig. 1a, Movie S1 and Fig. 2a, Movie S6). In agreement with previous studies in *Drosophila* embryos (Parry et al. 2003), Dup-depleted S2 cells entered mitosis with single chromatids (Fig. 1b–e, Movies S2-5). This allowed the unequivocal tracking of chromatids containing template DNA strands. Accordingly, single chromatids upon Dup depletion remained scattered up to several hours (Table 1), likely due to the establishment of unstable kinetochore attachments with spindle microtubule plus ends as result of reduced/absent centromeric tension (King and Nicklas 2000, Pinsky and Biggins 2005). Due to these unstable attachments a highly variable number of chromosomes/kinetochores remained close to the poles throughout mitosis (Fig. 1b–e, Movies S2–5, Fig. 2b, c and Movies S7–8). Interestingly, three out of four Dup-depleted cells (Table 1) showed a clear asymmetric distribution of chromosomes/kinetochores between the two poles immediately upon nuclear envelope breakdown and establishment of initial kinetochore-microtubule attachments (Fig. 2b–c, Movies S7–8). This correlated with a much higher microtubule organizing activity from one of the centrosomes, and spindle bipolarity was achieved by means of centrosome-independent mechanisms (Maiato et al. 2004). Importantly, all recorded *Drosophila* S2 cells undergoing MUGs eventually exited

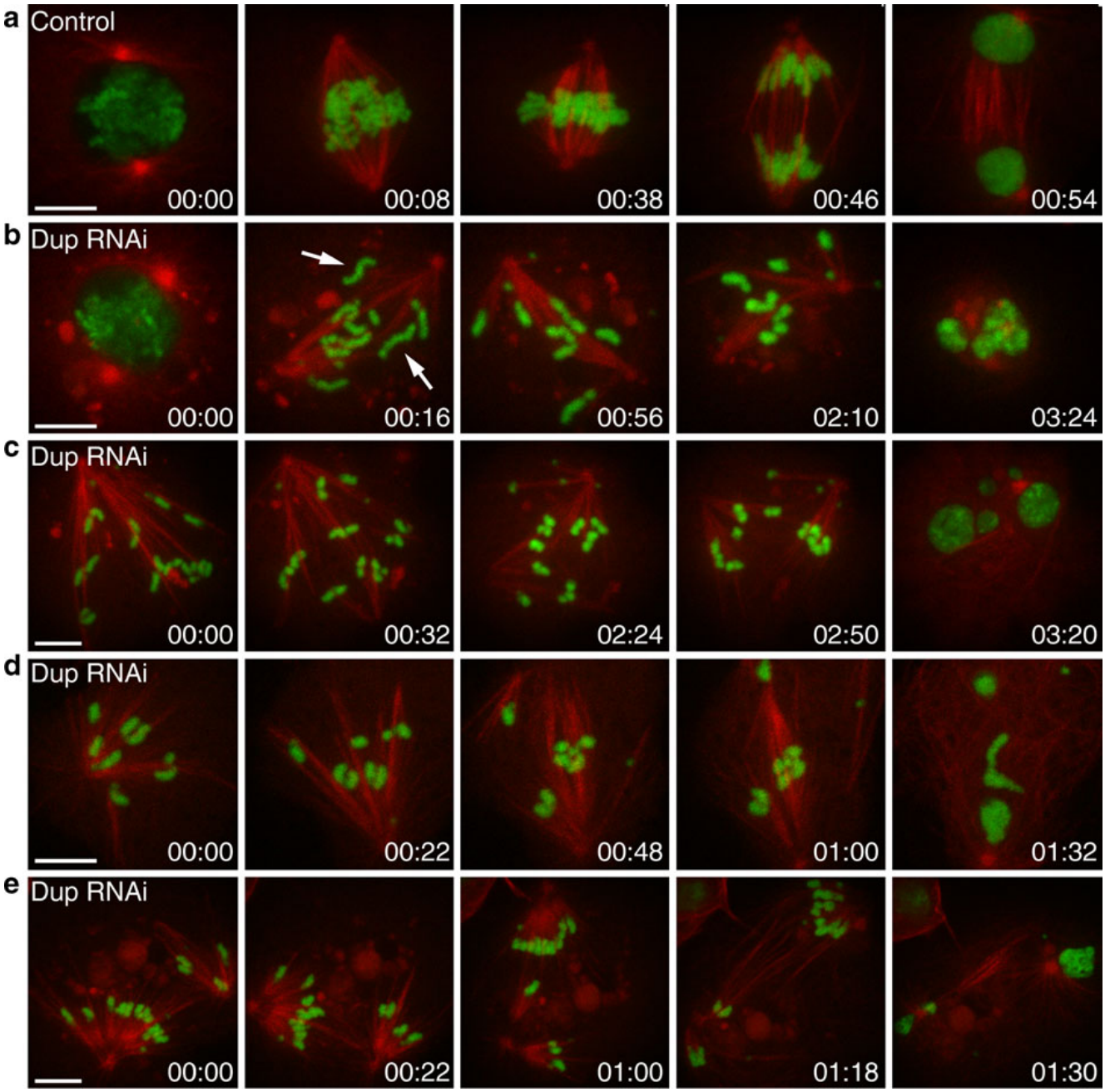

Fig. 1 Dup-depleted cells enter mitosis with unreplicated genomes (MUGs) with single, condensed chromatids. Live cell imaging of control and Dup-depleted *Drosophila* S2 cells stably expressing GFP-H2B Histone (*shown in green*) and mCherry-α-tubulin (*shown in red*). **a** Control cells containing replicated chromosomes aligned during metaphase and segregated evenly during anaphase. **b**–**e** Dup-depleted S2 cells enter MUGs with single, condensed chromatids (*arrows*) which remain scattered within the mitotic spindle. Spindle elongation and DNA decondensation can be observed at the end of MUGs. *Scale bar* 5 μm. Time is in h:min

mitosis (Table 1), as determined by spindle and cell elongation together with chromatin decondensation (Fig. 1b–e, Movies S2–5). This is consistent with previous studies in mammalian cells undergoing MUGs, which were shown to satisfy the SAC after a mitotic delay (Brinkley et al. 1988, O'Connell et al. 2008). Curiously, mammalian cells undergoing MUGs do not seem to elongate the spindle during anaphase B (Johnson and Wise 2010), which was not the case in *Drosophila* S2 cells (Fig. 1e, Movie S5 and Table 1).

Contrary to control *Drosophila* S2 cells in which chromosomes segregated evenly during anaphase (Fig. 1a, Movie S1 and Fig. 2a, movie S6), S2 cells undergoing MUGs showed a 3:1 bias (n=8 cells) in

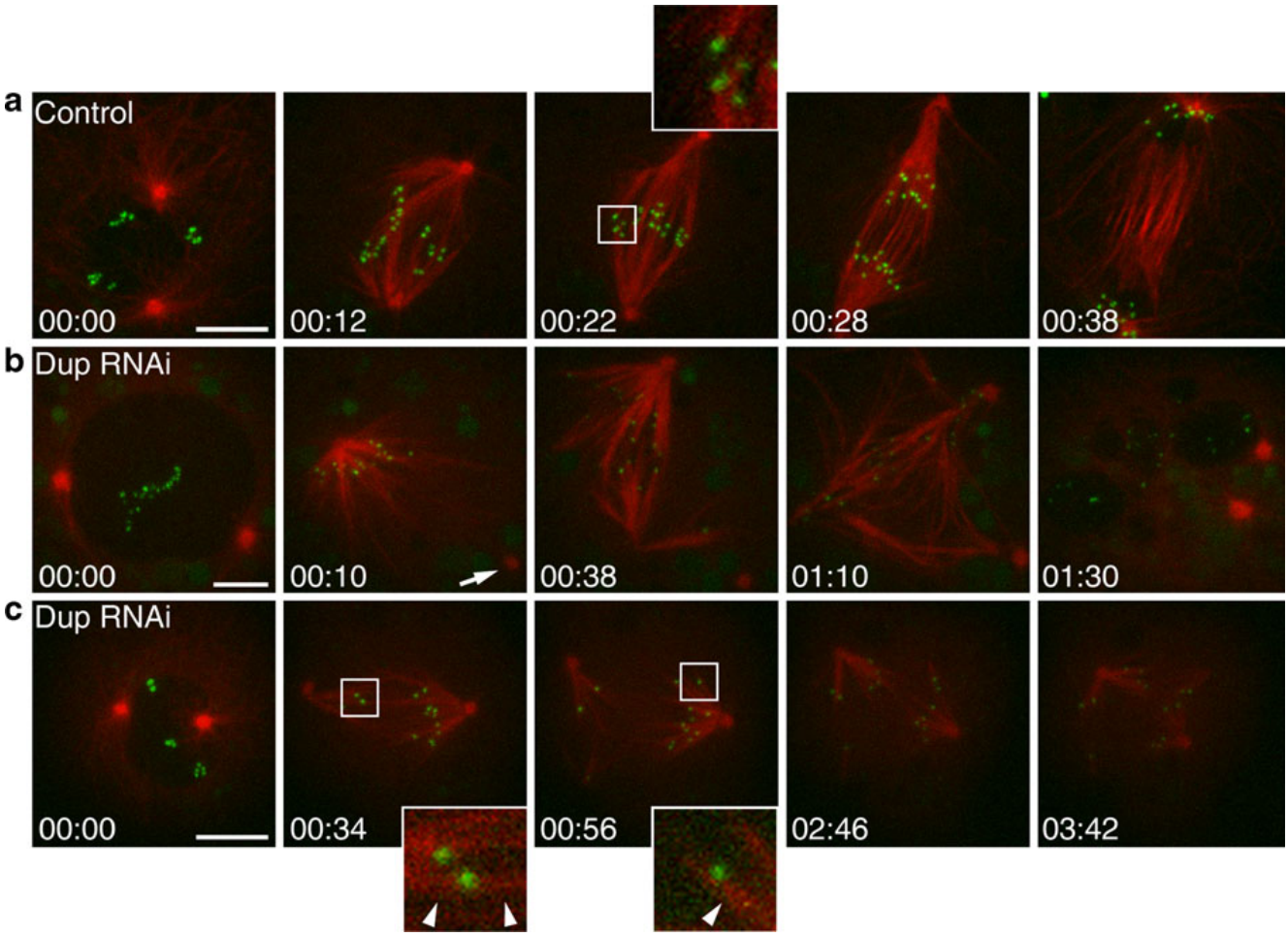

Fig. 2 Dup-depleted cells undergoing MUGs contain single kinetochores improperly attached to the mitotic spindle. Live cell imaging of control and Dup-depleted *Drosophila* S2 cells stably expressing GFP-α-tubulin (*shown in red*) and CID-mCherry (*shown in green*). **a** Control cells contain paired, bioriented kinetochores with amphitelic attachments (*boxed*, *enlarged*). **b**–**c** Single, unpaired kinetochores of Dup-depleted cells undergoing MUGs. **c** Kinetochores during MUGs are either merotelic (*left box*) or monotelic (*right box*) attached (*arrowheads on microtubules*). **b** Arrow is pointing to the single pole excluded from the mitotic spindle showing lower microtubule organization capacity. *Scale bar*, 5 μm. Time is in h:min

segregating single chromatids containing template DNA strands in an asymmetric vs. apparently symmetric fashion (Fig. 1d, e, Movies S4–5 and Table 1).

Discussion

Here, we have established the experimental conditions to generate MUGs in *Drosophila* S2 cells in culture (Fig. 3). MUGs represent an established model system that helped elucidating a number of important processes in mitosis, such as kinetochore-microtubule interactions, SAC satisfaction and the role of chromosomes/kinetochores in spindle assembly (Wise and Brinkley 1997, O'Connell et al. 2008, O'Connell et al. 2009, Johnson and Wise 2010). The ability of *Drosophila* S2 cells to preserve condensed DNA morphology during MUGs allowed the unequivocal tracking of single chromatids (Fig. 1b–e, Movies S2–5) containing template DNA strands, which is an advantage relative to mammalian systems where DNA condensation during MUGs is lost.

Although S2 cells are thought to divide in a symmetrical fashion, there are inherent asymmetries that are normally neglected. This is the case for the mother and daughter centrosomes, which will be inherited by the two daughter cells. The template and replicated DNA strands are also inherently asymmetric, in the sense that one is older than the other, but whether they segregate asymmetrically in this system remains unknown. Moreover, even if they do segregate asymmetrically, there is no obvious reasoning for such behaviour aside from the potential conservation of mechanisms that

Table 1 Summary of measured parameters from *Drosophila* S2 cells undergoing MUGs

MUGs	Mitotic entry	Interpolar distribution of single chromatids before NEB	Interpolar distribution of single chromatids after NEB	Mitotic exit	Minimal mitosis duration[a]	Spindle elongation in anaphase	Chromatid segregation in anaphase
Cell 1	Yes	Even	Asymmetric	Yes	1 h	Yes	Asymmetric
Cell 2	Yes	Even	Asymmetric	N.A.	>6 h	N.A.	N.A.
Cell 3	Yes	Even	Asymmetric	N.A.	>1 h	N.A.	N.A.
Cell 4	N.A.	N.A.	N.A.	Yes	>2 h	Yes	Asymmetric
Cell 5	N.A.	N.A.	N.A.	Yes	>2 h	Yes	Asymmetric
Cell 6	N.A.	N.A.	N.A.	Yes	>45 min	Yes	Even
Cell 7	N.A.	N.A.	N.A.	Yes	>2 h 20 min	Yes	Asymmetric
Cell 8	Yes	Even	Even	Yes	2 h	Yes	Even
Cell 9	N.A.	N.A.	N.A.	Yes	>2 h	Yes	Asymmetric
Cell10	N.A.	N.A.	N.A.	Yes	>20 min	Yes	Asymmetric

[a] Defined as the time between nuclear envelope breakdown until chromatin decondensation. In the cases where the entry /exit of mitosis is missing from our recordings, the indicated times are an underestimation of the real mitotic duration

N.A. data not available

maybe present in the stem cells from which S2 cells derived. Importantly, it is possible to induce polarized division in S2 cells in culture, for example through the ectopic expression of aPKC or Pins to cell–cell contact sites (Johnston et al. 2009). The powerful and flexible experimental tools together with the simple cytology of S2 cells makes this system potentially suited for the dissection of the molecular mechanism behind asymmetric DNA strand segregation, namely through the combination of high-resolution live cell imaging with loss-of-function studies.

Although beyond the scope of this work, we did notice that those S2 cell MUGs that were able to exit mitosis showed a 3:1 bias in asymmetric vs. apparently symmetric segregation of single chromatids containing template DNA strands. This was surprising in light of previous studies in CHO cells where it was shown that during MUGs small centromere-kinetochore fragments segregate evenly to the daughter cells without showing any strong bias or asymmetry (Johnson and Wise 2010). However, previous studies did detect two populations of CHO cells undergoing MUGs where some showed apparently equal segregation and others where segregation was uneven, depending on whether they had near "diploid" kinetochore numbers (Brinkley et al. 1988). In these cases, the reason for discrepancy might lie in the detection method of small kinetochore fragments, which in S2 cell MUGs does not represent a problem since entire chromatids can be tracked. Are these results in S2 cell MUGs relevant to the "immortal strand" hypothesis? Maybe not, and our results should be taken with caution given that just a small population of cells was analysed in the present study. Moreover, the observed bias might be due to many other mechanisms unrelated to template strand bias, such as asymmetry in the initial distribution of chromatids towards one of the two centrosomes or unequal microtubule nucleation capacity of centrosomes, which would bias the capture of a single chromatid by a particular spindle pole. Nevertheless, we do not think this to be the case as during MUGs initial kinetochore-microtubule attachments are unstable and therefore cannot account for the segregation bias observed several hours after alternating chromatid excursions to both spindle poles. This is further supported by the observation that those S2 cells undergoing MUGs that showed a very early bias of chromatids relative to one of the spindle poles immediately upon nuclear envelope breakdown (NEB) did not reveal any obvious asymmetry in their spatial distribution relative to both poles prior to NEB (Table 1). These situations are particularly relevant because they further provide an opportunity to dissect and visualize how the initial interactions between kinetochores from sister chromatids containing template DNA strands and microtubules from the mitotic apparatus are established. Finally, our results do show that there is no absolute bias/asymmetry in the segregation of all template DNA strands and, in the best case scenario, there might only be a segregation bias of template DNA strands from some, but not all, chromosomes. It will be interesting in the future to reproduce these

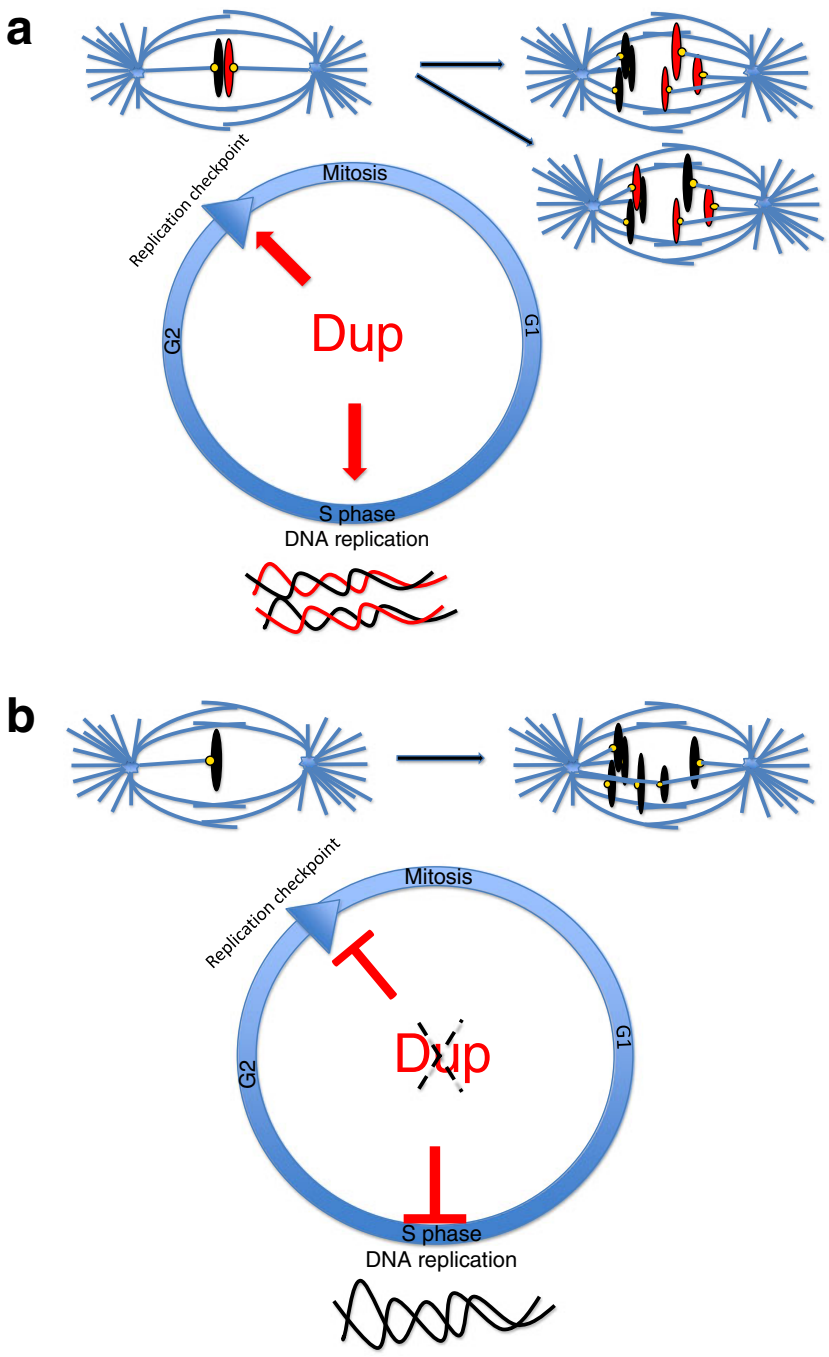

Fig. 3 Model of MUGs upon Dup depletion in *Drosophila* S2 cells. Model illustrates possible biased/asymmetric segregation of chromosomes in Dup-depleted cells in comparison to control. **a** In control cells chromatids equally segregate towards the mitotic poles. **b** Since Dup-depleted S2 cells only contain template DNA this system/strategy might be useful to investigate biased/asymmetric segregation of DNA strands

experiments upon induction of polarization and selective labelling of mother vs. daughter centrosomes in S2 cells using photo-conversion of centriolar proteins (Wang et al. 2009, Januschke et al. 2011).

One important aspect that deserves further consideration in systems undergoing MUGs is that kinetochores are not paired and therefore the entire tension/attachment status of chromosomes is likely to be very different from normal cells, which may influence the segregation pattern of chromatids containing template DNA strands. Accordingly, we observed that the attachments between single chromatids and spindle microtubules in Dup-depleted S2 cells are unstable, with chromatids often switching orientation between the two poles. This highly dynamic kinetochore-microtubule interactions and unstable attachments likely result from the lack of tension in the absence of sister chromatid cohesion and is probably the result of Aurora B-mediated corrections of improper kinetochore-microtubule

attachments (e.g. merotelic or monotelic) (Oliveira et al. 2010). Indeed, the majority of Dup-depleted chromatids are scattered around the mitotic spindle and only some are able to align to the spindle equator apparently through the establishment of merotelic attachments, similar to what has been reported in human cells undergoing MUGs (O'Connell et al. 2008). In these cases, segregation bias was shown to depend on the number of microtubules associated between pole and the merotelic kinetochore, favouring segregation towards the pole with the higher number of attached microtubules (Cimini et al. 2003, 2004).

Interestingly, all recorded S2 cells undergoing MUGs exited mitosis but took about three to four times longer than control S2 cells (Table 1). This contrasts with results in *Drosophila* embryos mutant for Dup, which arrested in mitosis as a result of activated SAC, with stabilized mitotic cyclins and Bub1 kinase present on kinetochores (Garner et al. 2001). On the other hand, mammalian cells undergoing MUGs were able to satisfy the SAC and exited from mitosis (O'Connell et al. 2008), although BubR1 levels on kinetochores were still high. These differences between systems undergoing MUGs indicate that the detailed mechanism of SAC satisfaction/mitotic exit remains to be elucidated and likely involves structural modifications within the kinetochore itself in addition to centromere stretching (Maresca and Salmon 2009, Uchida et al. 2009).

Our results in S2 cells in culture mirror previous experiments with *Drosophila* embryos mutant for Dup (Whittaker et al. 2000, Parry et al. 2003). This provides an important advantage over in vitro-limited HU/caffeine induced MUGs in mammalian cells in culture to investigate biased/asymmetric DNA strand segregation in vivo using the powerful genetic tools of *Drosophila*, including the analysis of hypomorphic mutations, in vivo RNAi and clonal cell analysis in specific tissues.

Acknowledgments We would like to thank António Pereira for insightful discussions on chromosome segregation in MUGs. We also acknowledge the GABBA PhD Program for support to D.D and D.P. Work in the laboratory of H.M. is funded by grants PTDC/SAU-GMG/099704/2008 and PTDC/SAU-ONC/112917/2009 from FCT (COMPETE-FEDER), the Human Frontier Science Program and the 7th framework program grant PRECISE from the European Research Council.

References

Armakolas A, Klar AJ (2006) Cell type regulates selective segregation of mouse chromosome 7 DNA strands in mitosis. Science 311:1146–1149

Armakolas A, Koutsilieris M, Klar AJ (2010) Discovery of the mitotic selective chromatid segregation phenomenon and its implications for vertebrate development. Curr Opin Cell Biol 22:81–87

Brinkley BR, Zinkowski RP, Mollon WL, Davis FM, Pisegna MA, Pershouse M, Rao PN (1988) Movement and segregation of kinetochores experimentally detached from mammalian chromosomes. Nature 336:251–254

Cairns J (1975) Mutation selection and the natural history of cancer. Nature 255:197–200

Charville GW, Rando TA (2011) Stem cell ageing and non-random chromosome segregation. Philos Trans R Soc B Biol Sci 366:85–93

Cimini D, Cameron LA, Salmon ED (2004) Anaphase spindle mechanics prevent mis-segregation of merotelically oriented chromosomes. Curr Biol 14:2149–2155

Cimini D, Moree B, Canman JC, Salmon ED (2003) Merotelic kinetochore orientation occurs frequently during early mitosis in mammalian tissue cells and error correction is achieved by two different mechanisms. J Cell Sci 116:4213–4225

Conboy MJ, Karasov AO, Rando TA (2007) High incidence of non-random template strand segregation and asymmetric fate determination in dividing stem cells and their progeny. PLoS Biol 5:e102

Escobar M, Nicolas P, Sangar F, Laurent-Chabalier S, Clair P, Joubert D, Jay P, Legraverend C (2011) Intestinal epithelial stem cells do not protect their genome by asymmetric chromosome segregation. Nat Commun 2:258

Garner M, van Kreeveld S, Su TT (2001) mei-41 and bub1 block mitosis at two distinct steps in response to incomplete DNA replication in *Drosophila* embryos. Curr Biol: CB 11:1595–1599

Januschke J, Llamazares S, Reina J, Gonzalez C (2011) *Drosophila* neuroblasts retain the daughter centrosome. Nat Commun 2:243

Johnson MK, Wise DA (2010) Distribution of kinetochore fragments during mitosis with unreplicated genomes. Cytoskeleton (Hoboken) 67:172–177

Johnston CA, Hirono K, Prehoda KE, Doe CQ (2009) Identification of an Aurora-A/PinsLINKER/Dlg spindle orientation pathway using induced cell polarity in S2 cells. Cell 138:1150–1163

King JM, Nicklas RB (2000) Tension on chromosomes increases the number of kinetochore microtubules but only within limits. J Cell Sci 113(Pt 21):3815–3823

Lark KG, Consigli RA, Minocha HC (1966) Segregation of sister chromatids in mammalian cells. Science 154:1202–1205

Lew DJ, Burke DJ, Dutta A (2008) The immortal strand hypothesis: how could it work? Cell 133:21–23

Maiato H, Lince-Faria M (2010) The perpetual movements of anaphase. Cell Mol Life Sci: CMLS 67:2251–2269

Maiato H, Rieder CL, Khodjakov A (2004) Kinetochore-driven formation of kinetochore fibers contributes to spindle assembly during animal mitosis. J Cell Biol 167:831–840

Maiato H, Sunkel CE, Earnshaw WC (2003) Dissecting mitosis by RNAi in *Drosophila* tissue culture cells. Biol Proced Online 5:153–161

Maresca TJ, Salmon ED (2009) Intrakinetochore stretch is associated with changes in kinetochore phosphorylation and spindle assembly checkpoint activity. J Cell Biol 184:373–381

Moutinho-Pereira S, Matos I, Maiato H (2010) *Drosophila* S2 cells as a model system to investigate mitotic spindle dynamics, architecture, and function. Methods Cell Biol 97:243–257

O'Connell CB, Loncarek J, Hergert P, Kourtidis A, Conklin DS, Khodjakov A (2008) The spindle assembly checkpoint is satisfied in the absence of interkinetochore tension during mitosis with unreplicated genomes. J Cell Biol 183:29–36

O'Connell CB, Loncarek J, Kalab P, Khodjakov A (2009) Relative contributions of chromatin and kinetochores to mitotic spindle assembly. J Cell Biol 187:43–51

Oliveira RA, Hamilton RS, Pauli A, Davis I, Nasmyth K (2010) Cohesin cleavage and Cdk inhibition trigger formation of daughter nuclei. Nat Cell Biol 12:185–192

Parry DH, Hickson GR, O'Farrell PH (2003) Cyclin B destruction triggers changes in kinetochore behavior essential for successful anaphase. Curr Biol: CB 13:647–653

Pinsky BA, Biggins S (2005) The spindle checkpoint: tension versus attachment. Trends Cell Biol 15:486–493

Rocheteau P, Gayraud-Morel B, Siegl-Cachedenier I, Blasco MA, Tajbakhsh S (2012) A subpopulation of adult skeletal muscle stem cells retains all template DNA strands after cell division. Cell 148:112–125

Schepers AG, Vries R, van den Born M, van de Wetering M, Clevers H (2011) Lgr5 intestinal stem cells have high telomerase activity and randomly segregate their chromosomes. EMBO J 30:1104–1109

Tajbakhsh S (2008) Stem cell identity and template DNA strand segregation. Curr Opin Cell Biol 20:716–722

Tajbakhsh S, Gonzalez C (2009) Biased segregation of DNA and centrosomes: moving together or drifting apart? Nat Rev Mol Cell Biol 10:804–810

Uchida KS, Takagaki K, Kumada K, Hirayama Y, Noda T, Hirota T (2009) Kinetochore stretching inactivates the spindle assembly checkpoint. J Cell Biol 184:383–390

Wang X, Tsai JW, Imai JH, Lian WN, Vallee RB, Shi SH (2009) Asymmetric centrosome inheritance maintains neural progenitors in the neocortex. Nature 461:947–955

Whittaker AJ, Royzman I, Orr-Weaver TL (2000) *Drosophila* double parked: a conserved, essential replication protein that colocalizes with the origin recognition complex and links DNA replication with mitosis and the down-regulation of S phase transcripts. Genes Dev 14:1765–1776

Wise DA, Brinkley BR (1997) Mitosis in cells with unreplicated genomes (MUGs): spindle assembly and behavior of centromere fragments. Cell Motil Cytoskeleton 36:291–302

A.2 - Polar ejection forces promote the conversion from lateral to end-on kinetochore-microtubule attachments on mono-oriented chromosomes

Report

Cell Reports

Polar Ejection Forces Promote the Conversion from Lateral to End-on Kinetochore-Microtubule Attachments on Mono-oriented Chromosomes

Graphical Abstract

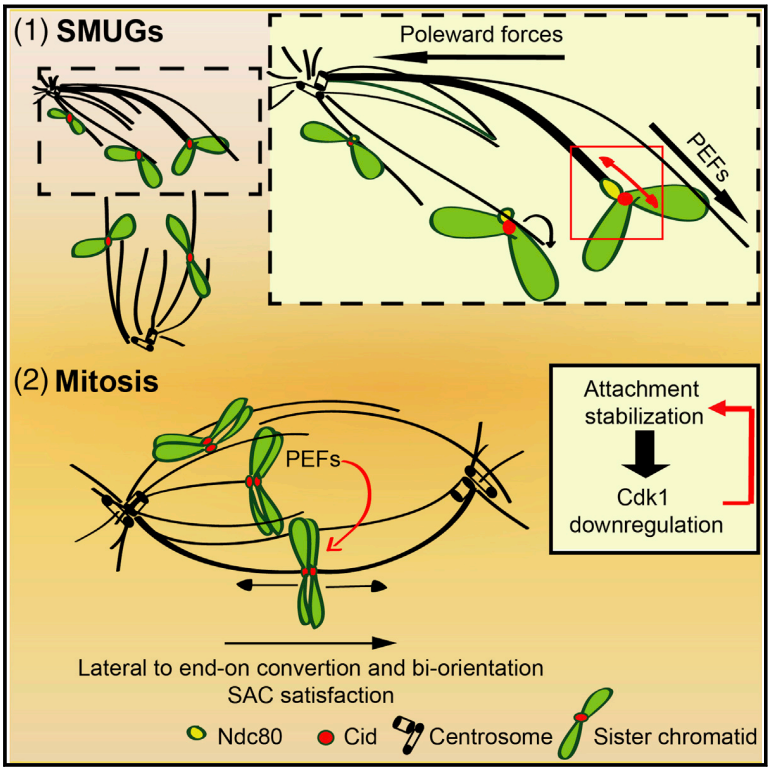

Authors

Danica Drpic, António J. Pereira, Marin Barisic, Thomas J. Maresca, Helder Maiato

Correspondence

maiato@ibmc.up.pt

In Brief

Tension on bi-oriented chromosomes plays a role in the stabilization of kinetochore-microtubule attachments. However, how kinetochore-microtubule attachments on mono-oriented chromosomes are first stabilized in the absence of tension remained unknown. Drpic et al. now show that polar ejection forces promote the transition from lateral to end-on attachments on mono-oriented chromosomes.

Highlights

- Spindle assembly checkpoint (SAC) can be satisfied after a delay in cells with mono-oriented chromosomes
- Mono-oriented chromosomes experience intra-kinetochore stretch
- Polar ejection forces promote SAC satisfaction independently of bi-orientation
- Polar ejection forces promote the conversion from lateral to end-on attachments

Drpic et al., 2015, Cell Reports *13*, 460–468
October 20, 2015 ©2015 The Authors
http://dx.doi.org/10.1016/j.celrep.2015.08.008

CellPress

OPEN ACCESS
CellPress

Cell Reports
Report

Polar Ejection Forces Promote the Conversion from Lateral to End-on Kinetochore-Microtubule Attachments on Mono-oriented Chromosomes

Danica Drpic,[1,2,3] António J. Pereira,[1,2] Marin Barisic,[1,2] Thomas J. Maresca,[4] and Helder Maiato[1,2,5,*]
[1]Chromosome Instability & Dynamics Laboratory, Instituto de Biologia Molecular e Celular, Universidade do Porto, Rua do Campo Alegre 823, 4150-180 Porto, Portugal
[2]Instituto de Investigação e Inovação em Saúde - i3S, Universidade do Porto, 4099-002 Porto, Portugal
[3]Graduate Program in Areas of Basic and Applied Biology (GABBA), Instituto de Ciencias Biomedicas Abel Salazar da Universidade do Porto, Rua de Jorge Viterbo Ferreira no. 228, 4050-313 Porto, Portugal
[4]Biology Department, University of Massachusetts, Amherst, Amherst, MA 01003, USA
[5]Cell Division Unit, Department of Experimental Biology, Faculty of Medicine, University of Porto, Alameda Prof. Hernâni Monteiro, 4200-319 Porto, Portugal
*Correspondence: maiato@ibmc.up.pt
http://dx.doi.org/10.1016/j.celrep.2015.08.008

SUMMARY

Chromosome bi-orientation occurs after conversion of initial lateral attachments between kinetochores and spindle microtubules into stable end-on attachments near the cell equator. After bi-orientation, chromosomes experience tension from spindle forces, which plays a key role in the stabilization of correct kinetochore-microtubule attachments. However, how end-on kinetochore-microtubule attachments are first stabilized in the absence of tension remains a key unanswered question. To address this, we generated *Drosophila* S2 cells undergoing mitosis with unreplicated genomes (SMUGs). SMUGs retained single condensed chromatids that attached laterally to spindle microtubules. Over time, laterally attached kinetochores converted into end-on attachments and experienced intra-kinetochore stretch/structural deformation, and SMUGs eventually exited a delayed mitosis with mono-oriented chromosomes after satisfying the spindle-assembly checkpoint (SAC). Polar ejection forces (PEFs) generated by Chromokinesins promoted the conversion from lateral to end-on kinetochore-microtubule attachments that satisfied the SAC in SMUGs. Thus, PEFs convert lateral to stable end-on kinetochore-microtubule attachments, independently of chromosome bi-orientation.

INTRODUCTION

During spindle assembly, the initial lateral interactions between chromosomes and microtubules are converted into stable end-on kinetochore-microtubule attachments that lead to chromosome bi-orientation (Magidson et al., 2011). After chromosome bi-orientation, the opposing spindle forces generate tension on centromeres that is important for the stabilization of correct kinetochore–microtubule attachments required for error-free chromosome segregation (Nicklas and Koch, 1969; Nicklas and Ward, 1994). Tension has also been shown to be sufficient to satisfy the spindle-assembly checkpoint (SAC) (Li and Nicklas, 1995), a surveillance mechanism that ensures that all chromosomes are attached to spindle microtubules before anaphase onset (Foley and Kapoor, 2013). Tension from spindle forces affects kinetochore chemistry through changes in phosphorylation of "tension-sensitive" proteins at kinetochores (Gorbsky and Ricketts, 1993; Nicklas et al., 1995). Aurora B, a mitotic kinase present on centromeres, plays a critical role in tension sensing and error correction (Biggins and Murray, 2001; Cheeseman et al., 2002; Lampson et al., 2004) by phosphorylating key substrates at the kinetochore-microtubule interface, such as the KMN network, in response to tension on bi-oriented chromosomes (DeLuca et al., 2006; Liu et al., 2009; Wang et al., 2011; Welburn et al., 2010). Importantly, recent works in human and *Drosophila* cells have shown that even in the absence of centromeric tension, an intra-kinetochore stretch or structural deformation is sufficient to satisfy the SAC (Maresca and Salmon, 2009; Uchida et al., 2009). However, the underlying mechanism remained unclear.

Chromokinesins are microtubule plus-end-directed motor proteins present on the chromosome arms harboring both chromatin- and microtubule-binding domains. As a consequence of their motor activities, chromokinesins move chromosomes away from the poles by generating random polar ejection forces (PEFs) (Barisic et al., 2014; Brouhard and Hunt, 2005; Levesque and Compton, 2001; Rieder et al., 1986; Wandke et al., 2012; Yajima et al., 2003). Recently, elevated PEFs were shown to stabilize erroneous kinetochore-microtubule attachments (Cane et al., 2013), suggesting a role in the stabilization of kinetochore-microtubule attachments. Here, we found that Chromokinesin-mediated PEFs promote the conversion from lateral to

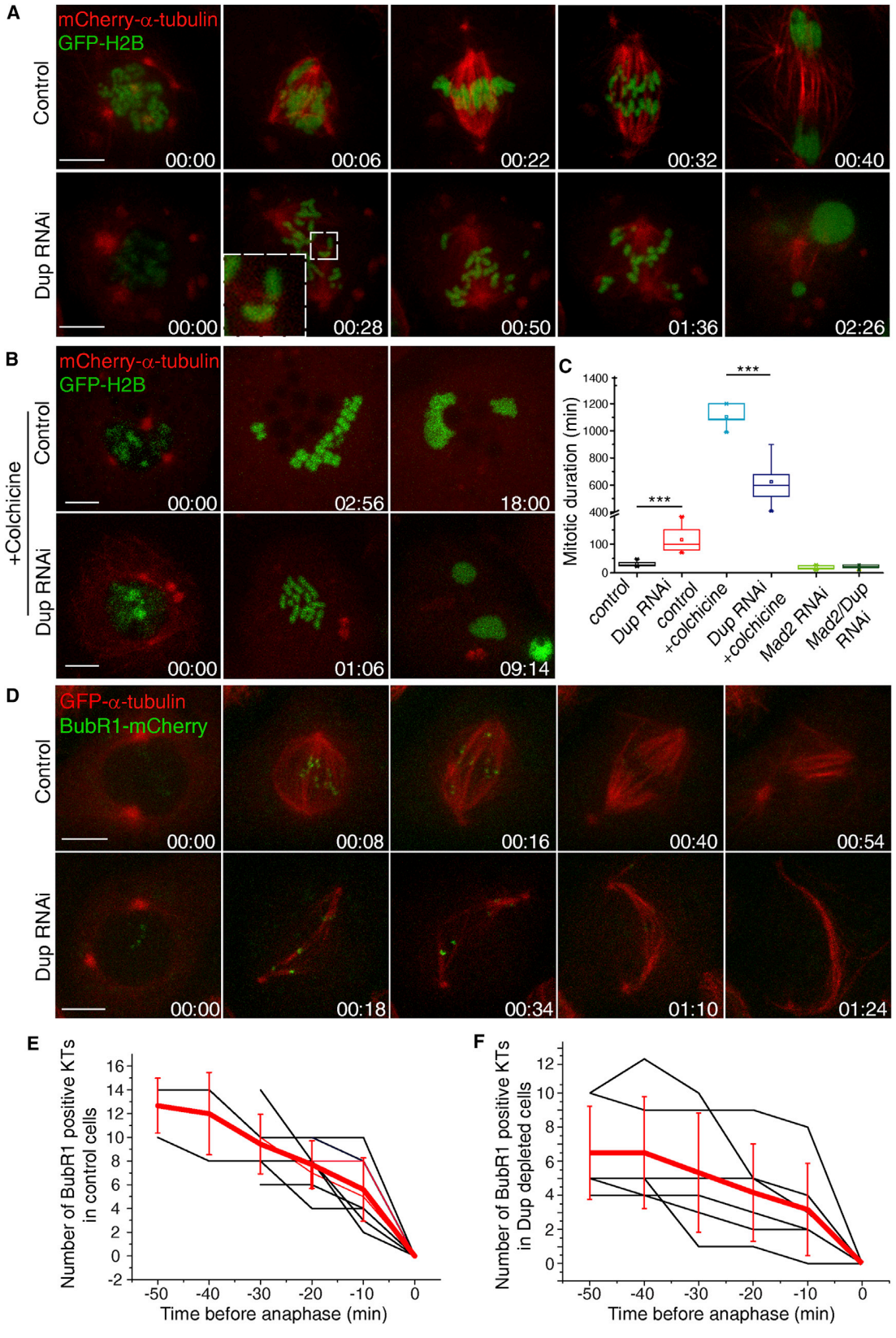

(legend on next page)

stable end-on kinetochore-microtubule attachments on mono-oriented chromosomes. These findings contribute to explain how initial end-on kinetochore-microtubule attachments are stabilized before bi-orientation.

RESULTS

The SAC Is Satisfied in Cells with Single Chromatids after a Mitotic Delay

To investigate which factors are responsible for kinetochore-microtubule attachment stability before bi-orientation, we established a system in *Drosophila* S2 cells undergoing mitosis with unreplicated genomes (SMUGs) (Drpic et al., 2013). This was achieved by RNAi-mediated depletion of Double parked (Dup), a conserved protein required for the initiation of DNA replication and post-replication checkpoint response (Whittaker et al., 2000). The main advantage of this system when compared to mammalian cells undergoing MUGs (Brinkley et al., 1988; O'Connell et al., 2009) is that SMUGs preserve their unreplicated genetic material condensed into single chromatids, which never experience bi-orientation due to the absence of sister kinetochores (Drpic et al., 2013). Thus, the function of individual kinetochores in SMUGs can be investigated in their native chromatid context.

Spinning-disk confocal live-cell imaging revealed that single chromatids in SMUGs were scattered along the spindle. Because of their low chromosome number, the status of kinetochore-microtubule attachments could be inferred by careful inspection of the respective z-sections (see Experimental Procedures). This indicated that SMUGs established mainly lateral and only few merotelic kinetochore-microtubule attachments. For instance, 20 min after nuclear envelope breakdown (NEB) we found that, on average, 8.0 ± 1.6 kinetochores per cell were laterally attached and 3.0 ± 0.82 kinetochores established merotelic attachments (mean ± SD, n = 5 cells; Figures 1A and S1A; Movie S1). Consequently, SMUGs significantly delayed mitotic exit (t = 111 ± 43 min, mean ± SD, n = 11 cells, p = < 0.001, t test) when compared to control cells (t = 31 ± 8 min, mean ± SD, n = 11 cells; Figures 1A and 1C; Movie S1). Indeed, while cyclin B1 levels abruptly decreased at the metaphase-anaphase transition in control cells, cyclin B1 levels decreased more slowly over time in SMUGs (Figures S1E and S1F), suggesting a delay in SAC satisfaction (see also Mirkovic et al., 2015 in this issue of *Cell Reports*). To investigate whether the delayed mitotic exit in SMUGs is SAC dependent, we co-depleted Mad2 and Dup by RNAi (Figures 1C, S1B, and S1C). We found that, similar to control cells, Mad2 co-depletion overcomes the mitotic delay in SMUGs (Mad2/Dup-depleted cells: t = 22.1 ± 6.0 min, mean ± SD, n = 31 cells; Mad2-depleted cells: t = 18.0 ± 5.6 min, mean ± SD, n = 19 cells), indicating that the mitotic delay in SMUGs is SAC dependent.

Next, we tested SAC response in SMUGs by adding colchicine immediately after NEB to generate unattached kinetochores and monitored mitotic progression by live-cell imaging. Both control cells and SMUGs were arrested in mitosis for more than 10 hr before undergoing slippage (Rieder and Maiato, 2004) (control t = 18.4 ± 1.23 hr, mean ± SD, n = 7 cells; SMUGs t = 10.4 ± 2.6 hr, mean ± SD, n = 24 cells; Figures 1B and 1C). These results indicate that SMUGs have an active SAC, which is, however, less robust than in control cells. Interestingly, the total levels of Mad2 and the recruitment of Mad2 and active Aurora B to unattached kinetochores in SMUGs were unaltered relative to controls; Figures S1D and S2A–S2D). Thus, despite normal SAC signaling at individual kinetochores, the number of cumulative unattached kinetochores that are able to inhibit the Anaphase Promoting Complex/Cyclosome (APC/C) in SMUGs is reduced by half relative to controls cells. This explains the weakened SAC response in SMUGs and is in line with previous reports in human cells (Collin et al., 2013; Dick and Gerlich, 2013). Importantly, these data strongly suggest that SMUGs normally exit mitosis after SAC satisfaction, as they took more than five times longer to slip out of mitosis in the presence of colchicine.

To directly test whether SMUGs satisfy the SAC after a mitotic delay, we investigated the behavior of another SAC protein, BubR1, using live-cell imaging of SMUGs stably expressing BubR1-mCherry/α-tubulin-GFP. BubR1 is normally recruited to unattached kinetochores and its levels decrease significantly as chromosomes bi-orient, becoming undetectable on anaphase kinetochores (Howell et al., 2004; Maiato et al., 2002). In contrast, BubR1 remains associated with kinetochores in cells that slip out of mitosis without satisfying the SAC (Brito and Rieder, 2006). We found that, despite of a mitotic delay, SMUGs lost BubR1 from kinetochores just before exiting from mitosis (Figures 1D–1F and Movie S2). This demonstrates that the SAC in SMUGs with single chromatids can be satisfied without bi-orientation.

Single Chromatids in SMUGs Experience Intra-kinetochore Stretch/Structural Deformation after a Mitotic Delay

Intra-kinetochore stretch or structural deformation is sufficient to satisfy the SAC even with reduced centromeric tension (Maresca and Salmon, 2009; Uchida et al., 2009). To investigate whether

Figure 1. Cells with Single Chromatids Satisfy the SAC after a Mitotic Delay

(A) Live-cell imaging of *Drosophila* S2 cells (control and Dup-depleted) stably expressing H2B-GFP and mCherry-α-tubulin. Dashed box indicates a single, condensed chromatid.

(B) Similar conditions, but in which cells were treated with 200 μM colchicine immediately after NEB.

(C) Quantification of mitotic duration (control n = 11 cells; Dup-depleted n = 11 cells; control cells treated with colchicine n = 7 cells; Dup-depleted cells treated with colchicine n = 24 cells; Mad2-depleted cells treated with colchicine n = 19 cells; Mad2/dup-depleted cells treated with colchicine, n = 31 cells).

(D) Live-cell imaging of S2 cells stably expressing BubR1-mCherry and GFP-α-tubulin.

(E and F) Quantification of the number of BubR1 positive kinetochores during normal mitosis (n = 10 cells) and SMUGs (n = 10 cells). Zero time point refers to anaphase onset.

***p < 0.001. Black lines indicate individual cells and red lines represent the average. Error bars, SD. Time = hr:min. Scale bar, 5 μm. See also Figures S1 and S2 and Movie S1.

SMUGs experience intra-kinetochore stretch/structural deformation, we measured the absolute distance between the inner kinetochore protein Cid-mCherry and the outer kinetochore protein Ndc80-GFP (Maresca and Salmon, 2009) at individual kinetochores (see Experimental Procedures) from control cells treated with colchicine (reference for relaxed kinetochores) or MG132 (reference for bi-oriented chromosomes under tension), as well as from Dup-depleted cells treated with MG132 for 2 hr (to normalize the mitotic delay). We found that under these conditions single chromatids in SMUGs experienced a significant intra-kinetochore stretch/structural deformation relative to relaxed kinetochores (Mann-Whitney rank-sum test, $p < 0.001$) that was almost comparable to bi-oriented chromosomes under tension (Figures 2A and 2C). In line with these measurements, we further observed intermediate levels of Aurora B-mediated phosphorylation of the outer kinetochore protein KNL1 (Welburn et al., 2010) relative to unattached controls and bi-oriented chromosomes (Figures 2B and 2C), suggesting that intra-kinetochore stretch/structural deformation positively correlates with kinetochore-microtubule attachment stability. Taken together, these data indicate that single chromatids in SMUGs experience sufficient intra-kinetochore stretch/structural deformation to satisfy the SAC.

PEFs Stabilize Kinetochore-Microtubule Attachments and Promote SAC Satisfaction Independently of Chromosome Bi-orientation

Elevated PEFs on chromosome arms after overexpression of the Chromokinesin Nod lead to the stabilization of syntelic kinetochore-microtubule attachments in *Drosophila* S2 cells (Cane et al., 2013). To test whether the kinetochore-microtubule stabilizing role of PEFs is involved in SAC satisfaction in SMUGs, we co-depleted Dup and Nod. This resulted in a SAC-dependent increase in mitotic duration when compared to Dup-depleted cells ($t = 208 \pm 109$ min, mean ± SD, $n = 25$ cells, $p = 0.007$, t test; Figures 3B and 3D; Movie S3). Co-depletion of both Chromokinesins, Nod and Klp3A, with Dup caused an even longer mitotic delay ($t = 304 \pm 66$ min, mean ± SD, $n = 8$ cells, $p \leq 0.001$, t test; Figures 3D and S3E). Interestingly, Nod depletion in control cells caused chromosome alignment defects and also significantly increased the duration of mitosis ($t = 44 \pm 12$ min, mean ± SD, $n = 26$, $p = 0.005$, Mann-Whitney rank-sum test; Figures 3A and 3D; Movie S3), in line with previous findings in human cells (Levesque and Compton, 2001; Magidson et al., 2011). This phenotype was exacerbated when Nod and Klp3A were co-depleted ($t = 62 \pm 29$ min, mean ± SD, $n = 20$, $p = 0.003$, t test; Figures 3D and S3E), suggesting that PEFs play an important role in the stabilization of kinetochore-microtubule attachments during a normal mitosis. Thus, in the absence of Chromokinesin-mediated PEFs, SAC satisfaction is delayed and the delay is more pronounced in the absence of chromosome bi-orientation.

One prediction from these data is that elevated PEFs should promote the stabilization of kinetochore-microtubule attachments and consequently accelerate SAC satisfaction in SMUGs. To test this, we overexpressed Nod-mCherry in Dup-depleted cells stably expressing GFP-α-tubulin (Cane et al., 2013). In agreement with our prediction, Nod overexpression significantly shortened the mitotic duration in Dup-depleted cells ($t = 46.5 \pm 22$ min, mean ± SD, $n = 12$ cells, $p \leq 0.001$, t test; Figures 3C and 3D; Movie S4). In contrast, elevated PEFs caused by Nod overexpression in control cells increased mitotic duration ($t = 67 \pm 27$ min, mean ± SD, $n = 22$ cells $p = 0.003$, Mann-Whitney rank-sum test; Figures 3C and 3D; Movie S4), which might be due to random ejection of chromosomes after stabilization of monotelic attachments, thereby preventing bi-orientation and timely SAC satisfaction (Barisic et al., 2014). Overall, these data suggest that Chromokinesin-mediated PEFs promote SAC satisfaction in SMUGs by stabilizing kinetochore-microtubule attachments independently of chromosome bi-orientation.

PEFs Promote the Conversion from Lateral to End-on Kinetochore-Microtubule Attachments on Mono-oriented Chromosomes

HeLa cells undergoing MUGs satisfy the SAC independently of bi-orientation mainly by establishing merotelic attachments (O'Connell et al., 2008). Due to opposite spindle forces, merotelic attachments might cause kinetochore deformation that generates sufficient intra-kinetochore stretch that would satisfy the SAC (Maresca and Salmon, 2009; Uchida et al., 2009). Importantly, the contribution of PEFs for SAC satisfaction could not be investigated in this system because kinetochores detach from chromatin, which remains decondensed during MUGs (Brinkley et al., 1988; O'Connell et al., 2009). Although we cannot exclude that, in addition to PEFs, some merotelic attachments contribute to SAC silencing in SMUGs, these attachments were rare, as indicated by our live-cell recordings and careful inspection of the respective z stacks (Figures 1A and S1A; Movie S1) (see also Mirkovic et al., this issue).

To test whether PEFs are required to satisfy the SAC in SMUGs, independently of chromosome bi-orientation and the establishment of merotelic attachments, we investigated the duration of mitosis in Nod-depleted cells with a monopolar spindle configuration (in which only monotelic attachments can be established), after co-depletion of the Kinesin-5 protein Klp61F by RNAi (Cane et al., 2013) (Figure 4A; Movie S5). We found that SMUGs with monopolar spindles were also able to exit mitosis after a delay ($t = 178 \pm 59$ min, mean ± SD, $n = 9$; Figure 4A; Movie S5), which was exacerbated after Nod co-depletion ($t = 379$ min ± 132 min, mean ± SD, $n = 4$, $p = 0.011$, Mann-Whitney rank-sum test; Figure 4A; Movie S5). Closer inspection of z stacks from live-cell images of monopolar spindles in SMUGs revealed a clear transition from lateral to end-on kinetochore-microtubule attachments prior to mitotic exit, and the presence of Nod-mediated PEFs promoted this transition (Figures 4B and 4C; Movie S5). Immunofluorescence analysis with a Mad1 antibody confirmed that the percentage of unattached kinetochores in SMUGs with monopolar spindles (35%) increased after Nod depletion (62%, $p = 0.028$, t test; Figure 4D). Overall, these data demonstrate that Chromokinesin-mediated PEFs promote the conversion from lateral to stable end-on kinetochore-microtubule attachments, independently of bi-orientation and merotely.

DISCUSSION

Chromosome bi-orientation is a critical requirement for accurate chromosome segregation during mitosis and requires that both kinetochores are stably attached to spindle microtubules.

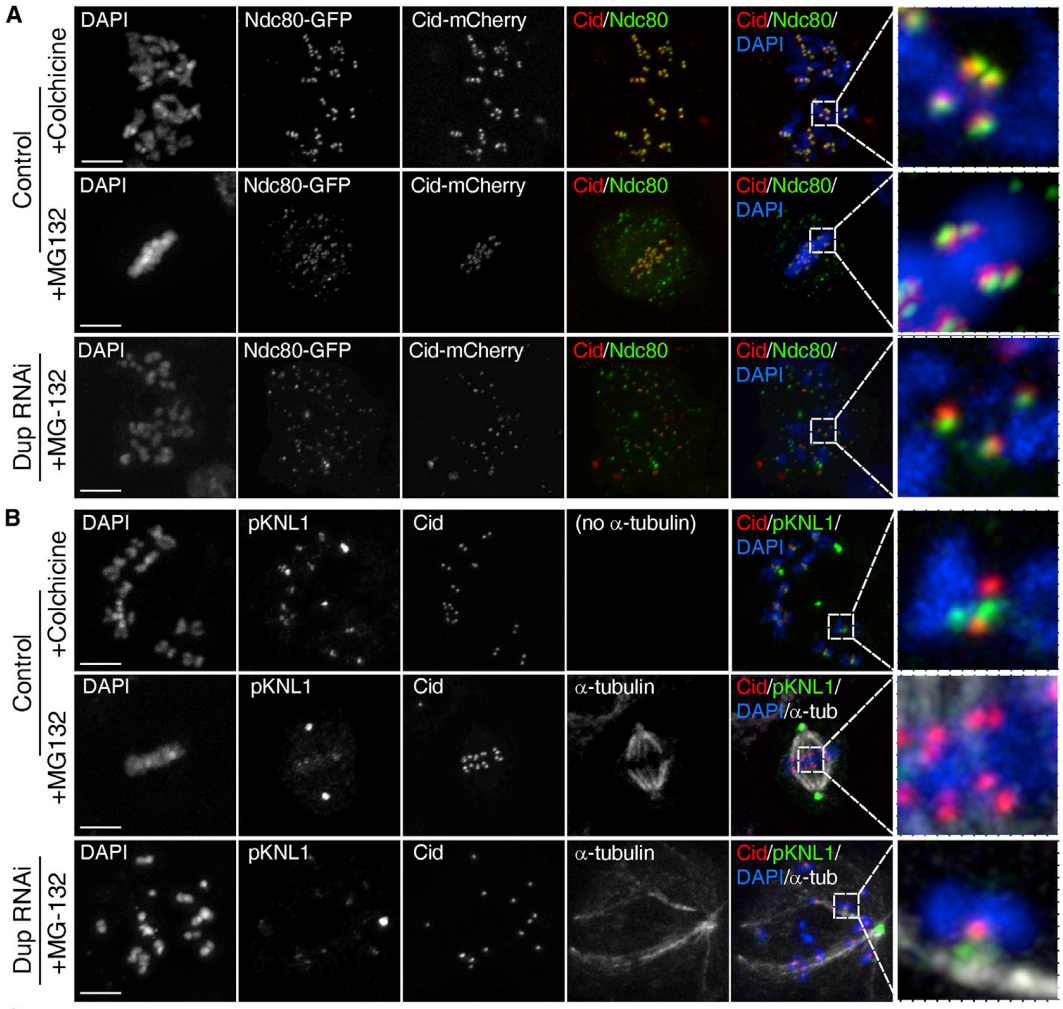

Treatment	Intra-KT stretch ± SD (nm)	Nr. of KTs	Mean Fluorescence Intensity of pKNL1/Cid ± SD (a.u.)	Nr. of KTs
Control + colchicine	103 ± 52	255	0.511 ± 0.385	351
Control + MG132	130 ± 62	890	0.353 ± 0.204	300
Dup + MG132	126 ± 68	475	0.438 ± 0.228	472

Figure 2. Single Chromatids in SMUGs Experience Intra-kinetochore Stretch after a Mitotic Delay

(A) Fixed control cells stably expressing Cid-mCherry/Ndc80-GFP were treated with colchicine or MG132 (2 hr) and compared with Dup-depleted cells treated with MG132 (2 hr).

(B) Immunofluorescence analysis of Aurora-B phosphorylation of the outer kinetochore protein KNL1 in SMUGs and control cells in the same conditions as in (A).

(C) Quantification of pKNL1 and intra-kinetochore stretch (shift) by measuring absolute distance between red (Cid) and green (Ndc80) centroids in control cells versus SMUGs.

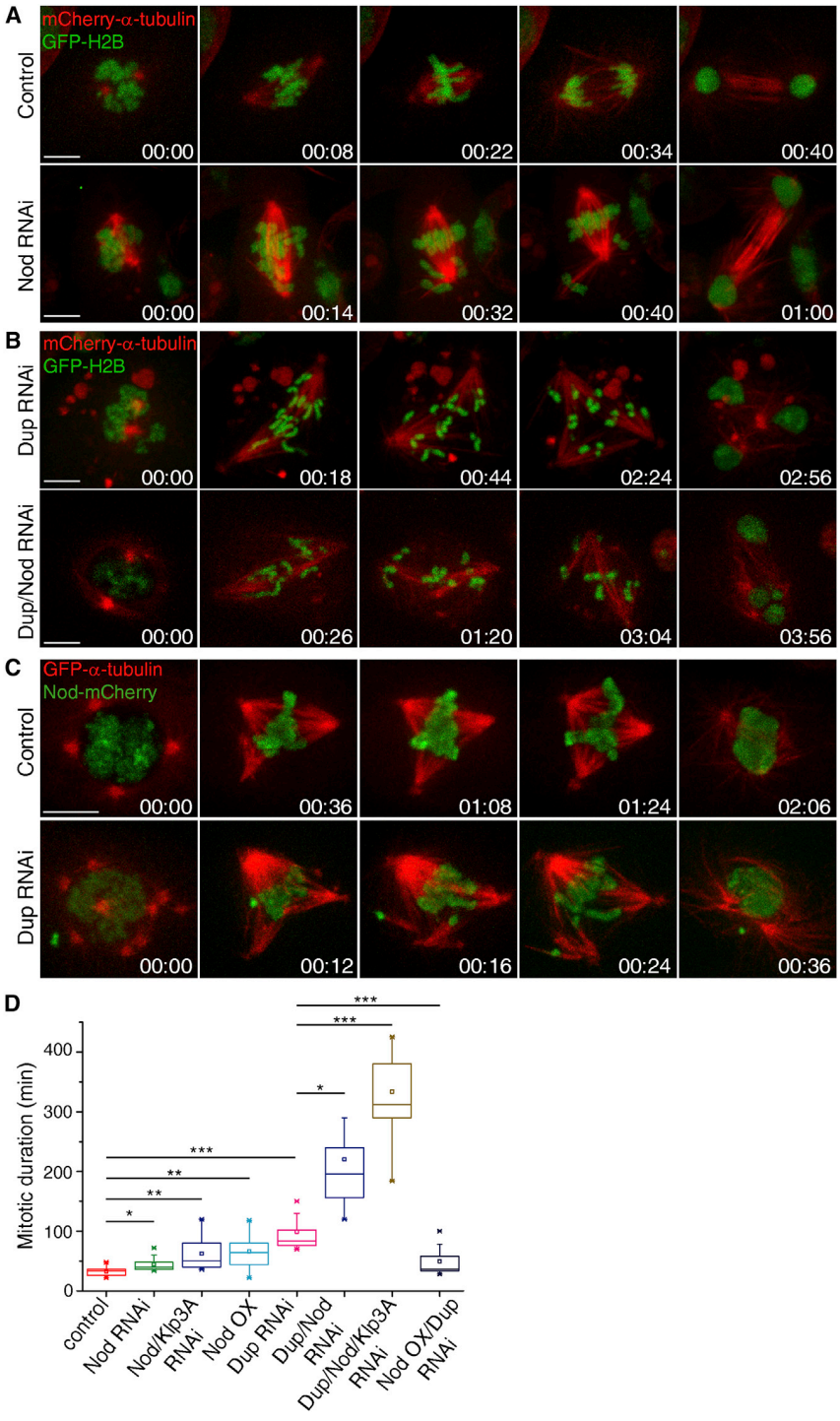

Figure 3. PEFs Are Involved in SAC Satisfaction Independently of Chromosome Bi-orientation

(A and B) Live-cell imaging of *Drosophila* S2 cells stably expressing H2B-GFP and mCherry-α-tubulin. The panels illustrate control, Nod-depleted, Dup-depleted, as well as Nod and Dup co-depleted situations, as indicated.

(C) Live-cell imaging of Nod-mCherry-over-expressing cells with and without Dup depletion.

(D) Mitotic duration of control (n = 11 cells), Nod-depleted (n = 26 cells), Nod/Klp3A-depleted (n = 20 cells), Nod-overexpressing (OX) (n = 22 cells), Dup-depleted (n = 10), Nod/Dup-depleted (n = 25), Nod/Klp3A/Dup-depleted (n = 8), and Nod OX SMUGs (n = 12). *p < 0.05, **p < 0.01, ***p < 0.001.

Time = hr:min. Scale bar, 5 μm. Error bars, SD. See also Figure S3.

Tension from spindle forces has long been known to stabilize correct kinetochore-microtubule attachments (King and Nicklas, 2000), but how the first end-on attachments are stabilized before the development of tension has remained unknown. Here, we found that PEFs promote the conversion from lateral to stable end-on kinetochore-microtubule attachments on mono-oriented chromosomes. Lateral attachments to spindle microtubules are insensitive to Aurora B activity (Kalantzaki et al., 2015) and are initially mediated by kinetochore Dynein, which is dominant over PEFs at the spindle poles (Barisic et al., 2014) and inhibits the action of the Ndc80 complex required for stable end-on attachments (Cheerambathur et al., 2013). Despite not being dominant at this stage, PEFs promote the exclusion of chromosomes from the central area of the mitotic spindle (Magidson et al., 2011), but chromosomes remain tethered to the microtubule walls by CENP-E/Kinesin-7 (Shrestha and Draviam, 2013), which slides chromosomes preferentially along detyrosinated microtubules toward the spindle equator (Barisic et al., 2015). At the equator PEFs become critical to stabilize end-on kinetochore-microtubule attachments required for chromosome bi-orientation (Barisic et al., 2014; Magidson et al., 2011; Wandke et al., 2012). In this context, our data can be best explained by a model in which the lateral to end-on conversion of kinetochore-microtubule attachments near the equator requires the contribution of Chromokinesin-mediated PEFs acting on the arms of mono-oriented chromosomes to counteract microtubule depolymerization-driven poleward motion. This might generate sufficient intra-kinetochore stretch or structural deformation (Maresca and Salmon, 2009; Uchida et al., 2009) that leads to the stabilization of end-on kinetochore-microtubule attachments. Cdk1 downregulation due to cyclin A and B1 degradation might generate positive feedback loops that, in coordination with PEFs, further stabilize kinetochore-microtubule attachments (Collin et al., 2013; Kabeche

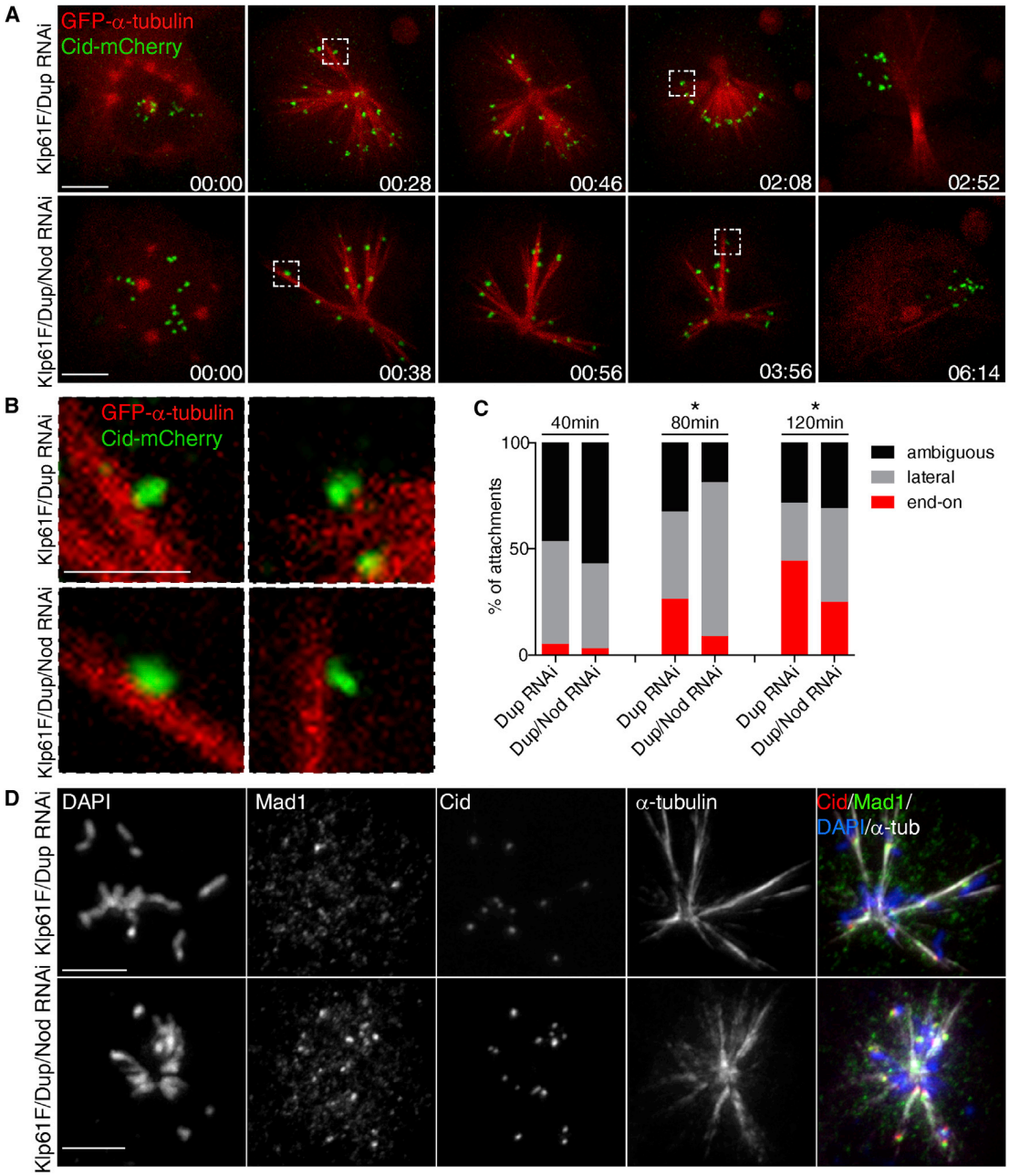

Figure 4. PEFs Promote the Conversion from Lateral to End-on Kinetochore-Microtubule Attachments on Mono-oriented Chromosomes

(A) Live-cell imaging of Klp61F/Dup and Klp61F/Dup/Nod-depleted S2 cells stably expressing GFP-α-tubulin and Cid-mCherry.

(B) Respective higher magnifications of lateral and end-on attachments from (A).

(C) Quantification of the different kinetochore-microtubule attachments (through z stacks) in Klp61F/Dup/Nod RNAi and Klp61F/Dup RNAi cells. The difference in the percentage of end-on attachments between Klp61F/Dup RNAi (n = 7 cells) and Klp61F/Dup/Nod RNAi cells (n = 5 cells) at 80 min and 120 min after NEB are statistically significant (Z-test compare proportions, $p < 0.05$).

(D) Immunofluorescence of Klp61F/Dup and Klp61F/Dup/Nod-depleted S2 cells. Nod depletion in monopolar SMUGs lead to increased number of Mad1 positive kinetochores. Time = hr:min. Scale bar, 5 μm.

Scale bar in higher magnification panels, 2 μm. *$p < 0.05$ relative to the previous time point, t test. Error bars, SD.

and Compton, 2013; Mirkovic et al., 2015). While this eventually leads to SAC satisfaction after a significant mitotic delay in SMUGs, we propose that during normal mitosis this mechanism contributes to the stabilization of initial end-on kinetochore-microtubule attachments, before tension from opposing spindle forces is established during bi-orientation.

EXPERIMENTAL PROCEDURES

Quantification of Kinetochore-Microtubule Attachments

In order to distinguish the different types of kinetochore-microtubule attachments in SMUGs, we performed live-cell imaging in *Drosophila* S2 cells stably expressing GFP-α-tubulin/Cid-mCherry. Images were analyzed using FIJI (ImageJ) software through z stacks (0.5 μm). Kinetochore-microtubule attachments were quantified after tracing microtubule positioning in relation to the Cid signal (kinetochores). When microtubules passed by the Cid signal the attachment was considered as lateral. When microtubules ended at the kinetochore they were considered as end-on attachments. Since in SMUGs chromosomes do not align in the spindle equator, merotelic attachments were rarely observed and were distinguished as having long K-fibers coming from opposite poles that ended on the same kinetochore.

Measurement of Intra-kinetochore Stretch/Deformation

Drosophila S2 cells stably expressing Cid-mCherry/Ndc80-GFP (Maresca and Salmon, 2009) were used for intra-kinetochore stretch measurements in fixed (4% paraformaldehyde) material and for live-cell imaging (intra-kinetochore stretch measurements over time). Sub-pixel determination of fluorescent spot localization was performed using a home-written MATLAB script (MathWorks). A sequential refinement of the spot position starts with manual (mouse) selection of the kinetochore ensemble to be measured. A neighborhood region of interest (ROI) (11 × 11 pixels) is defined around each selected point, the boundary of which is used to estimate average background signal per pixel. This background value is subtracted, and the centroid is then calculated to allow recentering of the ROI. This first part of the script is meant as a coarse correction of the mouse-defined points. Before fitting a circular two-dimensional Gaussian function to each ROI intensity map, an empirical parameter of 1/2 was chosen as the fraction of (highest gray value) ROI pixels to be fed into the fitting procedure thus avoiding the bias induced by residual fluorescence of adjacent structures (e.g., defocused adjacent kinetochores). Fitting is performed using the least-squares fitting routine *lsqcurvefit*.

Statistical Analysis

Statistical analyses were performed using SigmaStat. Additional procedures are available in Supplemental Experimental Procedures.

SUPPLEMENTAL INFORMATION

Supplemental Information includes Supplemental Experimental Procedures, three figures, and five movies and can be found with this article online at http://dx.doi.org/10.1016/j.celrep.2015.08.008.

AUTHOR CONTRIBUTIONS

D.D. performed and analyzed all the experiments; A.J.P. developed the algorithm to measure intra-kinetochore stretch on individual kinetochores; M.B. performed data analysis and designed experiments; T.J.M. provided reagents; H.M. performed data analysis, designed experiments, and supervised the work; D.D. and H.M. wrote the paper.

ACKNOWLEDGMENTS

We thank Raquel Oliveira for communicating results prior to publication. D.D. is supported by a fellowship from the GABBA PhD program from the University of Porto. T.J.M. is supported by an NIH grant (5 R01 GM107026) and by Research Grant No. 5-FY13-205 from the March of Dimes Foundation and support from the Charles H. Hood Foundation, Boston, MA. H.M. is funded by FLAD Life Science 2020 and PRECISE grant from the European Research Council.

Received: April 14, 2015
Revised: July 8, 2015
Accepted: August 3, 2015
Published: October 8, 2015

REFERENCES

Barisic, M., Aguiar, P., Geley, S., and Maiato, H. (2014). Kinetochore motors drive congression of peripheral polar chromosomes by overcoming random arm-ejection forces. Nat. Cell Biol. *16*, 1249–1256.

Barisic, M., Silva e Sousa, R., Tripathy, S.K., Magiera, M.M., Zaytsev, A.V., Pereira, A.L., Janke, C., Grishchuk, E.L., and Maiato, H. (2015). Mitosis. Microtubule detyrosination guides chromosomes during mitosis. Science *348*, 799–803.

Biggins, S., and Murray, A.W. (2001). The budding yeast protein kinase Ipl1/Aurora allows the absence of tension to activate the spindle checkpoint. Genes Dev. *15*, 3118–3129.

Brinkley, B.R., Zinkowski, R.P., Mollon, W.L., Davis, F.M., Pisegna, M.A., Pershouse, M., and Rao, P.N. (1988). Movement and segregation of kinetochores experimentally detached from mammalian chromosomes. Nature *336*, 251–254.

Brito, D.A., and Rieder, C.L. (2006). Mitotic checkpoint slippage in humans occurs via cyclin B destruction in the presence of an active checkpoint. Curr. Biol. *16*, 1194–1200.

Brouhard, G.J., and Hunt, A.J. (2005). Microtubule movements on the arms of mitotic chromosomes: polar ejection forces quantified in vitro. Proc. Natl. Acad. Sci. USA *102*, 13903–13908.

Cane, S., Ye, A.A., Luks-Morgan, S.J., and Maresca, T.J. (2013). Elevated polar ejection forces stabilize kinetochore-microtubule attachments. J. Cell Biol. *200*, 203–218.

Cheerambathur, D.K., Gassmann, R., Cook, B., Oegema, K., and Desai, A. (2013). Crosstalk between microtubule attachment complexes ensures accurate chromosome segregation. Science *342*, 1239–1242.

Cheeseman, I.M., Anderson, S., Jwa, M., Green, E.M., Kang, Js., Yates, J.R., 3rd, Chan, C.S., Drubin, D.G., and Barnes, G. (2002). Phospho-regulation of kinetochore-microtubule attachments by the Aurora kinase Ipl1p. Cell *111*, 163–172.

Collin, P., Nashchekina, O., Walker, R., and Pines, J. (2013). The spindle assembly checkpoint works like a rheostat rather than a toggle switch. Nat. Cell Biol. *15*, 1378–1385.

DeLuca, J.G., Gall, W.E., Ciferri, C., Cimini, D., Musacchio, A., and Salmon, E.D. (2006). Kinetochore microtubule dynamics and attachment stability are regulated by Hec1. Cell *127*, 969–982.

Dick, A.E., and Gerlich, D.W. (2013). Kinetic framework of spindle assembly checkpoint signalling. Nat. Cell Biol. *15*, 1370–1377.

Drpic, D., Barisic, M., Pinheiro, D., and Maiato, H. (2013). Selective tracking of template DNA strands after induction of mitosis with unreplicated genomes (MUGs) in Drosophila S2 cells. Chromosome Res. *21*, 329–337.

Foley, E.A., and Kapoor, T.M. (2013). Microtubule attachment and spindle assembly checkpoint signalling at the kinetochore. Nat. Rev. *14*, 25–37.

Gorbsky, G.J., and Ricketts, W.A. (1993). Differential expression of a phosphoepitope at the kinetochores of moving chromosomes. J. Cell Biol. *122*, 1311–1321.

Howell, B.J., Moree, B., Farrar, E.M., Stewart, S., Fang, G., and Salmon, E.D. (2004). Spindle checkpoint protein dynamics at kinetochores in living cells. Curr. Biol. *14*, 953–964.

Kabeche, L., and Compton, D.A. (2013). Cyclin A regulates kinetochore microtubules to promote faithful chromosome segregation. Nature *502*, 110–113.

Kalantzaki, M., Kitamura, E., Zhang, T., Mino, A., Novák, B., and Tanaka, T.U. (2015). Kinetochore-microtubule error correction is driven by differentially regulated interaction modes. Nat. Cell Biol. *17*, 421–433.

King, J.M., and Nicklas, R.B. (2000). Tension on chromosomes increases the number of kinetochore microtubules but only within limits. J. Cell Sci. *113*, 3815–3823.

Lampson, M.A., Renduchitala, K., Khodjakov, A., and Kapoor, T.M. (2004). Correcting improper chromosome-spindle attachments during cell division. Nat. Cell Biol. *6*, 232–237.

Levesque, A.A., and Compton, D.A. (2001). The chromokinesin Kid is necessary for chromosome arm orientation and oscillation, but not congression, on mitotic spindles. J. Cell Biol. *154*, 1135–1146.

Li, X., and Nicklas, R.B. (1995). Mitotic forces control a cell-cycle checkpoint. Nature *373*, 630–632.

Liu, D., Vader, G., Vromans, M.J., Lampson, M.A., and Lens, S.M. (2009). Sensing chromosome bi-orientation by spatial separation of aurora B kinase from kinetochore substrates. Science *323*, 1350–1353.

Magidson, V., O'Connell, C.B., Lončarek, J., Paul, R., Mogilner, A., and Khodjakov, A. (2011). The spatial arrangement of chromosomes during prometaphase facilitates spindle assembly. Cell *146*, 555–567.

Maiato, H., Sampaio, P., Lemos, C.L., Findlay, J., Carmena, M., Earnshaw, W.C., and Sunkel, C.E. (2002). MAST/Orbit has a role in microtubule-kinetochore attachment and is essential for chromosome alignment and maintenance of spindle bipolarity. J. Cell Biol. *157*, 749–760.

Maresca, T.J., and Salmon, E.D. (2009). Intrakinetochore stretch is associated with changes in kinetochore phosphorylation and spindle assembly checkpoint activity. J. Cell Biol. *184*, 373–381.

Mirkovic, M., Hutter, L.H., Novák, B., and Oliveira, R.A. (2015). Premature sister chromatid separation is poorly detected by the spindle assembly checkpoint as a result of system-level feedback. Cell Rep. *13*, this issue, 469–478.

Nicklas, R.B., and Koch, C.A. (1969). Chromosome micromanipulation. 3. Spindle fiber tension and the reorientation of mal-oriented chromosomes. J. Cell Biol. *43*, 40–50.

Nicklas, R.B., and Ward, S.C. (1994). Elements of error correction in mitosis: microtubule capture, release, and tension. J. Cell Biol. *126*, 1241–1253.

Nicklas, R.B., Ward, S.C., and Gorbsky, G.J. (1995). Kinetochore chemistry is sensitive to tension and may link mitotic forces to a cell cycle checkpoint. J. Cell Biol. *130*, 929–939.

O'Connell, C.B., Loncarek, J., Hergert, P., Kourtidis, A., Conklin, D.S., and Khodjakov, A. (2008). The spindle assembly checkpoint is satisfied in the absence of interkinetochore tension during mitosis with unreplicated genomes. J. Cell Biol. *183*, 29–36.

O'Connell, C.B., Loncarek, J., Kaláb, P., and Khodjakov, A. (2009). Relative contributions of chromatin and kinetochores to mitotic spindle assembly. J. Cell Biol. *187*, 43–51.

Rieder, C.L., and Maiato, H. (2004). Stuck in division or passing through: what happens when cells cannot satisfy the spindle assembly checkpoint. Dev. Cell *7*, 637–651.

Rieder, C.L., Davison, E.A., Jensen, L.C., Cassimeris, L., and Salmon, E.D. (1986). Oscillatory movements of monooriented chromosomes and their position relative to the spindle pole result from the ejection properties of the aster and half-spindle. J. Cell Biol. *103*, 581–591.

Shrestha, R.L., and Draviam, V.M. (2013). Lateral to end-on conversion of chromosome-microtubule attachment requires kinesins CENP-E and MCAK. Curr. Biol. *23*, 1514–1526.

Uchida, K.S., Takagaki, K., Kumada, K., Hirayama, Y., Noda, T., and Hirota, T. (2009). Kinetochore stretching inactivates the spindle assembly checkpoint. J. Cell Biol. *184*, 383–390.

Wandke, C., Barisic, M., Sigl, R., Rauch, V., Wolf, F., Amaro, A.C., Tan, C.H., Pereira, A.J., Kutay, U., Maiato, H., et al. (2012). Human chromokinesins promote chromosome congression and spindle microtubule dynamics during mitosis. J. Cell Biol. *198*, 847–863.

Wang, E., Ballister, E.R., and Lampson, M.A. (2011). Aurora B dynamics at centromeres create a diffusion-based phosphorylation gradient. J. Cell Biol. *194*, 539–549.

Welburn, J.P., Vleugel, M., Liu, D., Yates, J.R., 3rd, Lampson, M.A., Fukagawa, T., and Cheeseman, I.M. (2010). Aurora B phosphorylates spatially distinct targets to differentially regulate the kinetochore-microtubule interface. Mol. Cell *38*, 383–392.

Whittaker, A.J., Royzman, I., and Orr-Weaver, T.L. (2000). Drosophila double parked: a conserved, essential replication protein that colocalizes with the origin recognition complex and links DNA replication with mitosis and the down-regulation of S phase transcripts. Genes Dev. *14*, 1765–1776.

Yajima, J., Edamatsu, M., Watai-Nishii, J., Tokai-Nishizumi, N., Yamamoto, T., and Toyoshima, Y.Y. (2003). The human chromokinesin Kid is a plus end-directed microtubule-based motor. EMBO J. *22*, 1067–1074.